In vivo Hypoxia and *Aspergillus fumigatus* pathogenesis

Dissertation

zur Erlangung des akademischen Grades doctor rerum naturalium (Dr. rer. nat.)

vorgelegt dem Rat der Biologisch-Pharmazeutischen Fakultät der Friedrich-Schiller-Universität Jena

von Nora Grahl, Diplom Biologin

geboren am 10.07.1981 in Neuss

Gutachter:

1. Prof. Dr. Robert A. Cramer Jr., Montana State University
2. Prof. Dr. Erika Kothe, Friedrich-Schiller-Universität Jena
3. Prof. Dr. J. Andrew Alspaugh, Duke University Medical Center

Tag der mündlichen Prüfung: 28.11.2011

Table of content

1. Introduction

1.1 *Aspergillus fumigatus* and Aspergillosis

Over the last three decades life-threatening human fungal infections have increased due to advances in medical therapies such as solid-organ and hematopoietic stem cell transplantations, an increasing geriatric population, and HIV infections, which resulted in a significant rise in susceptible patients (McNeil *et al.*, 2001, Varkey & Perfect, 2008, Erjavec *et al.*, 2009). In the course of this development, the mold *Aspergillus fumigatus* has become the most prevalent airborne fungal pathogen (McCormick *et al.*, 2010). *A. fumigatus* is commonly found in soil and organic debris where it grows on dead or decaying matter recycling carbon and nitrogen (Millner *et al.*, 1977, Wilson *et al.*, 2002, Tekaia & Latge, 2005, Rhodes, 2006).

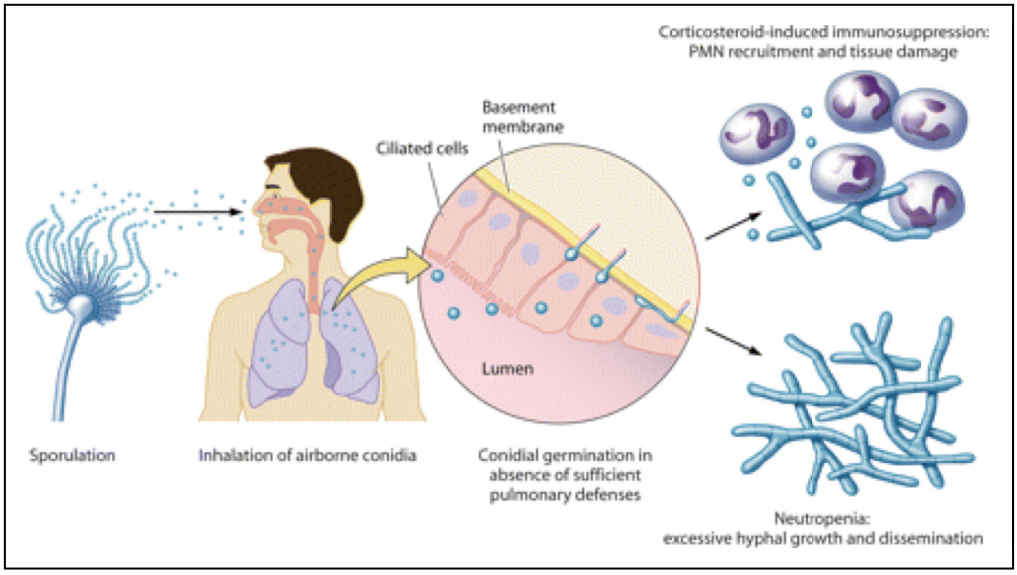

Figure 1: Infectious life cycle of *A. fumigatus*. *Aspergillus* is ubiquitous in the environment, and asexual reproduction leads to the production of airborne conidia. Inhalation by specific immunosuppressed patient groups results in conidium establishment in the lung, germination, and either PMN-mediated fungal control with significant inflammation (corticosteroid therapy) or uncontrolled hyphal growth with a lack of PMN infiltrates and, in severe cases, dissemination (neutropenia). (Dagenais and Keller, 2009)

Dissemination of *A. fumigatus* occurs through the release of small asexual conidia generated by a specialized structure, the conidiophore (Figure 1). Environmental reports indicate that several hundred *A. fumigatus* conidia are inhaled by humans each day (Chazalet *et al.*, 1998, Goodley *et al.*, 1994, Hospenthal *et al.*, 1998, Latge, 1999, Dagenais & Keller, 2009). With a size ranging from 2 to 3 µm, *A. fumigatus* conidia can infiltrate deep into the respiratory tract and reach the alveoli of the lung (Figure 1). In healthy individuals conidia are removed by the innate immune response where alveolar macrophages and neutrophils play a major role. Alveolar

macrophages engulf and kill *A. fumigatus* conidia as well as initiate a pro-inflammatory response that recruits neutrophils to the site of infection. Neutrophils are the second line of defense for the clearance of conidia and they are also able to target germlings and fungal hyphae (Segal *et al.*, 2010, Ibrahim-Granet *et al.*, 2010, Brakhage *et al.*, 2010). However, in patients with an impaired immune system *A. fumigatus* conidia can persist, form invasive hyphae, and cause disease (Figure 1).

A. fumigatus is responsible for a number of clinically relevant diseases with allergic bronchopulmonary aspergillosis (ABPA), Aspergilloma, and invasive pulmonary aspergillosis (IPA) the most prevalent. Patients suffering from asthma or cystic fibrosis can develop ABPA, a hypersensitive response to fungal antigens (Patterson & Strek, 2010, Antunes *et al.*, 2010, Moss, 2010, Riscili & Wood, 2009). Aspergilloma, which is sometimes also referred to as a “fungus ball”, describes a noninvasive *Aspergillus* infection that may occur in preexisting pulmonary cavities such as those that occur in tuberculosis patients (Riscili & Wood, 2009). IPA is the most lethal *Aspergillus*-related disease with mortality rates ranging from 30-90% depending on the patient population (Latge, 1999, Latge, 2001, Perfect *et al.*, 2001, Morgan *et al.*, 2005, Upton *et al.*, 2007, Dagenais & Keller, 2009, Baddley *et al.*, 2010). Patients most at risk for this life-threatening disease are those with acute leukemia, solid-organ and hematopoietic stem cell transplantations, as well as patients receiving prolonged corticosteroid treatment to prevent graft-versus-host disease or patients undergoing chemotherapy (Denning *et al.*, 1998, Patel & Paya, 1997, Ribaud *et al.*, 1999, Ribrag *et al.*, 1993, von Eiff *et al.*, 1994, Westney *et al.*, 1996, Marr *et al.*, 2002, Mikulska *et al.*, 2009, Post *et al.*, 2007, Bodey *et al.*, 1992, Latge, 1999, Dagenais & Keller, 2009). IPA is also a common infection in AIDS patients and individuals with genetic immunodeficiencies like chronic granulomatous disease (CGD) (Mylonakis *et al.*, 1998, Nash *et al.*, 1997, Denning *et al.*, 1998, Rex *et al.*, 1991, Latge, 1999).

When treating invasive fungal infections, early and appropriate antifungal therapy is essential for a successful outcome of disease. Three main classes of antifungal drugs are available to treat these infections: polyenes, azoles, and echinocandins. Polyenes like amphotericin B represent the oldest family of antifungal drugs and have a broad spectrum of activity (Chandrasekar, 2011). The biological activity of amphotericin B is mediated by binding to ergosterol, an essential component of the fungal cytoplasmic membrane, which results in increased membrane permeability, and ultimately, cell death (Chandrasekar, 2011). However,

amphotericin B usage is associated with significant nephrotoxicity and hepatotoxicity (Chandrasekar, 2011). The biologic activity of Echinocandins, the newest class of antifungal agents, is mediated by interference with fungal cell wall synthesis through inhibition of β-1,3-glucan synthesis, ultimately resulting in cell lysis (Chandrasekar, 2011). However, while echinocandins have a fungicidal effect on *Candida* spp., they only show static activity against *Aspergillus* spp. (Chandrasekar, 2011, Chen *et al.*, 2011). The antifungal class of triazoles is most commonly used in clinical practice with Voriconazole being the drug of choice for IPA treatment (Chandrasekar, 2011, Herbrecht *et al.*, 2002). Like Polyenes, azoles target the fungal cell membrane by inhibition of the ergosterol biosynthetic pathway (Chandrasekar, 2011).

However, over the last years in addition to the rising number of immunocompromised patients and increasing occurrence of fungal infections, emerging drug resistant *A. fumigatus* strains complicate successful treatment (Mayr & Lass-Florl, 2011, Snelders *et al.*, 2011). As treatment outcomes remain unacceptably poor, there is an urgent need for further extensive studies on *A. fumigatus* biology and aspergillosis pathogenesis to enrich our understanding of how this human fungal pathogen adapts to the mammalian host environment and causes disease. Consequently, new insights into *A. fumigatus* and aspergillosis pathogenesis will help identify potential new drug targets and other new therapeutic approaches to improve patient outcomes.

1.2 Hypoxia: An environmental stress faced *in vivo*

Once inhaled into the lower respiratory tract, *A. fumigatus* has to face, adapt, and respond to a number of *in vivo* microenvironmental challenges to cause disease. However, our understanding of the dynamic microenvironments encountered by the fungus in the mammalian lung, and the mechanisms by which it grows in these microenvironments, are poorly understood. Known *in vivo* environmental factors encountered by *A. fumigatus* during infection include: high temperature, changes in pH, oxidative stress, and a restricted nutrient supply. It was found that *A. fumigatus* possesses multi-faceted and robust mechanisms to overcome these challenges, which, in all probability, is based on the fact that these stresses are similar to those the mold has to overcome in its ecological niche, compost (Beffa *et al.*, 1998, Trautmann NM, 2003, van Heerden *et al.*, 2002, Rhodes, 2006, Cooney & Klein, 2008). As a member of the compost microflora, *A. fumigatus* also has to be able to

adapt to a wide range of oxygen levels, a characteristic that has largely been overlooked in the study of this pathogenic mold.

Oxygen concentrations in compost piles rapidly change with the metabolic activity of the microflora and range from atmospheric (21% at sea level) to hypoxic (1.5% and lower) (Wang W, 2007). Thus, organisms such as *A. fumigatus* that thrive in such environments likely have evolved mechanisms to tolerate hypoxia. Although *A. fumigatus* is considered an obligate aerobe, it has been observed to tolerate oxygen levels as low as 0.1% (Park *et al.*, 1992, Hall & Denning, 1994). In addition, studies have also suggested that *A. fumigatus* can grow in the complete absence of oxygen suggesting that it may actually be a facultative anaerobe (Tabak & Cooke, 1968).

In vivo, while it is unknown if *A. fumigatus* is exposed to hypoxic conditions, pathogens are often exposed to dynamic ranges of oxygen availability depending on their location in the mammalian body. In the alveoli of healthy lungs the oxygen levels are around 14%, substantially below atmospheric levels. Oxygen availability is also much lower in tissues with levels of 2-4% reported once oxygen reaches the capillaries and diffuses into surrounding tissues (Erecinska & Silver, 2001, Carlsson *et al.*, 2001, Studer *et al.*, 2000, West, 1984, Warn *et al.*, 2004). Inflammation, thrombosis, and necrosis associated with microbial infections are thought to decrease available oxygen concentrations even further. In addition, it has been described that hypoxic areas (oxygen levels ≤1%) due to decreased tissue perfusion occur in tumors and wounds (Matherne *et al.*, 1990, Van Belle *et al.*, 1987, Dewhirst, 1998, Arnold *et al.*, 1987, Simmen *et al.*, 1994, Nizet & Johnson, 2009).

While oxygen has not been directly measured at sites of *A. fumigatus* infections, lung histopathology shows significant host tissue damage caused by invasive fungal hyphae and subsequent host responses. These pathologic lesions most likely represent areas of poor oxygen availability to the pathogen and the host. Recent studies (Brock *et al.*, 2008, Ibrahim-Granet *et al.*, 2010) suggested that hypoxia may occur *in vivo* in the lung during *A. fumigatus* infections. A luciferase-producing *A. fumigatus* strain showed decreased luminescence after reaching a maximum intensity at day one post infection, despite an increase in fungal burden. The authors hypothesized that this observation may be due to severe tissue damage caused by the pulmonary lesions that decreased the oxygen availability in these lung areas. The lack of luminescence may be attributable to limited oxygen at the site of infection as oxygen is essential for the light-producing luciferase reaction. However, it

may also be possible that other unexplained mechanisms result in the decreased luminescence observed. Thus, whether hypoxia is an important component of the infection microenvironment during invasive pulmonary aspergillosis remains to be elucidated. Here, in this dissertation, I provide data that suggest hypoxia is an important component of invasive pulmonary aspergillosis pathophysiology.

1.3 Sensing changes in oxygen levels

To be able to respond and adapt to changes in oxygen tension, mechanisms for cellular oxygen sensing must be present. Different pathways involved in oxygen sensing and regulation of hypoxia adaptation have been identified in non-pathogenic and pathogenic fungi (Thiel *et al.*, 2005, Grahl & Cramer, 2010). To regulate the hypoxic gene response, the model organism *Saccharomyces cerevisiae* senses oxygen availability through cellular heme levels involving the transcriptional repressors of hypoxic genes Rox1p and Mot3p (Zhang & Hach, 1999, Hon *et al.*, 2003), and recent studies have suggested that cellular sterol levels are also used by *S. cerevisiae* to sense oxygen via the transcriptional regulators Upc2p and Ecm22p (Davies & Rine, 2006). Also in the human fungal pathogen *Candida albicans*, an Upc2p ortholog has been identified and shown to be activated in hypoxic conditions and in response to lowered sterol levels (Hoot *et al.*, 2008, Silver *et al.*, 2004, White & Silver, 2005, Synnott *et al.*, 2010). Upc2p null mutants display significant growth reductions in hypoxia and no longer filament, but Upc2p's link with pathogenesis is currently unknown.

An elegant model of oxygen sensing has been described in the fission yeast *Schizosaccharomyces pombe* whereby a transcriptional regulator in the sterol regulatory element binding protein family (SREBP) indirectly senses oxygen levels through monitoring cellular sterol levels (Hughes *et al.*, 2005, Todd *et al.*, 2006). SREBPs are conserved in a wide range of eukaryotes and are membrane bound transcription factors that sense oxygen dependent changes in sterol levels. In *S. pombe,* SREBP Sre1 was found to be a major regulator of the hypoxic response and essential for growth under these conditions (Hughes *et al.*, 2005, Bien & Espenshade, 2010, Todd *et al.*, 2006). Importantly, a functionally conserved SREBP pathway has been identified in the human fungal pathogen *Cryptococcus neoformans* (Chang *et al.*, 2007, Chun *et al.*, 2007, Bien *et al.*, 2009). The respective SREBP ortholog (Sre1) is required for growth in hypoxia and subsequently a null mutant of *sre1* is attenuated in virulence in murine models of cryptococcosis (Chang

et al., 2007, Chun *et al.*, 2007, Bien *et al.*, 2009). In addition, deletion of other components of the SREBP regulatory pathway in *C. neoformans* also resulted in hypoxia growth defects and attenuated virulence (Bien *et al.*, 2009, Chang *et al.*, 2009). Altogether, the data suggests an important role of the SREBP pathway in hypoxia adaptation and adaptation to host tissue microenvironments.

1.4 Hypoxia and *in vivo* energy metabolism

To colonize the host and cause disease, pathogens have to adapt their metabolism to be able to generate energy from available nutrients to support growth, development, and responses to external stresses. Most eukaryotes, like *A. fumigatus*, utilize aerobic or oxidative respiration, the most efficient pathway to produce chemical energy in the form of ATP. However, oxidative respiration is dependent on the presence of oxygen as the terminal electron acceptor. As oxygen limited microenvironments can occur during infection, pathogens must be able to activate alternative pathways to generate energy and support growth. In fact, respiratory flexibility, switching from aerobic respiration to various forms of anaerobic energy generating pathways with alternative electron acceptors has been implicated as an important virulence attribute in prokaryotic pathogens like e.g. *Mycobacterium tuberculosis* (Smith, 2003, Richardson, 2000, Shi *et al.*, 2005). However not much is known about how pathogenic fungi respond to low oxygen tensions. Recent transcriptional profiling studies of *C. albicans, C. neoformans*, and *A. fumigatus* found that hypoxia stimulates transcription of genes involved in glycolysis and fermentation, suggesting that these pathogens adapt to hypoxic conditions by switching to oxygen-independent energy producing pathways (Setiadi *et al.*, 2006, Synnott *et al.*, 2010, Chun *et al.*, 2007, Barker and Cramer personal communication). Interestingly, while genes of oxidative metabolism are repressed in *C. albicans* (Setiadi *et al.*, 2006, Synnott *et al.*, 2010), genes involved in oxidative respiration were increased in *C. neoformans*, indicating significant differences in hypoxia adaptation between these two fungal pathogens (Chun *et al.*, 2007). Furthermore, a *C. neoformans Agrobacterium tumefaciens* forward genetics approach identified a key role for fungal mitochondria in hypoxia adaptation (Ingavale *et al.*, 2008). However, it is unclear what the mechanisms are behind the respective mitochondrial mutant's inability to grow in hypoxia or whether this impacts *Cryptococcus* virulence.

Earlier work in the model yeast *S. cerevisiae* proposed that the fungal mitochondrial respiratory chain is involved in oxygen sensing, growth in hypoxia,

hypoxic signaling and hypoxic gene regulation through production of reactive oxygen and nitrogen species (Kwast *et al.*, 1999, David & Poyton, 2005, Castello *et al.*, 2006, Guzy *et al.*, 2007, Ingavale *et al.*, 2008, Poyton *et al.*, 2009a, Poyton *et al.*, 2009b). Furthermore, several studies have suggested that increased oxidative stress observed in hypoxia may act as a putative second messenger that activates redox-sensitive transcription factors to enable hypoxia adaptation though these transcription factors are undefined (Dirmeier *et al.*, 2002, Chandel & Budinger, 2007, Guzy *et al.*, 2007).

Taken together, these studies suggest that mitochondria, oxidative respiration, and energy metabolism flexibility might also play an important role in *Aspergillus* adaptation to and growth in oxygen limiting conditions. In this dissertation, I explore mechanisms by which *A. fumigatus* adapts to hypoxia.

1.5 Thesis

Data and observations from the above discussed studies led to the following overall thesis of this dissertation:

Hypoxia is a stress faced *in vivo* by *A. fumigatus* and the ability to sense, adapt to, and grow in hypoxic conditions is a virulence attribute of this human fungal pathogen.

The above overall thesis was sub-divided into the following sub-objectives:

1) To examine the involvement of the *A. fumigatus* sterol-regulatory element binding protein SrbA in oxygen-sensing, hypoxic adaptation, and fungal virulence.
2) To investigate the occurrence of *in vivo* hypoxic microenvironments during IPA and the role of ethanol fermentation for hypoxia adaptation and virulence of *A. fumigatus*.
3) To determine the importance of oxidative respiration as an energy producing pathway in hypoxia during *A. fumigatus* pathogenesis

2. Summary of Manuscripts

2.1 Manuscript I

Willger SD, Puttikamonkul S, Kim KH, Burritt JB, Grahl N, Metzler LJ, Barbuch R, Bard M, Lawrence CB, Cramer Jr. RA. (2008) A sterol-regulatory element binding protein is required for cell polarity, hypoxia adaptation, azole drug resistance, and virulence in *Aspergillus fumigatus*. PLoS Pathogens, 4(11) e1000200. doi:10.1371/journal.ppat.1000200.

Summary

The manuscript describes the characterization of the sterol-regulatory element binding protein (SREBP), SrbA, in *A. fumigatus*. It was shown that SrbA is essential for growth under hypoxic conditions and virulence of *A. fumigatus*. Furthermore, SrbA plays a critical role in ergosterol biosynthesis, triazole drug resistance, and cell polarity. Importantly, this study presents a new function for SREBP proteins in filamentous fungi, and strongly suggests that hypoxia adaptation is an important virulence attribute of pathogenic molds.

Author contribution

My contribution to this manuscript included murine virulence and histopathology studies, which were designed, conducted, and analyzed by Srisombat Puttikamonkul and me. In addition, I also designed, performed, and analyzed the macrophage killing assay and composed the corresponding text passages.

2.2 Manuscript II

Grahl N, and Cramer, RA. (2010) Regulation of hypoxia adaptation: An overlooked virulence attribute of pathogenic fungi? Medical Mycology, 22:1-16.

Summary

This manuscript is a review article focusing on the increasing evidence that pathogenic fungi have to adapt to rapidly changing oxygen levels during fungal infections. The review discusses in detail known oxygen-sensing mechanisms that non-pathogenic and pathogenic fungi utilize to adapt to hypoxic microenvironments and their possible relation to fungal virulence.

Author contribution

I undertook the literature search for this review article. I analyzed, described, and summarized the literature available and wrote the article in concert with Prof. Robert A. Cramer.

2.3 Manuscript III

Grahl N, Puttikamonkul S, Macdonald JM, Gamcsik MP, Ngo LY, Hohl MH, Cramer RA. (2011) *In vivo* hypoxia and a fungal alcohol dehydrogenase influence the pathogenesis of invasive pulmonary aspergillosis. PLoS Pathogens, 7(7): e1002145. doi:10.1371/journal.ppat.1002145.

Summary

This manuscript describes for the first time that hypoxic microenvironments occur at the site of *Aspergillus* infection during invasive disease. In addition, ethanol fermentation was shown to be utilized by *A. fumigatus* in hypoxia, but this pathway emerged to be not essential for growth under hypoxic conditions. However, it was found that a fungal alcohol dehydrogenase influences fungal pathogenesis in the lung as loss of this gene resulted in a significant increase of neutrophils to the site of infection. Altogether, the results in this manuscript suggest that fungal metabolism changes due to dynamic *in vivo* environmental conditions influence host-pathogen interactions.

Author contribution

All experiments were conceived, designed, and performed by me, in concert with Prof. Robert A. Cramer, with the exception of the ^{1}H-NMR metabolite profiling of broncheoalveolar lavage fluids which was done by Jeffrey M. Macdonald and Michael P. Gamcsik, the *in vitro* cytokine experiment with bone marrow derived macrophages which was done by Lisa Y. Ngo and Tobias M. Hohl, and the GCMS analysis of culture supernatants was done by the Montana State University Proteomics Core Facility. I wrote the article with Prof. Robert A. Cramer.

2.4 Manuscript IV

Grahl N, Magnani Dinamarco T, Willger SD, Goldman GH, Cramer RA. (Submitted) *Aspergillus fumigatus* mitochondrial electron transport chain mediates oxidative stress homeostasis, hypoxia responses, and fungal pathogenesis (submitted to Molecular Microbiology).

Summary

In this study it was shown that the main cytochrome respiratory pathway is important for germination and growth in normoxic and hypoxic conditions of *A. fumigatus*. The conventional electron transport chain and the alternative oxidase were also found to be involved in susceptibility or resistance to oxidative stress and macrophage killing respectively. In addition, a possible connection between the fungal electron transport chain and hypoxic activation of ethanol fermentation was demonstrated and, for the first time, it was shown that the respiration chain plays an important role for *A. fumigatus* pathogenesis.

Author contribution

All experiments were conceived, designed, and performed by me, in concert with Prof. Robert A. Cramer, with the exception of oxygen consumption experiments and the protein oxidation detection that were done by Taisa Magnani Dinamarco and Prof. Gustavo H. Goldman. I wrote the article with Prof. Robert A. Cramer.

OPEN ACCESS Freely available online

PLoS PATHOGENS

A Sterol-Regulatory Element Binding Protein Is Required for Cell Polarity, Hypoxia Adaptation, Azole Drug Resistance, and Virulence in *Aspergillus fumigatus*

Sven D. Willger[1], Srisombat Puttikamonkul[1], Kwang-Hyung Kim[2], James B. Burritt[3], Nora Grahl[1], Laurel J. Metzler[4], Robert Barbuch[4], Martin Bard[4], Christopher B. Lawrence[2], Robert A. Cramer Jr.[1]*

1 Department of Veterinary Molecular Biology, Montana State University, Bozeman, Montana, United States of America, **2** Virginia Bioinformatics Institute, Virginia Polytechnic Institute and State University, Blacksburg, Virginia, United States of America, **3** Department of Microbiology, Montana State University, Bozeman, Montana, United States of America, **4** Department of Biology, Indiana University-Purdue University, Indianapolis, Indiana, United States of America

Abstract

At the site of microbial infections, the significant influx of immune effector cells and the necrosis of tissue by the invading pathogen generate hypoxic microenvironments in which both the pathogen and host cells must survive. Currently, whether hypoxia adaptation is an important virulence attribute of opportunistic pathogenic molds is unknown. Here we report the characterization of a sterol-regulatory element binding protein, SrbA, in the opportunistic pathogenic mold, *Aspergillus fumigatus*. Loss of SrbA results in a mutant strain of the fungus that is incapable of growth in a hypoxic environment and consequently incapable of causing disease in two distinct murine models of invasive pulmonary aspergillosis (IPA). Transcriptional profiling revealed 87 genes that are affected by loss of SrbA function. Annotation of these genes implicated SrbA in maintaining sterol biosynthesis and hyphal morphology. Further examination of the SrbA null mutant consequently revealed that SrbA plays a critical role in ergosterol biosynthesis, resistance to the azole class of antifungal drugs, and in maintenance of cell polarity in *A. fumigatus*. Significantly, the SrbA null mutant was highly susceptible to fluconazole and voriconazole. Thus, these findings present a new function of SREBP proteins in filamentous fungi, and demonstrate for the first time that hypoxia adaptation is likely an important virulence attribute of pathogenic molds.

Citation: Willger SD, Puttikamonkul S, Kim K-H, Burritt JB, Grahl N, et al. (2008) A Sterol-Regulatory Element Binding Protein Is Required for Cell Polarity, Hypoxia Adaptation, Azole Drug Resistance, and Virulence in *Aspergillus fumigatus*. PLoS Pathog 4(11): e1000200. doi:10.1371/journal.ppat.1000200

Editor: Scott G. Filler, David Geffen School of Medicine at University of California Los Angeles, United States of America

Received July 29, 2008; **Accepted** October 9, 2008; **Published** November 7, 2008

Copyright: © 2008 Willger et al. This is an open-access article distributed under the terms of the Creative Commons Attribution License, which permits unrestricted use, distribution, and reproduction in any medium, provided the original author and source are credited.

Funding: RAC is currently supported by funding from the National Institutes of Health, COBRE grant RR020185, and the Montana State University Agricultural Experiment Station. M.B. acknowledges the support of NIH grant GM62104.

Competing Interests: The authors have declared that no competing interests exist.

* E-mail: rcramer@montana.edu

Introduction

Aspergillus fumigatus is a normally benign saprophytic fungus that may cause an often lethal invasive disease in immunocompromised patients, invasive pulmonary aspergillosis (IPA) [1,2]. Interestingly, while IPA can be caused by several *Aspergillus* species, the majority of IPA cases are caused by *A. fumigatus*. This may suggest that *A. fumigatus* contains unique attributes that allow it to cause disease [3]. Yet, the mechanisms utilized by *A. fumigatus* to survive and cause disease in immunocompromised hosts are not fully understood [4]. During infection, *A. fumigatus* causes significant damage to host tissue through invasive growth by hyphae and subsequent recruitment of immune effector cells. Thus, infection generates significant inflammation and necrosis in lung tissue that can be visualized by histopathology. These pathologic lesions also likely represent areas of poor oxygen availability to the pathogen and host.

At sites of *Aspergillus* infection, direct measurements of oxygen tension have not been recorded, however, it is well established that sites of inflammation contain significantly low levels of oxygen (hypoxia) [5–7]. Moreover, low oxygen tension has been observed in many compartments of inflamed as well as normal tissues [5–7]. In inflamed tissues, the blood supply is often interrupted because the vessels are congested with phagocytes [8,9]. Indeed, immune effector cells such as neutrophils often function effectively in severely hypoxic microenvironments and have evolved distinct mechanisms to deal with the absence of oxygen that are dependent upon the transcription factor hypoxia inducible factor (HIF) 1.

HIF1 is a heterodimeric transcription factor that consists of a constitutively expressed HIF1β subunit and an oxygen-tension-regulated HIF1α subunit. [10]. Increased HIF1α protein stability and activity of the HIF1 complex, in turn, regulate the transcription of many hypoxia-responsive genes, including those encoding many glycolytic enzymes, erythropoietin, adrenomedullin, and growth factors [11,12]. Genetic evidence of the importance of hypoxic environments in the regulation of immune responses was recently provided by a study of neutrophil-mediated lung inflammation [13]. Thus, since immune cells of the host have evolved mechanisms to function in hypoxia, it follows that invasive fungal pathogens like *A. fumigatus* are likely subjected to hypoxia during fungal pathogenesis.

While hypoxic adaptation has not been studied in the context of *A. fumigatus* pathogenesis, circumstantial evidence suggests that hypoxia plays a key role in the pathophysiology of IPA. For example, it has been postulated that the low rate of *Aspergillus* recovery from clinical specimens is due to adaptation by the fungus to hypoxic microenvironments found at sites of infection

Author Summary

The incidence of potentially lethal infections caused by normally benign molds has increased tremendously over the last two decades. One disease in particular, invasive pulmonary aspergillosis (IPA), caused by the common mold *Aspergillus fumigatus*, has become the leading cause of death due to invasive mycoses. Currently, we have a limited understanding of how this opportunistic pathogen causes disease in immunocompromised patients. In this study, we discover a previously unexplored mechanism required by this mold to cause disease, hypoxia (low oxygen) adaptation. We report that hypoxia adaptation in *A. fumigatus* is mediated in part by a highly conserved transcription factor, SrbA, a protein in the sterol regulatory element binding protein family. A null mutant of SrbA was unable to grow in hypoxia, displayed increased susceptibility to the azole class of antifungal drugs, and was avirulent in two distinct murine models of IPA. Importantly, we report the discovery of a novel function of SrbA in molds related to maintenance of cell polarity. The finding that SrbA regulates resistance to the azole class of antifungal drugs presents an opportunity to uncover new mechanisms of antifungal drug resistance in *A. fumigatus*.

[14,15]. Furthermore, there are often significant differences in the *in vivo* and *in vitro* test results of antifungal drug efficacies. These differences have been postulated to be linked to the occurrence of hypoxia *in vivo* as demonstrated by recent *in vitro* antifungal drug efficacy tests conducted in hypoxia [16,17]. Consequently, it seems probable that pathogenic molds such as *A. fumigatus* must possess mechanisms to adapt to hypoxic microenvironments found *in vivo* during infection.

In fact, switching from aerobic respiration to various forms of anaerobic respiration to deal with low oxygen levels has been implicated as an important virulence attribute in several prokaryotic pathogens [18,19]. However, in eukaryotic pathogens, mechanisms of how these organisms respond and adapt to hypoxia are largely unknown. Most of our knowledge on how fungi respond to hypoxia comes from studies in the model yeast *Saccharomyces cerevisiae*. Under aerobic conditions, heme biosynthesis activates the transcriptional regulator Hap1p [20]. Hap1p induces genes involved in respiration and oxidative stress-responses, but also activates the transcriptional repressors Rox1p and Mot3p, that down-regulate genes required for hypoxia adaptation [21]. However, in hypoxic conditions, Rox1p and Mot3p are expressed and this leads to transcriptional induction of genes involved in hypoxia adaptation [22]. Thus, hypoxic gene expression in yeast requires transcription factors that utilize Rox1p-binding sequences, low oxygen-response elements (LORE), and other regulatory elements within promoters [23,24]. Since *S. cerevisiae* is a facultative anaerobe, it is not surprising that homologs of these key hypoxia gene regulators have not been found in obligate aerobic filamentous fungi such as *A. fumigatus*.

Recently, a novel mechanism of hypoxia adaptation mediated by a highly conserved family of transcription factors, sterol regulatory element-binding proteins (SREBPs), was characterized in fission yeast, *Schizosaccharomyces pombe* [25]. SREBPs are a unique family of membrane bound transcription factors first identified in mammals as regulators of cholesterol and lipid metabolism [26–30]. Hughes et al. [25] proposed a model in *S. pombe* where SREBP (Sre1) and a sterol cleavage activating protein (SCAP, Scp1) monitor-oxygen dependent sterol synthesis as an indirect measure of oxygen supply. Importantly, Sre1 was found to be required for adaptation to hypoxia and regulated approximately 68% of the genes transcriptionally induced greater than 2-fold in response to anaerobic conditions [31].

Orthologs of Sre1 and Scp1 were recently identified and characterized in the human fungal pathogenic yeast, *Cryptococcus neoformans* [32,33]. As in fission yeast, the SREBP pathway mediated by Sre1 and Scp1 in *C. neoformans* was crucial for adaptation to hypoxia and sterol biosynthesis. Importantly, these mutants also failed to proliferate in host tissue, failed to cause fatal meningoencephalitis, and displayed hypersensitivity to the azole class of antifungal drugs [32,33]. In the yeast *S. cerevisiae and Candida albicans*, orthologs of SREBPs do not appear to exist. However, two similar genes, *Upc2 and Ecm22*, appear to serve similar functions as SREBPs. Conserved functions of these genes include their involvement in the ability of yeast to grow in hypoxia as well as regulation of sterol biosynthesis and resistance to antifungal drugs [34–40]. Taken together, these observations demonstrate an important link between sterol biosynthesis, hypoxia adaptation, azole drug resistance, and the virulence of pathogenic yeasts.

In this study, we report the identification and first characterization of a Sre1 homolog, SrbA, in an opportunistic pathogenic mold, *A. fumigatus*. Our results suggest that while certain aspects of SREBP function are conserved in yeast and filamentous fungi, significant differences exist that are unique to molds. Thus, our results further expand the spectrum of important functions mediated by SREBPs in eukaryotes, emphasize the importance of this pathway in human fungal pathogenesis, and suggest possible clinical significance of SREBPs related to antifungal drug efficacy.

Results

Identification of *srbA* in *Aspergillus fumigatus*

In order to determine if hypoxia adaptation is an important virulence attribute of filamentous fungi, we first conducted transcriptional profiling experiments using a long-oligo *A. fumigatus* microarray (version 3.0) of wild type *A. fumigatus* grown under hypoxic (1% O_2) conditions compared to fungus grown under normal conditions (~21% O_2). Analysis of this data revealed ten putative transcription factors that were transcriptionally induced more than 2-fold in response to hypoxia and thus could possibly act as a regulators of genes required for hypoxic adaptation in *A. fumigatus* (Willger and Cramer, unpublished data). Further bioinformatic analyses of these genes revealed that only one, AFUA_2g01260 (induced 5.02 fold in response to hypoxia), had similarity with a functionally characterized protein, Sre1 from *S. pombe* [25]. Sre1 shares similarity with mammalian SREBP proteins that regulate lipid and cholesterol homeostasis (reviewed in [29,30]). In addition, a Sre1 homolog has also recently been described in the human pathogenic yeast, *C. neoformans* as a regulator of hypoxia adaptation and fungal virulence [32,33]. AFUA_2g01260 contains 988 amino acid residues, which displayed low sequence percent identity with Sre1 from *S. pombe* (~13%) and *C. neoformans* (~10%). However, like Sre1 in both yeasts, the amino terminus (amino acids 1–425) of AFUA_2g01260 contains a basic helix-loop-helix (bHLH) leucine zipper DNA binding domain. In addition, AFUA_2g01260 is predicted to contain at least one, and likely two, transmembrane domains. The carboxyl terminus of AFUA_2g01260 is also predicted to contain a conserved domain of unknown function (DUF2014) that is found in other SREBP homologs. Consequently, these results suggest that AFUA_2g01260 is likely the SREBP homolog in *A. fumigatus*, and we consequently named this gene *srbA*

(*sreA* is already in use in *A. nidulans* for an unrelated gene). Additional BLAST analyses revealed that SrbA is highly conserved amongst the filamentous fungi with putative orthologs found in plant pathogens such as *Magnaporthe grisea and Alternaria brassicicola* and saprophytic molds such as *Neurospora crassa* and *Aspergillus nidulans*.

SrbA is required for hypoxia adaptation in *Aspergillus fumigatus*

To determine whether SrbA is involved in hypoxia adaptation and fungal virulence in filamentous fungi, we generated a null mutant of the gene encoding SrbA by replacement of the *srbA* coding sequence in *A. fumigatus* strain CEA17 with the auxotrophic marker *pyrG* from *A. parasiticus* as previously described [41,42] (Figure 1). The resulting *ΔsrbA* strain was named SDW1. Ectopic re-introduction of the wild type *srbA* allele into SDW1 (resulting in strain SDW2) allowed us to attribute all resulting phenotypes specifically to the absence of *srbA* in SDW1. All strains were rigorously confirmed with Southern blot (Figure 1) and PCR analyses (data not shown). The re-introduced *srbA* allele in SDW2 displayed similar mRNA abundance in response to hypoxia as the *srbA* allele in the wild type strain (data not shown). SDW1 and SDW2 both displayed normal hyphal growth rates compared to the wild type strain CEA10 in normoxic conditions on glucose minimal medium (GMM) (Figure 2A) ($P>0.01$). However, no hyphal growth of SDW1 was observed in hypoxic (1% O_2, 5% CO_2, 94% N_2) conditions whereas wild type strain CEA10 and reconstituted strain SDW2 grew at a normal rate with visual phenotypic differences in colony color and conidiation compared to growth in normoxia (Figure 2A and 2B). In hypoxia, the wild type strains displayed increased aerial hyphae, decreased conidia production, and consequently exhibited a fluffy colony morphology (Figure 2B). After 96 hours of incubation in hypoxia, SDW1 continued to display undetectable growth. However, upon transfer back to normoxic conditions, wild type growth rate was restored (data not shown). Addition of exogenous ergosterol or lanosterol did not rescue the SDW1 growth defect or alter wild type growth morphology in hypoxia (data not shown). These results indicate that *A. fumigatus* can rapidly adapt to hypoxic microenvironments, and that SrbA in *A. fumigatus* is involved in mediating this response by an undefined mechanism.

Transcriptional profiling of SDW1 in response to hypoxia

Given the dramatic phenotype observed in strain SDW1 in hypoxia and the sequence annotation that SrbA likely functions as a transcription factor, we next sought to determine which genes are regulated by SrbA under hypoxic conditions. Microarray experiments comparing the transcriptional profiles of wild type strain CEA10 and SDW1 exposed to hypoxia for 24 hours revealed 87 significant genes possibly regulated by SrbA (Table 1). Several genes previously shown to be involved in ergosterol biosynthesis in fungi were found to be transcriptionally repressed in the absence of SrbA including *ERG25*, *ERG24*, and *ERG3* (Table 1). Interestingly, besides *srbA* itself, the gene with the highest fold difference in expression in SDW1 is a non-ribosomal peptide synthetase, AFUA_1g10380 (NRPS1 or *pes1*) [43,44]. In addition, a significant number of genes involved in cell wall biosynthesis or homeostasis were observed to be repressed in SDW1 compared to wild type. These included genes known to be involved in cell wall biosynthesis such as alpha-galactosidase, alpha-glucosidase B, and genes involved in cell wall homeostasis such as chitinase. However, no obvious defects in cell wall biosynthesis were observed in the

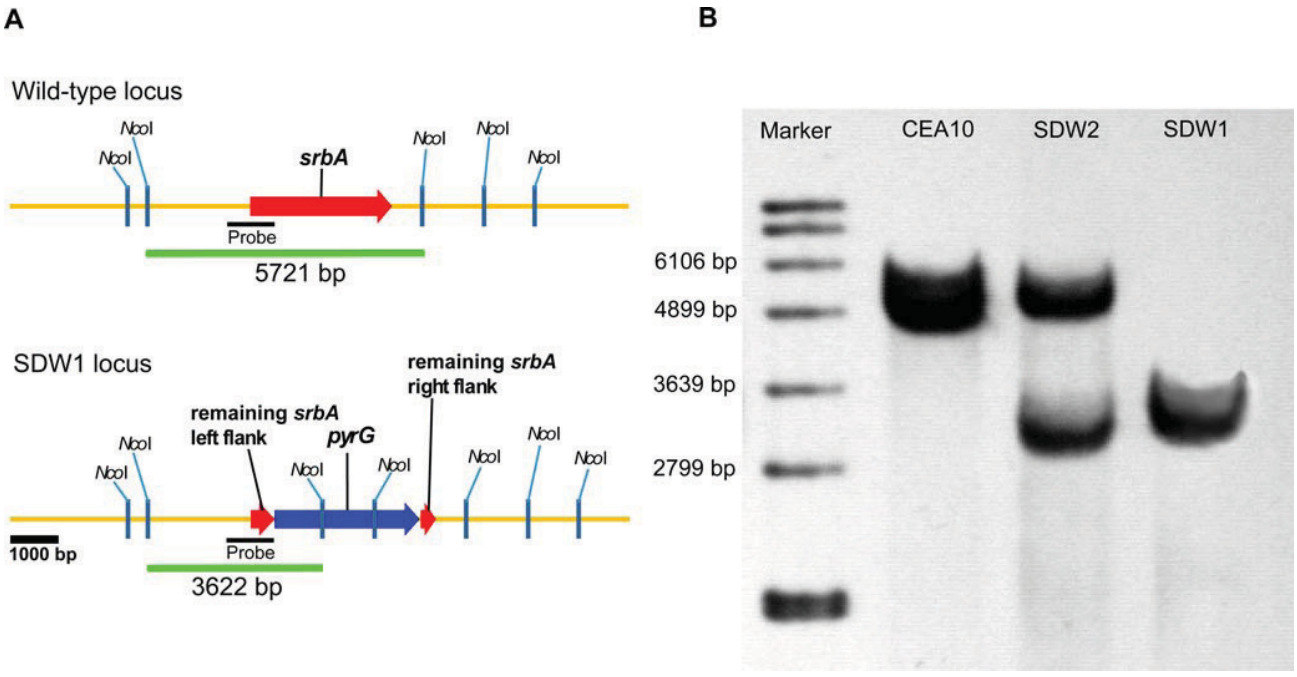

Figure 1. Generation and confirmation of a SrbA null mutant in *Aspergillus fumigatus*. (A) Schematic of wild type (CEA10) and SDW1 (SrbA null mutant) genomic loci. (B) Southern blot analysis of wild type, SDW1, and SDW2 strains. Genomic DNA from the respective strains was isolated and digested overnight with *Nco*I. An approximate 1 kb genomic region of the SrbA locus was utilized as a probe. The expected hybridization patterns and sizes were observed for the wild type CEA10 (5721 bp) and SrbA mutant (SDW1) (3622 bp) strains. In addition, confirmation of ectopic reconstitution of the SrbA null mutant was confirmed by the presence of the wild type *srbA* locus hybridization signal and persistence of the SrbA null mutant locus (strain SDW2).
doi:10.1371/journal.ppat.1000200.g001

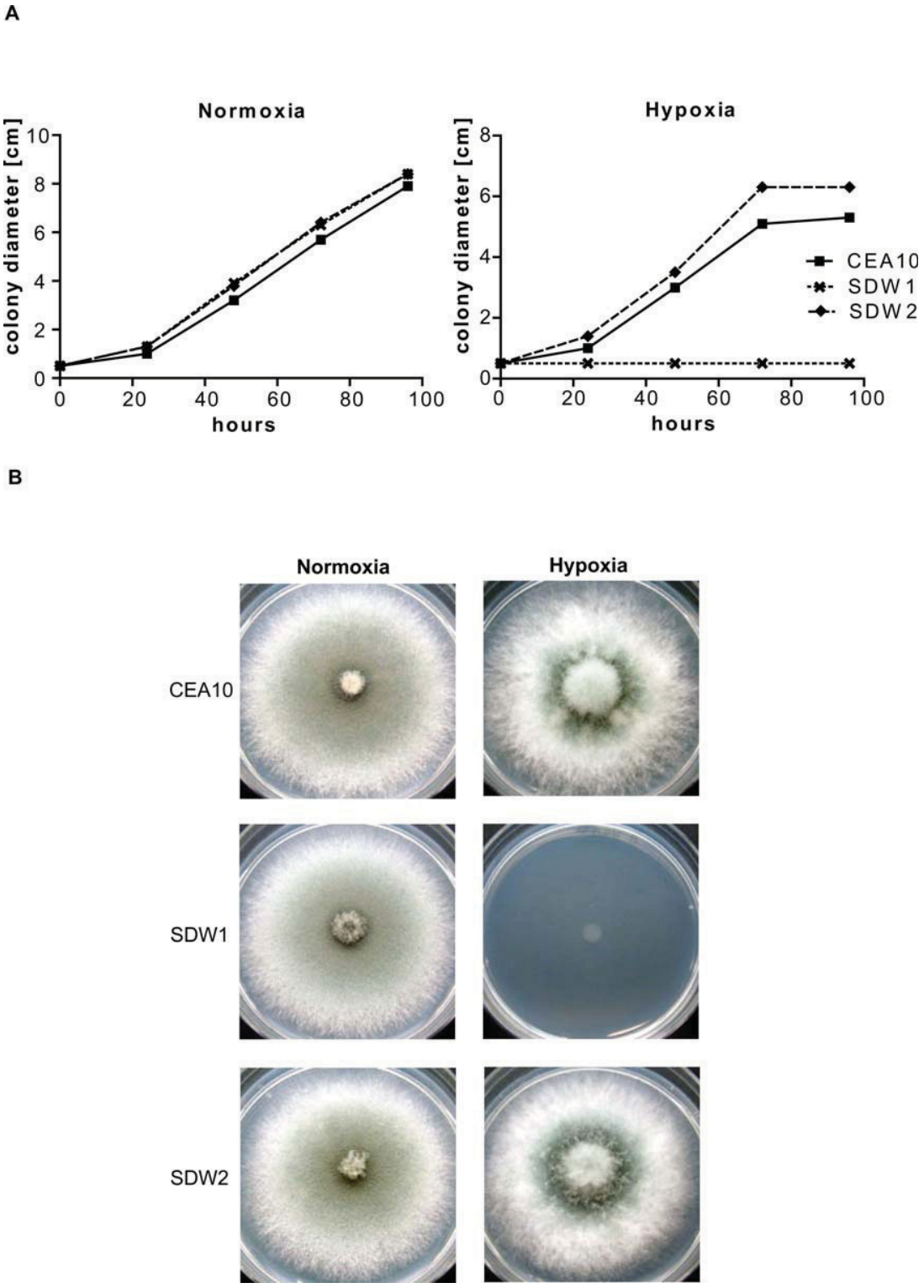

Figure 2. SrbA is required for hyphal growth under hypoxic conditions. 1×10^6 conidia of CEA10, SDW1 = *ΔsrbA*, SDW2 = *ΔsrbA+srbA* were plated on GMM plates and incubated at 37°C under normoxic and hypoxic conditions. (A) The diameter of the colony was measured over 96 h every 24 h. Under normoxic conditions no significant difference in growth speed and colony size or morphology could be observed ($P>0.01$). (B) Under hypoxic conditions the wild type CEA10 and the reconstituted strain SDW2 showed comparable growth ($P>0.01$) but the mutant strain SDW1 did not demonstrate any detectable growth. Error bars represent standard error from the triplicate experiments.
doi:10.1371/journal.ppat.1000200.g002

Table 1. Genes with higher expression in wild type than in the *srbA* null mutant in hypoxia.

TRANSPORTERS		
AFUA_4g01560	MFS myo-inositol transporter, putative	15.77
AFUA_1g10390	ABC multidrug transporter, putative	15.64
AFUA_3g01670	MFS hexose transporter, putative	14.12
AFUA_2g09450	carboxylic acid transport protein	12.18
AFUA_3g14170	high-affinity hexose transporter	11.31
AFUA_5g06720	MFS sugar transporter, putative	11.04
AFUA_7g06120	transmembrane transporter, putative	10.80
AFUA_3g12720	sugar transporter-like protein	9.08
AFUA_1g13350	transporter, putative	7.65
TRANSCRIPTION REGULATION		
AFUA_2g01260	HLH transcription factor, putative (srbA)	38.59
AFUA_3g12910	MmcR, putative	10.49
AFUA_8g00200	CalO6, putative	8.05
AFUA_2g07900	APSES transcription factor (StuA), putative	7.79
AFUA_1g16590	C2H2 transcription factor (BrlA), putative	7.14
AFUA_8g05460	bZIP transcription factor, putative	6.09
STEROL BIOSYNTHESIS		
AFUA_8g02440	c-4 methyl sterol oxidase (ERG25)	15.79
AFUA_2g00320	sterol delta 5,6-desaturase (ERG3)	13.57
AFUA_1g03150	c-14 sterol reductase (ERG24)	11.98
OXIDATIVE STRESS RESPONSE		
AFUA_1g10380	nonribosomal peptide synthase (NRPS), putative	23.36
AFUA_7g05070	FAD dependent oxidoreductase, putative	13.68
AFUA_5g08830	HEX1	10.66
AFUA_4g08710	short chain dehydrogenase, putative	9.82
AFUA_3g02270	mycelial catalase Cat1	9.15
AFUA_4g14530	theta class glutathione S-transferase	8.45
AFUA_3g01580	GMC oxidoreductase	6.56
AFUA_1g03250	oxidoreductase, short chain dehydrogenase/ reductase family, putative	6.25
CELL WALL RELATED		
AFUA_3g08110	cell wall protein, putative	21.29
AFUA_5g14740	fucose-specific lectin	15.00
AFUA_6g00430	IgE-binding protein	12.65
AFUA_5g00840	integral membrane protein	12.21
AFUA_5g03760	class III chitinase ChiA1	7.68
AFUA_4g09600	GPI anchored protein, putative	6.32
AFUA_2g05340	1,3-beta-glucanosyltransferase, putative	6.29
AFUA_1g05790	GPI anchored protein, putative	6.20
AFUA_5g07190	beta-glucosidase	6.04
SECONDARY METABOLISM		
AFUA_8g01220	arthrofactin synthetase B	8.38
AFUA_2g17600	polyketide synthetase PksP	6.40
OTHER METABOLIC PROCESSES		
AFUA_3g00810	cholestenol delta-isomerase, putative	18.48
AFUA_7g04930	alkaline serine protease (PR1), putative	13.09
AFUA_5g02130	alpha-galactosidase	12.92
AFUA_8g00190	cytochrome P450, putative	11.40
AFUA_1g16250	alpha-glucosidase B	9.95
AFUA_3g12960	cytochrome P450, putative	8.97
AFUA_3g07030	glutaminase A	8.24
AFUA_8g00620	dimethylallyl tryptophan synthase, putative	7.65
AFUA_4g09980	cytochrome P450 monooxygenase, putative	7.15
OTHER AND UNKNOWN GENES		
AFUA_6g03680	hypothetical protein	13.55
AFUA_3g07870	conserved hypothetical protein	13.23
AFUA_8g04380	conserved hypothetical protein	12.96
AFUA_8g00710	antimicrobial peptide, putative	12.92
AFUA_3g13110	hypothetical protein	12.88
AFUA_7g01930	ESDC	12.14
AFUA_4g08400	hypothetical protein	11.16
AFUA_6g01870	hypothetical protein	10.71
AFUA_4g14060	conserved hypothetical protein	10.60
AFUA_6g12180	conserved hypothetical protein	10.20
AFUA_6g13980	prenyltransferase, putative	10.04
AFUA_2g00500	conserved hypothetical protein	9.61
AFUA_8g04310	conserved hypothetical protein	9.26
AFUA_1g02290	conserved hypothetical protein	9.13
AFUA_7g05450	SUN domain protein (Uth1), putative	9.02
AFUA_2g15200	conserved hypothetical protein	8.86
AFUA_7g04870	hypothetical protein	8.71
AFUA_5g00700	hypothetical protein	8.69
AFUA_3g07730	hypothetical protein	8.65
AFUA_4g12700	hypothetical protein	8.60
AFUA_5g14920	hypothetical protein	8.59
AFUA_3g07340	hypothetical protein	8.53
AFUA_7g04120	DUF636 domain protein	8.23
AFUA_1g14340	metalloreductase, putative	8.01
AFUA_3g08210	hypothetical protein	7.95
AFUA_5g14680	hypothetical protein	7.80
AFUA_6g11890	dynamin GTPase, putative	7.72
AFUA_2g09030	secreted dipeptidyl peptidase	7.70
AFUA_4g13630	hypothetical protein	7.51
AFUA_2g09680	PB1 domain protein, putative	7.09
AFUA_7g04740	hypothetical protein	6.84
AFUA_3g12230	hypothetical protein	6.81
AFUA_5g02330	major allergen Asp F1	6.81
AFUA_6g14340	related to berberine bridge enzyme (imported)	6.64
AFUA_2g17550	yellowish-green 1	6.56
AFUA_8g04620	hypothetical protein	6.37
AFUA_4g14040	Hsp70 family protein	6.30
AFUA_5g14410	cysteine dioxygenase	6.30
AFUA_2g08820	hypothetical protein	6.24
AFUA_1g13610	SH3 domain protein	5.97
AFUA_4g14050	hypothetical protein	5.73

doi:10.1371/journal.ppat.1000200.t001

mutant strain, and thus the transcriptional profiling results are likely indirect effects of the altered cell polarity of the mutant (discussed below). Genes encoding several transporters were also found to be regulated by SrbA. Overall, these results suggest some similarities, such as with regard to ergosterol biosynthesis, with

genes regulated by SREBPs in *S. pombe* and *C. neoformans*. However, the overall set of genes putatively regulated by SrbA in *A. fumigatus* is significantly different from data obtained from Sre1 mutants in the yeast *S. pombe and C. neoformans*. Consequently, these results strongly suggest that SrbA plays a distinct role in filamentous fungal biology. These results subsequently directed experiments to further characterize the role of SrbA in *A. fumigatus* biology.

SrbA mediates resistance to the azole class of antifungal drugs

Given the number of ergosterol biosynthesis genes apparently regulated by SrbA, we next asked the question whether SrbA mediated resistance to the azole class of antifungal drugs that target ergosterol biosynthesis. In a screen for susceptibility to antifungal drugs using E-Test strips (AB Biodisk, kindly provided by Dr. Theodore White, Seattle Biomedical Research Institute) we found that SrbA is required for resistance to Fluconazole and Voriconazole, but not Amphotericin B or Caspofungin. All 3 strains showed equivalent minimal inhibitory concentrations (MIC) to Amphotericin B (0.25 μg/ml) and Caspofungin (0.125 μg/ml). The lack of effect of Caspofungin provides support for our hypothesis that the mutant is likely not directly affected in cell wall biosynthesis as possibly suggested by the transcriptional profiling data. However, while CEA10 and SDW2 showed resistance to Fluconazole as expected, SDW1 growth was inhibited at the surprisingly low MIC of 1 μg/ml (Figure 3). On the plates with Voriconazole we could observe that CEA10 and SDW2 were susceptible as expected (MIC of 0.125 μg/ml respectively). Similar to the results with Fluconazole, SDW1 was significantly more susceptible to Voriconazole and showed a MIC of only 0.012 μg/ml (Figure 3). These clinically significant results suggest that SrbA mediates resistance to the azole class of antifungal drugs by an undefined mechanism.

SrbA is required for cell polarity and hyphal morphogenesis

Visual inspection of SDW1 colony morphology in standard laboratory conditions did not reveal any apparent morphological phenotypes (Figure 2B). However, our transcriptional profiling experiments suggested possible alterations in cell wall biosynthesis, a critical component of hyphal morphology and growth, in the absence of SrbA. Consequently, we performed a more in depth analysis of SDW1 morphology. First, we utilized light microscopy to examine the growing edges of SDW1 colonies in normoxia. We observed a significant defect in hyphal tip branching in SDW1 that is not apparent in strains CEA10 and SDW2 (Figure 4). SDW1 hyphal tips display hyper-branching and a "blunted" abnormal morphological phenotype (Figure 4). This phenotype suggests that SrbA is involved in maintaining cell polarity that directs hyphal growth. Interestingly, this phenotype does not appear to alter the growth rate of the colony, which was comparable to the wild type under normoxic conditions (Figure 2A). Next, we utilized transmission electron microscopy (TEM) to further examine the cell wall and morphology of conidia and hyphae of SDW1. Confirming our suspicions that the mutant was not directly affected in cell wall biosynthesis we observed no clear cell wall

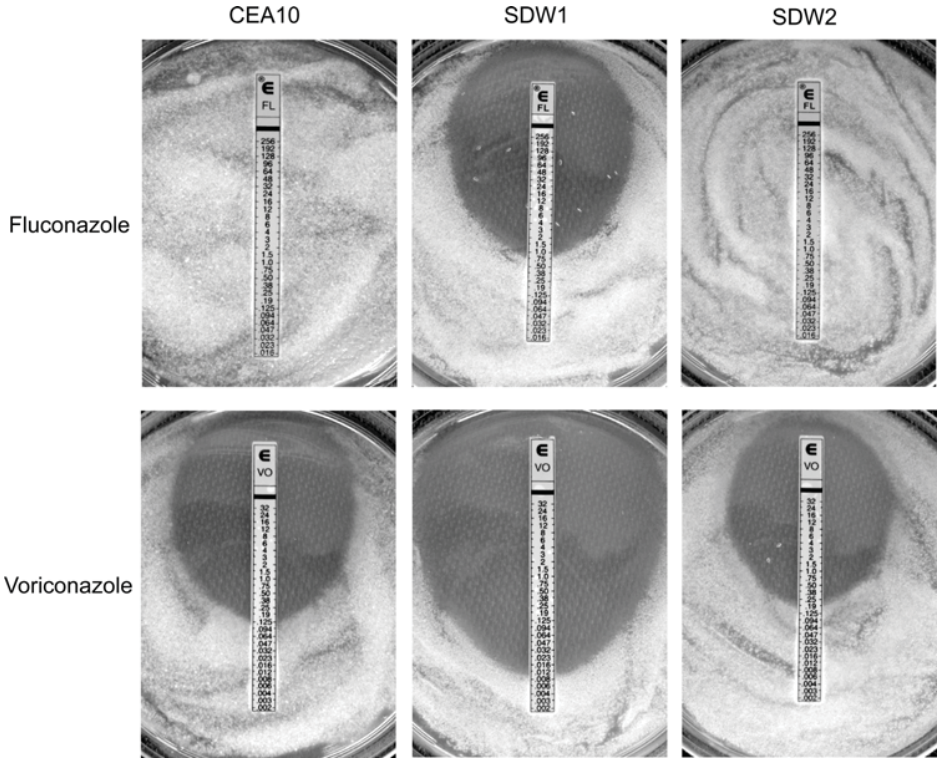

Figure 3. SrbA mediates resistance to Fluconazole (FL) and Voriconazole (VO) in *Aspergillus fumigatus*. A clear ellipse indicates the susceptibility to the respective drug. As expected, Fluconazole has no effect on CEA10 and SDW2, but in the absence of SrbA, SDW1 is highly susceptible to Fluconazole (MIC = 1.0 μg/ml). CEA10 and SDW2 are susceptible to Voriconazole (MIC for both = 0.125 μg/ml); however, SDW1 also displays increased susceptibility (MIC = 0.012 μg/ml) to this important antifungal agent. The numbers on the scale correspond to the Fluconazole and Voriconazole concentrations on the E-test strip (in micrograms per milliliter).
doi:10.1371/journal.ppat.1000200.g003

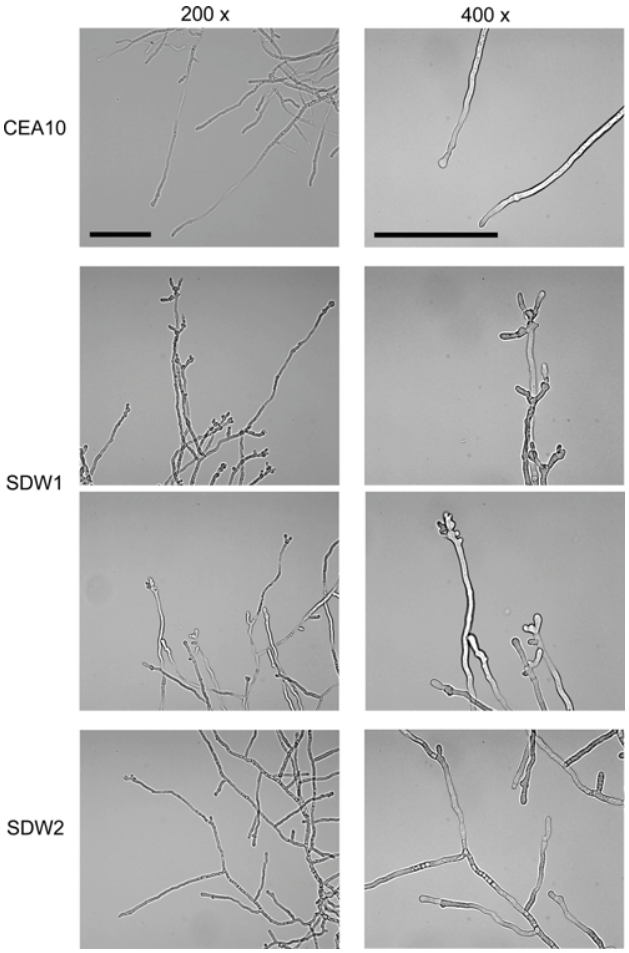

Figure 4. Hyphal morphology and growth of wild type strain CEA10 and SrbA null mutant SDW1. Strains were grown overnight on slides coated with GMM. Brightfield microscopy pictures of wild type CEA10 and SDW1 at 200-fold and 400-fold magnification. SDW1 showed abnormal hyphal formation and apparent cell polarity defect with multiple branches and unusual thick structures at the apical tips of the hyphae. Bars = 100 μm.
doi:10.1371/journal.ppat.1000200.g004

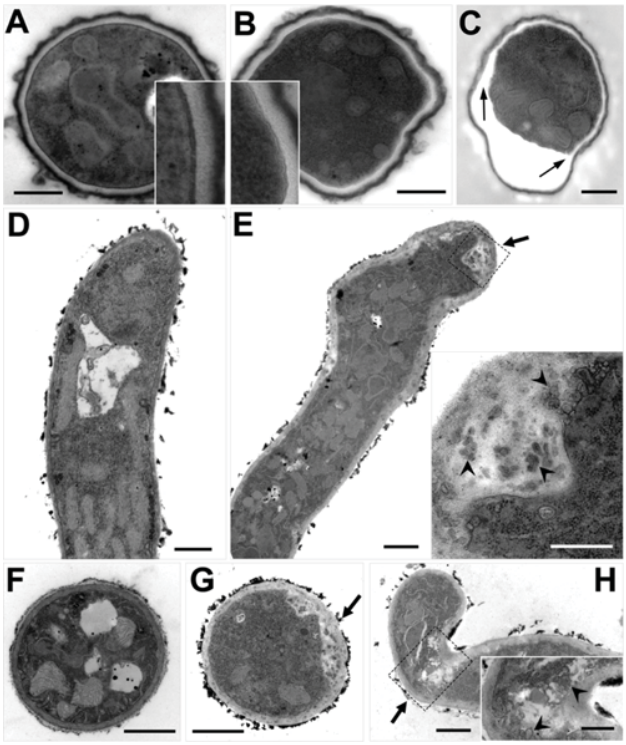

Figure 5. Abnormal cell wall-plasma membrane interface and hyphal morphology is evident in the absence of SrbA. (A–C) Transmission electron micrographs showing sections of conidia of wild type CEA10 (A) and SDW1 (B,C). Compared with the round wild type conidia having clear boundaries between plasma membrane and cell wall layers, most of the SDW1 conidia were distorted in shape and possessed faint, somewhat shriveled boundaries. Note that frequent "tearing" took place mainly at the cell wall – plasma membrane interface during microscopic examination of the SDW1 conidia (arrows). This phenotype was observed in over 80% of SDW1 conidia examined. Inset panels depict a 3× magnified view of the conidial cell wall region. Bars = 500 nm. (D–H). Transmission electron micrographs showing longitudinal and transverse hyphal sections of wild type CEA10 (D,F) and SDW1 (E,G,H). Close observation of the hyphal tips show phenotypic differences between wild type and SDW1. Abnormal cell wall – plasma membrane interfaces and apical swellings in SDW1 hyphae were frequently observed, while the wild type showed normal round-shaped apexes. With respect to cell wall morphology around the hyphal apex, SDW1 had an abnormally expanded cell wall (arrows) containing numerous electron dense objects (arrowheads), which likely resulted in hyphal tip bending (H). Inset panels depict a magnified view of the boxed region. Bars = 1 μm, except for the inset panels of E and H where they denote 500 nm.
doi:10.1371/journal.ppat.1000200.g005

defects. However, a general thickening of the intracellular space between the cell wall and plasma membrane is observed in SDW1 conidia and hyphae compared with the wild type (Figure 5A and 5B and 5D and 5E). A striking phenotype was consequently observed in conidia from SDW1 that suggested a significant defect in the cell wall-plasma membrane interface occurs in the absence of SrbA (Figure 5A and 5B). This defect is apparently exacerbated by the electron beam, which causes a separation between the cell wall and plasma membrane in SDW1 conidia (Figure 5C). This phenotype was observed in over 80% of the SDW1 conidia examined. However, the size and density of the mutant conidia were comparable to the wild type strain as measured by flow cytometry (data not shown). Since a defect in the cell wall plasma membrane interface was suggested, we examined viability of the SDW1 conidia by monitoring germination. These experiments revealed that viability, as measured by conidia germination, was not significantly different between the wild type, SDW1 and SDW2 strains (Figure 6) ($P>0.01$). Similar cell wall-plasma membrane defects were observed in the SDW1 hyphae compared with the wild type hyphae (Figure 5D and 5E). Importantly, an accumulation of electron dense objects was observed in the SDW1 hyphae. We hypothesize that these objects may be vesicles of the Spitzenkörper, and their abnormal location in the SDW1 hyphae may cause the observed altered cell polarity (Figure 5E and 5H). This phenotype was observed in over 50% of the SDW1 hyphae examined and never observed in the wild type strain. These results suggest that SrbA is critical for maintaining the cell wall – plasma membrane interface, and that SrbA is critical for normal hyphal branching and cell polarity in filamentous fungi by an undefined mechanism.

SrbA is required for normal sterol biosynthesis

Transcriptional profiling of SDW1 under hypoxia suggested that SrbA was involved in both early and late steps of the sterol

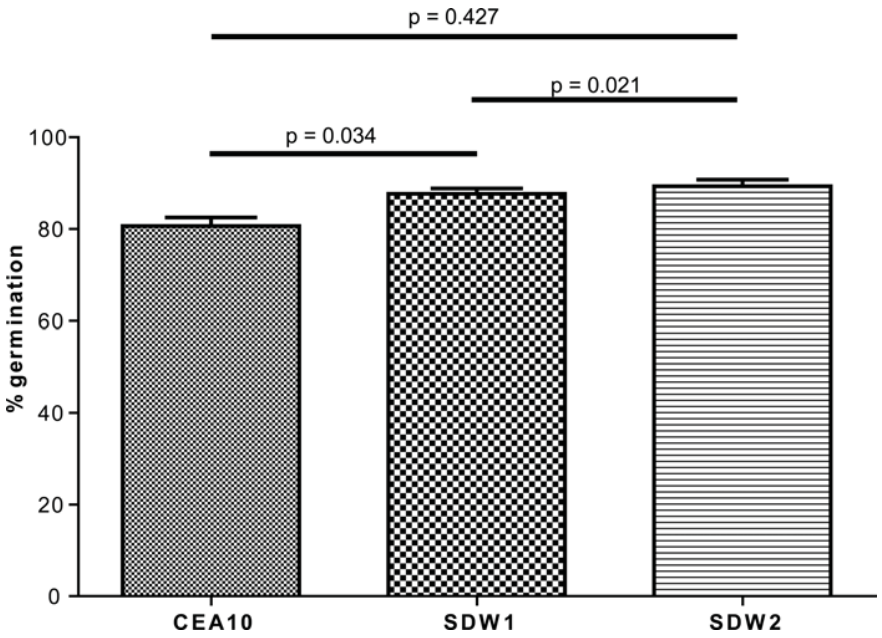

Figure 6. Conidia germination is not affected by loss of SrbA. Germination media was inoculated with approximately 10^6 conidia/ml of the *A. fumigatus* strains CEA10, SDW1, and SDW2. After 7 hours the germination rate was determined by counting a total of 100 spores and noting the number of germinated spores. Three replicates were performed. No significant difference in germination was observed between CEA10, SDW1, and SDW2 ($P>0.01$).
doi:10.1371/journal.ppat.1000200.g006

biosynthesis pathway. In addition, the abnormal conidial and hyphal morphology observed via light microscopy and TEM micrographs in SDW1 also suggested possible alterations in sterol content in the absence of SrbA. Thus, we examined the sterol profile of the SrbA null mutant SDW1 by GC-MS and compared it with the wild type strain CEA10. The GC-MS profiles demonstrated a significant accumulation of 4-methyl sterols in the SrbA null mutant, SDW1, that was not observed in the wild type strain CEA10 (Figure 7). Interestingly, both strains possessed significant amounts of ergosterol (Figure 7). The ratio of C-4 methylated sterols to ergosterol in the absence of SrbA is 1.94 whereas no C-4 methylated sterols accumulated in the wild type. Specifically, the accumulation of 4-methylfecosterol and 4,4-dimethylergosta-8,24(28)-dien-3β-ol in the absence of SrbA suggests a blockage at ERG25 in the sterol biosynthesis pathway in SDW1. These alterations are supported by the transcriptional profiling data, which suggests transcriptional regulation of ERG25 by SrbA in *A. fumigatus* (Table 1). Consequently, these results suggest a blockage of C4 demethylation in the absence of SrbA in *A. fumigatus*. In addition, these results suggest that ergosterol can still be synthesized in the absence of SrbA in *A. fumigatus*.

SrbA is required for fungal virulence in two distinct murine models

Next, we sought to determine whether SrbA was required for *A. fumigatus* virulence. To answer this important question, we utilized two distinct murine models of IPA. In the first model, outbred CD1 neutropenic mice infected with SDW1 displayed no symptoms associated with IPA (Figure 8A). This was in contrast to mice infected with the wild type CEA10 and reconstituted strain SDW2 that displayed well described symptoms of *A. fumigatus* infection including hunched posture, ruffled fur, weight loss, and increased respiration. Consequently, a significant difference in mortality was observed between the mice infected with SDW1 and mice infected with either SDW2 or CEA1O ($P = 0.0002$). Indeed, in this murine model, the SDW1 strain was completely avirulent (Figure 8A). We next asked the question whether mice infected with SDW1 were able to clear the infection. After 28 days, SDW1

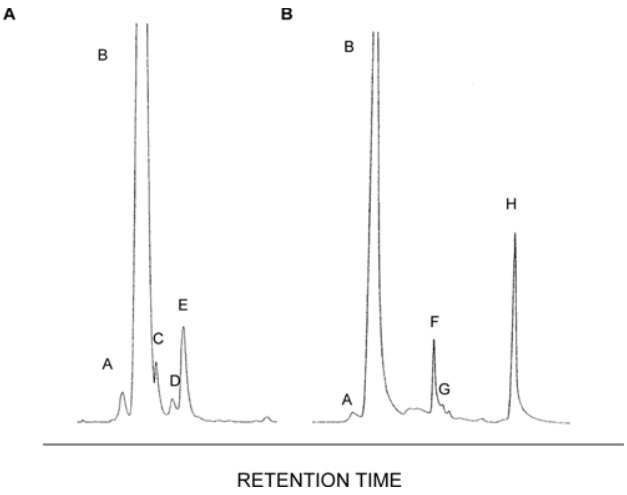

Figure 7. C4-demethylation is altered in the absence of SrbA. Representative GC-MS chromatograms of sterol extracts from wild type (A) and SDW1 (B). Key: A- ergosta-5,8,22-trien-3β-ol, B- ergosterol, C-ergosta-5,7,22,24(28)-tetraen-3β-ol, D- ergosta-5,7,24(28)-trien-3β-ol, E-24-ethylcholesta-5,7,22-trien-3β-ol, F- 4-methylfecosterol, G- 4methylergosta-5,8,24(28)-trien-3β-ol, H- 4,4-demethylergosta-8,24(28)-dien-3β-ol. An accumulation of 4-methyl sterols is observed in the absence of SrbA, suggesting a blockage in enzymes involved in sterol C-4 demethylation. The ratio of C-4 methylated sterols to ergosterol in the absence of SrbA was 1.94 whereas no C-4 methylated sterols accumulated in the wild type.
doi:10.1371/journal.ppat.1000200.g007

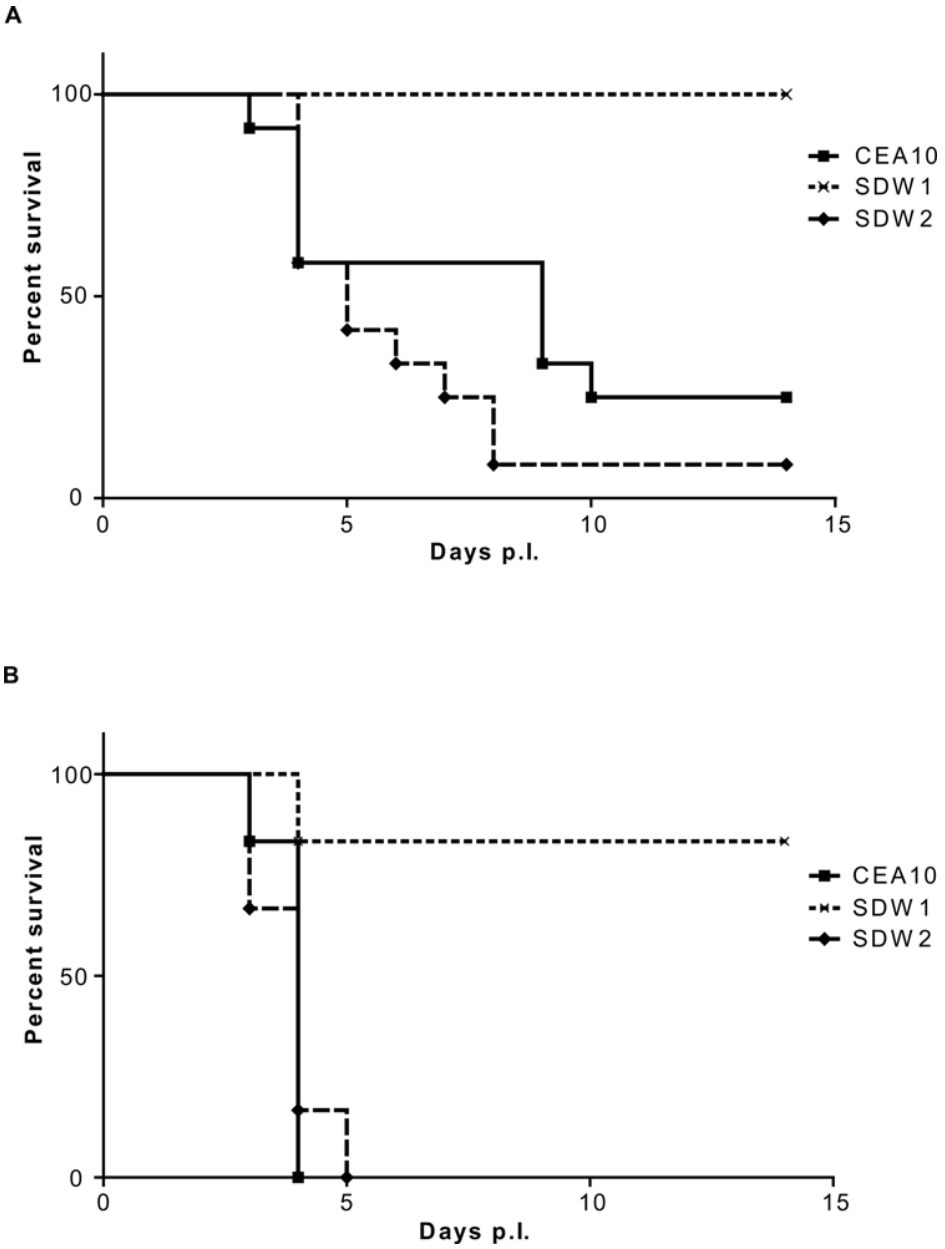

Figure 8. Role of SrbA in *Aspergillus fumigatus* virulence. (A) Outbred CD-1 mice (n = 12) were immunosuppressed by i.p. injection of cyclophosphamide (150 mg/kg) 2 days prior to infection and s.c. injection of Kenalog (40 mg/kg) 1 day prior to infection and injection of 150 mg/kg cyclophosphamide 3 days post-inoculation and 40 mg/kg Kenalog 6 days post-inoculation. Mice were inoculated intranasally with 10^6 conidia in a volume of 40 µl of wild type CEA10, *ΔsrbA* mutant strain SDW1 and the *srbA* reconstituted strain SDW2. P value for comparison between SDW1 and wild type CEA10, P = 0.0002. (B) gp91$^{phox-/-}$ mice (n = 6) were challenged intratracheally with 10^6 conidia in a volume of 40 µl of wild type CEA10, *ΔsrbA* mutant strain SDW1 and the *srbA* reconstituted strain SDW2. A log rank test was used for pair wise comparisons of survival levels among the strain groups. P value for comparison between SDW1 and wild type CEA10, P = 0.0054. SDW1 is significantly less virulent than the wild type CEA10 and the reconstituted strain SDW2 in both murine models. All animal experiments were repeated in duplicate with similar results.
doi:10.1371/journal.ppat.1000200.g008

infected mice displayed no visible or microscopic signs of infection. In particular, at days 14, 21, and 28 lung homogenates were taken from SDW1 infected mice and with the exception of one mouse, no fungal colonies were recoverable indicating that the mice had cleared the infection. Histopathological analyses of mice on days 14, 21 and 28 in this neutropenic model also confirmed the lack of fungal persistence and inflammation in mice infected with SDW1 (Figure 9).

Next, we examined the virulence of SDW1 in a murine model of X-linked chronic granulomatous disease (X-CGD) utilizing gp91$^{phox-/-}$ mice. These mice are deficient in NADPH oxidase activity and display hyper-susceptibility to *Aspergillus* species without the need for immunosuppression with chemotherapeautic agents [45,46]. Similar to the neutropenic mouse model, X-CGD mice infected with strain SDW1 had significant differences in survival compared with mice infected with wild type and

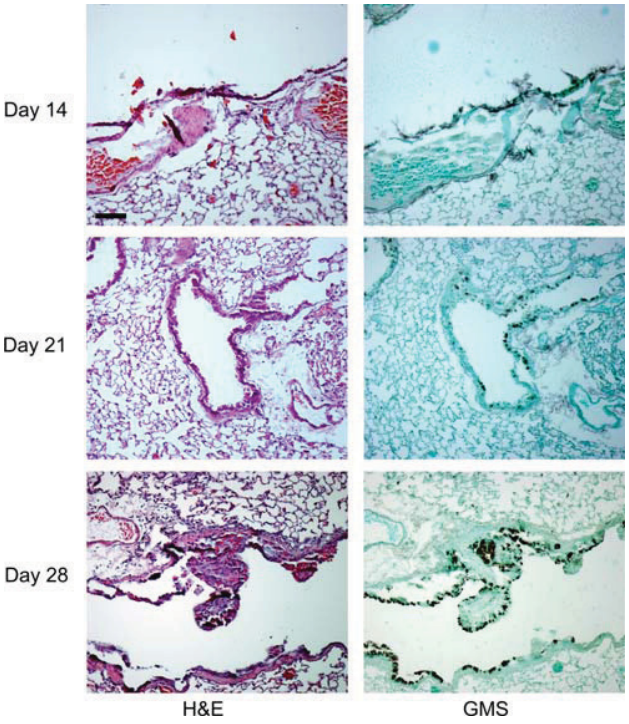

Figure 9. Representative histopathology of CD-1 mouse model SDW1 infected survivors. Hematoxylin and eosin (H&E) or Gommori's methenamine silver (GMS) stains at 100-fold magnification. No sign of inflammation or fungal burden was observed in any surviving animal on day +14, +21 and +28 of the infection. This result indicates that in this murine model, the immune system is capable of clearing the fungal infection in the absence of SrbA. Bar = 100 µm.
doi:10.1371/journal.ppat.1000200.g009

reconstituted strains (Figure 8B) (P = 0.005). Unlike the neutropenic mouse model, these mice all displayed symptoms of IPA during the preliminary stages of infection. These symptoms, likely due to the large inflammatory response characteristic of these mice when exposed to fungal antigens, included ruffled fur, hunched posture, and lethargic movement as early as 24 hours post-infection. However, only one mouse infected with SDW1 succumbed to the infection. In a repeat experiment, 3 additional X-CGD mice infected with SDW1 also succumbed on day 4 to the infection. Most likely, this was due to the hyper-inflammatory response that occurs in X-CGD mice and not death due to invasive fungal growth. Regardless, the majority of X-CGD mice infected with SDW1 survived the infection and displayed no symptoms of IPA by day 14. Histopathological analyses of these mice displayed standard pathological findings associated with *Aspergillus* infections in X-CGD mice including the development of granulomatous like lesions, massive influx of inflammatory cells (primarily neutrophils) to sites of infection, subsequent peribronchiolar and alveolar inflammation, and substantial fungal growth in silver stained tissue (Figures 10 and 11). On day 1 of the infection, fungal germination and growth is observed in mice infected respectively with all 3 strains of the fungus. This observation confirms the viability of SDW1 conidia *in vivo* (Figure 10). Semi-quantitative assessment of the percent of the lung affected by the infection, measured by inflammation and necrosis, of mice infected with the 3 strains respectively revealed no difference at this early time point (CEA10 = 1.3±0.5, SDW1 = 1.3±0.5, SDW2 = 1±0.0). Histopathology on day 4 of the infection, however, revealed extensive growth and proliferation of the wild type and reconstituted SDW2

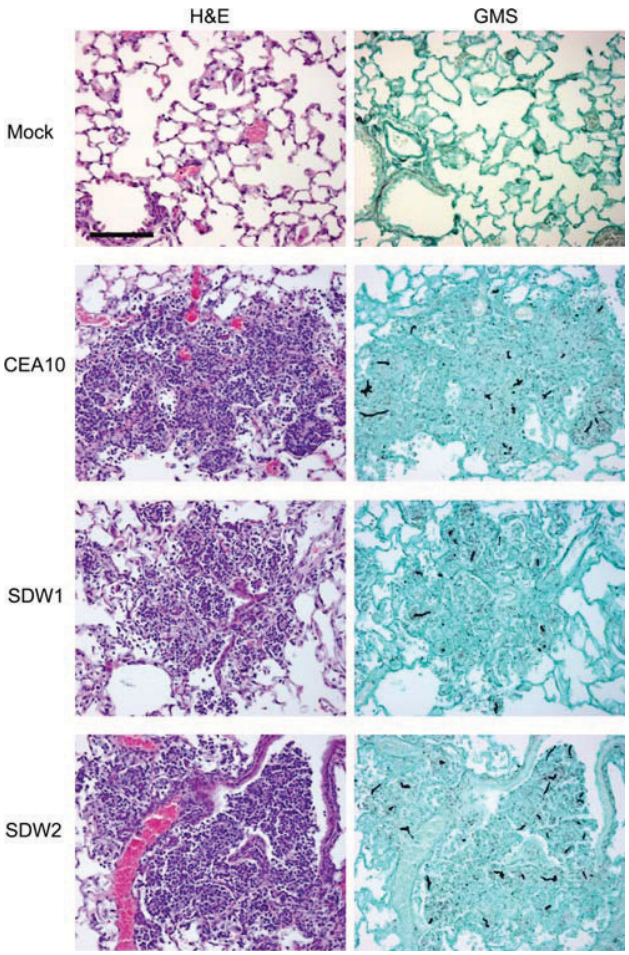

Figure 10. Histopathology of X-CGD mouse model 24 hours after infection. Mock = 0.01% Tween inoculated, WT = CEA10, SDW1 = *ΔsrbA*, SDW2 = *ΔsrbA+srbA*. Mice were inoculated with 1×10^6 conidia intratracheally, euthanized on day +1 after inoculation, lungs removed, fixed in formaldehyde, and stained with hematoxylin and eosin (H&E) or Gommori's methenamine silver (GMS) stain. On day 1 no difference in size and state of lesions could be observed in the infected mice. GMS staining revealed that fungal colonization and germination is observed in all infected animals but not the mock control. This result indicates that SDW1 conidia are viable *in vivo* during the early stages of infection. Bar = 100 µm.
doi:10.1371/journal.ppat.1000200.g010

strain, but minimal fungal growth and proliferation in mice infected with the SrbA null mutant SDW1 (Figure 11). Semi-quantitative assessment of the inflammation and necrosis observed in the lungs of mice infected with the 3 strains respectively at this time point revealed significant differences in the percent of the lung affected by the infection (CEA10 = 3.3±0.5, SDW1 = 2.3±0.5, SDW2 = 3.8±0.5). Lung homogenates from these mice also revealed that viable SDW1 fungus was recoverable from these mice at this time point. This data is consistent with the observed *in vitro* phenotype of the SDW1 strain in hypoxia. Histopathological analysis of SDW1 infected survivors in this model revealed persistence of granuloma like structures and fungal tissue (Figure 12). Lung homogenates from these animals revealed that the observed fungal tissue was still viable. These results indicate that despite normal growth rates *in vitro* in normoxic conditions, the SDW1 strain is severely attenuated in its ability to cause lethal disease in two distinct murine models of IPA.

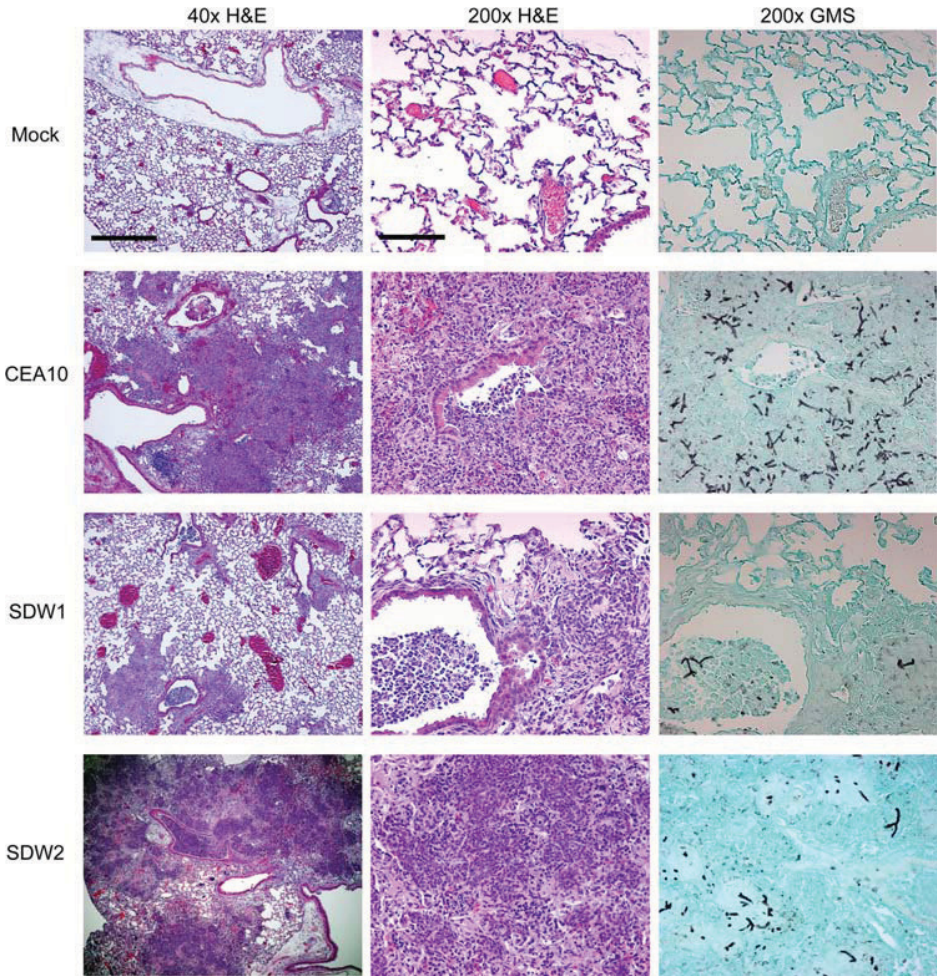

Figure 11. Histopathology of X-CGD mouse model day 4 after infection. Mock = 0.01% Tween inoculated, WT = CEA10, SDW1 = *ΔsrbA*, SDW2 = *ΔsrbA+srbA*. Mice were inoculated with 1×10^6 conidia intratracheally, euthanized on day +4 after inoculation, lungs removed, fixed in formaldehyde, and stained with hematoxylin and eosin (H&E) or Gommori's methenamine silver (GMS) stain. Significant inflammation, necrosis, and an influx of immune effector cells (primarily neutrophils) is observed on day +4 in all infected animals but not the mock control. However, lesions are more localized and not as extensive in mice infected with SDW1. Open alveoli and more localized inflammation are clearly observed in mice infected with SDW1. Interestingly, GMS staining revealed that fungal growth is less extensive in SDW1 as well. This result indicates that as the infection progresses, SDW1 is incapable of continued hyphal growth despite the absence of NADPH oxidase in this murine model. Bar = 500 μm for 40×; Bar = 100 μm for 200×.
doi:10.1371/journal.ppat.1000200.g011

SrbA is not required for oxidative stress resistance and resistance to macrophage killing

One possible mechanism that could explain the virulence defect of strain SDW1 is an increased susceptibility to oxidative stress as suggested by transcriptional profiling and altered conidia morphology. We examined the growth of CEA10, SDW1, and SDW2 in the presence of 1 mM and 2.5 mM hydrogen peroxide on glucose minimal media. After 48 hours, we observed no detectable difference in growth morphology or colony diameter. In addition, we next examined the ability of RAW264.7 macrophage-like cells to kill SDW1 conidia (Figure 13). As presented in figure 13, no significant difference in conidia killing was observed between CEA10, SDW1, and SDW2 ($P>0.01$). We conclude that increased susceptibility to oxidative stress and macrophage killing is not responsible for the virulence defect observed in the absence of SrbA.

Discussion

In this manuscript we present the first characterization of a SREBP in a filamentous fungus. In the yeasts *S. pombe* and *C. neoformans*, SREBP homologs are crucial for sterol biosynthesis, survival under hypoxic conditions, resistance to azole antifungal agents, and fungal virulence [25,32,33]. Our results confirm that some roles of SREBPs in filamentous fungi are conserved with yeast including, the response to hypoxia, sterol biosynthesis, and susceptibility to the azole class of antifungal drugs. However, our results suggest additional functions of SREBPs in filamentous fungi, most importantly a role in maintenance of cell polarity.

Similarities and differences between SrbA in *A. fumigatus* and Sre1 in the yeast *S. pombe* and *C. neoformans* were apparent from transcriptional profiles comparing the SREBP null mutants to their respective wild type strains in response to hypoxia. Unlike *C. neoformans*, we did not observe SrbA dependent genes involved in iron or copper uptake in *A. fumigatus* [32]. This may, however, be a reflection of the experimental conditions that did not place iron stress on the fungus in these experiments. Similar to *C. neoformans* and *S. pombe*, we observed SrbA dependent genes involved in ergosterol biosynthesis including ERG25, ERG24, and ERG3 [31–33]. This result suggests that regulation of ergosterol

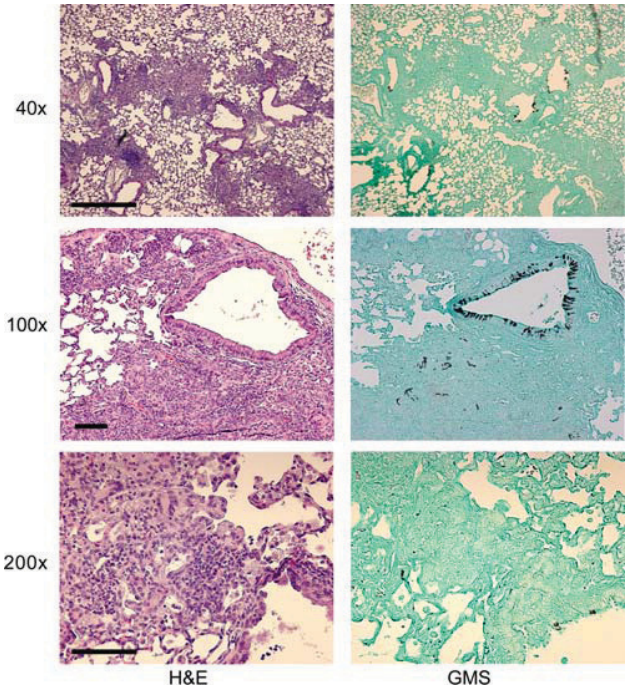

Figure 12. Representative histopathology of X-CGD mouse model SDW1 infected survivors. Hematoxylin and eosin (H&E) or Gommori's methenamine silver (GMS) stains. Resolution of inflammation and necrosis is observed in all surviving animals on day +14 of the infection. However, lesions are still apparent as is common in these mice, but necrosis and debris is significantly reduced. Fungal tissue remains evident on GMS stains indicating that despite surviving the infection, these mice have not entirely cleared the fungal infection. This result confirms the importance of a functional NADPH oxidase in resistance to *Aspergillus* infections, and suggests that increased hypoxia prevents proliferation of fungal tissue in the absence of SrbA. Bar = 500 μm for 40×; Bars = 100 μm for 100× and 200×.
doi:10.1371/journal.ppat.1000200.g012

biosynthesis is a conserved function of SREBPs in fungi. In *A. fumigatus*, the SrbA dependent regulation of ERG25 seems to be of particular significance as sterol profiles of the SrbA mutant indicated an accumulation of C-4 methyl sterols suggesting a block in ERG25 function. The effects of decreased ERG3 and ERG24 transcription in the SrbA null mutant is less clear. The accumulation of pathway intermediates may subsequently affect the expression of these genes, and thus, their regulation by SrbA may be indirect. Moreover, *A. fumigatus* is predicted to have 3 possible orthologs of ERG3 and two of ERG24, which likely indicates a complex regulatory mechanism for ergosterol biosynthesis in *A. fumigatus* that is mediated in part by SrbA under specific conditions such as hypoxia [47,48]. Indeed, single mutants of *erg3* genes result in no difference in their sterol profiles compared with wild type strains [49].

Other differences with yeast in the transcriptional profile of the SREBP mutant in *A. fumigatus* suggest important roles for SrbA in filamentous fungal biology. For example, a non-ribosomal peptide synthetase, NRPS1 (or *pes1*), had the highest change in expression between wild type and the SrbA null mutant [43,44]. This NRPS has been observed to mediate resistance to oxidative stress in *A. fumigatus* and displayed an attenuated virulence phenotype in a *Galleria mellonella* (wax moth) model of aspergillosis depending on inoculum dose [44]. NRPSs are not generally found in most yeast and are particularly abundant in filamentous fungi. Thus, this result suggests that the uncharacterized peptide produced by this NRPS may possibly be involved in hypoxia adaptation as regulated by SrbA in filamentous fungi. Interestingly, we did not observe any increased susceptibility to oxidative stress in the SrbA null mutant. Overall, however, unlike *C. neoformans* and *S. pombe*, we did not observe any genes with an annotation that would clearly point to a role in allowing *Aspergillus* to adapt to hypoxia. This result further illustrates that mechanisms of hypoxia adaptation are almost certainly different in molds than yeast.

Our examination of the SrbA null mutant colony morphology subsequently revealed abnormal branching at the hyphal tips in normoxia and an inability of hyphal growth in hypoxia. Further examination of the mutant with TEM suggested altered vesicle

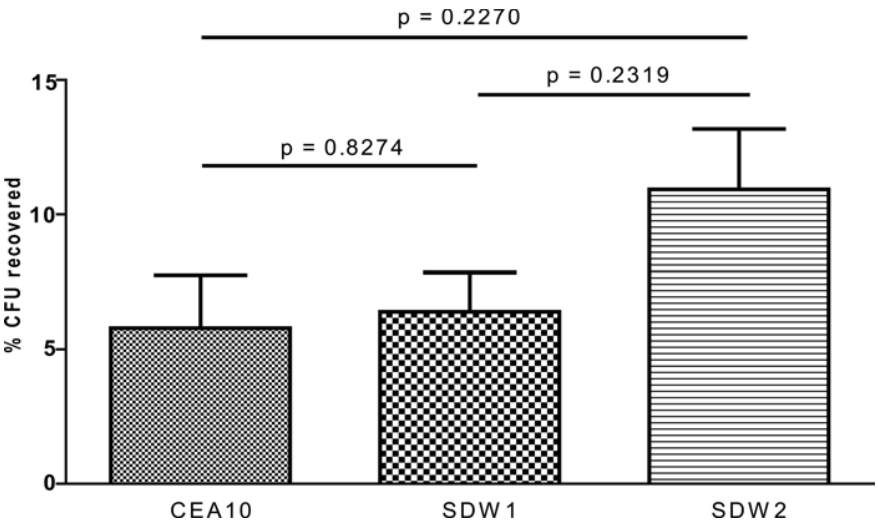

Figure 13. Loss of SrbA does not affect susceptibility to conidia killing by RAW264.7 cells. RAW264.7 cells (macrophages) were infected with a total of 1.25×10^6 freshly harvested *A. fumigatus* conidia of strains CEA10, SDW1, and SDW2 to obtain a conidia:macrophage ratio of 5:1. Conidia and macrophages were incubated together for 6 hours. After 6 hours, conidia were collected from the macrophages and plated onto glucose minimal media. Shown is the percent of recovered conidia after 6 hours incubation of two biological replicates. No significant difference in conidia killing was observed between CEA10, SDW1, and SDW2 ($P>0.01$).
doi:10.1371/journal.ppat.1000200.g013

translocation or formation in the hyphae. It is unclear whether these electron dense objects, which we hypothesize are vesicles, comprise the actual Spitzenkörper. At the apex of hyphae in filamentous fungi, the Spitzenkörper is an accumulation of vesicles that is critical for growth directionality [50,51]. Interestingly, Takeshita et al. (2008) recently observed that localization of key deposition proteins involved in polarized growth at the hyphal tip requires apical sterol-rich membranes [52]. Thus, we hypothesize that the altered hyphal morphology and excessive branching at the tips observed in the SrbA null mutant is due to the alteration in sterol composition of the sterol-rich microdomains in the membrane that are critical for localization of important vesicles and landmark proteins [53]. The alteration in sterol content may cause improper sorting of the vesicles to the apex of the hyphal tip. It is also likely then that the inability of the mutant to grow in hypoxia is related to the perturbation in sterol biosynthesis, a highly oxygen dependent pathway reported to require at least 22 molecules of oxygen.

We could not rescue the SrbA phenotype in hypoxia with addition of ergosterol or lanosterol (data not shown). Nor did exogenous addition of these sterols alter growth of the wild type strain in hypoxia as is the case for *S. cerevisiae*, which requires exogenous sterols for anaerobic growth. These results may suggest that *A. fumigatus* does not import exogenous sterols in hypoxic conditions, that SrbA may be in part responsible for exogenous sterol uptake, or that the defect is not due to loss of ergosterol or lanosterol. We feel that the latter explanation is most likely as *A. fumigatus* has been observed to take up and utilize exogenous cholesterol [54]. We observed that the *A. fumigatus* SrbA null mutant produced substantial levels of ergosterol even in the absence of SrbA. Thus, even though the ergosterol biosynthesis pathway appears blocked at ERG25 in the SrbA mutant, alternative mechanisms exist for *A. fumigatus* to produce ergosterol in the absence of SrbA and presumably ERG25 activity. This finding is consistent with a recent report which suggested that *A. fumigatus* likely possess at least three alternative pathways for ergosterol biosynthesis [48]. Also, an analysis of the *A. fumigatus* genome sequence revealed that *A. fumigatus* contains duplicate and even triplicate copies of many of the ergosterol biosynthesis genes [47,55]. Thus, it appears that *A. fumigatus* contains complex regulatory mechanisms, of which SrbA is a part, for the production of ergosterol that remain to be elucidated.

Based on our current knowledge of the pathophysiology of IPA, the *in vitro* phenotypes observed in the SrbA mutant would not predict a role for this protein in *A. fumigatus* virulence. However, the SrbA null mutant was virtually avirulent in two distinct murine models of IPA despite a normal growth rate of the fungus in standard laboratory conditions. Consequently, we believe two possible explanations exist for the observed avirulent phenotype of the SrbA null mutant. First, and we believe most likely, the inability of the SrbA null mutant to grow in hypoxia prevents invasive disease from being established. Once hypoxia is generated during *Aspergillus* infection, the mutant simply can no longer grow and proliferate, allowing what immune effector cells that remain functional the ability to ultimately clear the infection. An alternative hypothesis is that the altered hyphal morphology and excessive branching observed in the SrbA mutant in normoxic conditions results in a strain incapable of invasive growth or a strain more susceptible to clearance by the immune system. To examine these alternatives, we employed the use of two distinct murine models of IPA.

We first examined the SrbA mutant virulence phenotype in a persistently neutropenic mouse model characterized by the use of high doses of cyclophosphamide and Kenalog [42]. Currently, it is unclear what specific components of the immune system are affected in this model, but it is clear that differences in the immunosuppression regimen can significantly affect the outcome of infection [56,57]. In this model, significant inflammation and tissue necrosis is observed in histopathological examinations. We hypothesize that these sites of infection and inflammation in this model are hypoxic. Thus, we believe that *A. fumigatus* must overcome significant hypoxia during pulmonary infections, and the inability of the SrbA null mutant to adapt to hypoxic conditions results in rapid cessation of invasive growth and a lack of lethal disease. Our histopathological findings with the SrbA mutant strain revealed fungal growth in this model early in the infection. However, by day 14, we were unable to recover viable colonies from mice infected with the SrbA null mutant strain. Indeed, by day 14 of the infection, little evidence of inflammation or fungal burden was evident in mice infected with the SrbA null mutant. These two results suggest that growth of the fungus was halted and what immune effector cells present in the immunosuppressed mice were able to clear the infection. Furthermore, our *in vitro* experiments revealed that the growth defect of the SrbA mutant in hypoxia was not fungicidal but fungistatic. Thus, if growth simply were halted in the animals without immune system clearance, we would have expected to recover viable fungal colonies from the infected mice.

To further examine the apparent virulence defect of the SrbA null mutant, we utilized a mouse strain highly susceptible to *Aspergillus* infections, the X-CGD gp91$^{phox-/-}$ mice [45,46]. These mice exhibit a hyper-inflammatory response when exposed to *A. fumigatus* and other *Aspergillus* species. We chose this particular animal model for our experiments given the very specific defect in NADPH oxidase function in these mice, and with the hypothesis that the hyper-inflammatory response would generate significant hypoxia in the lung. Given the extreme susceptibility of these mice to *A. fumigatus*, we hypothesized that if the SrbA null mutant could grow and persist *in vivo*, even at a reduced rate, we should observe significant mortality in these mice. However, in contrast, we observed limited mortality in these mice when inoculated with the SrbA null mutant, strongly suggesting that the mutant simply cannot grow effectively *in vivo* to cause invasive disease. Unlike the neutropenic mouse model, extensive signs of chronic inflammation remained evident in the X-CGD mice post-day 14, consistent with previously reported results in these animals [45]. Furthermore, unlike the neutropenic mice, we could detect the persistence of viable SDW1 in the lungs of these surviving mice out to day 14.

Consequently, we conclude that these observations strongly suggest that the inability of the SrbA null mutant to grow in hypoxic microenvironments is primarily responsible for the avirulent phenotype of the mutant. Though the altered cell polarity of the SrbA mutant may contribute to the virulence defect, the fact that SrbA null mutant displayed normal growth rates *in vitro* in standard laboratory growth conditions suggests to us that the altered cell polarity did not significantly affect fungal growth. Furthermore, we also have examined the susceptibility of the SrbA null mutant conidia to macrophage (RAW264.7 cells) killing and found no difference with the wild type strain. In addition, the SrbA mutant did not display increased sensitivity to hydrogen peroxide. Taken together, we feel these observations strongly suggest that the virulence defect in the SrbA null mutant is due to its inability to grow in hypoxia.

An additional observation of clinical significance was the finding that SrbA mediates resistance to the azole class of antifungal drugs. Interestingly, loss of SrbA resulted in a strain of *A. fumigatus* highly susceptible to fluconazole, an azole that normally has minimal activity against *A. fumigatus* [58,59]. The mechanism(s) behind this

result are currently not known. Transcriptional profiling of the SrbA mutant revealed numerous transporters possibly regulated by SrbA. Thus, the mechanism behind the increased azole susceptibility may be due to loss of transcription in specific transporters in the SrbA mutant. This hypothesis is currently being tested in our laboratory. Second, a relationship between mitochondria function, sterol homeostasis, and azole drug resistance has been observed in the yeast *S. cerevisiae* and *Candida glabrata* [60,61]. Thus, the altered accumulation of sterol intermediates in the SrbA mutant may alter the resulting interaction with fluconazole and mitochondria. With a similar increase in susceptibility to azoles in the SREBP mutant in *C. neoformans*, it seems clear that further study of the SREBP pathway and azole drug resistance in pathogenic fungi is highly warranted. Identification of ways to inhibit this pathway *in vivo* may increase the efficacy of current azole antifungal agents [32,33]. Thus, further studies are needed to dissect this important pathway in yeast and molds to identify conserved targets that may be harnessed to treat patients with invasive mycoses.

Finally, in this study, we did not focus on elucidating the molecular mechanism behind SrbA regulation and activation in molds. However, several observations from our studies hint at possible mechanisms. First, we identified SrbA in a transcriptional profiling screen of *A. fumigatus* in response to hypoxia (induced >5 fold). This suggests that SrbA may be transcriptionally regulated in molds. However, HIF1 in humans also responds transcriptionally to hypoxia, but its activity is primarily post-translationally regulated [62,63]. In the yeast *S. pombe* and *C. neoformans*, it seems clear that Sre1 is regulated post-translationally in response to sterol biosynthesis perturbation that occurs in low oxygen environments. Indeed, Hughes et al. (2007) have identified 4-methyl sterols as the primary activating agent of Sre1 in *S. pombe* [64]. Thus, our finding that the SrbA null mutant in *A. fumigatus* accumulates 4-methyl sterols may also suggest that these sterols are the trigger for SrbA activation in *A. fumigatus*.

While many of the phenotypes we observed in the SrbA mutant in *A. fumigatus* may suggest that SrbA is regulated in a similar manner as Sre1 in yeast, our results may also suggest an alternative model in molds. First, despite extensive bioinformatic analyses, we were unable to identify a clear homolog of the sterol cleavage activating protein (SCAP). SCAP is highly conserved in yeast, mammals, and insects and thus it is surprising that bioinformatic searches were unable to identify a clear homolog in any filamentous fungi with genome sequences available. However, some candidates with minimal sequence similarity are being pursued in our laboratory. Second, the observation that sterol biosynthesis was altered in normoxia, likely resulting in altered cell polarity, suggests that in molds, SrbA plays a significant role in the biology of filamentous fungi in normoxic conditions. Third, though sequence identity was extremely low, generation of null mutants in putative site-1 (S1P) and site-2 (S2P) protease homologs in *A. fumigatus* did not demonstrate expected defects in hypoxic growth (Willger and Cramer, unpublished data). Additional proteases remain to be explored. We could, however, identify a clear Insig1 homolog, which we have named InsA. In mammals, Insig is a key regulator of SREBP function where it binds to SCAP and prevents SREBP cleavage in the presence of sterols by maintaining the SREBP-SCAP complex in the endoplasmic reticulum membrane [65,66]. We are currently characterizing a possible role for InsA in SREBP signalling in filamentous fungi. Interestingly, *C. neoformans* lacks an apparent Insig homolog and the Insig homolog in *S. pombe* does not appear to be required for regulation of SREBP signalling [25,32]. Taken together, these results suggest that while aspects of SrbA signalling in filamentous fungi may be conserved in yeast and mammals, it is likely that significant differences exist in molds that remain to be elucidated. What is clear, however, is that SREBPs play critical roles in the biology of fungi that have important implications for fungal virulence and how we manage and treat invasive fungal infections. Future studies on this pathway in *A. fumigatus* are likely to yield important insights into sterol metabolism, hypoxia adaptation, fungal growth, and mechanisms of azole drug resistance.

Materials and Methods

Strains and media

A. fumigatus strain CEA17 (a gift from Dr. J.P. Latgé, Institut Pasteur) was used to generate the *srbA* null mutant strain, SDW1 (*ΔsrbA::A. parasiticus pyrG pyrG1*). *A. fumigatus* strain CEA17 is a uracil-auxotrophic (*pyrG1*) mutant of *A. fumigatus* strain CEA10 [67,68]. In this study we used CEA10 (gift from Dr. Thomas Patterson, University of Texas- San Antonio Health Sciences Center) as the wild type, SDW1, and an ectopic complemented control strain SDW2 (*Δsrb::A. parasiticus pyrG+srbA*). All strains were stored as frozen stocks with 50% glycerol at −80°C. The strains were routinely grown in glucose minimal medium (GMM) with appropriate supplements as previously described [69] at 37°C. To prepare solid media 1.5% agar was added before autoclaving.

Strain construction

Generation of a *srbA* null mutant in *A. fumigatus* strain CEA17 was accomplished by replacing an ~2.2-kb internal fragment of the *srbA* coding region (~3.0 kb; GenBank accession no. XM_744169) with *A. parasiticus pyrG*. The replacement construct was generated by cloning a sequence homologous to the *srbA* locus into plasmid pJW24 (donated by Dr. Nancy Keller, University of Wisconsin—Madison). Homologous sequences, each ~1 kb in length and 5′ and 3′ of the *srbA* coding sequence, were cloned to flank *A. parasiticus pyrG* in pJW24. The resulting plasmid, pSRBAKO, was used as a template to amplify the ~5.1-kb disruption construct for use in fungal transformation. To complement the *ΔsrbA* strain SDW1 the *srbA* gene was amplified using genomic DNA of CEA10 as template and the primers 5′SrbAKOLF and 3′SrbAKORF. The ~5.9-kb PCR product was used in a fungal transformation and selection was for colonies able to grow under hypoxic conditions. The primers utilized in vector construction are presented in Table S1.

Generation of fungal protoplasts and polyethylene glycol-mediated transformation of *A. fumigatus* were performed as previously described [70]. Briefly, 10 μg of the *srbA*KO PCR-generated replacement construct was incubated on ice for 50 min with 1×10^7 fungal protoplasts in a total volume of 100 μl. Transformants were initially screened by PCR to identify potential homologous recombination events at the *srbA* locus. PCR was performed with primers designed to amplify only the disrupted *srbA* locus (5′SrbAKOLF and 3′PyrGKOLF; 5′PyrGKORF and 3′SrbAKORF) (Table S1). Homologous recombination was confirmed by Southern analysis with the digoxigenin labeling system (Roche Molecular Biochemicals, Mannheim, Germany) as previously described [71]. To eliminate the chance of heterokaryons, each transformant was streaked with sterile toothpicks a minimum of two times to obtain colonies from single conidia.

Hypoxic cultivation

Strains were grown on GMM plates at 37°C. Normoxic conditions were considered general atmospheric levels within the lab (~21% O_2). For hypoxic conditions a Hypoxia Incubation Chamber (MIC-101; Billups-Rothenberg, http://www.

hypoxiaincubator.com) was used. The chamber was maintained at 37°C and kept at ~1% oxygen level utilizing a gas mixture containing 1% O_2, 5% CO_2 and 94% N_2. In addition, hypoxia experiments requiring shake-flask cultures were conducted in a Biospherix C-Chamber with O_2 levels controlled by a PRO-Ox controller and CO_2 levels controlled with PRO-CO_2 controller (Biospherix, Lacona, NY). For these experiments, O_2 set point was 1% and CO_2 set point was 5%.

Colony growth was quantified as previously described [72]. Briefly, 5-µl aliquots containing 1×10^6 conidia from freshly harvested GMM plates were placed in the center of GMM agar plates. Plates were then cultured under normoxic or hypoxic conditions. Diameters of three colonies per *A. fumigatus* strain and condition were measured once daily over a period of 4 days. The average change in colony diameter per 24 h of growth was calculated from three independent cultures. Conidia were harvested with 20 ml of sterile 0.01% Tween 80, filtered through two layers of sterile miracloth (EMD Biosciences, La Jolla, CA), and quantified.

Isolation of total RNA

Conidia from freshly harvested GMM plates were inoculated in 5 ml GMM in a 6-well plate to a concentration of 1×10^7/ml. Cultures were grown aerobically for 24 h. For normoxic growth, cultures were maintained in atmospheric conditions. For hypoxic growth, cultures were placed in the hypoxic chamber for 24 h. Fungal mats were flash frozen in liquid nitrogen and lyophilized prior to total RNA extraction using TRIsure Reagent (Bioline) according to the manufacturer's instructions. RNA was further purified using the RNeasy Mini Kit (Qiagen) and re-suspended in DEPC-treated water. RNA integrity was confirmed with an Agilent Technologies Bioanalyzer.

Microarray-based transcriptional profiling

Total RNA was reverse transcribed by priming with oligo dT and utilizing aminoallyl-dUTP. The resultant cDNA was then coupled to Cy3- and Cy5-labeled probes (GE Healthcare), and hybridized to *Aspergillus fumigatus* version 3 microarrays from the pathogen functional resources center (PFGRC) as described in the TIGR standard operating procedures found at http://atarray.tigr.org. Labeled cDNA from wild type grown in hypoxic conditions was hybridized against cDNA from SDW1 grown in hypoxic conditions. Data for each strain represents six independent experiments and includes three dye swaps. Arrays were scanned on an Axon 4000B scanner with GenePix software at the Montana State University Functional Genomics Core facility (Axon Instruments). Array signals were bulk-normalized and filtered for flagged spots using MIDAS (available at http://www.tm4.org/midas.html). Data were log-transformed (base 2) and filtered for genes that contained data for at least three out of four arrays from each strain, and missing values were calculated through K-nearest neighbor algorithm using Significance Analysis of Microarrays (SAM) software [73] prior to statistical analysis by SAM. Statistically significant genes identified by SAM with 2-fold or greater changes in expression are listed in Table 1. A Delta cutoff in SAM that captured the maximum number of significant genes with a false discovery rate of zero was utilized. Microarray data has been deposited in the Gene Expression Omnibus (GEO) at the National Center for Biotechnology Information (NCBI) series accession number GSE12376.

Susceptibility testing

E-test strips (AB Biodisk, N.J.) plastic strips impregnated with a gradient of Fluconazole, Voriconazole, Caspofungin, or Amphotericin B were used per manufacturers' instructions. Each strip was placed onto a RPMI-1640 (Sigma Aldrich) agar plate containing a lawn of conidia and growth inhibition was measured after 24 and 48 h by direct observation of the plates at 37°C. No difference in results was observed between 24 and 48 h.

Sterol analyses

Sterols were extracted following published protocols [74]. Gas-chromatography-Mass spectrometry analyses were performed with a HP6890 GC coupled to a HP5973 mass selective detector. Electron impact MS (70 eV, scanning from 50 to 550amu, at 2.94 intervals/sec) was performed using the following conditions: HP-5 column (30 m×0.25 mm i.d., 0.25 mm film thickness), Helium as carrier gas (1 ml/min), detector temperature 180°C, column temperature 100°C to 300°C (100°C for 1 min, 7°C/min to 300°C then held for 15 min). All injections were run in splitless mode.

Electron microscopy

Conidia and mycelia of wild type and SDW1 were examined by transmission electron microscopy (TEM). Conidia released in sterile water from 5-day-old GMM plates and mycelia grown in liquid GMM for two days were collected by centrifugation at 5000× g for 10 min. The conidial and mycelial pellets were coated with 0.8% agarose and fixed in modified Karnovsky's fixative containing 2% paraformaldehyde and 2% (v/v) glutaraldehyde in 0.05 M sodium cacodylate buffer (pH 7.2) overnight at 4°C. After washing three times with 0.05 M sodium cacodylate buffer (pH 7.2) for 10 min each, samples were post-fixed with 1% (w/v) osmium tetraoxide in the same buffer for 2 hours at 4°C. The post-fixative was removed by washing briefly twice with distilled water at room temperature and the samples were *en bloc* stained with 0.5% uranyl acetate overnight at 4°C. The samples were then dehydrated in a graded ethanol series, rinsed with propylene oxide, and embedded in Eppon resin (Fluka AG, Zürich, CH). Ultrathin sections cut from the Eppon-embedded material with ultramicrotome (MT-X, RMC, USA) were collected on carbon-coated grids, stained with 2% uranyl acetate for 3 min, and with Reynold's lead solution [75] for 3 min. Examination was conducted with a JEM-1010 (JEOL, Tokyo, Japan) electron microscope operating at 60 kV.

Conidia Germination assay

For the conidia germination assay, *A. fumigatus* strains were grown in 25 ml GMM with 2% yeast extract. Cultures were inoculated with approximately 10^6 conidia/ml. After 7 hours the germination rate was determined by counting a total of 100 spores and noting the number of germinated spores. Counting was repeated three times for each strain and the mean and standard deviation are reported.

Murine virulence assays

In this study two different mouse models were used to assess the role of the transcription factor SrbA in fungal virulence. For the persistently neutropenic mouse model we used outbred CD1 (Charles River Laboratory, Raleigh, NC) male mice (26 to 28 g in size, 6–8 weeks old), which were housed six per cage and had access to food and water ad libitum. Mice were immunosuppressed with intraperitoneal (i.p.) injections of cyclophosphamide at 150 mg/kg 2 days prior to infection and with Kenalog injected subcutaneously (s.c.) at 40 mg/kg 1 days prior to infection. On day 3 post-infection (p.i.), repeat injections were given with cyclophosphamide (150 mg/kg i.p.) and on day 6 p.i. with Kenalog (40 mg/

kg s.c.). Twelve mice per *A. fumigatus* strain (CEA10, *srbA*-deficient mutant SDW1, or the reconstituted strain SDW2) were infected intranasally. For an alternative mouse model, we used breeder mice with a null allele corresponding to the X-linked $gp91^{phox}$ component of NADPH oxidase (B6.129S6-$Cyb^{btm1Din}$). Breeding pairs of these mice were obtained from the Jackson Laboratory (Bar Harbor, Maine) and reared in the Animal Resource Center at Montana State University. All animals were kept in specific-pathogen-free housing, and all manipulations were approved by the institutional internal review board (IACUC). To avoid exposing $gp91^{phox-/-}$ mice to bacterial infections, they were housed in microisolator cages in an environment of filtered air and given autoclaved food ad libitum and prophylactic treatment with sulfamethoxazole-trimethoprim in their sterile drinking water. The animals were used at 8 to 13 weeks of age. The mice were inoculated intratracheally following brief isoflurane inhalation, returned to their cages, and monitored at least twice daily.

Infection inoculum was prepared by growing the *A. fumigatus* isolates on GMM agar plates at 37°C for 3 days. Conidia were harvested by washing the plate surface with sterile phosphate-buffered saline-0.01% Tween 80. The resultant conidial suspension was adjusted to the desired concentration of 1×10^6 conidia/40 µl by hemacytometer count. Mice were observed for survival for 14 days after *A. fumigatus* challenge. Any animals showing distress were immediately sacrificed and recorded as deaths within 24 h. Mock mice were included in all experiments and inoculated with sterile 0.01% Tween 80. Lungs from all mice sacrificed during the experiment were removed for fungal burden assessment and histopathology. Experiments were repeated in duplicates with similar results. Survival was plotted on a Kaplan-Meier curve and a log-rank test used to determine significance of pair-wise survival (two-tailed $P<0.01$). No mock infected animals perished in either murine model in all experiments.

Histopathology

For histopathology studies, additional $gp91^{phox-/-}$ mice were infected as described above, and sacrificed at set time points of day 1 and day 4 after *A. fumigatus* challenge. When mice were sacrificed, lungs were removed on that day. Lung tissue was fixed in 10% phosphate-buffered formalin, embedded in paraffin, sectioned at 5 µm, and stained with hematoxylin and eosin (H&E) or Grocott methenamine silver (GMS) by using standard histological techniques. Microscopic examinations were performed on a Zeiss Axioscope 2-plus microscope and imaging system using Zeiss Axiovision version 4.4 software. Semi-quantitative analysis of inflammation and necrosis were scored on a scale of 1 to 5. The scale consisted of: 1 = 0 to 24% lung involvement, 2 = 25–49%, 3 = 50–74%, 4 = 75–99% 5 = 100%. H&E stained whole lungs from 4 mice infected with each respective strain were assessed to determine the percentage involvement and scored accordingly on days 1 and 4 of the infection in consultation with a pulmonary immunologist.

Macrophage assays

Macrophage killing of conidia was measured by serial dilution as previously described with slight modifications [76–78]. Briefly, 2.5×10^5 RAW264.7 cells in a volume of 500 ml were inoculated into 24 well tissue culture treated cell culture plates (Corning Incorporated, Corning, NY) in DMEM complete media and incubated overnight at 37°C, 5% CO_2. A total of 1.25×10^6 freshly harvested *A. fumigatus* conidia of the respective strains in DMEM complete media were inoculated into each well to give a conidia:macrophage ratio of 5:1. Co-incubation was performed at 37°C, 5% CO_2 for 1 hour, after which media was removed and cells were gently washed with 1× phosphate buffered saline (PBS) to remove non-phagocytosed conidia. At this time point, conidia from each strain were harvested from macrophages in one well to establish the baseline number of conidia engulfed. DMEM complete media was added back to the non-harvested wells and incubation proceeded for an additional 5 hours. Lysis of macrophages was performed by treating the cells with 200 ml of a 0.5% SDS solution for 10 minutes followed by addition of 200 ml of 1× PBS. The percentage of colony forming units (CFU) from conidia:macrophage co-incubations was determined relative to control conidia harvested at the one hour time point. Controls were performed by lysing macrophages as described above after phagocytosis of conidia for 1 hour and CFU counts were set to 100%. Experiments were performed with triplicate wells and repeated two times for each *A. fumigatus* strain.

Oxidative stress assay

For the oxidative stress assay, the *A. fumigatus* strains were grown on GMM plates with and without H_2O_2. GMM plates with 1 and 2.5 mM H_2O_2 were prepared. Plates were inoculated with approximately 100,000 spores in 5 µl and incubated at 37°C. Sensitivity to oxidative stress was determined by comparing the colony radius of 2-day-old cultures on plates with H_2O_2. The assay was repeated three times for each concentration. Growth of each strain on each plate was visually examined.

Statistical analysis

The software program Prism 5 (GraphPad, San Diego, Calif.) was used for all statistical tests of significance (to P values of ≤0.01). Normally, a two-sided t test was used to compare two groups of data, with Welch's correction being used if the groups had unequal variances. In cases in which a deviation from a normal distribution was suspected, a nonparametric test (Mann-Whitney test) was also applied. In those cases, we found that both the t test and Mann-Whitney test indicated the same results (i.e., both indicated significance or insignificance); however, typically one test gave a more conservative (larger, but still <0.01) P value. The P values we report are always the conservative values. Log-rank tests were utilized to determine significance of survival in animal studies.

Supporting Information

Table S1 Primers Used in This Study
Found at: doi:10.1371/journal.ppat.1000200.s001 (0.03 MB DOC)

Acknowledgments

We would like to thank Gayle Callis and the Dr. Allen Harmsen Laboratory at Montana State University for assistance with histopathology techniques, Kate McInnerney, Kerry Thompson, and Dr. Mike Franklin at the MSU Functional Genomics Core Facility for assistance with the microarrays, and Dr. Ted White for assistance with E-strip assays and constructive comments. Additional thanks to Julie Elser from the Cramer laboratory for assistance with these experiments, and Dr. John Perfect Duke University Medical Center and three anonymous reviewers for their constructive comments that improved the manuscript.

Author Contributions

Conceived and designed the experiments: SDW RACJ. Performed the experiments: SDW SP KHK JBB NG LJM RB MB RACJ. Analyzed the data: SDW SP KHK JBB NG LJM RB MB CBL RACJ. Contributed reagents/materials/analysis tools: SDW KHK JBB LJM RB MB CBL RACJ. Wrote the paper: SDW MB RACJ.

References

1. Tekaia F, Latge JP (2005) *Aspergillus fumigatus*: saprophyte or pathogen? Curr Opin Microbiol 8: 385–392.
2. Latge JP (1999) *Aspergillus fumigatus* and aspergillosis. Clin Microbiol Rev 12: 310–350.
3. Rhodes JC (2006) *Aspergillus fumigatus*: growth and virulence. Med Mycol 44 Suppl 1: S77–81.
4. Hohl TM, Feldmesser M (2007) *Aspergillus fumigatus*: principles of pathogenesis and host defense. Eukaryot Cell 6: 1953–1963.
5. Matherne GP, Headrick JP, Coleman SD, Berne RM (1990) Interstitial transudate purines in normoxic and hypoxic immature and mature rabbit hearts. Pediatr Res 28: 348–353.
6. Van Belle H, Goossens F, Wynants J (1987) Formation and release of purine catabolites during hypoperfusion, anoxia, and ischemia. Am J Physiol 252: H886–893.
7. Dewhirst MW (1998) Concepts of oxygen transport at the microcirculatory level. Semin Radiat Oncol 8: 143–150.
8. Arnold F, West D, Kumar S (1987) Wound healing: the effect of macrophage and tumour derived angiogenesis factors on skin graft vascularization. Br J Exp Pathol 68: 569–574.
9. Simmen HP, Battaglia H, Giovanoli P, Blaser J (1994) Analysis of pH, pO2 and pCO2 in drainage fluid allows for rapid detection of infectious complications during the follow-up period after abdominal surgery. Infection 22: 386–389.
10. Nakayama K, Frew IJ, Hagensen M, Skals M, Habelhah H, et al. (2004) Siah2 regulates stability of prolyl-hydroxylases, controls HIF1alpha abundance, and modulates physiological responses to hypoxia. Cell 117: 941–952.
11. Wenger RH (2002) Cellular adaptation to hypoxia: O2-sensing protein hydroxylases, hypoxia-inducible transcription factors, and O2-regulated gene expression. Faseb J 16: 1151–1162.
12. Maxwell PH, Dachs GU, Gleadle JM, Nicholls LG, Harris AL, et al. (1997) Hypoxia-inducible factor-1 modulates gene expression in solid tumors and influences both angiogenesis and tumor growth. Proc Natl Acad Sci U S A 94: 8104–8109.
13. Thiel M, Chouker A, Ohta A, Jackson E, Caldwell C, et al. (2005) Oxygenation inhibits the physiological tissue-protecting mechanism and thereby exacerbates acute inflammatory lung injury. PLoS Biol 3: e174. doi: 0.1371/journal.pbio.0030174.
14. Tarrand JJ, Han XY, Kontoyiannis DP, May GS (2005) *Aspergillus* hyphae in infected tissue: evidence of physiologic adaptation and effect on culture recovery. J Clin Microbiol 43: 382–386.
15. Tarrand JJ, Lichterfeld M, Warraich I, Luna M, Han XY, et al. (2003) Diagnosis of invasive septate mold infections. A correlation of microbiological culture and histologic or cytologic examination. Am J Clin Pathol 119: 854–858.
16. Warn PA, Sharp A, Guinea J, Denning DW (2004) Effect of hypoxic conditions on in vitro susceptibility testing of amphotericin B, itraconazole and micafungin against *Aspergillus* and *Candida*. J Antimicrob Chemother 53: 743–749.
17. Perkhofer S, Jost D, Dierich MP, Lass-Florl C (2008) Susceptibility testing of anidulafungin and voriconazole alone and in combination against conidia and hyphae of *Aspergillus spp*. under hypoxic conditions. Antimicrob Agents Chemother 52: 1873–1875.
18. Smith I (2003) *Mycobacterium tuberculosis* pathogenesis and molecular determinants of virulence. Clin Microbiol Rev 16: 463–496.
19. Richardson DJ (2000) Bacterial respiration: a flexible process for a changing environment. Microbiology 146(Pt 3): 551–571.
20. Zhang L, Hach A (1999) Molecular mechanism of heme signaling in yeast: the transcriptional activator Hap1 serves as the key mediator. Cell Mol Life Sci 56: 415–426.
21. Kastaniotis AJ, Zitomer RS (2000) Rox1 mediated repression. Oxygen dependent repression in yeast. Adv Exp Med Biol 475: 185–195.
22. Kwast KE, Burke PV, Staahl BT, Poyton RO (1999) Oxygen sensing in yeast: evidence for the involvement of the respiratory chain in regulating the transcription of a subset of hypoxic genes. Proc Natl Acad Sci U S A 96: 5446–5451.
23. Balasubramanian B, Lowry CV, Zitomer RS (1993) The Rox1 repressor of the *Saccharomyces cerevisiae* hypoxic genes is a specific DNA-binding protein with a high-mobility-group motif. Mol Cell Biol 13: 6071–6078.
24. Vasconcelles MJ, Jiang Y, McDaid K, Gilooly L, Wretzel S, et al. (2001) Identification and characterization of a low oxygen response element involved in the hypoxic induction of a family of *Saccharomyces cerevisiae* genes. Implications for the conservation of oxygen sensing in eukaryotes. J Biol Chem 276: 14374–14384.
25. Hughes AL, Todd BL, Espenshade PJ (2005) SREBP pathway responds to sterols and functions as an oxygen sensor in fission yeast. Cell 120: 831–842.
26. Briggs MR, Yokoyama C, Wang X, Brown MS, Goldstein JL (1993) Nuclear protein that binds sterol regulatory element of low density lipoprotein receptor promoter. I. Identification of the protein and delineation of its target nucleotide sequence. J Biol Chem 268: 14490–14496.
27. Wang X, Briggs MR, Hua X, Yokoyama C, Goldstein JL, et al. (1993) Nuclear protein that binds sterol regulatory element of low density lipoprotein receptor promoter. II. Purification and characterization. J Biol Chem 268: 14497–14504.
28. Rawson RB (2003) The SREBP pathway–insights from Insigs and insects. Nat Rev Mol Cell Biol 4: 631–640.
29. Espenshade PJ (2006) SREBPs: sterol-regulated transcription factors. J Cell Sci 119: 973–976.
30. Espenshade PJ, Hughes AL (2007) Regulation of sterol synthesis in eukaryotes. Annu Rev Genet 41: 401–427.
31. Todd BL, Stewart EV, Burg JS, Hughes AL, Espenshade PJ (2006) Sterol regulatory element binding protein is a principal regulator of anaerobic gene expression in fission yeast. Mol Cell Biol 26: 2817–2831.
32. Chang YC, Bien CM, Lee H, Espenshade PJ, Kwon-Chung KJ (2007) Sre1p, a regulator of oxygen sensing and sterol homeostasis, is required for virulence in *Cryptococcus neoformans*. Mol Microbiol 64: 614–629.
33. Chun CD, Liu OW, Madhani HD (2007) A Link between virulence and homeostatic responses to hypoxia during infection by the human fungal pathogen *Cryptococcus neoformans*. PLoS Pathog 3: e22. doi:10.1371/journal.ppat.0030022.
34. White TC, Silver PM (2005) Regulation of sterol metabolism in *Candida albicans* by the *UPC2* gene. Biochem Soc Trans 33: 1215–1218.
35. Vik A, Rine J (2001) Upc2p and Ecm22p, dual regulators of sterol biosynthesis in *Saccharomyces cerevisiae*. Mol Cell Biol 21: 6395–6405.
36. Silver PM, Oliver BG, White TC (2004) Role of *Candida albicans* transcription factor Upc2p in drug resistance and sterol metabolism. Eukaryot Cell 3: 1391–1397.
37. Shianna KV, Dotson WD, Tove S, Parks LW (2001) Identification of a UPC2 homolog in *Saccharomyces cerevisiae* and its involvement in aerobic sterol uptake. J Bacteriol 183: 830–834.
38. MacPherson S, Akache B, Weber S, De Deken X, Raymond M, et al. (2005) *Candida albicans* zinc cluster protein Upc2p confers resistance to antifungal drugs and is an activator of ergosterol biosynthetic genes. Antimicrob Agents Chemother 49: 1745–1752.
39. Dunkel N, Liu TT, Barker KS, Homayouni R, Morschhauser J, et al. (2008) A gain-of-function mutation in the transcription factor Upc2p causes upregulation of ergosterol biosynthesis genes and increased fluconazole resistance in a clinical *Candida albicans* isolate. Eukaryot Cell 7: 1180–1190.
40. Davies BS, Rine J (2006) A role for sterol levels in oxygen sensing in *Saccharomyces cerevisiae*. Genetics 174: 191–201.
41. Cramer RA Jr, Gamcsik MP, Brooking RM, Najvar LK, Kirkpatrick WR, et al. (2006) Disruption of a nonribosomal peptide synthetase in *Aspergillus fumigatus* eliminates gliotoxin production. Eukaryot Cell 5: 972–980.
42. Steinbach WJ, Cramer RA Jr, Perfect BZ, Asfaw YG, Sauer TC, et al. (2006) Calcineurin controls growth, morphology, and pathogenicity in *Aspergillus fumigatus*. Eukaryot Cell 5: 1091–1103.
43. Cramer RA Jr, Stajich JE, Yamanaka Y, Dietrich FS, Steinbach WJ, et al. (2006) Phylogenomic analysis of non-ribosomal peptide synthetases in the genus *Aspergillus*. Gene 383: 24–32.
44. Reeves EP, Reiber K, Neville C, Scheibner O, Kavanagh K, et al. (2006) A nonribosomal peptide synthetase (Pes1) confers protection against oxidative stress in *Aspergillus fumigatus*. Febs J 273: 3038–3053.
45. Morgenstern DE, Gifford MA, Li LL, Doerschuk CM, Dinauer MC (1997) Absence of respiratory burst in X-linked chronic granulomatous disease mice leads to abnormalities in both host defense and inflammatory response to *Aspergillus fumigatus*. J Exp Med 185: 207–218.
46. Pollock JD, Williams DA, Gifford MA, Li LL, Du X, et al. (1995) Mouse model of X-linked chronic granulomatous disease, an inherited defect in phagocyte superoxide production. Nat Genet 9: 202–209.
47. Ferreira ME, Colombo AL, Paulsen I, Ren Q, Wortman J, et al. (2005) The ergosterol biosynthesis pathway, transporter genes, and azole resistance in *Aspergillus fumigatus*. Med Mycol 43 Suppl 1: S313–319.
48. Alcazar-Fuoli L, Mellado E, Garcia-Effron G, Lopez JF, Grimalt JO, et al. (2008) Ergosterol biosynthesis pathway in *Aspergillus fumigatus*. Steroids 73: 339–347.
49. Alcazar-Fuoli L, Mellado E, Garcia-Effron G, Buitrago MJ, Lopez JF, et al. (2006) *Aspergillus fumigatus* C-5 Sterol Desaturases Erg3A and Erg3B: Role in Sterol Biosynthesis and Antifungal Drug Susceptibility. Antimicrob Agents Chemother 50: 453–460.
50. Riquelme M, Reynaga-Pena CG, Gierz G, Bartnicki-Garcia S (1998) What determines growth direction in fungal hyphae? Fungal Genet Biol 24: 101–109.
51. Grove SN, Bracker CE (1970) Protoplasmic organization of hyphal tips among fungi: vesicles and Spitzenkorper. J Bacteriol 104: 989–1009.
52. Takeshita N, Higashitsuji Y, Konzack S, Fischer R (2008) Apical Sterol-rich Membranes Are Essential for Localizing Cell End Markers That Determine Growth Directionality in the Filamentous Fungus *Aspergillus nidulans*. Mol Biol Cell 19: 339–351.
53. Alvarez FJ, Douglas LM, Konopka JB (2007) Sterol-rich plasma membrane domains in fungi. Eukaryot Cell 6: 755–763.
54. Xiong Q, Hassan SA, Wilson WK, Han XY, May GS, et al. (2005) Cholesterol import by *Aspergillus fumigatus* and its influence on antifungal potency of sterol biosynthesis inhibitors. Antimicrob Agents Chemother 49: 518–524.
55. Nierman WC, Pain A, Anderson MJ, Wortman JR, Kim HS, et al. (2005) Genomic sequence of the pathogenic and allergenic filamentous fungus *Aspergillus fumigatus*. Nature 438: 1151–1156.

56. Balloy V, Huerre M, Latge JP, Chignard M (2005) Differences in patterns of infection and inflammation for corticosteroid treatment and chemotherapy in experimental invasive pulmonary aspergillosis. Infect Immun 73: 494–503.
57. Stephens-Romero SD, Mednick AJ, Feldmesser M (2005) The pathogenesis of fatal outcome in murine pulmonary aspergillosis depends on the neutrophil depletion strategy. Infect Immun 73: 114–125.
58. Sabatelli F, Patel R, Mann PA, Mendrick CA, Norris CC, et al. (2006) In vitro activities of posaconazole, fluconazole, itraconazole, voriconazole, and amphotericin B against a large collection of clinically important molds and yeasts. Antimicrob Agents Chemother 50: 2009–2015.
59. White TC, Marr KA, Bowden RA (1998) Clinical, cellular, and molecular factors that contribute to antifungal drug resistance. Clin Microbiol Rev 11: 382–402.
60. Kaur R, Castano I, Cormack BP (2004) Functional genomic analysis of fluconazole susceptibility in the pathogenic yeast *Candida glabrata*: roles of calcium signaling and mitochondria. Antimicrob Agents Chemother 48: 1600–1613.
61. Kontoyiannis DP (2000) Modulation of fluconazole sensitivity by the interaction of mitochondria and erg3p in *Saccharomyces cerevisiae*. J Antimicrob Chemother 46: 191–197.
62. Semenza GL (1999) Regulation of mammalian O_2 homeostasis by hypoxia-inducible factor 1. Annu Rev Cell Dev Biol 15: 551–578.
63. Belaiba RS, Bonello S, Zahringer C, Schmidt S, Hess J, et al. (2007) Hypoxia up-regulates hypoxia-inducible factor-1alpha transcription by involving phosphatidylinositol 3-kinase and nuclear factor kappaB in pulmonary artery smooth muscle cells. Mol Biol Cell 18: 4691–4697.
64. Hughes AL, Lee CY, Bien CM, Espenshade PJ (2007) 4-Methyl sterols regulate fission yeast SREBP-Scap under low oxygen and cell stress. J Biol Chem 282: 24388–24396.
65. Engelking LJ, Evers BM, Richardson JA, Goldstein JL, Brown MS, et al. (2006) Severe facial clefting in Insig-deficient mouse embryos caused by sterol accumulation and reversed by lovastatin. J Clin Invest 116: 2356–2365.
66. Yang T, Espenshade PJ, Wright ME, Yabe D, Gong Y, et al. (2002) Crucial step in cholesterol homeostasis: sterols promote binding of SCAP to INSIG-1, a membrane protein that facilitates retention of SREBPs in ER. Cell 110: 489–500.
67. D'Enfert C, Diaquin M, Delit A, Wuscher N, Debeaupuis JP, et al. (1996) Attenuated virulence of uridine-uracil auxotrophs of *Aspergillus fumigatus*. Infect Immun 64: 4401–4405.
68. d'Enfert C (1996) Selection of multiple disruption events in *Aspergillus fumigatus* using the orotidine-5′-decarboxylase gene, *pyrG*, as a unique transformation marker. Curr Genet 30: 76–82.
69. Shimizu K, Keller NP (2001) Genetic involvement of a cAMP-dependent protein kinase in a G protein signaling pathway regulating morphological and chemical transitions in *Aspergillus nidulans*. Genetics 157: 591–600.
70. Bok JW, Keller NP (2004) LaeA, a regulator of secondary metabolism in *Aspergillus spp*. Eukaryot Cell 3: 527–535.
71. Cramer RA, Lawrence CB (2003) Cloning of a gene encoding an Alt a 1 isoallergen differentially expressed by the necrotrophic fungus *Alternaria brassicicola* during Arabidopsis infection. Appl Environ Microbiol 69: 2361–2364.
72. McNeil MM, Nash SL, Hajjeh RA, Phelan MA, Conn LA, et al. (2001) Trends in mortality due to invasive mycotic diseases in the United States, 1980–1997. Clin Infect Dis 33: 641–647.
73. Tusher VG, Tibshirani R, Chu G (2001) Significance analysis of microarrays applied to the ionizing radiation response. Proc Natl Acad Sci U S A 98: 5116–5121.
74. Gachotte D, Sen SE, Eckstein J, Barbuch R, Krieger M, et al. (1999) Characterization of the *Saccharomyces cerevisiae ERG27* gene encoding the 3-keto reductase involved in C-4 sterol demethylation. Proc Natl Acad Sci U S A 96: 12655–12660.
75. Reynolds ES (1963) The use of lead citrate at high pH as an electron opaque stain in electron microscopy. J Cell Biol 17: 208–212.
76. Jahn B, Rampp A, Dick C, Jahn A, Palmer M, et al. (1998) Accumulation of amphotericin B in human macrophages enhances activity against *Aspergillus fumigatus* conidia: quantification of conidial kill at the single-cell level. Antimicrob Agents Chemother 42: 2569–2575.
77. Liebmann B, Gattung S, Jahn B, Brakhage AA (2003) cAMP signaling in *Aspergillus fumigatus* is involved in the regulation of the virulence gene pksP and in defense against killing by macrophages. Mol Genet Genomics 269: 420–435.
78. Marr KA, Koudadoust M, Black M, Balajee SA (2001) Early events in macrophage killing of *Aspergillus fumigatus* conidia: new flow cytometric viability assay. Clin Diagn Lab Immunol 8: 1240–1247.

Medical Mycology
2009, 1–16, iFirst article

informa
healthcare

Review Article

Regulation of hypoxia adaptation: an overlooked virulence attribute of pathogenic fungi?

NORA GRAHL & ROBERT A. CRAMER JR.
Department of Veterinary Molecular Biology, Montana State University, Bozeman, Montana, USA

Over the past two decades, the incidence of fungal infections has dramatically increased. This is primarily due to increases in the population of immunocompromised individuals attributed to the HIV/AIDS pandemic and immunosuppression therapies associated with organ transplantation, cancer, and other diseases where new immunomodulatory therapies are utilized. Significant advances have been made in understanding how fungi cause disease, but clearly much remains to be learned about the pathophysiology of these often lethal infections. Fungal pathogens face numerous environmental challenges as they colonize and infect mammalian hosts. Regardless of a pathogen's complexity, its ability to adapt to environmental changes is critical for its survival and ability to cause disease. For example, at sites of fungal infections, the significant influx of immune effector cells and the necrosis of tissue by the invading pathogen generate hypoxic microenvironments to which both the pathogen and host cells must adapt in order to survive. However, our current knowledge of how pathogenic fungi adapt to and survive in hypoxic conditions during fungal pathogenesis is limited. Recent studies have begun to observe that the ability to adapt to various levels of hypoxia is an important component of the virulence arsenal of pathogenic fungi. In this review, we focus on known oxygen sensing mechanisms that non-pathogenic and pathogenic fungi utilize to adapt to hypoxic microenvironments and their possible relation to fungal virulence.

Keywords *Aspergillus fumigatus*, *Cryptococcus neoformans*, *Candida albicans*, fungal virulence, hypoxia, sterols

Downloaded By: [Montana State University Bozeman] At: 20:30 11 December 2009

Introduction – Significance of hypoxia during fungal pathogenesis

Recent advances in medical therapies, organ transplantation, HIV infections, and an increasing geriatric population have generated rising populations of immunocompromised patients. These events have all resulted in a significant increase in life-threatening human fungal infections over the last two decades [1]. The limited treatment options and high mortality rates associated with these infections has consequently led to a concerted effort to better understand mechanisms of fungal pathogenesis in mammals. The general rationale behind these studies is that a better understanding of how these organisms cause disease will allow us to develop better technologies for the treatment and prevention of these often lethal infections. One increasing area of fungal pathogenesis research is related to identifying and understanding the basic metabolic pathways utilized by these fungi to survive in the harsh and highly variable mammalian host environment.

Received 6 January 2009; Final revision received 2 April 2009; Accepted 4 April 2009
Correspondence: Robert A. Cramer Jr., PO Box 173610, Bozeman, MT 59717, USA. Tel: +1 406 994 7467; Fax: +1 406 994 4303; E-mail: rcramer@montana.edu

© 2009 ISHAM

DOI: 10.1080/13693780902947342

Downloaded By: [Montana State University Bozeman] At: 20:30 11 December 2009

The three main fungal pathogens that cause human mycoses, *Aspergillus fumigatus*, *Cryptococcus neoformans*, and *Candida albicans*, are typically opportunistic pathogens. These fungi are saprophytic organisms that have evolved a unique combination of attributes to survive in their natural environments. *Aspergillus fumigatus* is typically found in soil and decaying organic material such as compost heaps. *Cryptococcus neoformans* is typically found in pigeon droppings, soil and certain trees.

Unlike *Aspergillus* and *Cryptococcus* species, *Candida albicans* is rarely found in the soil or external environment. Instead, it is a normal inhabitant of the human microflora. Thus, *C. albicans* is already highly adapted to the host environment. *C. albicans* possess the ability to survive in disparate host environments, as illustrated by its ability to colonize diverse areas of the host (oral, vaginal, gastrointestinal areas). Coincidentally, many of these attributes, which allow fungal survival in their natural ecological niches, appear to also allow these fungi to cause disease in immunocompromised hosts. One overlooked environmental selection pressure found in natural environments of all three of the most common fungal pathogens of humans is low oxygen tension. Whether in the soil, a compost pile, pigeon guano, or the gut of a mammal, these fungi must deal with low levels of oxygen.

The focus of this review is on the increasing evidence that pathogenic fungi must adapt to rapidly changing oxygen levels during fungal infections. It is well established that oxygen levels vary throughout the mammalian body depending on numerous factors including tissue type and presence or absence of an inflammatory response. For example, oxygen levels in most mammalian tissues are found to be considerably below atmospheric levels (21%) [2–4]. Even in the alveoli of healthy lungs, the most oxygen rich organ and site of infection for many fungal pathogens, the oxygen level is around 14%. By the time oxygen reaches the capillaries and diffuses into surrounding tissues its availability is much lower with levels of 2–4% reported [5,6]. In addition, it is well established that at sites of inflammation available oxygen is significantly reduced compared to surrounding tissues [7–9]. Moreover, in inflamed tissues, the blood supply is often interrupted because the vessels are congested with phagocytes or the pathogen itself [10,11]. Thus, it seems highly probable that hypoxic microenvironments are generated during fungal infection.

Indeed, we can look no further than the host response to observe that fungal pathogens are likely exposed to severely low oxygen levels during infection. Immune effector cells, such as neutrophils, function effectively in severely hypoxic microenvironments. These and other cells of the host have evolved distinct mechanisms to deal with hypoxic microenvironments generated during microbial infections. Many of these host response mechanisms are dependent upon the global transcription factor, hypoxia inducible factor (HIF) 1.

HIF 1 is a heterodimeric transcription factor that consists of one of three α-subunits (HIF-1α, HIF-2α, and HIF-3α) and one β-subunit (HIF-1β), and is the central regulator of hypoxic gene expression in mammals (reviewed in [12,13]). Both the degradation and activity of the HIF-1α subunit are regulated by oxygen-dependent post-translational hydroxyl modifications. Under hypoxic conditions HIF-1α is not hydroxylated, leading to an accumulation of the HIF-1α subunit and expression of hypoxia-responsive genes, including those encoding many glycolytic enzymes, erythropoietin, adrenomedullin, and growth factors [14,15].

In a recent study of Acute Respiratory Distress Syndrome (ARDS) and acute inflammatory lung injury, Thiel *et al*. [16] provided evidence for the importance of hypoxic microenvironments in regulation of host immune responses. ARDS patients are normally treated with a life-saving oxygen therapy, but this therapy may have a dangerous side effect in patients with uncontrolled pulmonary inflammation. Thiel *et al*. [16] identified a local tissue hypoxia-driven and adenosin A2A receptor (A2AR)-mediated anti-inflammatory mechanism. Their data suggest that oxygenation may lead to elimination of the A2AR-mediated lung tissue-protecting pathway and thereby further exacerbate lung injury. Taken together, the above observations and studies indicate that mammalian immune system responses to microbial infection and inflammation are critically tied to hypoxic microenvironments.

While the role of hypoxia in the immune response to fungal pathogens is relatively unknown, it follows that since immune cells of the host have evolved mechanisms to function in hypoxia, mammalian fungal pathogens like *A. fumigatus*, *C. neoformans* and *C. albicans* are likely exposed to hypoxic conditions during fungal pathogenesis. Indeed, during *A. fumigatus* infection, our laboratory has recently observed significant increases in HIF-1α activity as the fungal infection progresses and inflammation and edema increase in the lung (Grahl and Cramer, unpublished data). In addition, a recent study by Brock *et al*. [17] demonstrated that hypoxia likely occurs *in vivo* in the lung during *A. fumigatus* infection. The authors constructed a luciferase-producing bioluminescent *A. fumigatus* strain, which was not attenuated in virulence in a

© 2009 ISHAM, *Medical Mycology*

murine model of invasive aspergillosis. Interestingly, luminescence from the lungs decreased after reaching a maximum at one day post infection, despite the high number of fungal hyphae present in histology examinations. The authors hypothesize that this phenomenon might be due to the severe tissue damage in and through the pulmonary lesions, which likely decrease the oxygen concentration in the lung tissue. Oxygen is essential for the light-producing reaction, and thus the lack of luminescence is likely attributable to the hypoxia at the site of infection [17].

Additional evidence that hypoxia may be a key component of the pathophysiology of invasive fungal infections comes from the observation that there are often significant differences in the *in vivo* and *in vitro* test results of antifungal drug efficacies. These differences have recently been postulated to be related to hypoxic conditions found *in vivo* as demonstrated by *in vitro* antifungal drug efficacy tests conducted in hypoxia [6,18]. Furthermore, recent studies have identified genes responsible for regulating fungal response to hypoxia, and some of these pathways have been observed to be essential for fungal virulence of mammals. Consequently, it seems probable that pathogenic fungi possess mechanisms to adapt to hypoxic microenvironments found *in vivo* during infection.

The purpose of this review is to summarize recent advances in our understanding of mechanisms that human fungal pathogens use to adapt to hypoxic conditions and to highlight the emerging importance of this area of research in the pathogenic fungi. While studies on hypoxia adaptation in these pathogenic fungi are limited, increasing research attention to this important component of their virulence arsenal has revealed similarities and differences with each other and the model yeast *S. cerevisiae* and *S. pombe*. Importantly, we should clarify the distinction between mechanisms of hypoxia *adaptation* and mechanisms of hypoxic *growth*. It seems clear that these are two distinct biological processes requiring a distinct set of genes and mechanisms. In our literature review, we did not find detailed studies defining these two likely different processes in the fungi. It is likely that periods of adaptation are different for diverse fungi. A close examination of the methodology used in the cited studies indicated that most, if not all, studies are focused on genes allowing the fungi to adapt to hypoxia (i.e., genes expressed/required in the early phase of exposure to hypoxia (within 48 hours of a switch to hypoxia), rather than genes required for actual fungal growth in these conditions. Where possible, we have attempted to highlight these distinctions. Finally, we have divided the manuscript into sections detailing fungi with Upc2p orthologs and fungi with SREBP orthologs given the emerging importance of these pathways in oxygen sensing and hypoxia adaptation in fungi.

Fungi with the SREBP analogue Upc2p

Saccharomyces cerevisiae

S. cerevisiae cells adapt to anaerobic conditions by inducing expression of a large number of genes, called 'hypoxic genes' [19–25]. The hypoxic genes encode oxygen-related functions in respiration, heme, and membrane biosynthesis that are required at higher levels when molecular oxygen is limited [20,26]. For the regulation of hypoxic genes, the cell senses oxygen availability through cellular heme levels [27,28], and recent studies suggest that oxygen availability can also be sensed through cellular sterol levels [29].

Oxygen sensing by heme

Molecular oxygen is required as a substrate in two consecutive steps of heme biosynthesis catalyzed by the enzymes coproporphyrinogen oxidase and protoporphyrinogen IX oxidase [30]. In the presence of oxygen (aerobic growth), heme accumulates, binds to the transcriptional activator Hap1p (Heme Activator Protein) and causes the formation of a Hap1p homodimer specific for DNA binding to the *cis*-element. Hap1p is a protein composed of a zinc-finger DNA binding domain at the N-terminus, a dimerization domain, a heme binding domain within the central region, a heme-responsive motif 7 (HRM7), and a transcriptional activation domain at the C-terminus [31–33]. The heme-Hap1p-complex acts as a transcriptional activator of genes containing its recognition site ($5'CGGN_6CGG$) [34–36], such as genes involved in respiration (reviewed in [20]).

In addition, the expression of the *ROX1* (Repressor Of hypoXic genes) gene is activated by the heme-Hap1p complex and Rox1p accumulates in the cell under aerobic conditions (reviewed in [26]). The Rox1p repressor binds to its recognition site upstream of the hypoxic genes to repress their transcription [37,38]. Rox1p binds to the DNA with its HMG domain and recruits the general repression complex, Tup1/Ssn6, which binds to the Rox1p repression domain (reviewed in [26]). The repression through Rox1p varies between hypoxic genes that do not have aerobic counterparts, which are expressed at detectable levels at all oxygen concentrations but their expression is higher when oxygen decreases, like *HEM13*, *OLE1*, *ERG11*, and the autorepressed *ROX1* itself, and hypoxic genes that

© 2009 ISHAM, *Medical Mycology*

Downloaded By: [Montana State University Bozeman] At: 20:30 11 December 2009

have an aerobic homologue, like *HMG1*/*HMG2*, *COX5A*/*COX5B*, *AAC1, AAC2*/*AAC3*, and *TIF51A*/*ANBI* (the first gene is aerobic – last and underlined anaerobic). The anaerobic gene is then completely repressed until very low oxygen concentrations are reached [38,39].

For some hypoxic genes, a second DNA binding protein Mot3p enhances Rox1p repression through helping recruit the Tup1p/Ssn6p complex. Two examples are the *ANBI* (ANaeroBically Induced) gene, encoding a subunit of eukaryotic initiation factor 5 (eIF-5a), an essential translation factor [40], and the *HEM13* gene, encoding the enzyme coproporphyrinogen III oxidase, which catalyzes the rate-limiting step in heme biosynthesis [41]. The hypoxic derepression of *HEM13* allows the cell to continue heme biosynthesis under limited available oxygen. The strongly repressed *ANBI* gene has one Mot3p and two Rox1p binding sites in its promoter region, while the promoter of the partially repressed *HEM13* contains one Rox1p and three Mot3p binding sites. The combination of binding sites determines the strength of repression. Multiple Mot3p binding sites plus a single Rox1p binding site are much weaker than multiple Rox1p binding sites plus a single Mot3p binding site [42]. Rox1p and Mot3p both interact with Ssn6p of the general repression complex and Rox1p stabilizes Mot3p binding to DNA through interactions with Tup1p/Ssn6p [42].

Under hypoxic or anaerobic growth conditions, heme levels are reduced. Hap1p still binds to its cognate site, but in the absence of heme, Hap1p forms a biochemically distinct High-Molecular-weight Complex, HMC, which contains Hap1p and four other proteins including Hsp28p and Ydj1p. This complex represses transcription [43]. Consequently, under hypoxic conditions, *ROX1* and *MOT3* expression is repressed resulting in the activation of hypoxic gene expression [26].

During adaptation to anaerobic conditions, a complex program of cell wall remodeling occurs in yeast. Under anaerobic conditions, major aerobic cell wall mannoproteins, encoded by *CWP1* and *CWP2,* are replaced by their anaerobic counterparts, encoded by the *DAN*/*TIR* genes. The *DAN*/*TIR* genes encode a group of eight cell wall mannoproteins that play a significant role in cell wall permeability [23,44]. *DAN*/*TIR* genes are regulated by heme, sterol levels, and three DNA binding transcription factors. The heme-dependent repressors Rox1p and Mot3p function synergistically to efficiently repress *DAN*/*TIR* genes under aerobic conditions [45]. In addition, the sterol depletion-dependent activator Upc2p acts through a consensus site termed *AR1* to induce the expression of *DAN*/*TIR* genes in anaerobic conditions [46]. Sertil *et al*. [47] observed that the histone deacetylase and global repressor Rpd3p is required for the expression of all the *DAN*/*TIR* genes and the hypoxic gene *ANBI*. Moreover, the authors propose that Rpd3p is recruited to the *DAN1* promoter under strict anaerobic conditions. The presence of Rpd3p at the promoter counteracts the function of the repressor Mot3p, which leads to stable binding of the activator Upc2p. Upc2p then recruits the chromatin remodeling complex Swi/Snf to reorganize chromatin, thereby facilitating the binding of the transcriptional machinery that results in the activation of gene expression [47]. Upc2p, together with the transcription factor Ecm22p, is also responsible for basal and induced expression of genes encoding enzymes of ergosterol biosynthesis in yeast (*ERG1*, *ERG2*, *ERG3*, *ERG7*, *ERG25*, *ERG26*, and *ERG27*), and it has been implicated in the uptake of sterols under hypoxic conditions [48–52].

Oxygen sensing by sterols

While heme has been thought to be the primary oxygen sensor in *S. cerevisiae*, recent studies suggest that sterol levels also play an important role. Upc2p and Ecm22p are functionally related to human sterol regulatory element binding protein (SREBP) with an N-terminal transcription factor domain and a C-terminal transmembrane domain. Although *S. cerevisiae* lacks an ortholog of SREBP, it seems that a potentially analogous oxygen-sensing mechanism exists in budding yeast regulated through Upc2p and Ecm22p. Marie *et al*. [53] have observed that Upc2p and Ecm22p are localized outside of the nucleus in sterol replete conditions, but in conditions of sterol depletion localization shifts toward the nucleus. The authors suggest that the N-terminal transcription factor domain is separated from the C-terminal transmembrane domain by proteolytic cleavage and enters the nucleus to activate gene expression, analogous to SREBP regulation of cholesterol biosynthesis in mammals.

Upc2p and Ecm22p both bind a sequence motif known as the sterol regulatory element (SRE) [48,49,54]. Nearly one-third of hypoxically induced genes in *S. cerevisiae* contain at least one potential Upc2p/Ecm22p binding site, suggesting that these transcription factors are major players in the adaptation to hypoxia [55]. The activation of target genes by Upc2p occurs in response to low sterol levels, which can be caused by blocks in ergosterol biosynthesis or by hypoxia. Davies and Rine [29] observed that both Upc2p and Ecm22p require a functional version of Hap1p for basal expression of *ERG2*, but when sterols

© 2009 ISHAM, *Medical Mycology*

Downloaded By: [Montana State University Bozeman] At: 20:30 11 December 2009

Downloaded By: [Montana State University Bozeman] At: 20:30 11 December 2009

are depleted Upc2p is independent of Hap1p, whereas Ecm22p still depends upon Hap1p for *ERG* gene activation. *ERG2*, *ERG3*, *ERG10*, *DAN2*, and *DAN4* are activated by Upc2p solely in response to sterol depletion whereas *DAN1* and *TIR1* respond to both sterols and heme [46].

Other oxygen sensing mechanisms

An additional hypoxic regulatory pathway involving an antagonistic interaction between the Ord1p repressor and the Yap1p factor (a transcriptional activator involved in oxidative stress response) has been discovered in *S. cerevisiae* and regulates both *TIR1* and *SRP1*. The hypoxic response of *TIR1*/*SRP1* (both encode cell wall mannoproteins) depends on the absence of heme but is Rox1p-independent. Under aerobic conditions, Ord1p binds to the *SRP1* promoter and expression is repressed. When conditions change to hypoxia, Yap1p also binds to the *SRP1* promoter, counteracts the Ord1p effect and *SRP1* is expressed [56].

Multiple pathways involved in regulating hypoxic and anoxic gene expression in yeast may exist. Studies of several other hypoxic/anaerobic genes including *SUT1*, encoding a putative Zn[II]2Cys6-transcription factor that facilitates the uptake and synthesis of sterols under hypoxic conditions [57], *GPD2*, encoding an isoenzyme of NAD-dependent glycerol 3-phosphate dehydrogenase [58], and members of the seripauperine (*PAU*) family, like *TIR1* [59] have demonstrated Rox1p-independent hypoxic/anaerobic induction, but the mechanisms by which this occurs are not yet understood.

Another recently described possible mechanism of hypoxia signaling in yeast involves the mitochondrial respiratory chain, the cytochrome c oxidase and reactive oxygen species [60,61]. It has been shown that mitochondria from yeast, rat liver, and plants are capable of nitrite (NO_2^-)-dependent nitric oxide (NO) synthesis [60,62–66]. This pathway is induced when cells experience hypoxia, and furthermore, Castello *et al.* [60] suggest that mitochondrially produced NO functions in a signaling pathway to the nucleus by reacting with the superoxide produced by hypoxic mitochondria [67] to form peroxynitrite ($ONOO^-$) that promotes protein tyrosine nitration of specific proteins that may be involved in a signaling pathway to the nucleus. Future research on this mechanism will likely uncover its specific role in hypoxia adaptation.

It seems clear that adaptation to hypoxia is a complex multi-faceted process regulated via the interaction of several different critical metabolic pathways in the cell. The major regulatory pathways discussed above are summarized in Fig. 1 and Table 1. We now turn our attention to other fungi and discuss similarities and differences with these hypoxia adaptation mechanisms in *S. cerevisiae*. As many of the pathogenic fungi employ different life-styles than *S. cerevisiae,* it is still unclear which of these pathways involved in regulating responses to hypoxia in baker's yeast are conserved in fungi that invade mammalian hosts.

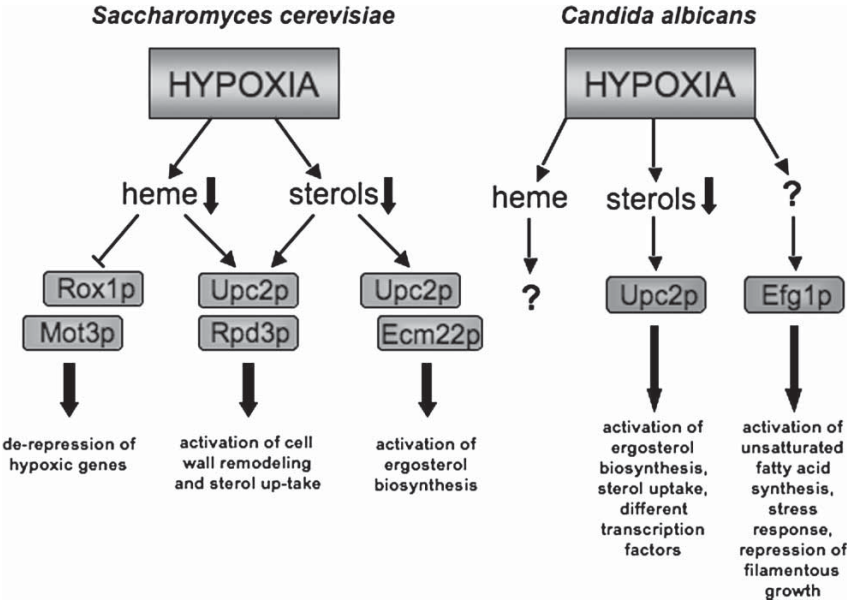

Fig. 1 Schematic of the oxygen sensing pathways in *Saccharomyces cerevisiae* and *Candida albicans*. The proteins are defined in the text.

© 2009 ISHAM, *Medical Mycology*

Downloaded By: [Montana State University Bozeman] At: 20:30 11 December 2009

Table 1 Hypoxia sensing mechanisms and pathways

Hypoxia sensing pathways	Mammals	*S. cerevisiae*	*C. albicans*	*S. pombe*	*C. neoformans*	*A. fumigatus*
HIF pathway	a) HIF-1a, HIF-2a, HIF-3a; HIF-1b	No homolog found	No homolog found	No homolog found	No homolog found	No homolog found
Heme level sensing pathways	No homolog found	a) Hap1p/ Rox1p/Mot3p	Rfg1p* (Rox1p homolog)	No homolog found	No homolog found	No homolog found
	No homolog found	b) Yap1p/Ord1p	Cap1p[x]	Pap1p[x]	No homolog found	AfYap1[x]
Sterol sensing pathways	b) SREBP-1(a/c)*, SREBP-2*, SCAP*, INSIG-1*, INSIG-2*, S1P*, S2P*	c) Upc2p[y]/ Ecm22p	Upc2p[y]	Sre1p, Scp1p, Ins1p*	a) Sre1p, Scp1p, Stp1p*	SrbA, InsA*
Tco1 hypoxia sensing pathways	Not known	No known	Nik1p[x]	No known	b) Tco1p	Bos1[x]
Regulated pathways in response to activation of hypoxia sensing pathways	Regulated by a): erythropoiesis and iron metabolism (e.g., erythropoietin and transferrin); oxygen transport (e.g., adrenomedullin) glucose uptake and glycolysis (e.g., glucose transporter 1, Lactate dehydrogenase A)	Regulated by a): e.g., heme biosynthesis (*HEM13*), cell wall remodeling (*DAN/TIR* genes); fatty acid synthesis (*OLE1*); eIF-5a factor subunit AnbIp; respiration and ATP exchange (*COX5b*; *ACC3*)	Regulated by Upc2p: azole drug resistance and sterol biosynthesis (*ERG11*); several transcription factors (*INO2*, *ACE2*, *SUT1*, *UPC2*); corticosteroid uptatke (*CBP1*);	Regulated by Sre1p: heme biosynthesis (*HEM13*, *HEM14*, *HEM15*); sphingolipid biosynthesis (e.g., *SPBC887.15c*); fatty acid biosynthesis (e.g., *CUT6*); ergosterol biosynthesis (e.g., *ERG1*, *ERG5*, *ERG6*, *ERG11*, *ERG25*)	Regulated by a): iron uptake (e.g., *SIT1* and *FRE7*); azol drug resistance and sterol biosynthesis (e.g., *ERG3*, *ERG11*, *ERG25*); crucial for virulence	Regulated by SrbA: resistance to azole drugs and sterol biosynthesis (*erg25*, erg24, and *erg3*); transporters and cell wall related genes; cell polarity; crucial for virulence
	Regulated by b): lipid synthesis (cholesterol biosynthesis and uptake)	Regulated by b): cell wall mannoproteins (*TIR1/SRP1*)			Regulated by b): no impact on expression of hypoxic genes-may be post-transcriptional regulation?; required for virulence	
		Regulated by c): cell wall remodeling (*DAN/TIR* genes); ergosterol biosynthesis and sterol uptake (e.g., *ERG2*, *ERG3*, *ERG10*, *DAN2*, *DAN4*)				

*No role in hypoxia response.
[x]role in hypoxia unknown.
[y]SREBP analog.

© 2009 ISHAM, *Medical Mycology*

Downloaded By: [Montana State University Bozeman] At: 20:30 11 December 2009

Candida albicans

Candida albicans is an important human fungal pathogen that causes superficial skin infections as well as deep-seated infections, suggesting that its ability to switch between normoxia and hypoxia is a major determinant of its virulence [68]. In *C. albicans* little is known about mechanisms utilized by this yeast to adapt to hypoxic microenvironments. However, our current knowledge suggests that the transcriptional response to hypoxia differs significantly between *C. albicans* and *S. cerevisiae* in important aspects. Although both are generally referred to as facultative anaerobes, genetics studies, conditions required for anaerobic growth, and genome analyses seem to suggest that these hemiascomycota yeast respond differently to changes in oxygen levels.

First, a homologue (Rfg1p) of the *S. cerevisiae* Rox1p has been identified in *C. albicans*, but Rfg1p does not play a role in the regulation of hypoxic genes in this pathogenic yeast as in *S. cerevisiae* (Table 1). Instead, Rfg1p is a transcriptional regulator that controls filamentous growth, and in that role, is critical for *C. albicans* virulence [69].

Second, *S. cerevisiae* genes involved in glycolysis and fermentation are not stimulated by hypoxia [25,70], but hypoxia induces these genes and genes involved in hyphal growth in *C. albicans* while genes of oxidative metabolism are repressed [68]. During normoxic conditions the global transcription factor Efg1p regulates the expression of genes involved in glycolysis and respiration, but it has no role in controlling the expression of respiratory genes and is not required to upregulate glycolytic gene expression in hypoxia [68,71]. Efg1p also promotes filamentation under normoxic conditions. Recently, it was observed that under hypoxic conditions Efg1p promotes the synthesis of unsaturated fatty acids, the up-regulation of genes involved in the stress response (*HSP12*, *DDR48*, *CTA1*) and represses filamentous growth in *C. albicans*. Thus, the regulatory role of Efg1p in *C. albicans* strongly depends on oxygen [68,72]. Transcriptional analyses observed that Efg1p is required to allow hypoxic regulation of about half of all genes that are normally regulated by hypoxia in *C. albicans*. In an *efg1* mutant, hypoxic upregulation (e.g., *CTA1*) or downregulation (e.g., *RIP1*) of several genes is abolished, and some genes, like *OLE1* encoding a fatty acid desaturase, are ineffectively expressed in hypoxia. Another major function of Efg1p is to prevent hypoxic regulation of numerous genes that are not normally up- or down-regulated under hypoxia [71]. Despite the fact that Efg1p is a major regulator of the hypoxic response in *C. albicans*, a homozygous *efg1* mutant shows no severe change in virulence in comparison to the wild-type [73].

Another transcription factor in *C. albicans* affected by hypoxia, Ace2p, is required for filamentation in response to hypoxic conditions. Ace2p also induces fermentative growth and represses respiration, but it is possible that the effect of Ace2p on metabolism is restricted to normal oxygen conditions. This remains to be tested [74]. Interestingly, an *ace2* null mutant is almost avirulent in an immunocompetent mouse model, while there is only a low degree of attenuation in a neutropenic mouse model [75,76]. This may suggest that different states of the immune system may affect the development of hypoxia *in vivo* i.e. the lack of neutrophils in the neutropenic model minimizes the inflammatory response and hence hypoxic microenvironments encountered by the invading fungus. This remains to be examined and confirmed.

As in *S. cerevisiae* [23,44,46], the cell-wall proteome of *C. albicans* is sensitive to changes in environmental conditions which helps the cell to adjust to harsh environments. For example, iron deprivation and hypoxic conditions affect the expression of cell-wall protein encoding genes, such as iron acquisition and iron-uptake genes, i.e., *RBT5* a gene encoding a predicted GPI protein involved in iron acquisition [68,77,78]. Numerous oxygen-dependent reactions in the cell are carried out by iron-containing enzymes [79]. During hypoxic conditions, there may be competition for iron by iron-containing enzymes, which might lead to an increased expression of cell-wall protein encoding genes involved in iron-acquisition and iron-uptake [80].

Oxygen sensing in Candida albicans

In *S. cerevisiae* it has been observed that the cell senses oxygen availability through cellular heme and sterol levels [27–29]. In *C. albicans*, no apparent homolog of *ScHAP1* exists, but in recent studies a close ortholog of *S. cerevisiae* Upc2p and Ecm22p, both involved in sensing sterol depletion, has been identified. Upc2p, a transcription factor of the zinc cluster family, is an important regulator of the sterol biosynthesis and azole drug resistance in *C. albicans* [81,82] (Fig. 2). Hoot *et al*. [83] showed that transcriptional regulation of *UPC2* expression occurs through Upc2p-dependent as well as a novel Upc2p-independent mechanism. Whether there is also a post-translational control mechanism as described for the mammalian sterol regulator SREBP (discussed in detail below) or as suggested for the *Sc*Upc2p remains to be determined.

Upc2p binds *in vivo* to the promoters of several ergosterol biosynthesis genes and other genes involved

© 2009 ISHAM, *Medical Mycology*

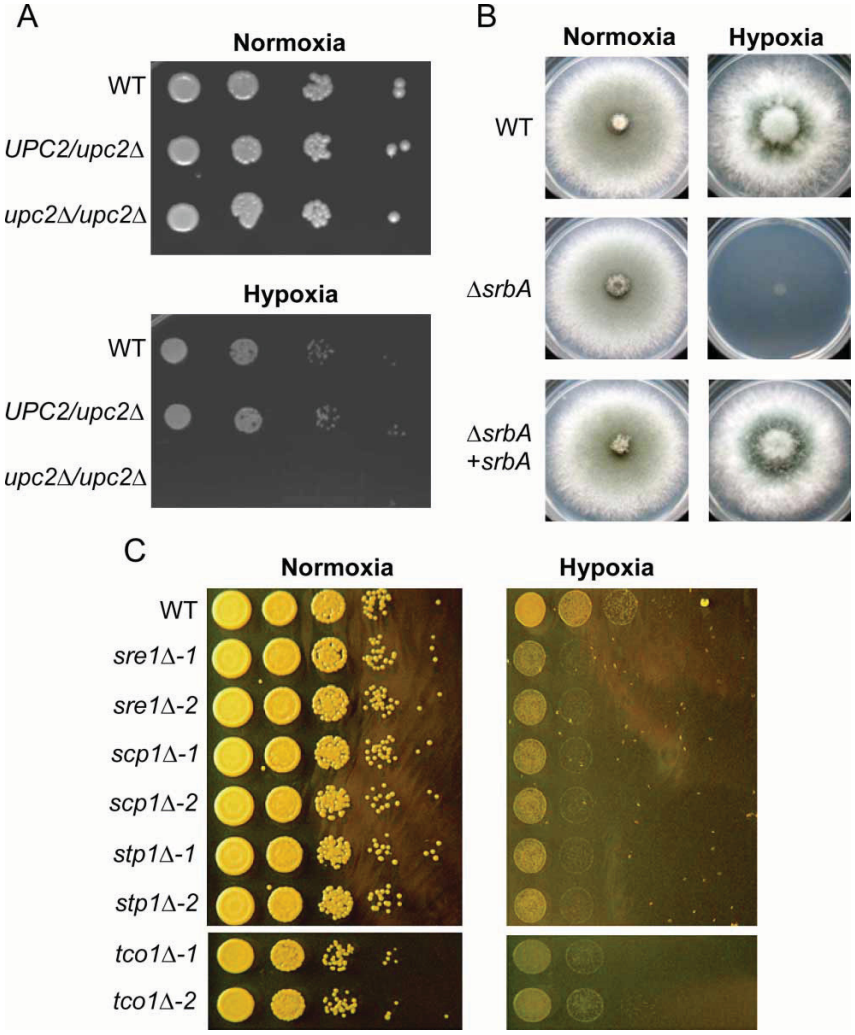

Fig. 2 Mutants in SREBP Pathway and Tco1 are sensitive to hypoxia. Growth in normoxic and hypoxic conditions. (A) *Candida albicans*: a heterozygous *UPC2/upc2*Δ and a homozygous *upc2*Δ/*upc2*Δ *C. albicans* strain were serially diluted and spotted on CSM plates and grown at 30°C. The top panel shows growth in aerobic conditions after 48 h. The bottom panel shows growth in hypoxic conditions after 96 h. Under hypoxic conditions the wild-type (WT) and the heterozygous strain showed comparable growth but the homozygous deletion strain did not demonstrate any detectable growth (Courtesy Chelsea Samaniego and Dr Theodore C. White); (B) *Aspergillus fumigatus*: 1×10^6 conidia were plated on GMM plates and incubated at 37°C under normoxic and hypoxic conditions for 48 h. The wild-type and the reconstituted strain grew comparably under hypoxic conditions while no growth was detectable for the mutant strain (modified from Willger *et al.* [124]); (C) *Cryptococcus neoformans*: *C. neoformans* cultures diluted to $OD_{600nm} = 0.6$ were diluted serially in 10-fold increments prior to being spotted onto YPD plates. The plates were incubated in normoxic or hypoxic conditions in the dark at 37°C. Under hypoxic conditions all mutants in the SREBP pathway and the *tco1*Δ mutants showed reduced growth compared to the wild-type (modified from Chun *et al.* [100]).

or predicted to be involved in lipid metabolism. Znaidi *et al.* [84] observed that up-regulation of *ERG11* during hypoxia is strictly Upc2p dependent. Upc2p also binds the promoters of four genes encoding transcription factors (*INO2*, *ACE2*, *SUT1*, and *UPC2* itself). One of them, Sut1p, controls sterol uptake in *S. cerevisiae* [57,85] suggesting that in *C. albicans* Upc2p and Sut1p may interact in a sterol regulatory network [84].

Interestingly, Upc2p also binds to the promoter of *CBP1*, which was shown to encode a corticosteroid binding protein in *C. albicans* [86]. *C. albicans* appears to take up steroids and possibly metabolic precursors from the host, and Upc2p seems to play a role in corticosteroid uptake from mammals and in adaptation of *C. albicans* to hypoxic conditions in the host [84]. Thus, an emerging theme with studies in *S. cerevisiae* and *C. albicans* is the role of sterol homeostasis in adaptation to hypoxic microenvironments. This theme will also be expanded on in additional fungi discussed below with the discovery of SREBP orthologs. A summary of the known hypoxia regulation mechanisms in *C. albicans* is presented in Fig. 1 and Table 1.

Fungi with SREBP orthologs

Schizosaccharomyces pombe

Recently, a novel mechanism of hypoxia adaptation mediated by a highly conserved family of transcription factors, the SREBPs, was characterized in *Schizosaccharomyces pombe* [87]. *S. pombe*, also called 'fission yeast', is a non-pathogenic yeast that is used as a model organism in molecular and cell biology. SREBPs are a family of endoplasmic reticulum (ER) membrane bound transcription factors first identified in mammals as regulators of cholesterol and fatty acid synthesis

© 2009 ISHAM, *Medical Mycology*

Downloaded By: [Montana State University Bozeman] At: 20:30 11 December 2009

Downloaded By: [Montana State University Bozeman] At: 20:30 11 December 2009

[88–92]. SREBPs contain two transmembrane segments and are inserted into ER membranes in a hairpin fashion such that the N- and C-terminal ends of the protein are in the cytosol. SREBP is synthesized as an inactive membrane-bound precursor that forms a complex with SCAP (SREBP Cleavage-Acting Protein), a multispan membrane protein that is a component of the sterol sensor [90]. Under conditions with enough available sterols, the SREBP-SCAP complex is retained in the ER membrane through binding of SCAP to the resident ER protein Insig [93]. In sterol-depleted cells, SCAP changes its confirmation, which releases the SREBP-SCAP complex from Insig [94]. SCAP then escorts SREBP from the ER to the Golgi apparatus where SREBP is activated by two sequential proteolytic events catalyzed by site-1 and site-2 proteases that release the N-terminal transcription factor domain from the membrane, allowing the transcription factor to enter the nucleus and direct the transcription of target genes [90,95].

In *S. pombe* apparent orthologs of SREBP (*SRE1*), SCAP (*SCP1*) and Insig (*INS1*) have been identified and characterized. Sre1p is cleaved and activated in response to sterol depletion and hypoxia, and stimulates transcription of genes required for adaptation to hypoxia such as genes involved in heme, sphingolipid, ubiquinone, and ergosterol biosynthesis (Fig. 3 and Table 1) [87,96]. Thus, in fission yeast, Sre1p and Scp1p appear to monitor-oxygen dependent sterol synthesis as an indirect measure of oxygen supply. Interestingly, there does not appear to be an impact of Ins1p on the SREBP pathway in fission yeast. In addition, Hughes and Espenshade [97] recently identified another component of this pathway, Ofd1p. Ofd1p is a prolyl 4-hydroxylase-like 2-oxoglutarate-Fe(II) dioxygenase that accelerates Sre1p degradation in the presence of oxygen. The N-terminal dioxygenase domain is an oxygen sensor that regulates the activity of the C-terminal degradation domain [97]. Altogether, the SREBP pathway functions as an oxygen sensor and is required for adaptation to hypoxia in fission yeast. However, the critical function of Sre1 in allowing hypoxic adaptation and subsequent growth is not clearly defined. It seems likely that Sre1 is playing a pleiotropic role in regulating many different genes required for yeast cells to adapt and grow in hypoxia.

Orthologs of the SREBP pathway were recently identified and characterized in the human fungal pathogens *C. neoformans* and *A. fumigatus.* Yet, the exact components and the mechanism behind SREBP regulation largely remain to be determined in these pathogenic fungi. Moreover, it appears that the SREBP pathway is similar in function to the Upc2p mediated pathway in *S. cerevisiae* and *C. albicans*, but the mechanisms behind the similarities and differences between these two pathways is currently not clear.

Cryptococcus neoformans

Unlike the Ascomycete yeast *S. cerevisiae* and *C. albicans*, the Basidiomycete yeast *Cryptococcus neoformans* is generally considered an obligate aerobe. *Cryptococcus* species cause the disease Cryptococcosis

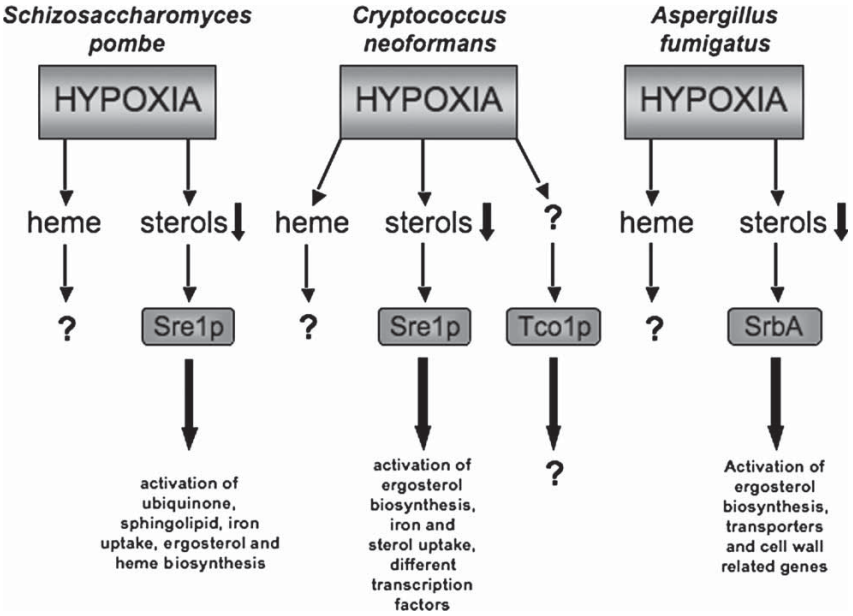

Fig. 3 Schematic of the oxygen sensing pathways in *Schizosaccharomyces pombe*, *Cryptococcus neoformans* and *Aspergillus fumigatus.* The proteins are defined in the text.

© 2009 ISHAM, *Medical Mycology*

Downloaded By: [Montana State University Bozeman] At: 20:30 11 December 2009

in both immunocompromised and apparently healthy hosts and are the most common cause of fungal meningitis [98]. *C. neoformans* is primarily found in pigeon droppings and soil contaminated with avian guanos throughout the world [99]. One would speculate that these environments are relatively oxygen poor suggesting that *C. neoformans* likely has evolved mechanisms to adapt to low oxygen microenvironments. In the laboratory, *C. neoformans* grows optimally under atmospheric oxygen conditions (21%), but oxygen concentrations in the human brain are drastically lower than in the atmosphere and vary significantly among anatomical sites [2]. Thus, in order to establish an infection in the brain, it seems likely that *C. neoformans* must adapt to reduced oxygen levels during infection. Therefore, discovering the mechanisms utilized by *C. neoformans* to sense and adapt to low-oxygen conditions is an important area of research aimed towards understanding the pathobiology of this pathogenic yeast. Yet, until recently, the importance of hypoxia adaptation in *C. neoformans* biology and virulence has been largely unstudied.

Recent whole-genome microarray-based transcriptional profiling of *C. neoformans* in a hypoxic microenvironment has started to reveal genes and pathways regulated in response to hypoxia. Among them are genes involved in hexose uptake (sugar transporter and hexose transporter), ethanol production (pyruvate decarboxylase and alcohol dehydrogenases), and sterol metabolism (ergosterol biosynthesis genes) [100]. The possibility of fermentation being important for hypoxic growth during infection is supported by another study, where ethanol was found in cerebral tissue of rats infected with *C. neoformans* [101]. Yet the importance of fermentation pathways in this obligate aerobe's ability to cause disease and grow in hypoxic microenvironments is unknown. However, as with other yeasts we have discussed, and the filamentous mold *A. fumigatus*, sterol biosynthesis and homeostasis seems to be a common mechanism regulating adaptation to low oxygen environments in fungi.

The SREBP pathway in Cryptococcus neoformans

Orthologs of SREBP (*SRE1*), SCAP (*SCP1*) and a Site-2-protease (*STP1*) were identified and characterized in *C. neoformans* [100,102]. *C. neoformans* appears to lack an identifiable homologue of Insig, the ER retention-protein that controls ER-to-Golgi transport of SREBP-SCAP complex in mammalian cells. This finding is consistent with *S. pombe* data which suggests that Insig is not required for sterol-dependent regulation of Sre1p and Scp1p [87,102]. However, as in fission yeast, the SREBP pathway mediated by Sre1p and Scp1p in *C. neoformans* is crucial for adaptation to hypoxia and sterol biosynthesis (Fig. 2). In addition, unlike in *S. pombe*, Sre1p controls low-oxygen expression of genes required for two different pathways of iron uptake (*SIT1* and *FRE7*) [102], which might be crucial for survival under hypoxic conditions. Importantly, *sre1*Δ mutants fail to proliferate in host tissue, fail to cause fatal meningoencephalitis, and display hypersensitivity to the azole class of antifungal drugs (Table 1 and Fig. 3) [100,102]. It is unclear if the virulence defect is due to deficiencies in iron homeostasis, a known virulence attribute of pathogenic fungi, or the inability of *C. neoformans* to grow in low oxygen microenvironments in the absence of Sre1p. The two phenotypes are likely not mutually exclusive given the importance of iron in ergosterol biosynthesis. However, it is clear that *C. neoformans* needs Sre1p activation to adapt to the host environment. Mechanisms linking ergosterol biosynthesis, iron homeostasis, and fungal virulence in this pathogenic yeast remain unknown. Identification and characterization of additional components of the SREBP pathway are likely to yield important insights into how this pathogenic yeast causes disease.

In order to identify novel Sre1p pathway components in *C. neoformans*, Lee *et al.* [103] observed that responses to cobalt chloride [$CoCl_2$) in *C. neoformans* mimic certain aspects of hypoxia by targeting enzymes in the sterol biosynthesis pathway. $CoCl_2$ has been widely used as a hypoxia-mimicking agent in mammalian systems [104–108], but the mechanisms by which it induces hypoxia-mimicking responses are not fully understood. However, Sre1p is required for adaptation to $CoCl_2$ in *C. neoformans.* Upon $CoCl_2$ treatment, Sre1p is likely activated in response to sterol defects caused by the inhibition of several enzymatic steps in the ergosterol biosynthetic pathway. $CoCl_2$ treatment leads to increased levels of sterol intermediates, including the substrates of Erg25p, 4,4-dimethylfecosterol and 4-methylfecosterol, demonstrating that Sre1p regulates sterol homeostasis in response to $CoCl_2$. $CoCl_2$-induced sterol synthesis inhibition and Sre1p activation has also been observed in *S. pombe*, suggesting a conserved role for Sre1p in the adaptation to elevated levels of transition metals [103,109].

Consequently, $CoCl_2$ treatment has been used to screen for pathways involved in oxygen sensing in *C. neoformans.* In this context Ingavale *et al.* [109] observed that $CoCl_2$ sensitivity and/or oxygen sensing and adaptation processes in *C. neoformans* have a complex nature. Importantly they identified several mutants with increased sensitivity to $CoCl_2$ and they

© 2009 ISHAM, *Medical Mycology*

observed that most of the $CoCl_2$ sensitive mutants are also sensitive to low oxygen concentrations. Mutants included genes involved in the sterol biosynthesis pathway such as *SCP1*, *SRE1, ERG5*, mutants in genes involved in mitochondrial function and energy metabolism such as H^+ transporting ATP synthase, NADH:ubiquinone oxidoreductase or ATP:ADP anitporter, and various transporters and enzymes such as hexose transport related protein, seroheme synthase, amino acid transporter and myo-inositol oxygenase. The role of these genes and pathways in fungal virulence has yet to be explored, but the apparent role of the mitochondria in hypoxia adaptation in *C. neoformans* echoes the recent findings in *S. cerevisiae* discussed above.

The two-component like (Tco) system in Cryptococcus neoformans

Additional studies observed that the Sre1p pathway acts in parallel with a two-component signal transduction like pathway controlled by Tco1p in hypoxic adaptation of *C. neoformans* [100]. Tco1p is a member of a highly conserved family of fungal-specific histidine kinases. Tco1p negatively regulates the expression of melanin formation and, redundantly with Tco2p, positively regulates the HOG MAPK pathway [which is dispensable for virulence) [110]. Interestingly, it has been shown that Tco1p is required for growth under hypoxic conditions and for virulence of *C. neoformans* (Fig. 2) [100,110]. However, it is unclear how this pathway is involved in hypoxic adaptation and fungal virulence (Fig. 3). In contrast to mutants in *SRE1*, the *tco1* mutant shows no detectable defects in the regulation of any of the known hypoxic genes ([100], unpublished data). As a result Chun *et al*. [100] hypothesize that the Tco1p pathway might act post-transcriptionally. However, this result may also indicate that novel pathways or altered function of existing known pathways regulated by Tco1p are involved in hypoxia adaptation. Clearly, however, these data suggest that oxygen sensing in *C. neoformans* is highly complex, and likely important for virulence of this organism.

Aspergillus fumigatus

A. fumigatus is a saprophytic, obligate aerobic filamentous fungus commonly found in soil and compost piles. Its primary ecological function is to recycle carbon and nitrogen through the environment [111–113]. As with most fungi, it seems self-evident that these microenvironments would place significant oxygen related stress on the mold. While *A. fumigatus* is responsible for a number of clinically relevant diseases, invasive pulmonary aspergillosis (IPA) is the most lethal with mortality rates ranging from 60–90% [114–116]. Interestingly, while IPA can be caused by several *Aspergillus* species, the majority of IPA cases are caused by *A. fumigatus*. This may suggest that *A. fumigatus* contains unique attributes that allow it to cause disease [117].

Currently, we have a limited understanding of the *in vivo* growth mechanisms of *A. fumigatus* during IPA [118]. Given that the lung is the primary site of infection for this mold, it may be counter-intuitive to think that low oxygen levels would be a critical component of the pathophysiology of IPA. However, during infection, *A. fumigatus* causes significant damage to host tissue through invasive growth by hyphae and subsequent recruitment of immune effector cells (depending on the immune system status of the host). Thus, infection generates significant inflammation and necrosis in lung tissue that can be visualized by histopathology. These pathologic lesions also likely represent areas of poor oxygen availability to the pathogen and host. Thus, it is likely that to cause disease *A. fumigatus* must adapt to hypoxic conditions.

In general, mechanisms of hypoxia adaptation in molds have gone largely unstudied. Tarrand *et al*. [119,120] hypothesized that the low rate of *Aspergillus* recovery from clinical material is due to adaptation by the fungus to the physiologic temperature and hypoxic milieu found *in vivo*. However, recent studies with *A. fumigatus* suggest that it cannot grow in anaerobic environments [121]. Interestingly, studies with the relatively non-pathogenic model mold *A. nidulans* observed that while the mold could not proliferate without oxygen, ethanol fermentation was required for its long-term survival in anaerobic conditions [122,123]. Indeed, analyses of *Aspergillus* genome sequences have revealed numerous potential fermentation pathways in these molds. Yet, as obligate aerobes, it remains unclear what function these pathways may serve in hypoxia adaptation and fungal virulence. Recent studies in our laboratory have identified ethanol fermentation during *A. fumigatus* infection in a murine model of IPA indicating that fermentation may be a component of the virulence arsenal of this mold (Grahl *et al*. unpublished data). However, our knowledge about the mechanisms by which *A. fumigatus*, an obligate aerobe, adapts to hypoxic environments remains extremely limited.

The SREBP pathway in Aspergillus fumigatus

Recently, our laboratory identified and characterized an SREBP (Sre1p) ortholog, SrbA, in *A. fumigatus* [124]. As in *C. neoformans*, SrbA is crucial for

© 2009 ISHAM, *Medical Mycology*

Downloaded By: [Montana State University Bozeman] At: 20:30 11 December 2009

adaptation to hypoxia, mediates resistance to the azole class of antifungal drugs and is involved in sterol biosynthesis in *A. fumigatus* (Fig. 2 and Fig. 3). In addition, unlike *C. neoformans*, but similar to *S. pombe,* transcriptional profiling of the SrbA null mutant suggested that SrbA does not appear to be involved in iron uptake or homeostasis in *A. fumigatus.* However, these studies may have been limited by the type of media utilized, and direct studies regarding the role of SrbA in iron homeostasis in this pathogenic mold are ongoing.

Importantly, *srbA* null mutants are almost avirulent in two distinct murine models of IPA. While our results strongly suggest that the virulence defect is due to the inability of this mutant to grow in hypoxia due to the loss of hypoxia adaptation mechanisms regulated by SrbA, as with *C. neoformans,* other potential hypotheses may explain the attenuation of virulence [124]. For example, SrbA plays an important role in maintenance of cell polarity in *A. fumigatus* [124]. We hypothesize that the accumulation of sterol intermediates leads to dysfunction in the formation or localization of sterol microdomains known to be required for maintaining cell polarity. Thus, the alteration of cell polarity may inhibit the ability of the SrbA mutant to cause disease. Yet, the mutant displays a normal growth rate *in vitro* suggesting that the altered cell polarity does not alter growth in these conditions. Altogether, these data promote the hypothesis that hypoxia plays a key role in the pathophysiology of IPA. At the least, it is apparent that SREBPs are critical components of fungal virulence in both pathogenic yeast and molds.

So far the molecular mechanism behind SrbA regulation and activation in molds is unclear. In the yeast *S. pombe* and *C. neoformans*, it seems evident that Sre1p is regulated post-translationally in response to sterol biosynthesis perturbation that occurs in low oxygen environments. Indeed, Hughes *et al*. [125] have identified 4-methyl sterols as the primary activating agent of Sre1p in *S. pombe* and *C. neoformans.* Thus, our finding that the SrbA null mutant in *A. fumigatus* accumulates 4-methyl sterols may also suggest that these sterols are the trigger for SrbA activation in *A. fumigatus* [124].

While many of the phenotypes observed in the *A. fumigatus srbA* mutant may suggest that SrbA is regulated in a similar manner as Sre1p in yeast, our results may also suggest an alternative model in molds. For example, despite intense bioinformatic analyses, we have been unable to identify clear homologs of SCAP or the proteases required for Sre1p activation. We have, however, identified a potential Insig1 homolog (*insA*) and we are currently characterizing a possible role for InsA in SREBP signaling in filamentous fungi. Yet, given the conservation of SCAP across many organisms, it is surprising that an ortholog does not appear to be present in the *Aspergilli*. It may be that another protein with a divergent sequence performs a similar function as SCAP, or it may suggest that a novel mechanism of SREBP regulation and activation exists in molds. Studies to examine these potential mechanisms are ongoing in our laboratory.

Conclusion

In this review we have attempted to survey the known mechanisms utilized by fungi to regulate adaptation to hypoxic microenvironments. It is clear that we are just beginning to understand the mechanisms human fungal pathogens use to survive *in vivo* during infection. With the possible exception of SREBPs, the molecular mechanisms utilized by pathogenic fungi to adapt to hypoxic microenvironments found at sites of infection remain to be elucidated. A master regulator of hypoxia adaptation, such as HIF1 found in mammals, has not been identified in fungi. It remains to be seen whether one exists, or, if as suggested by current data, fungi rely on multiple mechanisms to sense oxygen levels and adapt to low oxygen environments.

In any case, we feel that this area of pathogenic fungal physiology has been ignored for too long. Certainly, some mechanisms of hypoxia adaptation, perhaps such as heme biosynthesis, are likely to be conserved between *S. cerevisiae* and the human pathogenic fungi. However, the different life-styles and selection pressures on non-pathogenic and pathogenic fungi likely have resulted in unique mechanisms of hypoxia adaptation. Thus, solely relying on *S. cerevisiae* as a model for how pathogenic regulate adaptation to hypoxic microenvironments is likely not appropriate. Regardless, it seems clear that mechanisms of hypoxia adaptation have important implications for fungal virulence and how we manage and treat invasive fungal infections. Therefore, future studies on discovering the conserved and unique pathways utilized by the major fungal pathogens of humans to adapt to hypoxia are likely to yield important insights into sterol metabolism, fungal growth, mechanisms of drug resistance, and fungal virulence.

Acknowledgements

RAC is currently supported by funding from the National Institutes of Health, COBRE grant RR020185, and the Montana State University Agricultural Experiment Station.

© 2009 ISHAM, *Medical Mycology*

Downloaded By: [Montana State University Bozeman] At: 20:30 11 December 2009

Declaration of interest: The authors report no conflicts of interest. The authors alone are responsible for the content and writing of the paper.

References

1 McNeil MM, Nash SL, Hajjeh RA, *et al*. Trends in mortality due to invasive mycotic diseases in the United States, 1980–1997. *Clin Infect Dis* 2001; **33**: 641–647.
2 Erecinska M, Silver IA. Tissue oxygen tension and brain sensitivity to hypoxia. *Respir Physiol* 2001; **128**: 263–276.
3 Carlsson PO, Palm F, Andersson A, Liss P. Markedly decreased oxygen tension in transplanted rat pancreatic islets irrespective of the implantation site. *Diabetes* 2001; **50**: 489–495.
4 Studer L, Csete M, Lee SH, *et al*. Enhanced proliferation, survival, and dopaminergic differentiation of CNS precursors in lowered oxygen. *J Neurosci* 2000; **20**: 7377–7383.
5 West JB. *Respiratory Physiology – The Essentials*, 3 edn. Baltimore, MD, USA: Williams & Wilkins, 1985.
6 Warn PA, Sharp A, Guinea J, Denning DW. Effect of hypoxic conditions on *in vitro* susceptibility testing of amphotericin B, itraconazole and micafungin against *Aspergillus* and *Candida*. *J Antimicrob Chemother* 2004; **53**: 743–749.
7 Matherne GP, Headrick JP, Coleman SD, Berne RM. Interstitial transudate purines in normoxic and hypoxic immature and mature rabbit hearts. *Pediatr Res* 1990; **28**: 348–353.
8 Van Belle H, Goossens F, Wynants J. Formation and release of purine catabolites during hypoperfusion, anoxia, and ischemia. *Am J Physiol* 1987; **252**(5 Pt 2): H886–893.
9 Dewhirst MW. Concepts of oxygen transport at the microcirculatory level. *Semin Radiat Oncol* 1998; **8**: 143–150.
10 Arnold F, West D, Kumar S. Wound healing: the effect of macrophage and tumour derived angiogenesis factors on skin graft vascularization. *Br J Exp Pathol* 1987; **68**: 569–574.
11 Simmen HP, Battaglia H, Giovanoli P, Blaser J. Analysis of pH, pO2 and pCO2 in drainage fluid allows for rapid detection of infectious complications during the follow-up period after abdominal surgery. *Infection* 1994; **22**: 386–389.
12 Schofield CJ, Ratcliffe PJ. Signalling hypoxia by HIF hydroxylases. *Biochem Biophys Res Commun* 2005; **338**: 617–626.
13 Gordan JD, Simon MC. Hypoxia-inducible factors: central regulators of the tumor phenotype. *Curr Opin Genet Dev* 2007; **17**: 71–77.
14 Wenger RH. Cellular adaptation to hypoxia: O2-sensing protein hydroxylases, hypoxia-inducible transcription factors, and O2-regulated gene expression. *Faseb J* 2002; **16**: 1151–1162.
15 Maxwell PH, Dachs GU, Gleadle JM, *et al*. Hypoxia-inducible factor-1 modulates gene expression in solid tumors and influences both angiogenesis and tumor growth. *Proc Natl Acad Sci USA* 1997; **94**: 8104–8109.
16 Thiel M, Chouker A, Ohta A, *et al*. Oxygenation inhibits the physiological tissue-protecting mechanism and thereby exacerbates acute inflammatory lung injury. *PLoS Biol* 2005; **3**: e174.
17 Brock M, Jouvion G, Droin-Bergere S, *et al*. Bioluminescent *Aspergillus fumigatus*, a new tool for drug efficiency testing and in vivo monitoring of invasive aspergillosis. *Appl Environ Microbiol* 2008; **74**: 7023–7035.
18 Perkhofer S, Jost D, Dierich MP, Lass-Florl C. Susceptibility testing of anidulafungin and voriconazole alone and in combination against conidia and hyphae of *Aspergillus* spp. under hypoxic conditions. *Antimicrob Agents Chemother* 2008; **52**: 1873–1875.
19 Lowry CV, Zitomer RS. Oxygen regulation of anaerobic and aerobic genes mediated by a common factor in yeast. *Proc Natl Acad Sci USA* 1984; **81**: 6129–6133.
20 Zitomer RS, Lowry CV. Regulation of gene expression by oxygen in *Saccharomyces cerevisiae*. *Microbiol Rev* 1992; **56**: 1–11.
21 Choi JY, Stukey J, Hwang SY, Martin CE. Regulatory elements that control transcription activation and unsaturated fatty acid-mediated repression of the *Saccharomyces cerevisiae OLE1* gene. *J Biol Chem* 1996; **271**: 3581–3589.
22 Evangelista CC, Jr, Rodriguez Torres AM, Limbach MP, Zitomer RS. Rox3 and Rts1 function in the global stress response pathway in baker's yeast. *Genetics* 1996; **142**: 1083–1093.
23 Sertil O, Cohen BD, Davies KJ, Lowry CV. The DAN1 gene of *S. cerevisiae* is regulated in parallel with the hypoxic genes, but by a different mechanism. *Gene* 1997; **192**: 199–205.
24 Kwast KE, Burke PV, Staahl BT, Poyton RO. Oxygen sensing in yeast: evidence for the involvement of the respiratory chain in regulating the transcription of a subset of hypoxic genes. *Proc Natl Acad Sci USA* 1999; **96**: 5446–5451.
25 ter Linde JJ, Liang H, Davis RW, *et al*. Genome-wide transcriptional analysis of aerobic and anaerobic chemostat cultures of *Saccharomyces cerevisiae*. *J Bacteriol* 1999; **181**: 7409–7413.
26 Zitomer RS, Carrico P, Deckert J. Regulation of hypoxic gene expression in yeast. *Kidney Int* 1997; **51**: 507–513.
27 Zhang L, Hach A. Molecular mechanism of heme signaling in yeast: the transcriptional activator Hap1 serves as the key mediator. *Cell Mol Life Sci* 1999; **56**: 415–426.
28 Hon T, Dodd A, Dirmeier R, *et al*. A mechanism of oxygen sensing in yeast. Multiple oxygen-responsive steps in the heme biosynthetic pathway affect Hap1 activity. *J Biol Chem* 2003; **278**: 50771–50780.
29 Davies BS, Rine J. A role for sterol levels in oxygen sensing in *Saccharomyces cerevisiae*. *Genetics* 2006; **174**: 191–201.
30 Labbe-Bois R, Labbe P. *Tetrapyrrole and heme biosynthesis in the yeast Saccharomyces cerevisiae*. In: Dailey HA (ed.). Biosynthesis of Heme and Chlorophylls. New York: McGraw-Hill Publishing Co, 1990: 235–285.
31 Creusot F, Verdiere J, Gaisne M, Slonimski PP. *CYP1* [*HAP1*) regulator of oxygen-dependent gene expression in yeast. I. Overall organization of the protein sequence displays several novel structural domains. *J Mol Biol* 1988; **204**: 263–276.
32 Pfeifer K, Kim KS, Kogan S, Guarente L. Functional dissection and sequence of yeast HAP1 activator. *Cell* 1989; **56**: 291–301.
33 Zhang L, Guarente L. Heme binds to a short sequence that serves a regulatory function in diverse proteins. *Embo J* 1995; **14**: 313–320.
34 Pfeifer K, Arcangioli B, Guarente L. Yeast *HAP1* activator competes with the factor *RC2* for binding to the upstream activation site UAS1 of the *CYC1* gene. *Cell* 1987; **49**: 9–18.
35 Cerdan ME, Zitomer RS. Oxygen-dependent upstream activation sites of *Saccharomyces cerevisiae* cytochrome c genes are related forms of the same sequence. *Mol Cell Biol* 1988; **8**: 2275–2279.
36 Zhang L, Guarente L. The yeast activator *HAP1* – a *GAL4* family member – binds DNA in a directly repeated orientation. *Genes Dev* 1994; **8**: 2110–2119.
37 Lowry CV, Zitomer RS. *ROX1* encodes a heme-induced repression factor regulating *ANB1* and *CYC7* of *Saccharomyces cerevisiae*. *Mol Cell Biol* 1988; **8**: 4651–4658.
38 Balasubramanian B, Lowry CV, Zitomer RS. The Rox1 repressor of the *Saccharomyces cerevisiae* hypoxic genes is a specific

© 2009 ISHAM, *Medical Mycology*

Downloaded By: [Montana State University Bozeman] At: 20:30 11 December 2009

DNA-binding protein with a high-mobility-group motif. *Mol Cell Biol* 1993; **13**: 6071–6078.
39 Deckert J, Perini R, Balasubramanian B, Zitomer RS. Multiple elements and auto-repression regulate Rox1, a repressor of hypoxic genes in *Saccharomyces cerevisiae*. *Genetics* 1995; **139**: 1149–1158.
40 Kang HA, Schwelberger HG, Hershey JW. The two genes encoding protein synthesis initiation factor eIF-5A in *Saccharomyces cerevisiae* are members of a duplicated gene cluster. *Mol Gen Genet* 1992; **233**: 487–490.
41 Zagorec M, Labbe-Bois R. Negative control of yeast coproporphyrinogen oxidase synthesis by heme and oxygen. *J Biol Chem* 1986; **261**: 2506–2509.
42 Klinkenberg LG, Mennella TA, Luetkenhaus K, Zitomer RS. Combinatorial repression of the hypoxic genes of *Saccharomyces cerevisiae* by DNA binding proteins Rox1 and Mot3. *Eukaryot Cell* 2005; **4**: 649–660.
43 Zhang L, Hach A, Wang C. Molecular mechanism governing heme signaling in yeast: a higher-order complex mediates heme regulation of the transcriptional activator *HAP1*. *Mol Cell Biol* 1998; **18**: 3819–3828.
44 Abramova N, Sertil O, Mehta S, Lowry CV. Reciprocal regulation of anaerobic and aerobic cell wall mannoprotein gene expression in *Saccharomyces cerevisiae*. *J Bacteriol* 2001; **183**: 2881–2887.
45 Sertil O, Kapoor R, Cohen BD, Abramova N, Lowry CV. Synergistic repression of anaerobic genes by Mot3 and Rox1 in *Saccharomyces cerevisiae*. *Nucleic Acids Res* 2003; **31**: 5831–5837.
46 Abramova NE, Cohen BD, Sertil O, *et al*. Regulatory mechanisms controlling expression of the *DAN*/*TIR* mannoprotein genes during anaerobic remodeling of the cell wall in *Saccharomyces cerevisiae*. *Genetics* 2001; **157**: 1169–1177.
47 Sertil O, Vemula A, Salmon SL, Morse RH, Lowry CV. Direct role for the Rpd3 complex in transcriptional induction of the anaerobic *DAN*/*TIR* genes in yeast. *Mol Cell Biol* 2007; **27**: 2037–2047.
48 Vik A, Rine J. Upc2p and Ecm22p, dual regulators of sterol biosynthesis in Saccharomyces cerevisiae. *Mol Cell Biol* 2001; **21**: 6395–6405.
49 Germann M, Gallo C, Donahue T, *et al*. Characterizing sterol defect suppressors uncovers a novel transcriptional signaling pathway regulating zymosterol biosynthesis. *J Biol Chem* 2005; **280**: 35904–35913.
50 Lewis TL, Keesler GA, Fenner GP, Parks LW. Pleiotropic mutations in *Saccharomyces cerevisiae* affecting sterol uptake and metabolism. *Yeast* 1988; **4**: 93–106.
51 Crowley JH, Leak FW, Jr, Shianna KV, Tove S, Parks LW. A mutation in a purported regulatory gene affects control of sterol uptake in *Saccharomyces cerevisiae*. *J Bacteriol* 1998; **180**: 4177–4183.
52 Wilcox LJ, Balderes DA, Wharton B, *et al*. Transcriptional profiling identifies two members of the ATP-binding cassette transporter superfamily required for sterol uptake in yeast. *J Biol Chem* 2002; **277**: 32466–32472.
53 Marie C, Leyde S, White TC. Cytoplasmic localization of sterol transcription factors Upc2p and Ecm22p in *S. cerevisiae*. *Fungal Genet Biol* 2008; **45**: 1430–1438.
54 Davies BS, Wang HS, Rine J. Dual activators of the sterol biosynthetic pathway of *Saccharomyces cerevisiae*: similar activation/regulatory domains but different response mechanisms. *Mol Cell Biol* 2005; **25**: 7375–7385.
55 Kwast KE, Lai LC, Menda N, *et al*. Genomic analyses of anaerobically induced genes in *Saccharomyces cerevisiae*: functional roles of Rox1 and other factors in mediating the anoxic response. *J Bacteriol* 2002; **184**: 250–265.
56 Bourdineaud JP, De Sampaio G, Lauquin GJ. A Rox1-independent hypoxic pathway in yeast. Antagonistic action of the repressor Ord1 and activator Yap1 for hypoxic expression of the *SRP1*/*TIR1* gene. *Mol Microbiol* 2000; **38**: 879–890.
57 Ness F, Bourot S, Regnacq M, *et al*. *SUT1* is a putative Zn[II]2Cys6-transcription factor whose upregulation enhances both sterol uptake and synthesis in aerobically growing *Saccharomyces cerevisiae* cells. *Eur J Biochem* 2001; **268**: 1585–1595.
58 Ansell R, Granath K, Hohmann S, Thevelein JM, Adler L. The two isoenzymes for yeast NAD+-dependent glycerol 3-phosphate dehydrogenase encoded by *GPD1* and *GPD2* have distinct roles in osmoadaptation and redox regulation. *Embo J* 1997; **16**: 2179–2187.
59 Rachidi N, Martinez MJ, Barre P, Blondin B. *Saccharomyces cerevisiae* PAU genes are induced by anaerobiosis. *Mol Microbiol* 2000; **35**: 1421–1430.
60 Castello PR, David PS, McClure T, Crook Z, Poyton RO. Mitochondrial cytochrome oxidase produces nitric oxide under hypoxic conditions: implications for oxygen sensing and hypoxic signaling in eukaryotes. *Cell Metab* 2006; **3**: 277–287.
61 Castello PR, Woo DK, Ball K, *et al*. Oxygen-regulated isoforms of cytochrome c oxidase have differential effects on its nitric oxide production and on hypoxic signaling. *Proc Natl Acad Sci USA* 2008; **105**: 8203–8208.
62 Gupta KJ, Stoimenova M, Kaiser WM. In higher plants, only root mitochondria, but not leaf mitochondria reduce nitrite to NO, *in vitro* and *in situ*. *J Exp Bot* 2005; **56**: 2601–2609.
63 Nohl H, Staniek K, Sobhian B, *et al*. Mitochondria recycle nitrite back to the bioregulator nitric monoxide. *Acta Biochim Pol* 2000; **47**: 913–921.
64 Nohl H, Staniek K, Kozlov AV. The existence and significance of a mitochondrial nitrite reductase. *Redox Rep* 2005; **10**: 281–286.
65 Planchet E, Jagadis Gupta K, Sonoda M, Kaiser WM. Nitric oxide emission from tobacco leaves and cell suspensions: rate limiting factors and evidence for the involvement of mitochondrial electron transport. *Plant J* 2005; **41**: 732–743.
66 Tischner R, Planchet E, Kaiser WM. Mitochondrial electron transport as a source for nitric oxide in the unicellular green alga *Chlorella sorokiniana*. *FEBS Lett* 2004; **576**: 151–155.
67 Dirmeier R, O'Brien KM, Engle M, *et al*. Exposure of yeast cells to anoxia induces transient oxidative stress. Implications for the induction of hypoxic genes. *J Biol Chem* 2002; **277**: 34773–34784.
68 Setiadi ER, Doedt T, Cottier F, Noffz C, Ernst JF. Transcriptional response of *Candida albicans* to hypoxia: linkage of oxygen sensing and Efg1p-regulatory networks. *J Mol Biol* 2006; **361**: 399–411.
69 Kadosh D, Johnson AD. Rfg1, a protein related to the *Saccharomyces cerevisiae* hypoxic regulator Rox1, controls filamentous growth and virulence in *Candida albicans*. *Mol Cell Biol* 2001; **21**: 2496–2505.
70 Becerra M, Lombardia-Ferreira LJ, Hauser NC, *et al*. The yeast transcriptome in aerobic and hypoxic conditions: effects of *hap1*, *rox1*, *rox3* and *srb10* deletions. *Mol Microbiol* 2002; **43**: 545–555.
71 Ernst JF, Tielker D. Responses to hypoxia in fungal pathogens. *Cell Microbiol* 2008; **11**: 183–190.
72 Doedt T, Krishnamurthy S, Bockmuhl DP, *et al*. APSES proteins regulate morphogenesis and metabolism in *Candida albicans*. *Mol Biol Cell* 2004; **15**: 3167–3180.
73 Lo HJ, Kohler JR, DiDomenico B, *et al*. Nonfilamentous *C. albicans* mutants are avirulent. *Cell* 1997; **90**: 939–949.

© 2009 ISHAM, *Medical Mycology*

Downloaded By: [Montana State University Bozeman] At: 20:30 11 December 2009

74 Mulhern SM, Logue ME, Butler G. *Candida albicans* transcription factor Ace2 regulates metabolism and is required for filamentation in hypoxic conditions. *Eukaryot Cell* 2006; **5**: 2001–2013.
75 Kelly MT, MacCallum DM, Clancy SD, *et al*. The *Candida albicans CaACE2* gene affects morphogenesis, adherence and virulence. *Mol Microbiol* 2004; **53**: 969–983.
76 MacCallum DM, Findon H, Kenny CC, *et al*. Different consequences of *ACE2* and *SWI5* gene disruptions for virulence of pathogenic and nonpathogenic yeasts. *Infect Immun* 2006; **74**: 5244–5248.
77 Lan CY, Rodarte G, Murillo LA, *et al*. Regulatory networks affected by iron availability in *Candida albicans*. *Mol Microbiol* 2004; **53**: 1451–1469.
78 Weissman Z, Kornitzer D. A family of *Candida* cell surface haem-binding proteins involved in haemin and haemoglobin-iron utilization. *Mol Microbiol* 2004; **53**: 1209–1220.
79 Kaplan J, McVey Ward D, Crisp RJ, Philpott CC. Iron-dependent metabolic remodeling in *S. cerevisiae*. *Biochim Biophys Acta* 2006; **1763**: 646–651.
80 Sosinska GJ, de Groot PW, Teixeira de Mattos MJ, *et al*. Hypoxic conditions and iron restriction affect the cell-wall proteome of *Candida albicans* grown under vagina-simulative conditions. *Microbiology* 2008; **154**(Pt 2): 510–520.
81 MacPherson S, Akache B, Weber S, *et al*. *Candida albicans* zinc cluster protein Upc2p confers resistance to antifungal drugs and is an activator of ergosterol biosynthetic genes. *Antimicrob Agents Chemother* 2005; **49**: 1745–1752.
82 Silver PM, Oliver BG, White TC. Role of *Candida albicans* transcription factor Upc2p in drug resistance and sterol metabolism. *Eukaryot Cell* 2004; **3**: 1391–1397.
83 Hoot SJ, Oliver BG, White TC. *Candida albicans* UPC2 is transcriptionally induced in response to antifungal drugs and anaerobicity through Upc2p-dependent and -independent mechanisms. *Microbiology* 2008; **154**(Pt 9): 2748–2756.
84 Znaidi S, Weber S, Al-Abdin OZ, *et al*. Genomewide location analysis of *Candida albicans* Upc2p, a regulator of sterol metabolism and azole drug resistance. *Eukaryot Cell* 2008; **7**: 836–847.
85 Bourot S, Karst F. Isolation and characterization of the *Saccharomyces cerevisiae SUT1* gene involved in sterol uptake. *Gene* 1995; **165**: 97–102.
86 Malloy PJ, Zhao X, Madani ND, Feldman D. Cloning and expression of the gene from *Candida albicans* that encodes a high-affinity corticosteroid-binding protein. *Proc Natl Acad Sci USA* 1993; **90**: 1902–1906.
87 Hughes AL, Todd BL, Espenshade PJ. SREBP pathway responds to sterols and functions as an oxygen sensor in fission yeast. *Cell* 2005; **120**: 831–842.
88 Briggs MR, Yokoyama C, Wang X, Brown MS, Goldstein JL. Nuclear protein that binds sterol regulatory element of low density lipoprotein receptor promoter. I. Identification of the protein and delineation of its target nucleotide sequence. *J Biol Chem* 1993; **268**: 14490–14496.
89 Wang X, Briggs MR, Hua X, *et al*. Nuclear protein that binds sterol regulatory element of low density lipoprotein receptor promoter. II. Purification and characterization. *J Biol Chem* 1993; **268**: 14497–14504.
90 Rawson RB. The SREBP pathway – insights from Insigs and insects. *Nat Rev Mol Cell Biol* 2003; **4**: 631–640.
91 Espenshade PJ. SREBPs: sterol-regulated transcription factors. *J Cell Sci* 2006; **119**(Pt 6): 973–976.
92 Espenshade PJ, Hughes AL. Regulation of sterol synthesis in eukaryotes. *Annu Rev Genet* 2007; **41**: 401–427.
93 Yang T, Espenshade PJ, Wright ME, *et al*. Crucial step in cholesterol homeostasis: sterols promote binding of SCAP to INSIG-1, a membrane protein that facilitates retention of SREBPs in ER. *Cell* 2002; **110**: 489–500.
94 Brown AJ, Sun L, Feramisco JD, Brown MS, Goldstein JL. Cholesterol addition to ER membranes alters conformation of SCAP, the SREBP escort protein that regulates cholesterol metabolism. *Mol Cell* 2002; **10**: 237–245.
95 DeBose-Boyd RA, Brown MS, Li WP, *et al*. Transport-dependent proteolysis of SREBP: relocation of site-1 protease from Golgi to ER obviates the need for SREBP transport to Golgi. *Cell* 1999; **99**: 703–712.
96 Todd BL, Stewart EV, Burg JS, Hughes AL, Espenshade PJ. Sterol regulatory element binding protein is a principal regulator of anaerobic gene expression in fission yeast. *Mol Cell Biol* 2006; **26**: 2817–2831.
97 Hughes BT, Espenshade PJ. Oxygen-regulated degradation of fission yeast SREBP by Ofd1, a prolyl hydroxylase family member. *Embo J* 2008; **27**: 1491–1501.
98 Chen S, Sorrell T, Nimmo G, *et al*. Epidemiology and host- and variety-dependent characteristics of infection due to *Cryptococcus neoformans* in Australia and New Zealand. Australasian Cryptococcal Study Group. *Clin Infect Dis* 2000; **31**: 499–508.
99 Kwon-Chung KJ, Bennett JE. *Medical Mycology*. Philadelphia, PA: Lea & Febiger, 1992.
100 Chun CD, Liu OW, Madhani HD. A link between virulence and homeostatic responses to hypoxia during infection by the human fungal pathogen *Cryptococcus neoformans*. *PLoS Pathog* 2007; **3**: e22.
101 Himmelreich U, Dzendrowskyj TE, Allen C, *et al*. Cryptococcomas distinguished from gliomas with MR spectroscopy: an experimental rat and cell culture study. *Radiology* 2001; **220**: 122–128.
102 Chang YC, Bien CM, Lee H, Espenshade PJ, Kwon-Chung KJ. Sre1p, a regulator of oxygen sensing and sterol homeostasis, is required for virulence in *Cryptococcus neoformans*. *Mol Microbiol* 2007; **64**: 614–629.
103 Lee H, Bien CM, Hughes AL, *et al*. Cobalt chloride, a hypoxia-mimicking agent, targets sterol synthesis in the pathogenic fungus *Cryptococcus neoformans*. *Mol Microbiol* 2007; **65**: 1018–1033.
104 Goldberg MA, Glass GA, Cunningham JM, Bunn HF. The regulated expression of erythropoietin by two human hepatoma cell lines. *Proc Natl Acad Sci USA* 1987; **84**: 7972–7976.
105 Wang GL, Semenza GL. General involvement of hypoxia-inducible factor 1 in transcriptional response to hypoxia. *Proc Natl Acad Sci USA* 1993; **90**: 4304–4308.
106 Wang G, Hazra TK, Mitra S, Lee HM, Englander EW. Mitochondrial DNA damage and a hypoxic response are induced by CoCl[2] in rat neuronal PC12 cells. *Nucleic Acids Res* 2000; **28**: 2135–2140.
107 Huang Y, Du KM, Xue ZH, *et al*. Cobalt chloride and low oxygen tension trigger differentiation of acute myeloid leukemic cells: possible mediation of hypoxia-inducible factor-1alpha. *Leukemia* 2003; **17**: 2065–2073.
108 Grasselli F, Basini G, Bussolati S, Bianco F. Cobalt chloride, a hypoxia-mimicking agent, modulates redox status and functional parameters of cultured swine granulosa cells. *Reprod Fertil Dev* 2005; **17**: 715–720.
109 Ingavale SS, Chang YC, Lee H, *et al*. Importance of mitochondria in survival of *Cryptococcus neoformans* under low oxygen

© 2009 ISHAM, *Medical Mycology*

Downloaded By: [Montana State University Bozeman] At: 20:30 11 December 2009

conditions and tolerance to cobalt chloride. *PLoS Pathog* 2008; **4**: e1000155.
110 Bahn YS, Kojima K, Cox GM, Heitman J. A unique fungal two-component system regulates stress responses, drug sensitivity, sexual development, and virulence of *Cryptococcus neoformans*. *Mol Biol Cell* 2006; **17**: 3122–3135.
111 Millner PD, Marsh PB, Snowden RB, Parr JF. Occurrence of *Aspergillus fumigatus* during composting of sewage sludge. *Appl Environ Microbiol* 1977; **34**: 765–772.
112 Tekaia F, Latge JP. *Aspergillus fumigatus*: saprophyte or pathogen? *Curr Opin Microbiol* 2005; **8**: 385–392.
113 Wilson DM, Mubatanhema W, Jurjevic Z. Biology and ecology of mycotoxigenic *Aspergillus* species as related to economic and health concerns. *Adv Exp Med Biol* 2002; **504**: 3–17.
114 Latge JP. *Aspergillus fumigatus* and aspergillosis. *Clin Microbiol Rev* 1999; **12**: 310–350.
115 Perfect JR, Cox GM, Lee JY, *et al*. The impact of culture isolation of *Aspergillus* species: a hospital-based survey of aspergillosis. *Clin Infect Dis* 2001; **33**: 1824–1833.
116 Latge JP. The pathobiology of *Aspergillus fumigatus*. *Trends Microbiol* 2001; **9**: 382–389.
117 Rhodes JC. *Aspergillus fumigatus*: growth and virulence. *Med Mycol* 2006; **44**(Suppl. 1): S77–81.
118 Hohl TM, Feldmesser M. *Aspergillus fumigatus*: principles of pathogenesis and host defense. *Eukaryot Cell* 2007; **6**: 1953–1963.
119 Tarrand JJ, Lichterfeld M, Warraich I, *et al*. Diagnosis of invasive septate mold infections. A correlation of microbiological culture and histologic or cytologic examination. *Am J Clin Pathol* 2003; **119**: 854–858.
120 Tarrand JJ, Han XY, Kontoyiannis DP, May GS. *Aspergillus* hyphae in infected tissue: evidence of physiologic adaptation and effect on culture recovery. *J Clin Microbiol* 2005; **43**: 382–386.
121 Taubitz A, Bauer B, Heesemann J, Ebel F. Role of respiration in the germination process of the pathogenic mold *Aspergillus fumigatus*. *Curr Microbiol* 2007; **54**: 354–360.
122 Lockington RA, Borlace GN, Kelly JM. Pyruvate decarboxylase and anaerobic survival in *Aspergillus nidulans*. *Gene* 1997; **191**: 61–67.
123 Kelly JM, Drysdale MR, Sealy-Lewis HM, Jones IG, Lockington RA. Alcohol dehydrogenase III in *Aspergillus nidulans* is anaerobically induced and post-transcriptionally regulated. *Mol Gen Genet* 1990; **222**: 323–328.
124 Willger SD, Puttikamonkul S, Kim KH, *et al*. A sterol-regulatory element binding protein is required for cell polarity, hypoxia adaptation, azole drug resistance, and virulence in *Aspergillus fumigatus*. *PLoS Pathog* 2008; **4**: e1000200.
125 Hughes AL, Lee CY, Bien CM, Espenshade PJ. 4-Methyl sterols regulate fission yeast SREBP-Scap under low oxygen and cell stress. *J Biol Chem* 2007; **282**: 24388–24396.

Downloaded By: [Montana State University Bozeman] At: 20:30 11 December 2009

© 2009 ISHAM, *Medical Mycology*

OPEN ACCESS Freely available online

PLoS PATHOGENS

In vivo Hypoxia and a Fungal Alcohol Dehydrogenase Influence the Pathogenesis of Invasive Pulmonary Aspergillosis

Nora Grahl[1], Srisombat Puttikamonkul[1], Jeffrey M. Macdonald[2], Michael P. Gamcsik[2], Lisa Y. Ngo[3], Tobias M. Hohl[3], Robert A. Cramer[1]*

1 Department of Immunology and Infectious Diseases, Montana State University, Bozeman, Montana, United States of America, **2** Joint Department of Biomedical Engineering, University of North Carolina, Chapel Hill, and North Carolina State University, Raleigh, North Carolina, United States of America, **3** Infectious Disease Sciences, Vaccine and Infectious Disease Division, Clinical Research Division, Fred Hutchinson Cancer Research Center, Seattle, Washington, United States of America

Abstract

Currently, our knowledge of how pathogenic fungi grow in mammalian host environments is limited. Using a chemotherapeutic murine model of invasive pulmonary aspergillosis (IPA) and ^{1}H-NMR metabolomics, we detected ethanol in the lungs of mice infected with *Aspergillus fumigatus*. This result suggests that *A. fumigatus* is exposed to oxygen depleted microenvironments during infection. To test this hypothesis, we utilized a chemical hypoxia detection agent, pimonidazole hydrochloride, in three immunologically distinct murine models of IPA (chemotherapeutic, X-CGD, and corticosteroid). In all three IPA murine models, hypoxia was observed during the course of infection. We next tested the hypothesis that production of ethanol *in vivo* by the fungus is involved in hypoxia adaptation and fungal pathogenesis. Ethanol deficient *A. fumigatus* strains showed no growth defects in hypoxia and were able to cause wild type levels of mortality in all 3 murine models. However, lung immunohistopathology and flow cytometry analyses revealed an increase in the inflammatory response in mice infected with an alcohol dehydrogenase null mutant strain that corresponded with a reduction in fungal burden. Consequently, in this study we present the first *in vivo* observations that hypoxic microenvironments occur during a pulmonary invasive fungal infection and observe that a fungal alcohol dehydrogenase influences fungal pathogenesis in the lung. Thus, environmental conditions encountered by invading pathogenic fungi may result in substantial fungal metabolism changes that influence subsequent host immune responses.

Citation: Grahl N, Puttikamonkul S, Macdonald JM, Gamcsik MP, Ngo LY, et al. (2011) *In vivo* Hypoxia and a Fungal Alcohol Dehydrogenase Influence the Pathogenesis of Invasive Pulmonary Aspergillosis. PLoS Pathog 7(7): e1002145. doi:10.1371/journal.ppat.1002145

Editor: Scott G. Filler, David Geffen School of Medicine at University of California Los Angeles, United States of America

Received January 28, 2011; **Accepted** May 17, 2011; **Published** July 21, 2011

Copyright: © 2011 Grahl et al. This is an open-access article distributed under the terms of the Creative Commons Attribution License, which permits unrestricted use, distribution, and reproduction in any medium, provided the original author and source are credited.

Funding: Work in this study was supported by funding from the National Institutes of Health, COBRE grant RR020185 (M. Quinn PI, RAC project 2 leader), NIH/NIAID grant R01AI81838 (RAC), equipment grant from the M. J. Murdock Charitable Trust, and the Montana State University Agricultural Experiment Station. The funders had no role in study design, data collection and analysis, decision to publish, or preparation of the manuscript.

Competing Interests: The authors have declared that no competing interests exist.

* E-mail: rcramer@montana.edu

Introduction

The incidence of life-threatening human fungal infections has increased during the last three decades as medical therapies, organ transplantations, an increasing geriatric population, and HIV infections have generated a significant rise in the number of susceptible patients [1,2,3]. *Aspergillus fumigatus*, a commonly encountered mold found in soil and organic debris [4,5], is responsible for a number of clinically relevant diseases in immunocompromised and immunocompetent individuals. Among these, invasive pulmonary aspergillosis (IPA) is the most lethal with mortality rates ranging from 30–90% depending on the patient population [6,7,8,9,10,11].

To cause lethal disease, *A. fumigatus* must face and overcome a number of *in vivo* microenvironment challenges once it is inhaled into the lower respiratory tract. However, our understanding of the dynamic microenvironments encountered by the fungus in the mammalian lung, and the mechanisms by which it grows in these microenvironments, are poorly understood. Arguably, understanding the mechanisms by which *A. fumigatus* is able to grow in the mammalian host environment will lead to either improvement of existing therapeutic options or development of novel treatments through the identification of novel drug targets. Some of the previously studied environmental factors encountered by *A. fumigatus* during *in vivo* growth include: high temperature, changes in pH, oxidative stress, and a restricted nutrient supply. In all probability, these stresses are similar to those that the mold has to overcome to be a highly competitive member of the compost microflora, and subsequently it has evolved multi-faceted and robust mechanisms to overcome these challenges [12,13,14,15,16].

An important characteristic of *A. fumigatus's* saprophytic lifestyle that has largely been overlooked is its ability to adapt to a wide range of oxygen levels. *Aspergillus* species are generally considered obligate aerobes, but *A. fumigatus* has been observed to tolerate oxygen levels as low as 0.1% [17,18]. In compost piles, oxygen concentrations range from atmospheric (21%) to hypoxic (1.5% and lower) and rapidly change with the metabolic activity of the compost microflora [19]. Thus, organisms such as *A. fumigatus* that thrive in such environments likely have evolved mechanisms to tolerate hypoxia. With regard to fungal-human interactions, oxygen availability in mammalian tissues is also substantially below atmospheric levels [20,21,22]. Even in the alveoli of healthy

Author Summary

Metabolic flexibility is important for human pathogens like *Aspergillus fumigatus* as it allows adaptation to dynamic infection induced microenvironments. Consequently, identification of fungal metabolic pathways critical for *in vivo* growth may uncover novel virulence mechanisms and new therapeutic opportunities. To date, the mechanisms used by *A. fumigatus* to adapt to microenvironments in immunosuppressed mammalian hosts are poorly understood. In this study we discover that *A. fumigatus* is exposed to oxygen limiting microenvironments during invasive pulmonary aspergillosis (IPA). Thus, this result builds on growing evidence that suggests hypoxia is a significant *in vivo* stress encountered by human fungal pathogens. We tested the hypothesis that genes encoding enzymes involved in ethanol fermentation are important for *in vivo* fungal responses to hypoxia. We consequently observed a significant increase in the inflammatory response that correlated with reduced fungal growth in the lungs of mice inoculated with an alcohol dehydrogenase null mutant. Altogether, our study suggests that fungal responses to *in vivo* hypoxic microenvironments can directly affect host immune responses to the invading fungal pathogen. A better understanding of these mechanisms will increase our understanding of IPA and other human diseases caused by fungi and could potentially lead to improved therapeutic options.

lungs, the most aerated organ and primary site of *Aspergillus* deposition, the oxygen level is around 14%. By the time oxygen reaches the capillaries and diffuses into surrounding tissues its availability is much lower with levels of 2–4% reported [23,24]. Thus, microorganisms that colonize, inhabit and infect mammalian hosts are subject to dynamic ranges of oxygen availability depending on their location in the mammalian body. Moreover, the collateral effects of microbial infections, inflammation, thrombosis, and necrosis, are often thought to decrease available oxygen concentrations even further [25,26,27,28]. However, the occurrence and effects of hypoxia on the outcome of human fungal infections, especially those that primarily occur in the lung, are poorly understood [29,30].

Recent evidence supporting the hypothesis that hypoxia is a significant component of fungal pathogenesis comes from studies on the sterol-regulatory element binding protein (SREBP) transcription factor in *Cryptococcus neoformans* and *A. fumigatus*. Null mutants of the respective SREBP in each fungal pathogen were incapable of growth in hypoxic conditions and subsequently were also avirulent in murine models of cryptococcosis and IPA [31,32,33]. Though the virulence defect in these SREBP mutants may be caused by other pleiotropic factors, their ability to grow in normoxic but not hypoxic conditions strongly suggests that adaptation and growth in hypoxia are contributing factors to the avirulence of these strains. Yet, as mentioned, whether hypoxia occurs during an invasive fungal infection in commonly used murine models of fungal disease is unknown.

In this study, we observe for the first time that hypoxic microenvironments do occur in three immunologically distinct murine models of IPA. We also observe that a key gene, which encodes an enzyme required for the last step of ethanol fermentation in response to hypoxia, influences IPA pathogenesis through modulation of the inflammatory response. Thus, we conclude that *in vivo* hypoxic microenvironments do occur during IPA and that fungal responses to these conditions can influence fungal pathogenesis. These results lay the foundation for further studies to identify how human pathogenic fungi adapt to hypoxia and how these adaptation mechanisms ultimately influence the outcome of fungal pathogenesis in mammals.

Results

In vivo ethanol production by *A. fumigatus* in a murine model of invasive pulmonary aspergillosis

In order to gain an understanding of the important metabolic pathways utilized by *Aspergillus fumigatus* during growth in the mammalian lung, we examined qualitative production of metabolites in a chemotherapeutic murine model of invasive pulmonary aspergillosis (IPA) utilizing broncheoalveolar lavages (BAL) and ^{1}H-NMR. Our chemotherapeutic model of IPA is characterized by the use of cyclophosphamide and the corticosteroid triamcinolone to induce immunosuppression. Visual inspection of the BAL sample spectra taken from uninfected control mice and mice inoculated with *A. fumigatus* on day +3 post-inoculation revealed a relatively small number of identifiable metabolites and few differences. Identifiable metabolites in all samples included taurine, choline, creatine, acetate, and lactate (Figure S1). Given the low complexity of BAL samples that are predominately 0.7% saline, this result is not surprising. Surprisingly, however, ethanol was detected in 4 of the 10 mice infected with *A. fumigatus*, but in none of the uninfected controls (Figure S1). Attempts to detect ethanol at later time points during infection using BALs or lung homogenates were not successful. Thus, the extent of ethanol production *in vivo* during IPA remains to be determined.

However, to support the hypothesis that the ethanol production was fungal in origin, we next tested whether *A. fumigatus* was capable of fermenting glucose to ethanol *in vitro* in glucose minimal media (1% glucose) under normoxic or hypoxic conditions. While no ethanol was detectable after 24 h in either condition, we could detect ethanol in the culture supernatants after 48, 72, and 96 h of growth in hypoxia (1% oxygen, Figure 1). The glucose levels expectedly dropped during the time course of the shake flask cultures, from 55 mM at time zero to less than 4 mM at 96 h, and this corresponded with a decrease in detectable ethanol (Figure 1). Fermentation is associated with hypoxic or anoxic environments in many organisms including plant pathogenic fungi, Crabtree negative yeast, pathogenic bacteria, and even plants [34,35,36,37,38,39,40]. We thus hypothesized that *A. fumigatus* encounters hypoxic or anoxic microenvironments during IPA.

Hypoxia occurs in murine models of invasive pulmonary aspergillosis

To test the hypothesis that *A. fumigatus* encounters hypoxia during IPA, we used a hypoxia marker, pimonidazole hydrochloride, a nitroheterocyclic drug whose hypoxia-dependent activation by cellular mammalian nitroreductases (severe hypoxia: 10 mmHg partial oxygen pressure, $\leq$1% oxygen) leads to the formation of covalent intracellular adducts with thiol groups on proteins, peptides, amino acids, and the drug itself [41,42,43,44]. The resulting protein adducts are effective immunogens and can be used to "visualize" hypoxia *in vivo* with immunofluorescence.

We tested for the development of hypoxia *in vivo* in three immunologically distinct murine models of IPA (chemotherapeutic, corticosteroid, and X-CGD) (Figure 2). Each model represents a different clinically relevant mechanism of immunosuppression. As mentioned, the chemotherapeutic model attempts to reproduce the immunological state of severely immunosuppressed patients who have often undergone a bone marrow transplant. This model is characterized by a severe depletion of neutrophils and other important immune effector cells needed to prevent and control

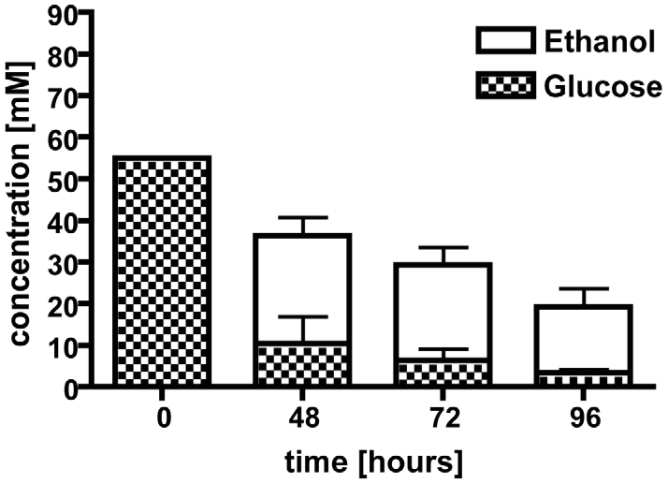

Figure 1. Culture supernatants were used in a high performance liquid chromatography (HPLC) analysis to determine ethanol production and glucose consumption. After 48 hours under hypoxic conditions, ethanol was detected along with a decrease in glucose concentration. Ethanol concentrations decrease over time with a peak at 48 hours. Each value represents mean ± standard error (n = 2 independent cultures). *,**,#$p<0.05$.
doi:10.1371/journal.ppat.1002145.g001

invasive fungal infections. Another patient population highly susceptible to invasive fungal infections is those patients on high doses of corticosteroids for treatment of graft versus host disease or other autoimmune type diseases. In our model of this patient population, we utilized a single high dose of the corticosteroid triamcinolone. Unlike the chemotherapeutic model, this model is not characterized by depletion of effector cells, but rather by a suppression of their antifungal activity that leads to altered inflammatory responses. Finally, we utilized transgenic mice that are deficient in the gp91 Phox subunit of the NADPH oxidase. These mice are a close model for the genetic disorder chronic granulomatous disease (CGD), and are highly susceptible to *Aspergillus* infection.

In the Triamcinolone model, histopathology of *A. fumigatus* inoculated mice show lesions with a strong influx of immune cells (blue) and strong growth of fungal hyphae (green) invading into the lung parenchyma from the airways (Figure 2A, Figure S2). By day 3 p.i., hypoxia could readily be detected in the center of larger lesions (red), and while the hypoxic areas of the lesions are comparable on day 3.5 p.i., they are significantly expanded on day 4 p.i.. The isotype control staining of the same lesions in subsequent tissue sections, as well as complete staining of tissue sections from inoculated mice without hypoxyprobe injections, demonstrate the specificity of the hypoxyprobe and antibodies utilized (Figure 2A).

In contrast to the Triamcinolone model, lesions in the chemotherapeutic model are dominated by massive fungal growth causing significant tissue necrosis with minimal inflammation (Figure 2B, Figure S2). Given the severe neutropenia associated with this model, this result is expected. Despite the strong reduction in the inflammatory response and extensive fungal growth in this model, we were able to detect hypoxia in these lesions at similar time points to the Triamcinolone model (Figure 2A and B). However, it is clear that the amount and extent of hypoxia is significantly reduced in this murine model.

In mice that lack the $gp91^{phox}$ component of NADPH oxidase (a model of X-CGD) the lesion size gradually increased during the time course of infection from day 3 to day 5, which was due to a strong increase in the inflammatory response of the host [45]. Fungal growth in this model was strongly reduced in comparison to the other two tested murine models (Figure 2C, Figure S2). On day 3 p.i. minimal amounts of hypoxia were detected, but by day 4 p.i. significant levels of hypoxia were observed in the center of the lesions. On day 5 p.i. hypoxia was abundantly present in the center of the lesions, and throughout the surrounding tissue indicating that significant parts of the lung experience hypoxia in this murine model of IPA (Figure 2C). Indeed, in some animals in this model almost the entire lung seemed hypoxic at later time points just prior to mortality (data not shown). Taken together, these data confirm that *A. fumigatus* encounters hypoxic microenvironments (oxygen concentrations $\leq 1\%$) and a dynamic range of oxygen availability during murine models of IPA. The extent of hypoxia, fungal growth, and host immune responses in the different models suggests that the host inflammatory response plays an important, but not exclusive, role in the generation of the hypoxic microenvironment.

Generation and characterization of ethanol fermentation deficient mutants

Given the evidence that *A. fumigatus* encounters hypoxia during IPA and that production of ethanol occurs *in vivo* during infection and is normally used by microbes to survive in low oxygen environments [34,35,36,37,38,39], we next tested the hypothesis that ethanol fermentation was a key mechanism for hypoxia adaptation and fungal virulence.

To determine the effects of ethanol fermentation on IPA pathogenesis, we searched the *A. fumigatus* genome sequence for genes encoding enzymes known to be involved in ethanol fermentation [46,47]. Using the *A. nidulans pdcA* (pyruvate decarboxylase) (*An_pdcA* – AN4888) gene sequence for a BLASTX search of the *A. fumigatus* genome (CADRE genome database) we identified three potential candidates that may encode for pyruvate decarboxylases and named them *pdcA* (AFUB_038070: 85% identity to *An_pdcA*), *pdcB* (AFUB_096720: 39% identity to *An_pdcA*), and *pdcC* (AFUB_062480: 33% identity to *An_pdcA*) (Table 1). Protein sequence analysis (InterProScan Sequence Search, http://www.ebi.ac.uk/Tools/InterProScan/) suggested all three *A. fumigatus* proteins were pyruvate decarboxylases

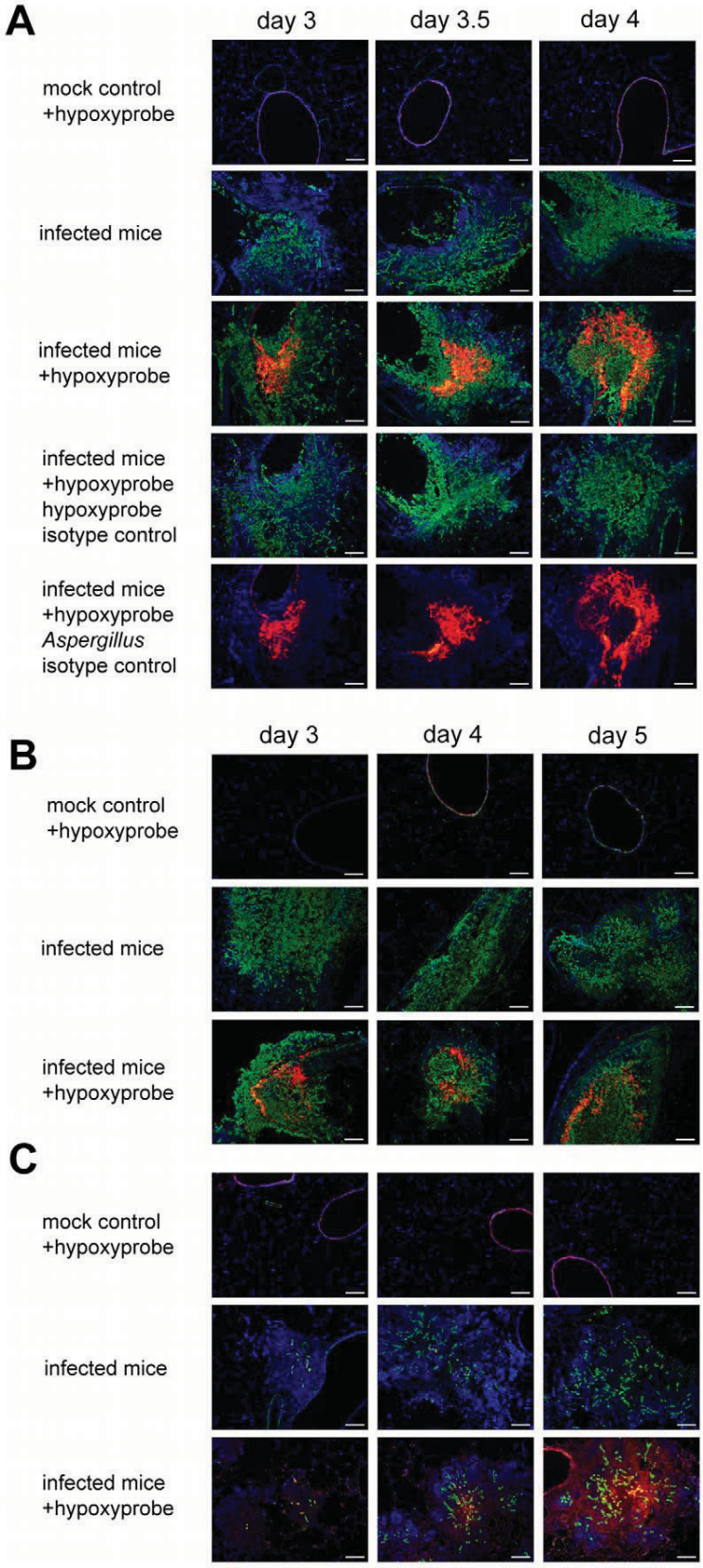

Figure 2. Identification of hypoxic microenvironments at the site of *A. fumigatus* infections in murine lungs. The following three distinct mouse IPA models were utilized: (**A**) triamcinolone (corticosteroid) model, (**B**) chemotherapy model, and (**C**) X-CGD mouse model. Mice were

euthanized on indicated days after inoculation (mock control = 0.01% Tween inoculated, infected mice = inoculated with *A. fumigatus* strain CEA10). Prior to sacrifice, Hypoxyprobe-1 (60 mg/kg) was intravenously injected into indicated mice (+hypoxyprobe) and allowed to circulate for 60 to 90 min. After tissue preparation specific antibodies were used to detect Hypoxyprobe-1 bound to proteins (red) and *A. fumigatus* hyphae (green). Isotype controls were only stained with either one of the secondary antibodies to verify specific staining. Host cell nuclei were counterstained with DAPI (blue). Merged pictures show co-localization of the fungal hyphae (green), surrounding immune cells (blue), and Hypoxyprobe-1 (red) in all three IPA mouse models. Isotype controls and infected mice without Hypoxyprobe-1 injection show that no unspecific staining occurred. Bar = 100 μm.
doi:10.1371/journal.ppat.1002145.g002

(Table 1). In a similar manner, the known alcohol dehydrogenase (Adh) gene sequences of *A. nidulans* (AdhI: *An_alcA* – AN8979, AdhII: *An_alcB* – AN3741, and AdhIII: *An_alcC* – AN2286) were used to identify the most likely genes encoding alcohol dehydrogenases in *A. fumigatus*. However, as the *Aspergillus fumigatus* genome contains several predicted alcohol dehydrogenases we restricted our search to proteins with high identity and similarity to the *A. nidulans* Adh proteins (*alcA* – AFUB_087590: 87% identity and 94% similarity to *An_alcA*, *alcB* – AFUB_089920: 79% identity and 89% similarity to *An_alcB*, and *alcC* – AFUB_053780: 80% identity and 91% similarity to *An_alcC*) (Table 1).

Given the findings that *A. fumigatus* utilizes ethanol fermentation in *in vitro* and possibly *in vivo* hypoxic environments and the apparent gene redundancy in the predicted ethanol fermentation pathway, we next sought to determine which of the genes transcriptionally responds to hypoxia. Quantitative real-time PCR comparing the mRNA abundance of the ethanol fermentation genes under hypoxic and normoxic conditions revealed an immediate increase in mRNA abundance of all three *pdc* genes as well as the *alcC* gene to hypoxic growth conditions (Figure 3). While mRNA abundance levels of *pdcB* and *pdcC* show a ~9-fold higher normalized fold expression after 24 h in hypoxia, *pdcA* mRNA showed a 64-fold increase compared to normoxic culture conditions. This data suggest that PdcA is the primary pyruvate decarboxylase that responds to hypoxia in *A. fumigatus*. With regard to the alcohol dehydrogenase encoding genes, the mRNA abundance of *alcC* significantly increased in response to hypoxia while mRNA abundance of the other two alcohol dehydrogenase encoding genes did not (Figure 3). These data suggest that *alcC* is the primary gene encoding an alcohol dehydrogenase that responds to hypoxia in *A. fumigatus*.

To determine whether these genes are involved in ethanol fermentation, we generated null mutants of the genes encoding PdcA, PdcB, PdcC, and AlcC by replacement of the coding sequence in *A. fumigatus* strain CEA17 with the auxotrophic marker pyrG from *A. parasiticus* (Figure 4 and data not shown). A *pdcA/pdcB* double mutant was also generated. Ectopic re-introduction of the wild type *pdcA* and *alcC* allele into Δ*pdcA* and Δ*alcC* (resulting in strains *pdcA* recon and *alcC* recon) allowed us to attribute all resulting phenotypes specifically to the absence of *pdcA* or *alcC*. The genotype of all strains was confirmed with PCR analyses (data not shown) and Southern blots (Figure 4 and data not shown). Southern blot analysis of the *alcC* recon strain revealed a double insertion of the *alcC* encoding sequence in the genome and the *alcC* recon strain displayed a 10-fold higher mRNA abundance in response to hypoxia as the *alcC* allele in the wild type strain (data not shown). However, the double insertion had no detectable phenotypic effect on the reconstituted strain, since the *alcC* recon strain showed the same phenotype as the wild type in all further experiments with only a slight but statistically insignificant increase in ethanol production (Figure 5B).

Next, we examined the ability of the generated null mutant strains to produce ethanol in response to *in vitro* hypoxic growth conditions. The loss of *pdcA* decreases Pdc enzyme activity in hypoxia by approximately 80% (Figure 5A) and the activity can be restored to wild type levels in the *pdcA* recon strain. The Δ*pdcB* and Δ*pdcC*, as well as the Δ*alcC* strain showed no significant decrease in Pdc activity (data not shown), confirming the hypothesis that *pdcA* is the most important *pdc* gene in *A. fumigatus* for production of ethanol, at least *in vitro*. However there is still residual activity detectable in the Δ*pdcA* and the Δ*pdcA*/Δ*pdcB* strains (0.0047 ± 0.0041 in normoxia and 0.0039 ± 0.0064 in hypoxia; data not

Table 1. Genes involved in *A. fumigatus* ethanol fermentation pathway.

Gene ID	Gene Name	Query Gene	Similarity	Identity	Domains	Enzyme
AFUB_038070	**pdcA**	**AN_pdcA**	**93%**	**85%**	C-terminal TPP-binding, central domain, N-terminal TPP-binding domain	Pyruvate decarboxylase
AFUB_096720	**pdcB**	**AN_pdcA**	**57%**	**39%**	C-terminal TPP-binding, central domain, N-terminal TPP-binding domain	Pyruvate decarboxylase
AFUB_062480	**pdcC**	**AN_pdcA**	**47%**	**33%**	TPP-binding enzyme conserved site, C-terminal TPP-binding, central domain, N-terminal TPP-binding domain	Pyruvate decarboxylase
AFUB_087590	**alcA**	**AN_alcA**	**94%**	**87%**	zinc-containing conserved site, GroES-like domain, ADH C-terminal domain, ADH GroES-like domain, NAD(P)-binding domain	Alcohol Dehydrogenase
AFUB_089920	**alcB**	**AN_alcB**	**89%**	**79%**	zinc-containing conserved site, GroES-like domain, ADH C-terminal domain, ADH GroES-like domain, NAD(P)-binding domain	Alcohol Dehydrogenase
AFUB_053780	**alcC**	**AN_alcC**	**91%**	**80%**	zinc-containing conserved site, GroES-like domain, ADH C-terminal domain, ADH GroES-like domain, NAD(P)-binding domain	Alcohol Dehydrogenase

AN = Aspergillus nidulans.
TPP = Thiamine pyrophosphate.
ADH = alcohol dehydrogenase.
doi:10.1371/journal.ppat.1002145.t001

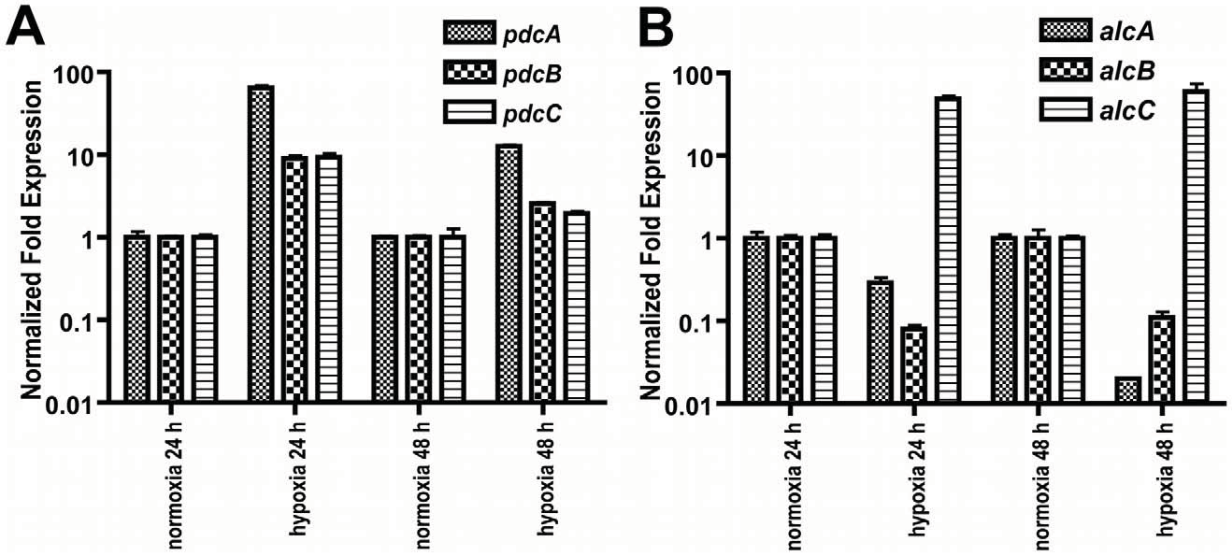

Figure 3. Normalized fold expression of *pdc* genes and *alc* genes in *A. fumigatus* under normoxic and hypoxic conditions. (**A**) mRNA levels of all three *pdc* genes increase in hypoxia with *pdcA* being the most responsive. mRNA levels of the *pdc* genes show a reduction in hypoxia over time. (**B**) Of the three tested *alc* genes only mRNA from *alcC* is increased in response to hypoxia. Quantification of mRNA was achieved by quantitative real-time PCR. Values are normalized to β–tubulin and shown relative to normoxia. Results are the mean and standard deviation of three replicates.
doi:10.1371/journal.ppat.1002145.g003

shown). A triple mutant of all three putative PDC encoding genes would need to be generated to definitively answer whether the observed residual activity from the cell free extracts is indeed real Pdc activity.

Using the culture supernatants from the above experiments we examined the amount of ethanol produced by the respective fungal strains. The *pdcB* and *pdcC* null mutant strains show a slight but statistically insignificant decrease in ethanol production that is essentially similar to wild type levels (CEA10: 0.071±0.035%; Δ*pdcB*: 0.047±0.002; Δ*pdcC*: 0.040±0.006; P>0.4). Importantly, no ethanol could be detected in Δ*pdcA* and Δ*alcC* culture supernatants, while the wild type and respective reconstituted strains produced ethanol (Figure 5B). These results support the gene expression and Pdc enzyme activity assays that suggest PdcA is the primary Pdc and that AlcC is the primary alcohol dehydrogenase required for *in vitro* ethanol production in *A. fumigatus*. The function of the remaining Pdc and Alc genes in *A. fumigatus* thus is not currently clear.

To determine whether ethanol fermentation is important for growth under hypoxic conditions, we examined radial growth on solid media under normoxic and hypoxic conditions. As previously described, *A. fumigatus* grows well under hypoxic conditions on the fermentable carbon source glucose [18,31] (Figure 5C). Surprisingly, the ethanol fermentation deficient mutants show no growth defect on glucose containing media under hypoxic (1% or 0.2% O_2 (data not shown)) conditions compared to the wild type and the reconstituted strains (Figure 5C). In addition, the wild type and mutant strains are all also able to grow on the non-fermentable carbon sources ethanol, lactate and glycerol, although the growth rate is decreased compared to growth on glucose (data not shown). Germination rates were the same for all strains utilized and no defects in conidia viability were observed (data not shown). Liquid biomass quantification with the respective mutant strains also revealed no growth differences between wild type and ethanol deficient strains in hypoxia (data not shown). Taken together, these results suggest that PdcA and AlcC are the primary enzymes involved in ethanol fermentation in *A. fumigatus*, but that other unidentified mechanisms are utilized to grow under hypoxic conditions on fermentable carbon sources when ethanol fermentation is not possible.

Deletion of alcohol dehydrogenase III in *A. fumigatus* alters the pathogenesis of invasive pulmonary aspergillosis

Despite the general lack of a pathogenesis associated phenotype of the *in vitro* ethanol production deficient strains, ethanol itself has been observed to have significant immunomodulatory properties [48,49,50,51,52]. In addition, utilizing quantitative real-time PCR we found that *alcC* is expressed *in vivo* during fungal pathogenesis on day 3 and 4 post inoculation in the triamcinolone model (Figure 6) suggesting that this gene and the enzyme it encodes may be important for *in vivo* growth. Therefore, we sought to determine the effects of loss of PdcA and AlcC on the pathogenesis of IPA. We first examined the virulence of the Δ*pdcA* and Δ*alcC* strains in the chemotherapeutic and X-linked chronic granulomatous disease (X-CGD, $gp91^{phox-/-}$ mice) murine models of IPA [45,53]. Irrespective of the fungal strain, *A. fumigatus* infected mice, in both models, displayed well described symptoms of *A. fumigatus* infection including hunched posture, ruffled fur, weight loss, and increased respiration as early as day +2 of inoculation. Subsequently, no difference in mortality was observed between the null mutant *(*Δ*alcC,* Δ*pdcA,* and Δ*pdcA*Δ*pdcB*) and wild type strains (Figure 7 and data not shown).

To further examine the impact of the mutant strains on the pathogenesis of IPA in these murine models, lung histopathology was performed. Lungs from X-CGD mice displayed the expected histopathology for this model including a large inflammatory response with reduced fungal growth (Figure S3). In this model, histopathology of wild type and Δ*alcC* inoculated mice looked identical at all time points examined (Figure S3). In the chemotherapy model, pulmonary lesions of wild type infected

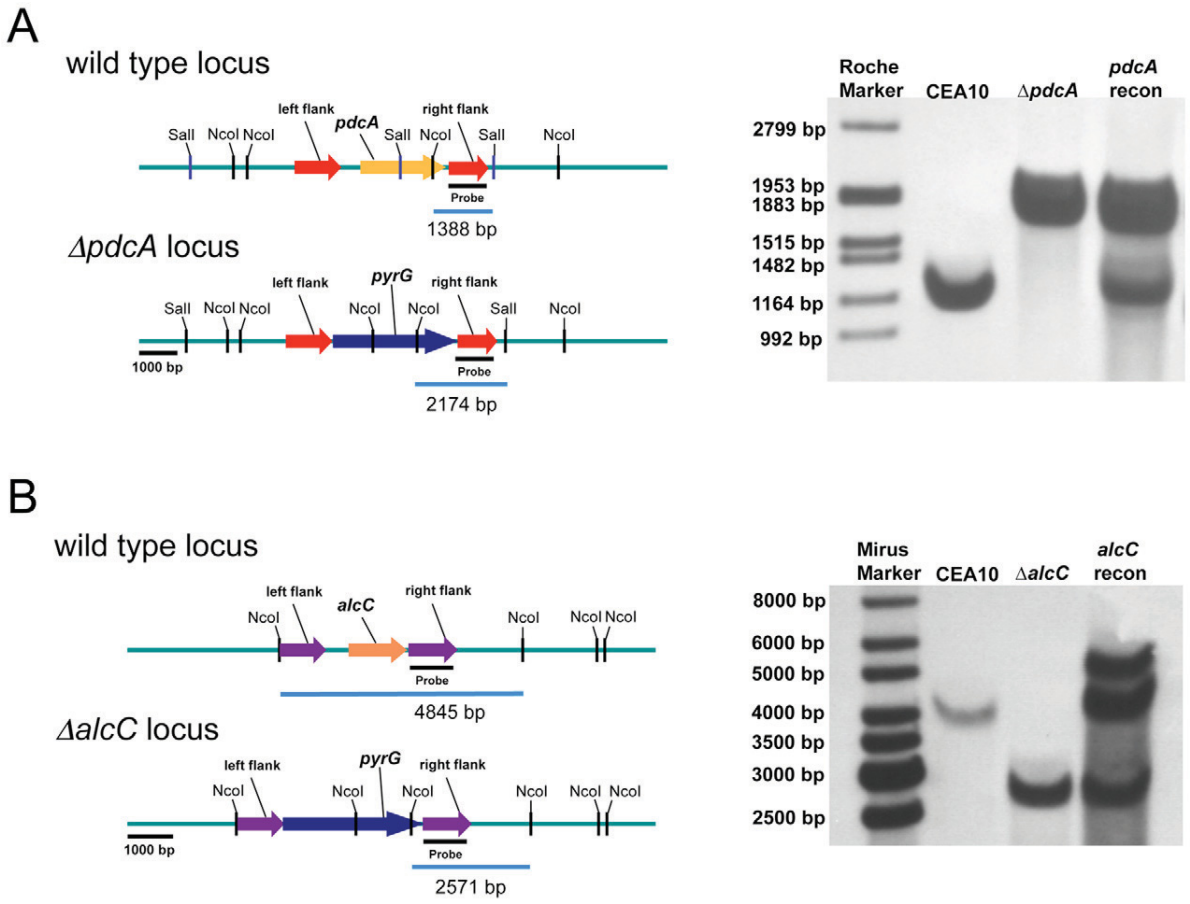

Figure 4. Generation and confirmation of PdcA and AlcC null mutants in *A. fumigatus*. Schematic of wild type (CEA10), PdcA (**A**), and AlcC (**B**) null mutant genomic loci. (**A**) Southern blot analysis of wild type, Δ*pdcA*, and *pdcA* recon strains as well as (**B**) wild type, Δ*alcC*, and *alcC* recon strains. Genomic DNA from the respective strains was isolated and digested overnight with SalI and NcoI in the case of PdcA and with only NcoI for AlcC. An approximate 1 kb genomic region was utilized as a probe. The expected hybridization patterns and sizes were observed for all strains tested. In addition, confirmation of ectopic reconstitution was confirmed by the presence of the wild type locus hybridization signal and persistence of the null mutant locus. The *alcC* reconstituted strain showed a double re-insertion of the *alcC* locus.
doi:10.1371/journal.ppat.1002145.g004

animals show substantial fungal growth and invasion of the lung parenchyma with a minimal influx of immune cells but extensive tissue necrosis, hemorrhaging, edema, and tissue damage (Figure 8A). Importantly, mice inoculated with Δ*alcC* show lesions with reduced fungal growth and more inflamed tissue compared to wild type inoculated mice (despite the overall lesion sizes being comparable between the two inoculation groups) (Figure 8A). Taken together, this result suggests that AlcC plays a potential role in the pathogenesis of IPA.

To explore this hypothesis further, we utilized the Triamcinolone (corticosteroid) model of IPA. IPA in mice treated with corticosteroids have previously been observed to induce hyper-inflammatory responses that are speculated to be the primary cause of mortality in this model [54]. Thus, we rationalized that any changes in the inflammatory response to *A. fumigatus* in the absence of AlcC would be potentiated in this model. As in the chemotherapeutic and X-CGD murine models, Δ*alcC* infected animals displayed wild type levels of mortality in the Triamcinolone model (Figure 7C). A similar change in gross histopathology of the Triamcinolone compared to the chemotherapeutic model infected with the Δ*alcC* strain is also observed (Figure 8B). Consistent with the observations in the chemotherapy model, Δ*alcC* inoculated animals show less fungal growth but increased levels of inflammation (Figure 8B).

Altogether these observations suggest that loss of AlcC results in an increased inflammatory response to *A. fumigatus*. To further characterize and quantify these histopathology observations, we analyzed the cellular infiltrates in BAL fluids of Triamcinolone treated mice from 2 different inoculation experiments using flow cytometry and differential cell counts. On day 3 p.i., Δ*alcC* inoculated mice show an increased quantity of $F4/80^+/CD11c^+$ cells and a significant increase in $GR\text{-}1^+/CD11b^+$ cells in the BAL fluids compared to wild type infected animals (Figure 9A and B, and Figure S4 and S5). $F4/80^+/CD11c^+$ cells most likely represent macrophages while $GR\text{-}1^+/CD11b^+$ cells are most likely neutrophils. As expected, control mice BALs contained $F4/80^+/CD11c^+$ cells but nearly no $GR\text{-}1^+/CD11b^+$ cells. Furthermore, differential cell counts of BAL fluids revealed that macrophages, monocytes and particularly neutrophils were the dominant cell types found in the BAL samples of *A. fumigatus* inoculated mice. Consistent with the observed histopathology as well as the flow cytometry data, differential cell count numbers of neutrophils were significantly increased in Δ*alcC* inoculated mice ($p<0.05$; Figure 9C and D).

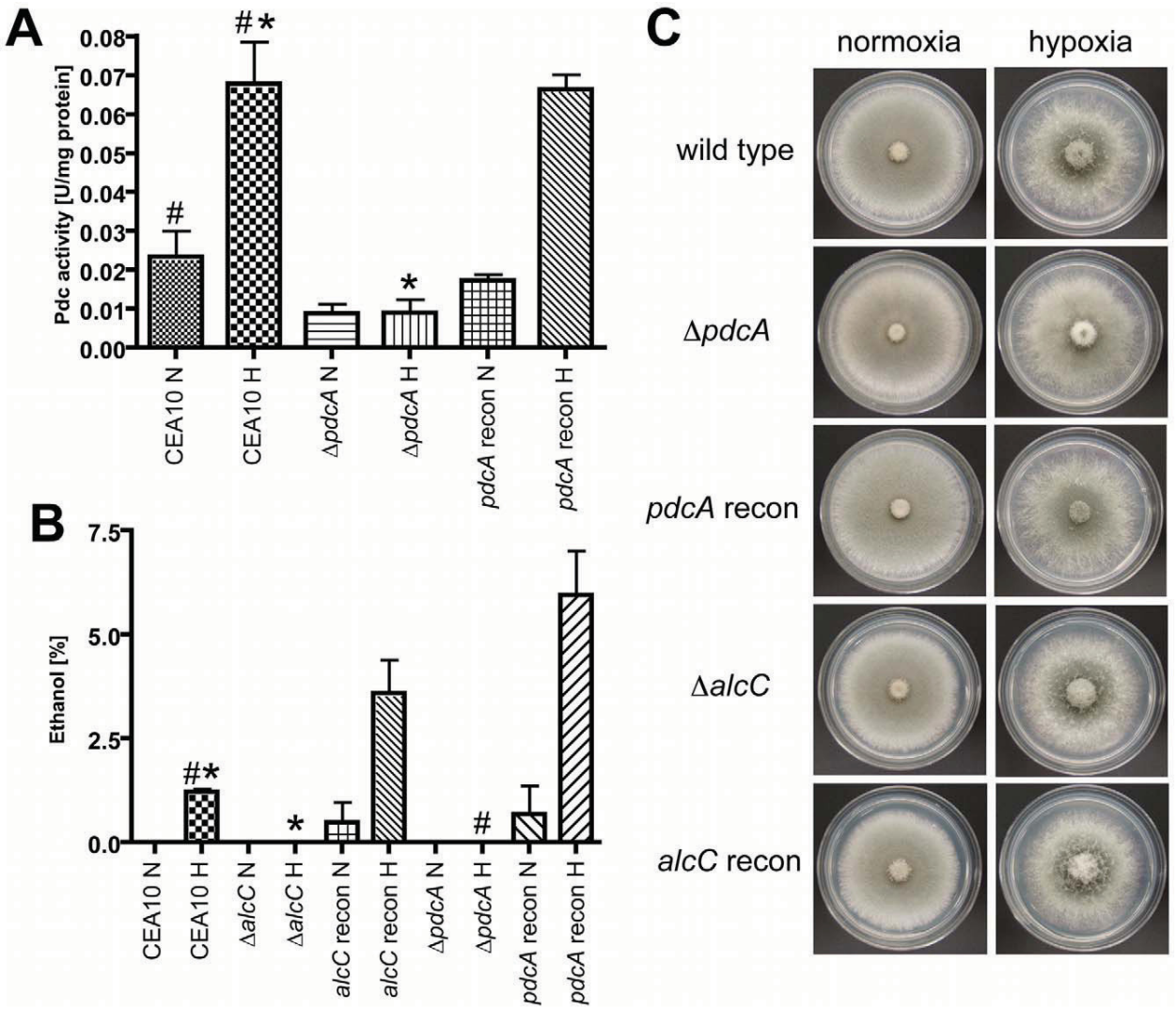

Figure 5. PdcA and AlcC are required for *in vitro* ethanol fermentation but not hypoxic growth of *A. fumigatus*. (**A**) After 48 hours in hypoxia, mycelia were harvested and pyruvate decarboxylase activity (Pdc) of cell free extracts was determined. Compared to CEA10, the Δ*pdcA* strain showed a ~80% reduction of Pdc activity under hypoxic conditions, which could be restored in the reconstituted strain (*,# $p<0.01$) (**B**) Ethanol concentration in culture supernatants was determined with GCMS, showing that PdcA and AlcC are required for ethanol production of *A. fumigatus*. Each value represents mean ± standard error (n = 3 for each condition for each strain). (*,# $p<0.01$). **(C)** $1x10^6$ conidia of CEA10, Δ*pdcA*, *pdcA* recon, Δ*alcC*, and *alcC* recon were plated on GMM (glucose) plates and incubated at 37°C for 48 h under normoxic or hypoxic conditions. All strains showed comparable growth and morphology in all tested conditions.
doi:10.1371/journal.ppat.1002145.g005

Taken together, these data support the histopathology observations that indicate an increased inflammatory response in mice infected with Δ*alcC*.

To further quantify the differences in immune response to Δ*alcC*, we examined the production of cytokines normally associated with neutrophil recruitment in mice (murine IL-8 homologs, KC and MIP2). We observed that protein levels of the two murine neutrophil chemo-attractants KC and MIP-2 were significantly increased in BALs from Δ*alcC* inoculated animals compared with wild type (Figure 10A and B; $p<0.05$). IL-6 was also slightly elevated while TNF-α protein levels were reduced in comparison to BAL fluids of mice inoculated with the wild type (Figure 10C and D; $p>0.05$). Altogether, these results indicate that loss of AlcC modulates the immune response of the host to *A. fumigatus* causing increased recruitment of immune effector cells to the site of infection, particularly neutrophils, and associated altered cytokine responses.

The *A. fumigatus* Δ*alcC* strain shows reduced *in vivo* fungal growth and causes wild type levels of tissue damage

The comparison of histopathology between wild type and Δ*alcC* inoculated mice suggested reduced fungal growth by the Δ*alcC* strain in both the chemotherapy and the Triamcinolone murine models (Figure 8). In order to confirm this important observation, we quantified the pulmonary fungal burden on days 3 and 4 p.i. by quantitative RT-PCR. Consistent with the GMS histopathology, qRT-PCR confirmed a reduced pulmonary fungal burden in mice inoculated with Δ*alcC* compared to wild type (Figure 11). In addition, we examined LDH (lactate dehydrogenase) and Albumin

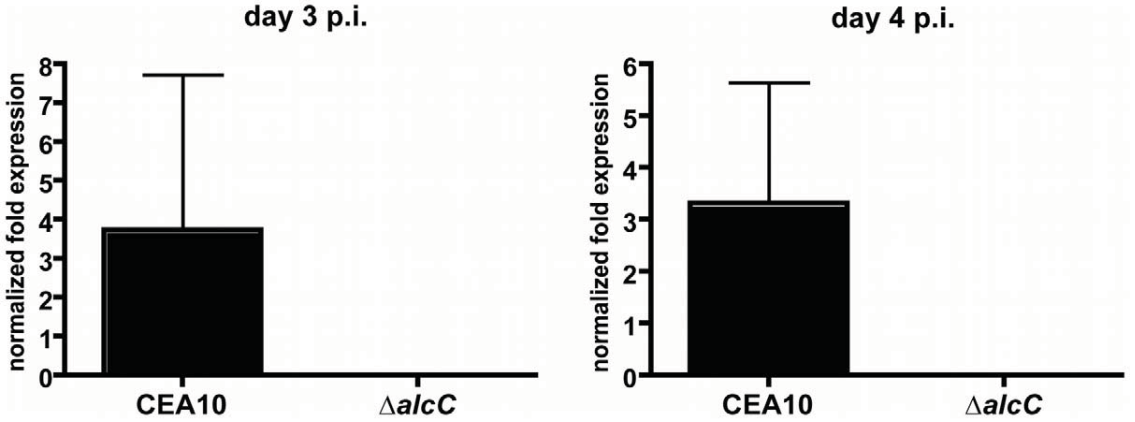

Figure 6. Normalized fold expression of the *A. fumigatus alcC* gene *in vivo* during fungal pathogenesis. Outbred CD1 mice were immunosuppressed by single injection of Triamcinolone (40 mg/kg) 1 day prior to *A. fumigatus* intranasal inoculation. Lungs were harvested on indicated days and whole RNA was prepared. Quantification of mRNA was achieved by quantitative real-time PCR using fungal specific primers. Values are normalized to *tefA* and shown relative to mock control animals. Results are the mean and standard deviation of three replicates.
doi:10.1371/journal.ppat.1002145.g006

release in BAL fluid to determine the degree of tissue damage caused by Δ*alcC* and the wild type strain. Intriguingly, both strains cause the same levels of LDH and Albumin release on day 3 and 4 post inoculation (Figure 12). Collectively, the lower fungal burden, the increased host inflammatory response, and the wild type level of tissue damage in response to Δ*alcC* strongly suggest the *A. fumigatus* alcohol dehydrogenase, AlcC, plays an important role in IPA.

The increased inflammatory response of the host to the Δ*alcC* strain is not caused by changes in the cell wall

The observed altered host response and reduced fungal burden in animals infected with Δ*alcC* led us to question the mechanism behind these phenotypes. As inflammatory responses to fungal pathogens are often mediated by the fungal cell wall, we tested whether loss of AlcC resulted in unexpected changes to the cell wall of this strain that could account for the *in vivo* phenotypes.

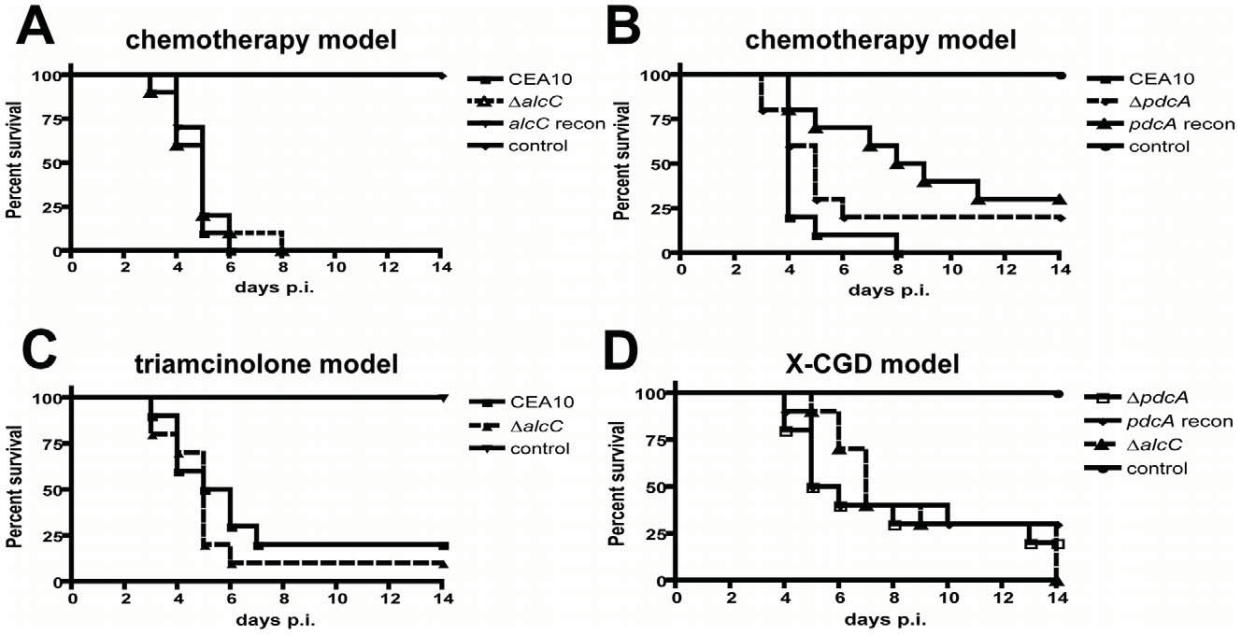

Figure 7. Loss of ethanol fermentation does not affect survival of *A. fumigatus* infected mice. (**A**) (**B**) Outbred CD-1 mice were immunosuppressed by intraperitoneal (i.p.) injection of 175 mg/kg cyclophosphamide 2 days prior to infection and 150 mg/kg 3 days post-inoculation, and subcutaneous (s.c.) injection of Triamcinolone (40 mg/kg) 1 day prior to infection and 6 days post-infection. Mice were inoculated with $\sim 10^4$ conidia of the indicated strains by inhalation of an aerosol in a Hinner's chamber. (**C**) For the triamcinolone model outbred CD-1 mice were immunosuppressed on day -1 by s.c. injection of Kenalog (40 mg/kg), followed by inhalation-inoculation with 10^4 conidia on day 0. (**D**) $gp91^{phox-/-}$ mice were challenged intranasally with 10^6 conidia in a volume of 25 μl of the indicated strains. The ethanol deficient mutant strains, Δ*alcC* and Δ*pdcA*, showed no difference in mortality compared to the wild type or reconstituted strains in any of the tested IPA models ($p>0.2$, Log-Rank Test). 10 animals were inoculated per experiment per inoculation group and the experiments were repeated in duplicate.
doi:10.1371/journal.ppat.1002145.g007

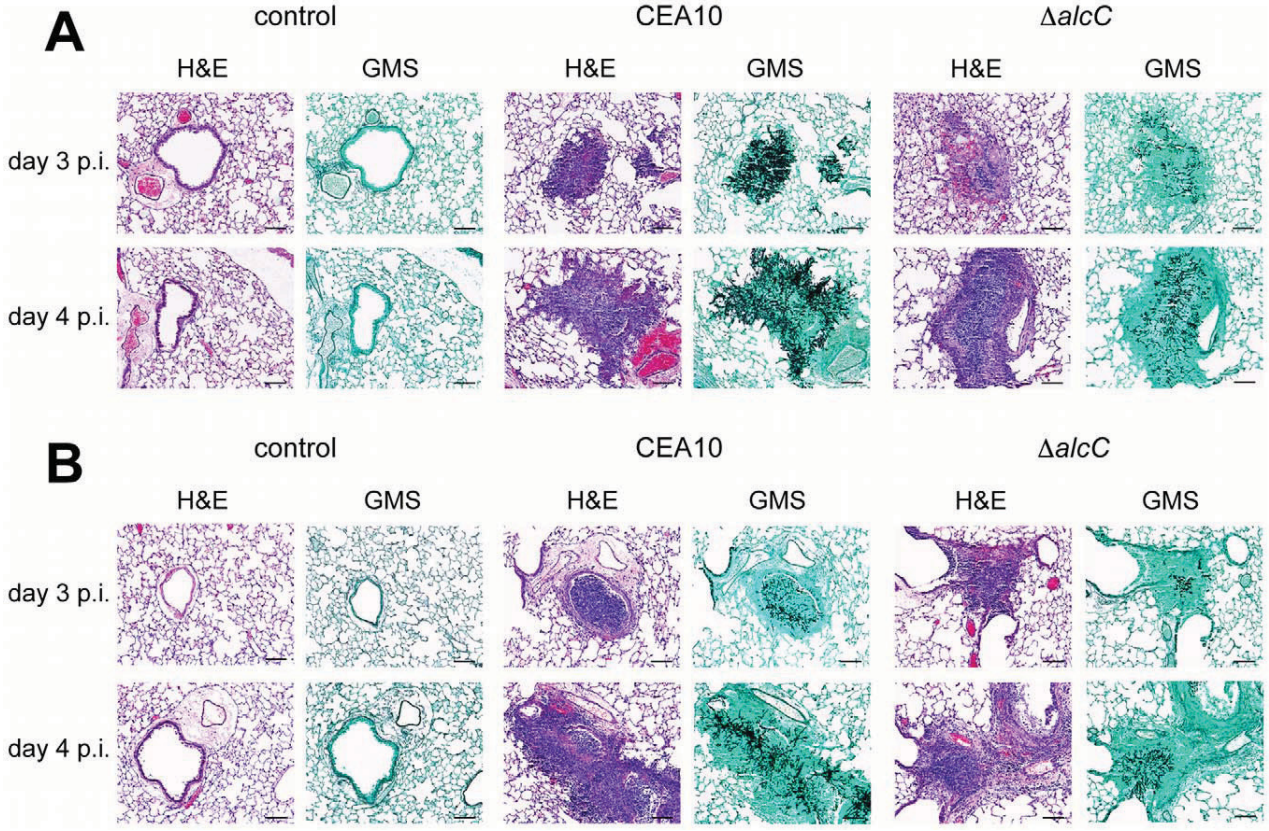

Figure 8. Representative histopathology of the chemotherapy and triamcinolone mouse models 3 and 4 days after inoculation. Mice were inoculated with $1x10^4$ conidia by inhalation (Control = 0.01% Tween inoculated), euthanized on indicated days, lungs removed, fixed, and stained with hematoxylin and eosin (H&E) or Gommori's methenamine silver (GMS) stain. (**A**) In the chemotherapy IPA model wild type inoculated mice show substantial fungal growth and a strongly reduced influx of immune cells, while lesions of Δ*alcC* inoculated mice show reduced fungal growth and an increased inflammatory response on day 3 and day 4 p.i.. (**B**) Lung histopathology of triamcinolone model mice showed reduced fungal growth of the wild type with robust inflammation compared to (A) and an even further reduction in growth of Δ*alcC* with an apparent increase in inflammation and cellular influx. Bar = 100 μm.
doi:10.1371/journal.ppat.1002145.g008

Conidia and ultraviolet (UV) irradiated germlings or hyphae from *A. fumigatus* wild type or Δ*alcC* were co-incubated with bone marrow-derived macrophages (BMMØ) and inflammatory cytokine responses were measured (Figure 13). No differences in the secretion of TNF-α or MIP-2 by BMMØ were observed to any of the tested *A. fumigatus* growth stages with regard to Δ*alcC* or wild type strains. Moreover, no difference in the response to chemical cell wall perturbing agents (caspofungin and congo red) was observed with Δ*alcC* (data not shown). Thus, our data suggest that the increased inflammatory response observed in Δ*alcC* inoculated mice is not caused by changes in the fungal cell wall. Thus, the exact mechanism for the altered pathogenesis in mice inoculated with Δ*alcC* remains to be determined.

Discussion

Metabolic adaptability and flexibility are important attributes for pathogens to successfully colonize, infect, and cause disease in a wide range of hosts. Importantly, these processes are dynamic, and pathogen and host metabolism are likely to change as the result of the host-pathogen interaction, which alters the localized microenvironment. In this study, we present new insights into the pathogenesis of IPA in commonly used experimental murine models. We present data that confirms previous circumstantial data that suggested that hypoxia may be part of the pathogenesis of IPA [55,56]. To our knowledge, this is the first confirmation of the occurrence of *in vivo* hypoxic microenvironments in an invasive fungal infection. Our results thereby add a "new" *in vivo* stress to which human fungal pathogens must adapt to cause lethal disease, and it will be intriguing to define the occurrence of hypoxia in other models of human fungal disease.

To determine whether hypoxia actually occurs in the lung during IPA, we used the hypoxia marker, pimonidazole hydrochloride, which is an investigational oncology probe used as a hypoxia-imaging agent in clinical studies to detect reduced oxygen concentrations in animal and human tumors [43,44,57,58,59]. In our study, we observed that lesions in lungs of mice infected with *A. fumigatus* are hypoxic, as evidenced by the formation of a stable adduct between reduced pimonidazole and host proteins at sites of *A. fumigatus* infection. However, the extent and timing of hypoxia development differed between the immunologically distinct murine models of infection. While hypoxia did occur to some degree in all three models, the chemotherapy model exhibited the least amount of hypoxia in terms of size of the hypoxic area in the lung. This result suggests that the influx and activity of host cells is a strong contributor to the development of hypoxia. However, the persistence of hypoxia in this model, albeit not as extensive as in the other models, also suggests that fungal activities/components

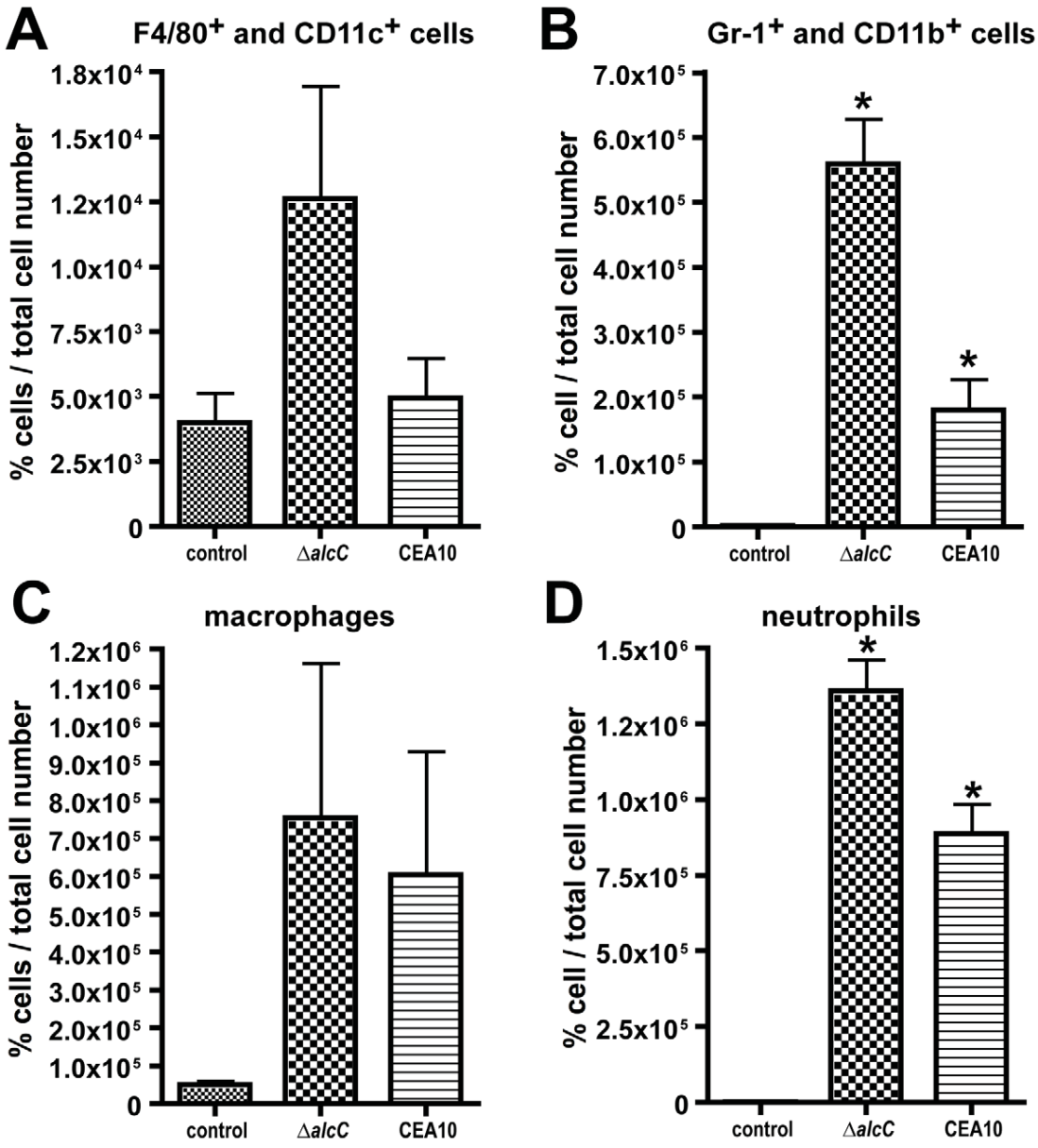

Figure 9. Characterization of cellular infiltrates in broncheoalveolar (BAL) fluids of triamcinolone immunosuppressed mice. Flow cytometry was used to identify (**A**) F4/80$^+$/CD11c$^+$ and (**B**) GR-1$^+$/CD11b$^+$ cells. Figures S3 and S4 show the corresponding Dot plots. Both cell types are elevated in Δ*alcC* inoculated mice. In agreement, differential cell counts demonstrate that macrophage and monocyte numbers were slightly increased in mice inoculated with Δ*alcC* (**C**) while neutrophil numbers were significantly elevated (**D**). *$p<0.05$. Results are presented as mean and standard error of N = 5 mice. The experiment was repeated in duplicate with similar results.
doi:10.1371/journal.ppat.1002145.g009

contribute to hypoxic lesion. For example, a recent study has observed that *A. fumigatus* can modulate host angiogenesis by secretion of secondary metabolites such as gliotoxin, which may further compromise tissue perfusion and ultimately contribute to coagulative necrosis, and thus limit oxygen delivery to sites of infection [60]. Importantly, though hypoxia was not detected on day +1 or day +2 of infection in any of our models we cannot rule out, and indeed would expect, that conidia and growing hyphal tips experience low oxygen tensions as they are engulfed by various host cells and ultimately penetrate the lung parenchyma and invade into the vasculature. Thus, we conclude that during colonization and subsequent infection, *A. fumigatus* is exposed to a dynamic range of oxygen levels in the lung.

The significance of hypoxia, and the timing and extent to which it occurs during IPA, remain important areas of investigation. One important question that we have started to explore in this study is related to the potential clinical significance of fungal mechanisms of hypoxia adaptation. Previous studies in our and other laboratories with fungal SREBPs have suggested that fungal adaptation to hypoxia is critical for virulence. If true, these mechanisms would become an attractive therapeutic target. However, SREBPs are transcription factors that likely modulate

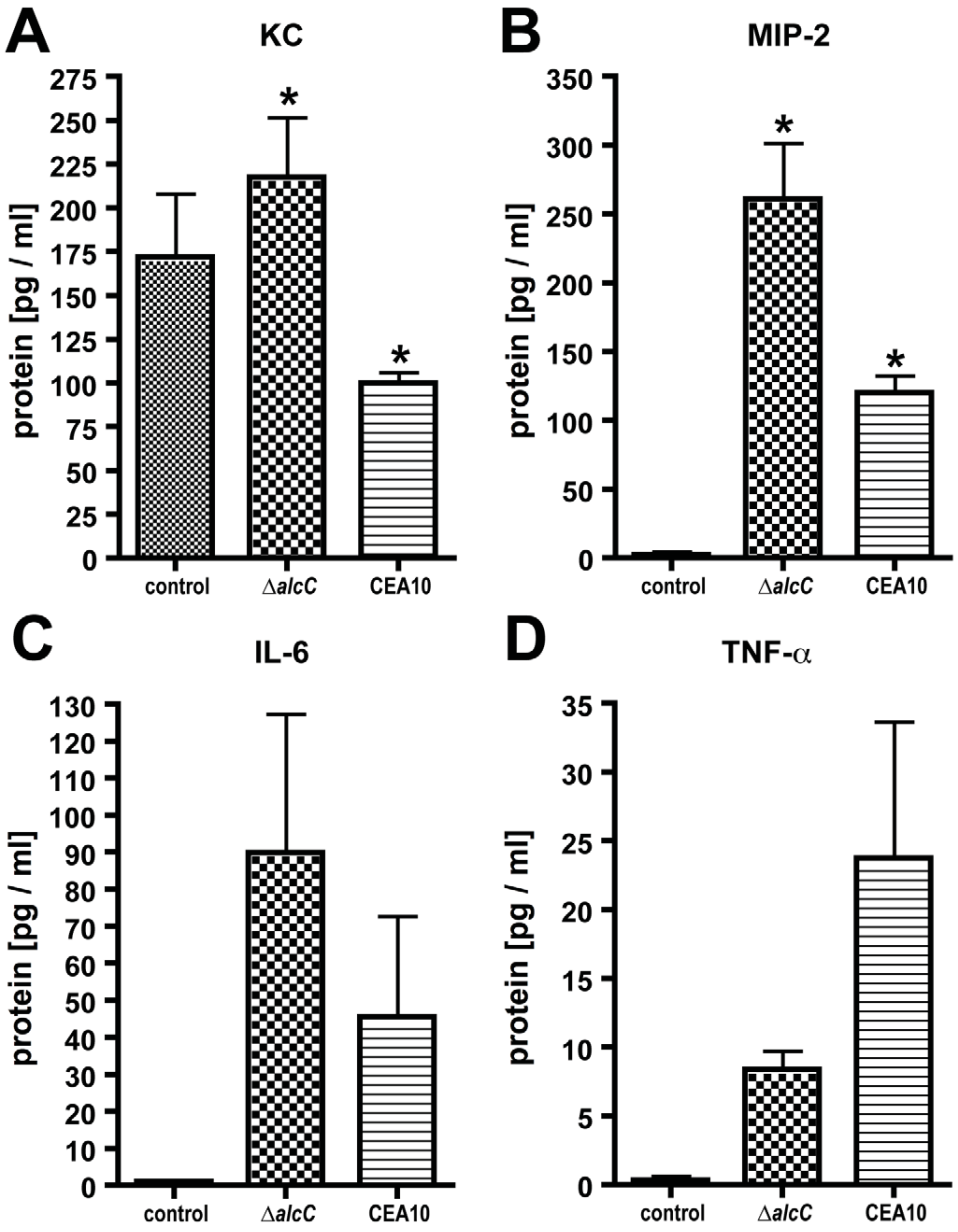

Figure 10. Cytokine production in response to *A. fumigatus* wild type and Δ*alcC* inoculation. (**A**) KC, (**B**) MIP-2, (**C**) IL-6, and (**D**) TNF-α concentrations were determined in BAL fluids on day 3 post inoculation. Significant differences between the two inoculation groups could be observed for KC and MIP-2 protein levels. *$p<0.05$. Results are the mean and standard error of N = 5 mice.
doi:10.1371/journal.ppat.1002145.g010

numerous important mechanisms of fungal physiology, and thus it is not currently possibly to attribute the avirulence phenotype of these strains solely to their inability to grow in hypoxia. In general, mechanisms of hypoxia adaptation in human fungal pathogens are unexplored.

Most eukaryotic cells, like *A. fumigatus*, obligatorily use oxygen to carry out many of their biochemical reactions. Oxygen is a key component of energy production where it functions as a terminal electron acceptor in the formation of ATP from glucose during aerobic respiration. When exposed to microenvironments with limited levels of oxygen, many microorganisms utilize fermentation as a potential metabolic mechanism for dealing with the lack of oxygen [34,35,36,37,38,39,40]. Fermentation allows the fungus to replenish sources of NAD^+ and thus to generate ATP through continued use of glycolysis. Importantly, our interest in hypoxia and fungal pathogenesis began with the discovery of ethanol in BAL samples from *A. fumigatus* infected mice immunosuppressed with our chemotherapeutic model (Figure S1). Thus, in this study, we explored the potential role of ethanol fermentation in *A. fumigatus* hypoxia adaptation and fungal virulence by identifying and characterizing the ethanol fermentation pathway genes in this pathogen.

Our *in vitro* molecular genetic analyses strongly suggest that the main route of ethanol fermentation in *A. fumigatus* is through the pyruvate decarboxylase, PdcA, and subsequent alcohol dehydrogenase, AlcC. Null mutants in both of these genes were unable to

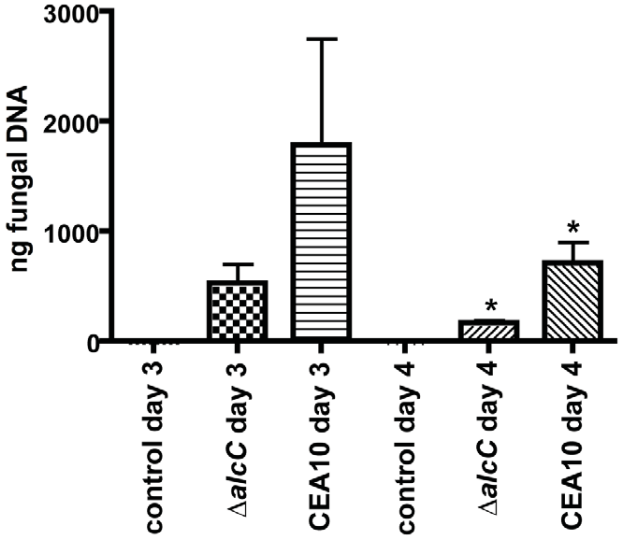

Figure 11. Decreased fungal burden in Δ*alcC* inoculated mice. Outbred CD1 mice were immunosuppressed by subcutaneous injection of triamcinolone (40 mg/kg) 1 day prior to *A. fumigatus* inoculation in a Hinner's inhalation chamber. Fungal burden in the lungs was determined by quantitative real-time PCR based on the 18S rRNA gene of *A. fumigatus*. Data are presented as total fungal genomic DNA normalized to input DNA. The mean and standard error are presented (N = 3 mice for the control group and N = 7 mice for both inoculation groups). * $p<0.01$.
doi:10.1371/journal.ppat.1002145.g011

produce detectable ethanol *in vitro* under hypoxic conditions. These results are in agreement with observations in *Aspergillus nidulans*, where a *pdcA* deletion strain also fails to produce ethanol [61] and *alcC* activity is induced by hypoxic conditions [62]. However, our results also suggest that ethanol fermentation per se is not required for fungal growth *in vitro* as none of the ethanol fermentation deficient strains displayed any growth differences in *in vitro* normoxic or hypoxic growth conditions. We cannot definitively rule out that a small amount of undetectable ethanol fermentation still occurs in our mutant strains, however, we feel it is more likely that other fermentation pathways exist and/or that sufficient mitochondrial respiration still occurs under the conditions examined to support robust growth.

Despite the persistent growth of the ethanol fermentation deficient stains under hypoxia, the Δ*alcC* displayed a very different phenotype *in vivo* in our murine models of IPA. In our three immunologically distinct models of IPA, no difference in mortality could be observed in mice infected with the wild type and ethanol fermentation mutant strains. However, histopathology of the chemotherapy and Triamcinolone models indicated an increased influx of immune cells and reduced fungal growth in Δ*alcC* inoculated mice. These observations were confirmed by flow cytometry and differential cell counts as well as quantitative fungal burden measurements by qRT-PCR. Although, we observed less fungal burden in Δ*alcC* inoculated mice, the overall lesion size was comparable to wild type caused lesions and both strains caused the same level of tissue damage as measured by LDH and Albumin assays. This result is probably due to the increased influx of neutrophils and macrophages to sites of Δ*alcC* infection. It is tempting to speculate then that Δ*alcC* inoculated mice might succumb to the infection because of the increased host

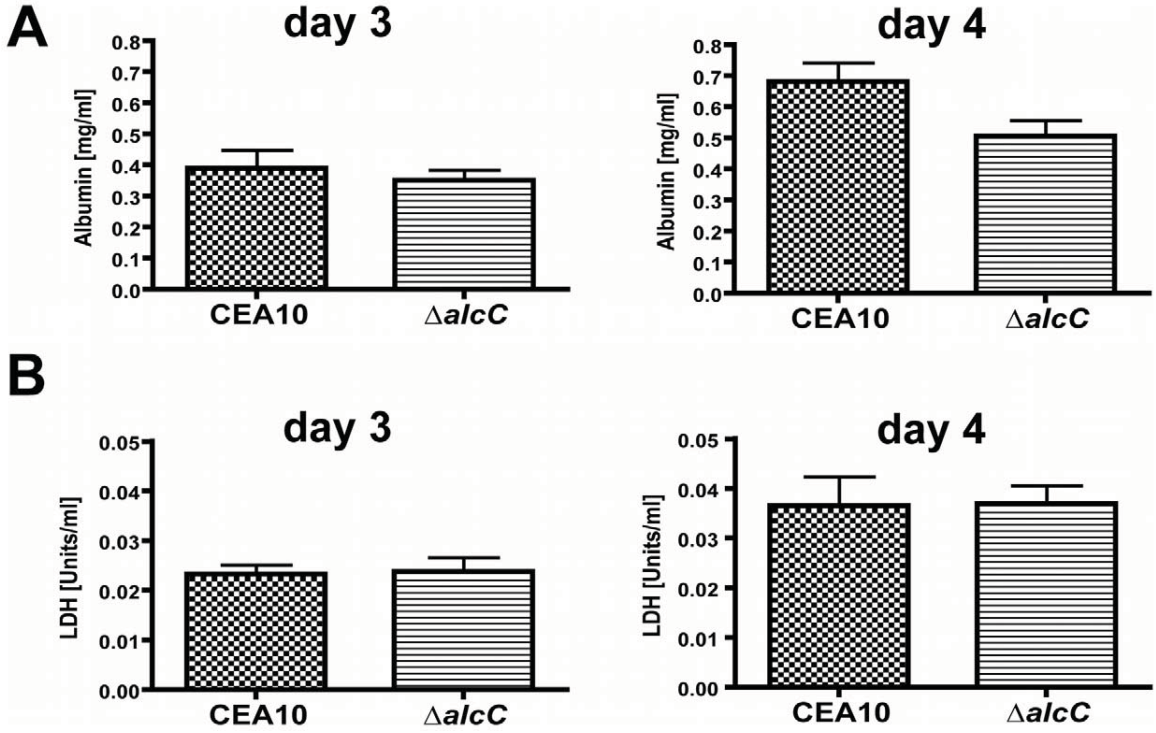

Figure 12. Wild type levels of tissue damage in Δ*alcC* inoculated mice. (**A**) BAL albumin and (**B**) BAL lactate dehydrogenase (LDH) levels in Triamcinolone immunosuppressed CD1 mice (40 mg/kg 1 day prior to infection) were determined on day 3 and 4 p. i. in wild type (CEA10) and Δ*alcC* inoculated mice demonstrating no significant differences between inoculation groups.
doi:10.1371/journal.ppat.1002145.g012

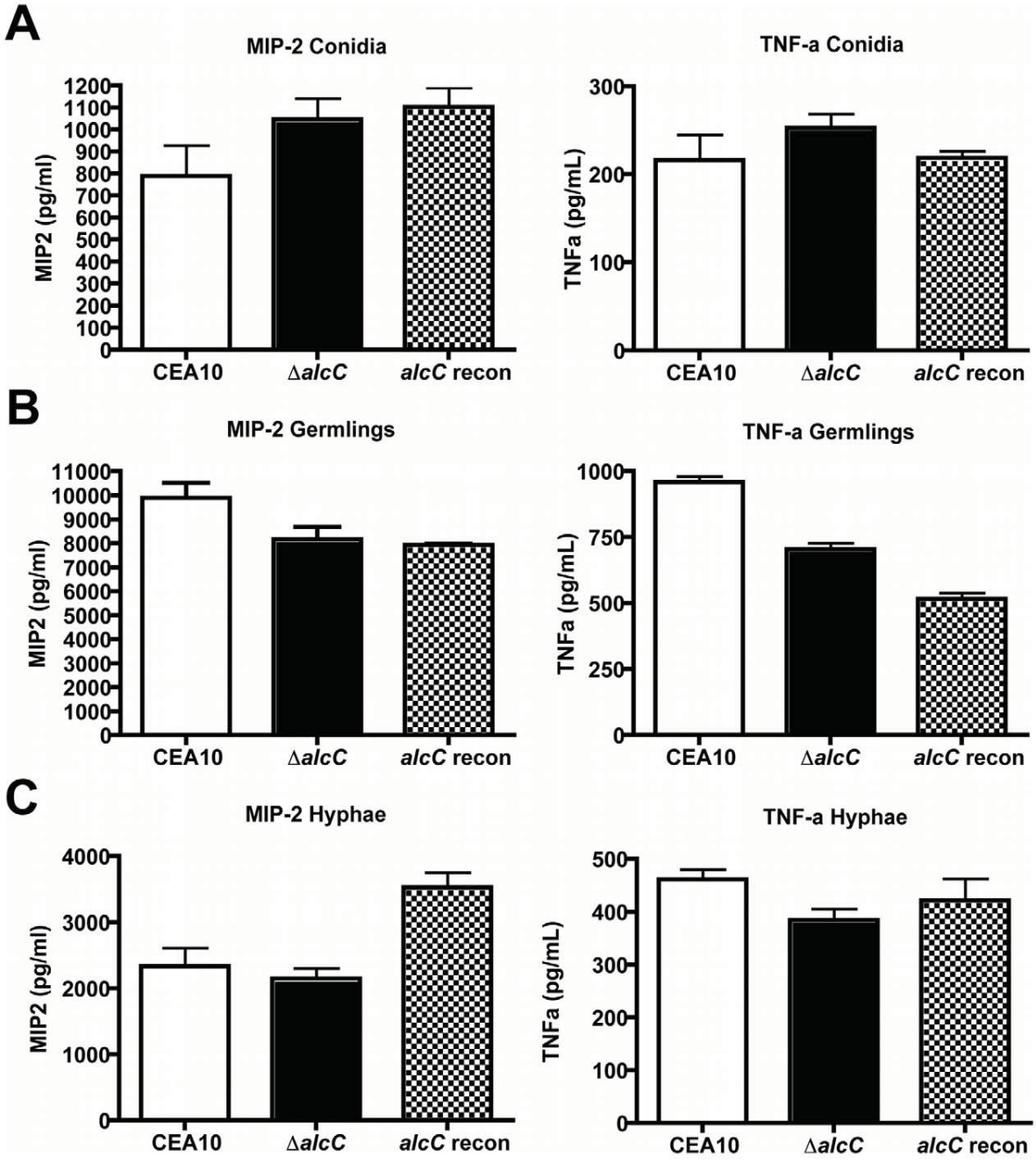

Figure 13. Increased cytokine response is not caused by cell wall changes of the Δ*alcC* strain. Secretion of MIP-2 and TNF-α by bone marrow-derived macrophages (cultured as described in Materials and Methods) incubated for 18 hours with *A. fumigatus* conidia (A), UV irradiated germlings (B), or UV irradiated hyphae (C). Presented are the average concentration and standard deviation in 3 wells per condition of one representative experiment. $P>0.05$ for all comparisons.
doi:10.1371/journal.ppat.1002145.g013

inflammatory response rather than by the invasive growth of the mold. The decrease in fungal burden in mice infected with the Δ*alcC* strain might suggest that this response is partially effective at limiting fungal growth, but with collateral damage to the host that results in mortality. Of note, Mehrad *et al.* recently observed that an overproduction of KC results in a lower fungal burden and higher levels of neutrophil recruitment in a murine model of IPA, which leads to more resistance to *A. fumigatus* infections [63]. As we observed increases in KC and MIP2 levels in response to Δ*alcC* with a concomitant decrease in fungal burden, it may be possible that the increased inflammatory response to Δ*alcC* is at least partially antifungal.

The *in vivo* phenotype of Δ*alcC* raises some intriguing questions about the mechanism behind the observed increase in host inflammatory response and subsequent reduction in fungal burden. Previous observations have indicated that ethanol is a potent immunosuppressive agent, and thus it seems reasonable to hypothesize that loss of ethanol production at the site of infection

at least partially explains the observations with Δ*alcC* [48,49,52,64,65,66,67,68]. Acute and chronic ethanol exposures have been shown to alter the immune response to both bacterial and viral pathogens [69,70,71]. Ethanol decreases clearance of pneumococci and *Klebsiella* species from the lungs of ethanol-fed mice, which is mainly due to an impaired response of the phagocytic cells [72]. With regard to fungal pathogens, Zuiable *et al.* observed that human blood monocytes incubated with ethanol have impaired killing of *Candida albicans* [51]. Along these lines of thinking it may be possible that *A. fumigatus* is able to partially suppress localized host immune responses by utilizing ethanol fermentation in response to hypoxic microenvironments during IPA. However, to confirm this hypothesis, more sensitive detection methods for the localized and low levels of ethanol produced at the site of *A. fumigatus* infection are needed.

Currently, ethanol detection in our murine models is inconsistent as exhibited by our initial experiment with BALs and ^{1}H-NMR. BALs only sample the airway and do not sample localized infection sites located in the lung parenchyma so it is potentially not surprising that this method may not consistently detect a small molecule in the lung such as ethanol. To overcome this potential limitation, we attempted to utilize whole lung homogenates and two different ethanol detection methods including an enzymatic based approach and a GC-MS approach. Unfortunately, either the complexity of the samples, the chemical nature of ethanol itself, or the metabolism at the site of infection prevented reproducible detection of ethanol. Thus, currently, we cannot directly attribute the increased inflammatory response observed with Δ*alcC* to loss of ethanol production. However, development of more sensitive detection methods is underway in our laboratory.

It is intriguing to note that the possibility of fermentation being important for hypoxic growth during fungal infections is further supported by the finding of ethanol in cerebral tissue of rats infected with *C. neoformans* [73]. Moreover, in support of the hypothesis that it is at least a secreted factor that is affecting the host response to Δ*alcC*, UV killed wild type and Δ*alcC* strains at 3 distinct growth phases do not exhibit a difference in pro-inflammatory responses *ex vivo* with bone marrow derived macrophages (Figure 13). Thus, the most likely culprit for an altered inflammatory response, the fungal cell wall, appears to not be altered in Δ*alcC*. Future studies will continue to probe the mechanism behind the reduced fungal growth and increased inflammatory response of Δ*alcC*.

Altogether, in this study we present the first *in vivo* observations of hypoxic microenvironments during an invasive pulmonary fungal infection and shed light on how the mold *A. fumigatus* adapts to low oxygen environments to cause disease. These results, along with other published data from our laboratory, continue to support the hypothesis that hypoxia adaptation and growth is an important component of the pathogenesis of IPA [29,31,74]. Our results further emphasize the dynamic and complex interactions that occur between fungi and their hosts during an invasive pulmonary fungal infection. Future studies will continue to explore the effects of infection localized microenvironment stresses on invasive pulmonary aspergillosis pathogenesis. It will be intriguing to learn if other human fungal pathosystems also involve significant levels of hypoxia at sites of infection and whether ethanol fermentation pathway mutants also alter the host response.

Materials and Methods

Strains and media

A. fumigatus strain CEA17 (gift from Dr. J.P. Latgé, Institut Pasteur, Paris, France) was used to generate the *pdcA* (AFUB_038070; Δ*pdcA*::*A. parasiticus pyrG pyrG1*), *pdcB* (AFUB_096720; Δ*pdcB*::*A. parasiticus pyrG pyrG1*), *pdcC* (AFUB_062480; Δ*pdcC*::*A. parasiticus pyrG pyrG1*), and *alcC* (AFUB_053780; Δ*alcC*::*A. parasiticus pyrG pyrG1*) null mutant strains. *A. fumigatus* strain CEA17 is a uracil-auxotrophic (*pyrG1*) mutant of *A. fumigatus* strain CEA10 [75,76]. In this study, we used CEA10 (CBS144.89) (gift from Dr. J.P. Latgé, Institut Pasteur, Paris, France) as the wild type strain in all experiments except the ^{1}H-NMR metabolite profiling experiment which utilized strain AF293, Δ*pdcA*, Δ*pdcB*, Δ*pdcC*, Δ*alcC*, and the ectopic complemented control strains, *pdcA* recon (Δ*pdcA*::*A. parasiticus pyrG* + *pdcA*) and *alcC* recon (Δ*alcC*::*A. parasiticus pyrG* + *alcC*). All strains were routinely grown in glucose minimal medium (GMM) with appropriate supplements as previously described [77] at 37°C. To prepare solid media 1.5% agar was added before autoclaving.

Strain generation

Generation of the *pdc* null mutants and the *alcC* null mutant in *A. fumigatus* strain CEA17 were accomplished by replacing the ORF of the target genes with *A. parasiticus pyrG*. The replacement construct was generated by cloning a sequence homologous to the gene locus into plasmid pJW24 (donated by Dr. Nancy Keller, University of Wisconsin – Madison). Homologous sequences, each ~1 kb in length and 5′ and 3′ of the gene coding sequence, were cloned to flank *A. parasiticus pyrG* in pJW24. The resulting plasmids, pPDCAKO, pPDCBKO, pPDCCKO, and pALCCKO, were used as templates to amplify a disruption construct (3.6–4.7 kb) for use in fungal transformation.

To complement the Δ*pdcA* and Δ*alcC* strains the genes were amplified using genomic DNA of CEA10 as template and primers ~1 kb 5′ and ~500 bp 3′ of the gene coding sequence. The PCR products were cloned in front of the hygromycin B resistance gene into plasmid pBC-hygro (Silar 1995, obtained from the Fungal Genetics Stock Center, Dr. Kevin McCluskey) using SpeI and NotI restriction sites [78,79]. The resulting plasmids, pBC-hyrgo-PDCA and pBC-hygro-ALCC, were used as template to amplify complementation constructs (~7.4 kb), which were used in a fungal transformation and selection was for colonies able to grow on media containing 150 μg/ml hygromycin B. The primers utilized in vector construction are presented in Table S1.

Standard fungal protoplast transformation was used to generate mutant and reconstituted strains as previously described [31]. Transformants were initially screened by PCR to identify potential homologous recombination events at the gene locus using primers designed to amplify only the mutated gene locus (Table S1). Single conidia of each transformant were prepared and screened by PCR to eliminate the chance of heterokaryons. Homologous recombination was confirmed by Southern analysis with the digoxigenin labeling system (Roche Molecular Biochemicals, Mannheim, Germany) as previously described [80].

Hypoxic cultivation

Strains were grown on or in GMM at 37°C. Normoxic conditions were considered general atmospheric levels within the lab (~21%). For hypoxic conditions two different devices were used, a Biospherix C-Chamber with O_2 levels controlled by a PRO-Ox controller and CO_2 levels controlled with PRO-CO_2 controller (Biospherix, Lacona, NY, USA) and an INVIVO$_2$ 400 Hypoxia Workstation (Ruskinn Technology Limited, Bridgend, UK). For these experiments, the O_2 set point was 1% and the CO_2 set point was 5%. Oxygen levels were maintained with 94% N_2 and a gas regulator. Colony growth was quantified as previously described [31].

Pyruvate decarboxylase activity assay

For normoxic samples, strains were grown in GMM with $1x10^6$ conidia/ml, 300 rpm, at 37°C for 16 hrs. 25 ml of the normoxic culture were mixed with 15 ml of fresh GMM and incubated for an additional 24 hrs under hypoxic conditions (130 rpm, 37°C). Mycelia of normoxic and hypoxic cultures were harvested, rinsed twice with distilled water, transferred to 2 ml screw cap tubes with 0.1 mm glass beats, immediately frozen in liquid nitrogen and weighed. After adding 1 ml of extraction buffer (100 mM KH_2PO_4, 2 mM $MgCl_2$, and 1 mM DTT), the samples were twice placed in a mini beadbeater (Biospec products, Bartlesville, OK, USA) for 30 sec with 5 min on ice in between. After centrifugation (13,000 rpm, 20 min, 4°C) the cell free extracts were transferred to new, cold reaction tubes and kept on ice until use. The protein concentration of the cell free extracts was defined by using the Coomassie Plus – The Better Bradford Assay Kit (Pierce, Rockford, IL, USA) following the method recommended by supplier.

Enzyme activity was determined using a method adapted from Lockington *et al.* 1997 [61]. The assay volume was adjusted to 200 µl for use in 96-well plates. 25 µl cell free extract (sample and control) or 25 µl extraction buffer (blank) were added to wells in duplicates and then 175 µl of the sample mix (50 mM histidine-HCl, 0.35 mM $MgCl_2$, 0.35 mM TPP, 67 mM pyruvate, 6 U yeast ADH, 0.5 mM fresh NADH, added up with water to 175 µl) were added to the samples and the blank, and 175 µl of the control mix (sample mix without pyruvate) were added to the cell free extract as controls. The rate of decrease in absorbance at 340 nm was followed in a Spectramax Plus (Molecular Devices, Sunnyvale, CA, USA), measuring every 10 sec, at 37°C over 5 min after mixing for 1 sec.

The pyruvate decarboxylase activity was calculated as described by http://cmbe.engr.uga.edu/assays/pyruvatedecarboxylase.pdf. The calculation had to be adjusted to the reduced length of the light path in the 96-well plate by multiplying the molar extinction coefficient for NADH (6.22 L/mmol for a path length of 1 cm) with 0.788. Experiments were done in three separate biological replicates and the mean and standard error calculated with Prism software version 5.0b (GraphPad Software Inc.).

Ethanol detection

To detect ethanol in the culture supernatant of *in vitro* fungal cultures, high performance liquid chromatography (HPLC) was performed using a Shimadzu system (Kyoto, Japan), consisting of a solvent delivery module, a low pressure gradient pump unit, a degasser, an autoinjector, a column oven and a refractive index. The column used for the analytical separation was the Aminex Fermentation Monitoring column (150 mm×7.8 mm, BioRad, Hercules, CA). The mobile phase consisted of 0.001 M H_2SO_4, the flow rate was 0.8 ml/min, the column temperature was 60°C, and the sample injection volume was 25 µl. As external standard ethanol solutions with known concentration (2, 1, 0.5, 0.1, 0.05, 0.01 (v/v) %) were used in every experiment and a standard curve was generated and used to determine concentration. Data was normalized to mycelial dry weight.

In addition, a Shimadzu (Kyoto, Japan) QP2010 GC/MS with an electron ionization (EI) source was used for metabolite separation and identification. A 30 m 0.25 mm id 0.25 um film thickness, RTX-5MS (5% Diphenyl - 95% dimethyl polysiloxane) fused silica capillary column from Restek (Bellefonte, PA) was used for all separations. The GC column was temperature programmed as follows: 5 min isothermal at 100°C, then raised at 20°C/minute to 120°C, and held for 30 seconds. Helium gas served as the carrier gas at a flow rate of 0.73 ml/min. Split injections were performed at a 1 to 20 ratio. The injection port was held constant at 200°C. The interface temperature was set at 200°C and the ion source at 200°C. EI fragmentation was performed scanning from 40 to 400 at 0.2 seconds/scan. The instrument was calibrated with Perfluorotributylamine (PFTBA) prior to analysis. Standards of ethanol were analyzed for rention time and a response curve using a 3 point serial dilution. These response curves were used to calculate detected compounds in each sample. One micro-liter of each sample and standard was used for analysis. Identification was matched to NIST 21 and NIST 107 libraries commercially purchased as well as secondary confirmation with standards, previously mention, purchased from Sigma (Saint Louis, MO).

For the culture samples, strains were grown as described above in the pyruvate decarboxylase assay description. After 24/48/72/96 hrs 2 ml of the culture supernatant were transferred into sterile reaction tubes on ice, and filtered through a Millipore membrane filter (0.45 µm, Millipore, Yonezawa, Japan) into HPLC vials (Sun Sri, Rockwood, TN). Experiments were done in three biological replications.

Isolation of total RNA and transcriptional profiling

Conidia from freshly harvested GMM plates were inoculated in 5 ml GMM in a 6-well plate to a concentration of 1×10^7 conidia/ml. Cultures were grown aerobically for 24 h. For normoxic growth, cultures were maintained in atmospheric conditions. For hypoxic growth, cultures were placed in the hypoxic chamber for 24 h. Fungal mats were flash frozen in liquid nitrogen and lyophilized prior to disruption using a bead beater. To assess fungal gene expression *in vivo*, the triamcinolone immunosuppression model was utilized as described below. Mice were sacrificed on day 3 and 4 post inoculation, and lungs were harvested and immediately frozen in liquid nitrogen. Samples were freeze-dried and homogenized with glass beads on a Mini-Beadbeater (BioSpec Products, Inc., Bartlesville, OK, USA). Total RNA was extracted using TRIsure Reagent (Bioline, Tauton, MA, USA) according to the manufacturer's instructions. After treatment with DNase I (Ambion, Austin, TX, USA), 500 ng of total RNA were used to generate first-strand cDNA with the reverse transcriptase kit (Qiagen, Hilden, Germany). Real-time PCR assays were performed with 20 µl reaction volumes that contained 1x iQ SYBR green master mix (Biorad, Hercules, CA, USA), 0.2 µM of each primer (Table S1), and 2 µl of a 1:5 dilution of the cDNA using a Bio-Rad MyiQ single Color real-time PCR detection System with iCycler. No-RT controls for each primer set were also assayed to confirm that no DNA contamination was present, respectively. Real-time PCRs were performed in triplicates, and the expression levels of all genes of interest were normalized to ß–tubulin levels or *tefA* (translation elongation factor alpha subunit) levels for *in vivo* experiments. The thermal cycling parameters consisted of a 3-min Taq polymerase hot start at 95°C, followed by template amplification of 40 cycles of 95°C for 10 sec, 58°C for 30 sec. Fluorescence was measured during the annealing/extension step (58°C) and a disassociation analysis (melting curve) was performed to confirm that a single amplified product was present. Following amplification, data was analyzed with the Bio-Rad iQ5 2.0 Standard Edition Optical System Software. The ΔΔCt method of analysis was used to determine fold changes of gene expression in the mutants relative to the wild type CEA10 strain.

Murine models of invasive pulmonary aspergillosis

The virulence of the *A. fumigatus* strains was tested in three immunologically distinct murine models of invasive pulmonary aspergillosis. All animals were housed five per cage in an environment with HEPA filtered air, autoclaved food at libitum,

and prophylactic treatment with antibiotic water containing clindamycin (150 mg/ml), vancomycin (1 mg/L) and gentamicin (100 mg/ml). CD1 male and female mice, 6–8 weeks old were used in all experiments for the triamcinolone and chemotherapeuatc murine models. Mice were obtained from Charles River Laboratories (Raleigh, NC) or from a breeding colony located in the Animal Resources Center (ARC) at Montana State University. For the Chronic Granulomatous Disease murine model, 6–8 week old mice with a null allele corresponding to the X-linked gp91^{phox} component of NADPH oxidase (B6.129S6-Cyb^{btm1Din}) were bred in the ARC at Montana State University [45].

For the triamcinolone (corticosteroid) model mice were immunosuppressed with a single dose of Kenalog (Bristol-Myers Squibb Company, Princeton, NJ, USA) injected subcutaneously (s.c.) at 40 mg/kg 1 day prior to inoculation. For the chemotherapy model mice were immunosuppressed with intraperitoneal (i.p.) injections of cyclophosphamide (Baxter Healthcare Corporation, Deerfield, IL, USA) at 175 mg/kg 2 days prior to inoculation and with Kenalog injected subcutaneously (s.c.) at 40 mg/kg 1 day prior to inoculation. On day 3 post-inoculation (p.i.), repeat injections were given with cyclophosphamide (150 mg/kg i.p.) and on day 6 p.i. with Kenalog (40 mg/kg s.c.).

For the detection of hypoxia *in vivo*, 15 unanesthetized mice inhaled 40 ml of an aerosolized suspension of 1×10^9 conidia/ml of *A. fumigatus* strain CEA10. 6 uninfected control mice inhaled 40 ml of aerosolized 0.01% Tween 80 in a Hinners inhalational chamber for 45 min as previously described [81]. One *A. fumigatus* infected mouse was sacrificed immediately after infection, lungs were removed, homogenized and the number of CFU was determined ($\sim1\times10^4$ conidia per mouse). After hypoxyprobe injection (see below), mice were sacrificed at set time points after *A. fumigatus* challenge and lungs were processed for hypoxyprobe immunohistochemistry.

For survival studies and histopathology, 10 mice per *A. fumigatus* strain (CEA10, Δ*pdcA*, *pdcA* recon., Δ*alcC*) either inhaled 40 ml of an aerosolized suspensions of $1x10^9$ conidia/ml (control mice inhaled 40 ml of aerosolized 0.01% Tween 80) or the animals were inoculated intranasally with 1×10^6 conidia in 25 µl and monitored twice a day. Infection inoculum was prepared by growing the *A. fumigatus* isolates on GMM agar plates at 37°C for 3 days. Conidia were harvested by washing the plate surface with sterile phosphate-buffered saline 0.01% Tween 80. The resultant conidial suspension was adjusted to the desired concentration by hemacytometer count.

Mice were observed for 14 days after *A. fumigatus* challenge. Any animals showing distress were immediately sacrificed and recorded as deaths within 24 hrs. No mock infected animals perished in either murine model in all experiments. Lungs from all mice sacrificed on different time points during the experiment were removed for fungal burden assessment, infiltrate and cytokine analysis as well as histopathology. Animal experiments were all repeated in duplicate.

Ethics statement

This study was carried out in strict accordance with the recommendations in the Guide for the Care and Use of Laboratory Animals of the National Institutes of Health. The animal experimental protocol was approved by the Institutional Animal Care and Use Committee (IACUC) at Montana State University (Federal-Wide Assurance Number: A3637-01).

Histopathology

For histopathology, CD1 mice were inoculated as described above, and sacrificed at set time points after *A. fumigatus* challenge. When mice were sacrificed, lungs were removed on that day. Lung tissue was fixed in 10% phosphate-buffered formalin, embedded in paraffin, sectioned at 5 µm, and stained with hematoxylin and eosin (H&E) or Gomori methenamine silver (GMS) by using standard histological techniques. Microscopic examinations were performed on a Nikon Eclipse 80i microscope and imaging system (Nikon Instruments Inc., Melville, NY, USA). A total of 3 mice were examined at each respective time point.

^{1}H-NMR metabolite profiling of broncheoalveolar lavage fluid

The chemotherapeutic murine model of IPA was utilized in these experiments. Mice were inoculated in the Hinner's chamber with either 0.01% Tween 80 or *A. fumigatus* wild type strain AF293. A total of 10 mice were used in each treatment group. On day +3 post infection, BALs were performed with each BAL a final total volume of ~1.5 ml. Deuterated water was added to 600 µL of each BAL to provide a field frequency lock and an internal standard of 0.03% 3-(Trimethylsilyl)-Propionic acid-D_4 sodium salt (TSP) was added to each sample to provide a chemical shift reference at 0 ppm. For ^{1}H-NMR, a one-pulse sequence was used with a 2-second pre-saturation pulse and 7-second repetition time. The resulting one-dimensional spectra were compared using MestReC NMR analysis software (Mestrelab Research) to monitor the presence and absence of identifiable metabolites.

Hypoxyprobe – treatment, staining and immunohistological identification

Mice were intravenously injected with hypoxyprobe at a dose of 60 mg/kg weight of the mouse (Hypoxyprobe Inc., Burlington, MA, USA). After 60 to 90 min, mice were sacrificed by pentobarbital anesthesia (100 µg/g body weight) followed by exsanguination. The left lung of each mouse was filled with OCT (frozen tissue matrix) and after embedding in OCT immediately frozen in liquid nitrogen. The lungs were cryosectioned into 5 µm sections and stored at −80°C until stained. After thawing, the sections are fixed in cold acetone (4°C) for 15 min, followed by washing the sections (PBS, 2×5 min) and blocking with normal serum block (NSB: PBS +10% goat serum +1.25% mouse serum) at RT. After 30 min, sections were washed and incubated overnight at 4°C with the mouse monoclonal antibody FITC-Mab1 (Hypoxyprobe-1 Plus Kit, Hypoxyprobe Inc., Burlington, MA, USA) diluted 1:400 in NSB and with a rabbit polyclonal antibody to *Aspergillus* (Abcam Inc., Cambridge, MA, USA). *Aspergillus* isotype control slides were incubated only with FITC-Mab1 and hypoxyprobe isotype control slides only with the *Aspergillus* antibody. Isotype controls are a measure of unspecific staining of the secondary antibody. After another wash, sections were incubated for 60 min at room temperature with DyLight 594-conjugated mouse Anti-FITC (Jackson ImmunoResearch Laboratories, West Grove, PA) and AlexaFluor488-conjugated goat Anti-rabbit (Invitrogen, Carlsbad, CA, USA) diluted 1:400. After another washing step, prolong Gold antifade reagent with DAPI (Invitrogen, Carlsbad, CA, USA) was added to each section. Microscopic examinations were performed on a Zeiss Axioscope 2-plus microscope and imaging system (Zeiss, Jena, Germany). For each time point, a total of 2 to 4 mice were examined and experiments were repeated in triplicate.

Evaluation of pulmonary infiltrate by flow cytometry and cell differentiation

Broncheoalveolar lavages (BALs) were performed by intratracheal instillation and extraction of 3 ml 1x PBS. Total lung lavage

cell numbers were determined by hemacytometer count, spun onto glass slides, and stained with Diff-Quick (Fisher Scientific, Pittsburgh, PA, USA) for differential counting. For flow cytometry, BAL cells were centrifuged and resuspended in phosphate-buffered saline with 2% calf serum and an anti-mouse Fc receptor antibody (Trudeau Institute, Saranac Lake, NY, USA) to a concentration of approximately 10^7 cells/ml. The cells were then stained with a mixture of fluorophore-conjugated antibodies against mouse GR-1 (APC-Cy7) (BD Pharmingen, San Diego, CA, USA), F4/80 (PE-Cy7) (eBioscience, San Diego, CA, USA), CD11b (AlexaFluor700) (BioLegend, San Diego, CA, USA), and CD11c (APC) (purified from the hamster cell line N418 (ATCC, Manassas, VA, USA) and fluorophore-conjugated using the AlexaFluor633 protein labeling kit (Invitrogen, Carlsbad, CA, USA)) and then examined on a BD LSR flow cytometer (BD Biosciences, San Jose, CA, USA). Analysis of cytometry data was performed with FlowJo software Version 8.8.7 DMG and numbers of relevant cell types were determined by combining flow cytometry data (percentage of a given cell type) with BAL cell counts. Data presented are the mean and standard error of N = 5 mice at each time point.

Detection of cytokines, chemokines and other signal proteins in BAL fluids

The BD Cytometric Bead Array Mouse Inflammation Kit (BD Biosciences, San Jose, CA, USA) was used according to the manufacturers instructions to quantitatively measure IL-6, IL-10, MCP-1, IFN-γ, TNF-α, and IL-12p70 protein levels in mouse BAL fluids utilizing a FACSCalibur flow cytometer (Becton Dickinson, Mountain View, CA, USA). IL-17, MIP-2, KC, and VEGF levels in mouse BAL samples were determined using the mouse cytokine/chemokine Milliplex Map Kit (Millipore Corporation, Billerica, MA, USA) according to the manufacturers instructions and then examined and analyzed on the BioPlex 200 System (Bio-Rad, Hercules, CA, USA). Data presented are the mean and standard error of N = 5 mice at each time point.

Determination of LDH and Albumin levels in BAL fluids

In vivo lung tissue damage was determined by measurement of LDH and Albumin levels in mouse BAL samples by using a LDH assay (CytoTox 96 Non-Radioactive Cytotoxicity Assay, Promega, Madison, WI, USA) and an albumin assay (Albumin (BCG) Reagent Set, Eagle Diagnostics, Cedar Hill, TX, USA) according to the manufacturers' instructions.

Determination of *in vivo* fungal burden

To assess fungal burden in lungs, the triamcinolone immunosuppression model was utilized as described above. Mice were sacrificed on day 3 and 4 post inoculation, and lungs were harvested and immediately frozen in liquid nitrogen. Samples were freeze-dried, homogenized with glass beads on a Mini-Beadbeater (BioSpec Products, Inc., Bartlesville, OK, USA), and DNA extracted with the E.N.Z.A. fungal DNA kit (Omega Bio-Tek, Norcross, GA, USA). Quantitative PCR was performed as described previously [82].

In vitro cytokine response

Bone marrow cells were eluted from the tibias and femurs of 8–12 week old C57BL/6 mice, lysed of red blood cells, and cultured in RP20 (RPMI, 20% FCS, 5 mM HEPES buffer, 1.1 mM L-glutamine, 0.5 U/ml penicillin, and 50 mg/ml streptomycin) supplemented with 30% (v/v) L929 cell supernatant (source of M-CSF). Bone marrow cells were plated in a volume of 20 ml at a density of 2.5×10^6 cells/ml in 10 ml Petri dishes. The medium was exchanged on day 3. Adherent bone marrow-derived macrophages (BMMØs) were harvested on day 6. Cells were washed and plated in 0.2 ml RP10 at a density of 5×10^5 cells/ml in 96 well plates and stimulated for 18 hours with conidia (5×10^5 per well), UV irradiated germlings (10^5/well), or UV irradiated hyphae (2×10^4/well) prepared as described before [83]. After 18 hours co-culture supernatants were collected for ELISA. Commercially available ELISA kits for TNF (BD Biosciences, San Jose, CA, USA) and MIP-2 (R&D Systems, Minneapolis, MN, USA) were used according to the manufacturers' instructions.

Supporting Information

Figure S1 Representative 400 MHz ^{1}H-NMR spectra of broncheoalveolar lavage (BAL) fluid from a mouse with a day +3 *A. fumigatus* pulmonary infection (top spectra) or an uninfected mouse (bottom spectra). Known metabolites are labeled on the infected mouse spectra. Substantial amounts of ethanol are seen in the infected mouse samples.
(TIF)

Figure S2 Hypoxic microenvironments at the site of *A. fumigatus* infection. Single color channel pictures were merged to show overlapping localization of fungal tissue (green), hypoxia (red), and inflammation (DAPI stained nuclei).
(TIF)

Figure S3 Representative histopathology of X-CGD mice inoculated with wild type (CEA10) or Δ*alcC* conidia using a Hinner's inhalational chamber. Mice were euthanized on indicated days p.i., lungs removed, fixed, and stained with hematoxylin and eosin (H&E) or Gommori's methenamine silver (GMS) stain. Lung histopathology showed strongly reduced fungal growth of both strains with simultaneous massive inflammation. No difference could be observed between infection groups. Bar = 100 μm.
(TIF)

Figure S4 Flow cytometry Dot plot for F4/80 and CD11c.
(TIF)

Figure S5 Flow cytometry Dot plot for GR-1 and CD11b.
(TIF)

Table S1 Nucleotide sequences of primers used for deletion and complementation strain constructions as well as real-time PCR.
(XLS)

Acknowledgments

The authors would like to thank Dr. Allen Harmsen and members of the Harmsen laboratory, especially Trent Bushmaker, as well as Dr. Nicole Meissner, David Taylor, Dr. Joshua Obar, and Dr. Steve Swain in the department of Immunology and Infectious Diseases at Montana State University for use of resources related to the hypoxyprobe and immunology studies. The authors would also like to thank Dr. James Raleigh (Department of radiation oncology, University of North Carolina) for insightful comments about hypoxyprobe.

Author Contributions

Conceived and designed the experiments: NG JMM MPG TMH RAC. Performed the experiments: NG SP JMM MPG LYN TMH RAC. Analyzed the data: NG SP JMM MPG LYN TMH RAC. Contributed reagents/materials/analysis tools: JMM MPG RAC. Wrote the paper: NG RAC.

References

1. McNeil MM, Nash SL, Hajjeh RA, Phelan MA, Conn LA, et al. (2001) Trends in mortality due to invasive mycotic diseases in the United States, 1980–1997. Clin Infect Dis 33: 641–647.
2. Varkey JB, Perfect JR (2008) Rare and emerging fungal pulmonary infections. Semin Respir Crit Care Med 29: 121–131.
3. Erjavec Z, Kluin-Nelemans H, Verweij PE (2009) Trends in invasive fungal infections, with emphasis on invasive aspergillosis. Clin Microbiol Infect 15: 625–633.
4. Millner PD, Marsh PB, Snowden RB, Parr JF (1977) Occurrence of *Aspergillus fumigatus* during composting of sewage sludge. Appl Environ Microbiol 34: 765–772.
5. Tekaia F, Latge JP (2005) *Aspergillus fumigatus*: saprophyte or pathogen? Curr Opin Microbiol 8: 385–392.
6. Latge JP (1999) *Aspergillus fumigatus* and aspergillosis. Clin Microbiol Rev 12: 310–350.
7. Latge JP (2001) The pathobiology of *Aspergillus fumigatus*. Trends Microbiol 9: 382–389.
8. Perfect JR, Cox GM, Lee JY, Kauffman CA, de Repentigny L, et al. (2001) The impact of culture isolation of *Aspergillus* species: a hospital-based survey of aspergillosis. Clin Infect Dis 33: 1824–1833.
9. Morgan J, Wannemuehler KA, Marr KA, Hadley S, Kontoyiannis DP, et al. (2005) Incidence of invasive aspergillosis following hematopoietic stem cell and solid organ transplantation: interim results of a prospective multicenter surveillance program. Med Mycol 43(Suppl 1): S49–58.
10. Upton A, Kirby KA, Carpenter P, Boeckh M, Marr KA (2007) Invasive aspergillosis following hematopoietic cell transplantation: outcomes and prognostic factors associated with mortality. Clin Infect Dis 44: 531–540.
11. Baddley JW, Andes DR, Marr KA, Kontoyiannis DP, Alexander BD, et al. (2010) Factors associated with mortality in transplant patients with invasive aspergillosis. Clin Infect Dis 50: 1559–1567.
12. Beffa T, Staib F, Lott Fischer J, Lyon PF, Gumowski P, et al. (1998) Mycological control and surveillance of biological waste and compost. Med Mycol 36(Suppl 1): 137–145.
13. Trautmann NM RT, Krasny ME (2003) Monitoring Compost pH. Ithaca, NY: Cornell University Composting Resources.
14. van Heerden I, Cronje C, Swart SH, Kotze JM (2002) Microbial, chemical and physical aspects of citrus waste composting. Bioresour Technol 81: 71–76.
15. Rhodes JC (2006) *Aspergillus fumigatus*: growth and virulence. Med Mycol 44(Suppl 1): S77–81.
16. Cooney NM, Klein BS (2008) Fungal adaptation to the mammalian host: it is a new world, after all. Curr Opin Microbiol 11: 511–516.
17. Park MK, Myers RA, Marzella L (1992) Oxygen tensions and infections: modulation of microbial growth, activity of antimicrobial agents, and immunologic responses. Clin Infect Dis 14: 720–740.
18. Hall LA, Denning DW (1994) Oxygen requirements of *Aspergillus* species. J Med Microbiol 41: 311–315.
19. Wang W WX, Liu J, Masaharu, I, Yasuo I, Cui Z (2007) Effect of oxygen concentration on the composting process and maturity. Compost Sci Util 15: 184–190.
20. Erecinska M, Silver IA (2001) Tissue oxygen tension and brain sensitivity to hypoxia. Respir Physiol 128: 263–276.
21. Carlsson PO, Palm F, Andersson A, Liss P (2001) Markedly decreased oxygen tension in transplanted rat pancreatic islets irrespective of the implantation site. Diabetes 50: 489–495.
22. Studer L, Csete M, Lee SH, Kabbani N, Walikonis J, et al. (2000) Enhanced proliferation, survival, and dopaminergic differentiation of CNS precursors in lowered oxygen. J Neurosci 20: 7377–7383.
23. West JB (1984) 1984 Armstrong lecture. Hypoxic man: lessons from extreme altitude. Aviat Space Environ Med 55: 1058–1062.
24. Warn PA, Sharp A, Guinea J, Denning DW (2004) Effect of hypoxic conditions on *in vitro* susceptibility testing of amphotericin B, itraconazole and micafungin against *Aspergillus* and *Candida*. J Antimicrob Chemother 53: 743–749.
25. Matherne GP, Headrick JP, Coleman SD, Berne RM (1990) Interstitial transudate purines in normoxic and hypoxic immature and mature rabbit hearts. Pediatr Res 28: 348–353.
26. Van Belle H, Goossens F, Wynants J (1987) Formation and release of purine catabolites during hypoperfusion, anoxia, and ischemia. Am J Physiol 252: H886–893.
27. Dewhirst MW (1998) Concepts of oxygen transport at the microcirculatory level. Semin Radiat Oncol 8: 143–150.
28. Tarrand JJ, Han XY, Kontoyiannis DP, May GS (2005) *Aspergillus* hyphae in infected tissue: evidence of physiologic adaptation and effect on culture recovery. J Clin Microbiol 43: 382–386.
29. Grahl N, Cramer RA, Jr. (2010) Regulation of hypoxia adaptation: an overlooked virulence attribute of pathogenic fungi? Med Mycol 48: 1–15.
30. Ernst JF, Tielker D (2009) Responses to hypoxia in fungal pathogens. Cell Microbiol 11: 183–190.
31. Willger SD, Puttikamonkul S, Kim KH, Burritt JB, Grahl N, et al. (2008) A sterol-regulatory element binding protein is required for cell polarity, hypoxia adaptation, azole drug resistance, and virulence in *Aspergillus fumigatus*. PLoS Pathog 4: e1000200.
32. Chun CD, Liu OW, Madhani HD (2007) A link between virulence and homeostatic responses to hypoxia during infection by the human fungal pathogen *Cryptococcus neoformans*. PLoS Pathog 3: e22.
33. Chang YC, Bien CM, Lee H, Espenshade PJ, Kwon-Chung KJ (2007) Sre1p, a regulator of oxygen sensing and sterol homeostasis, is required for virulence in *Cryptococcus neoformans*. Mol Microbiol 64: 614–629.
34. Zhou Z, Takaya N, Shoun H (2010) Multi-energy metabolic mechanisms of the fungus *Fusarium oxysporum* in low oxygen environments. Biosci Biotechnol Biochem 74: 2431–2437.
35. Panagiotou G, Villas-Boas SG, Christakopoulos P, Nielsen J, Olsson L (2005) Intracellular metabolite profiling of *Fusarium oxysporum* converting glucose to ethanol. J Biotechnol 115: 425–434.
36. Kiers J, Zeeman AM, Luttik M, Thiele C, Castrillo JI, et al. (1998) Regulation of alcoholic fermentation in batch and chemostat cultures of *Kluyveromyces lactis* CBS 2359. Yeast 14: 459–469.
37. Merico A, Galafassi S, Piskur J, Compagno C (2009) The oxygen level determines the fermentation pattern in *Kluyveromyces lactis*. FEMS Yeast Res 9: 749–756.
38. van Dijken JP, van den Bosch E, Hermans JJ, de Miranda LR, Scheffers WA (1986) Alcoholic fermentation by 'non-fermentative' yeasts. Yeast 2: 123–127.
39. Lara AR, Taymaz-Nikerel H, Mashego MR, van Gulik WM, Heijnen JJ, et al. (2009) Fast dynamic response of the fermentative metabolism of *Escherichia coli* to aerobic and anaerobic glucose pulses. Biotechnol Bioeng 104: 1153–1161.
40. Ismond KP, Dolferus R, de Pauw M, Dennis ES, Good AG (2003) Enhanced low oxygen survival in *Arabidopsis* through increased metabolic flux in the fermentative pathway. Plant Physiol 132: 1292–1302.
41. Raleigh JA, Franko AJ, Koch CJ, Born JL (1985) Binding of misonidazole to hypoxic cells in monolayer and spheroid culture: evidence that a side-chain label is bound as efficiently as a ring label. Br J Cancer 51: 229–235.
42. Arteel GE, Thurman RG, Raleigh JA (1998) Reductive metabolism of the hypoxia marker pimonidazole is regulated by oxygen tension independent of the pyridine nucleotide redox state. Eur J Biochem 253: 743–750.
43. Raleigh JA, Calkins-Adams DP, Rinker LH, Ballenger CA, Weissler MC, et al. (1998) Hypoxia and vascular endothelial growth factor expression in human squamous cell carcinomas using pimonidazole as a hypoxia marker. Cancer Res 58: 3765–3768.
44. Ljungkvist AS, Bussink J, Rijken PF, Raleigh JA, Denekamp J, et al. (2000) Changes in tumor hypoxia measured with a double hypoxic marker technique. Int J Radiat Oncol Biol Phys 48: 1529–1538.
45. Morgenstern DE, Gifford MA, Li LL, Doerschuk CM, Dinauer MC (1997) Absence of respiratory burst in X-linked chronic granulomatous disease mice leads to abnormalities in both host defense and inflammatory response to *Aspergillus fumigatus*. J Exp Med 185: 207–218.
46. Nierman WC, Pain A, Anderson MJ, Wortman JR, Kim HS, et al. (2005) Genomic sequence of the pathogenic and allergenic filamentous fungus *Aspergillus fumigatus*. Nature 438: 1151–1156.
47. Fedorova ND, Khaldi N, Joardar VS, Maiti R, Amedeo P, et al. (2008) Genomic islands in the pathogenic filamentous fungus *Aspergillus fumigatus*. PLoS Genet 4: e1000046.
48. Rimland D, Hand WL (1980) The effect of ethanol on adherence and phagocytosis by rabbit alveolar macrophages. J Lab Clin Med 95: 918–926.
49. Goral J, Karavitis J, Kovacs EJ (2008) Exposure-dependent effects of ethanol on the innate immune system. Alcohol 42: 237–247.
50. Tamura DY, Moore EE, Partrick DA, Johnson JL, Offner PJ, et al. (1998) Clinically relevant concentrations of ethanol attenuate primed neutrophil bactericidal activity. J Trauma 44: 320–324.
51. Zuiable A, Wiener E, Wickramasinghe SN (1992) *In vitro* effects of ethanol on the phagocytic and microbial killing activities of normal human monocytes and monocyte-derived macrophages. Clin Lab Haematol 14: 137–147.
52. Szabo G, Mandrekar P (2009) A recent perspective on alcohol, immunity, and host defense. Alcohol Clin Exp Res 33: 220–232.
53. Pollock JD, Williams DA, Gifford MA, Li LL, Du X, et al. (1995) Mouse model of X-linked chronic granulomatous disease, an inherited defect in phagocyte superoxide production. Nat Genet 9: 202–209.
54. Balloy V, Huerre M, Latge JP, Chignard M (2005) Differences in patterns of infection and inflammation for corticosteroid treatment and chemotherapy in experimental invasive pulmonary aspergillosis. Infect Immun 73: 494–503.
55. Brock M, Jouvion G, Droin-Bergere S, Dussurget O, Nicola MA, et al. (2008) Bioluminescent *Aspergillus fumigatus*, a new tool for drug efficiency testing and *in vivo* monitoring of invasive aspergillosis. Appl Environ Microbiol 74: 7023–7035.
56. Ibrahim-Granet O, Jouvion G, Hohl TM, Droin-Bergere S, Philippart F, et al. (2010) *In vivo* bioluminescence imaging and histopathopathologic analysis reveal distinct roles for resident and recruited immune effector cells in defense against invasive aspergillosis. BMC Microbiol 10: 105.
57. Raleigh JA, Chou SC, Bono EL, Thrall DE, Varia MA (2001) Semiquantitative immunohistochemical analysis for hypoxia in human tumors. Int J Radiat Oncol Biol Phys 49: 569–574.
58. Raleigh JA, Chou SC, Calkins-Adams DP, Ballenger CA, Novotny DB, et al. (2000) A clinical study of hypoxia and metallothionein protein expression in squamous cell carcinomas. Clin Cancer Res 6: 855–862.

59. Kizaka-Kondoh S, Konse-Nagasawa H (2009) Significance of nitroimidazole compounds and hypoxia-inducible factor-1 for imaging tumor hypoxia. Cancer Sci 100: 1366–1373.
60. Ben-Ami R, Lewis RE, Leventakos K, Kontoyiannis DP (2009) *Aspergillus fumigatus* inhibits angiogenesis through the production of gliotoxin and other secondary metabolites. Blood 114: 5393–5399.
61. Lockington RA, Borlace GN, Kelly JM (1997) Pyruvate decarboxylase and anaerobic survival in *Aspergillus nidulans*. Gene 191: 61–67.
62. Kelly JM, Drysdale MR, Sealy-Lewis HM, Jones IG, Lockington RA (1990) Alcohol dehydrogenase III in *Aspergillus nidulans* is anaerobically induced and post-transcriptionally regulated. Mol Gen Genet 222: 323–328.
63. Mehrad B, Wiekowski M, Morrison BE, Chen SC, Coronel EC, et al. (2002) Transient lung-specific expression of the chemokine KC improves outcome in invasive aspergillosis. Am J Respir Crit Care Med 166: 1263–1268.
64. Zhang P, Nelson S, Summer WR, Spitzer JA (1997) Acute ethanol intoxication suppresses the pulmonary inflammatory response in rats challenged with intrapulmonary endotoxin. Alcohol Clin Exp Res 21: 773–778.
65. Brown LA, Harris FL, Bechara R, Guidot DM (2001) Effect of chronic ethanol ingestion on alveolar type II cell: glutathione and inflammatory mediator-induced apoptosis. Alcohol Clin Exp Res 25: 1078–1085.
66. Brown LA, Harris FL, Guidot DM (2001) Chronic ethanol ingestion potentiates TNF-alpha-mediated oxidative stress and apoptosis in rat type II cells. Am J Physiol Lung Cell Mol Physiol 281: L377–386.
67. Guidot DM, Modelska K, Lois M, Jain L, Moss IM, et al. (2000) Ethanol ingestion via glutathione depletion impairs alveolar epithelial barrier function in rats. Am J Physiol Lung Cell Mol Physiol 279: L127–135.
68. Holguin F, Moss I, Brown LA, Guidot DM (1998) Chronic ethanol ingestion impairs alveolar type II cell glutathione homeostasis and function and predisposes to endotoxin-mediated acute edematous lung injury in rats. J Clin Invest 101: 761–768.
69. Messingham KA, Faunce DE, Kovacs EJ (2002) Alcohol, injury, and cellular immunity. Alcohol 28: 137–149.
70. Nelson S, Kolls JK (2002) Alcohol, host defence and society. Nat Rev Immunol 2: 205–209.
71. Zhang P, Bagby GJ, Happel KI, Summer WR, Nelson S (2002) Pulmonary host defenses and alcohol. Front Biosci 7: d1314–1330.
72. Nelson S, Bagby GJ, Bainton BG, Summer WR (1989) The effects of acute and chronic alcoholism on tumor necrosis factor and the inflammatory response. J Infect Dis 160: 422–429.
73. Himmelreich U, Dzendrowskyj TE, Allen C, Dowd S, Malik R, et al. (2001) Cryptococcomas distinguished from gliomas with MR spectroscopy: an experimental rat and cell culture study. Radiology 220: 122–128.
74. Willger SD, Grahl N, Cramer RA, Jr. (2009) *Aspergillus fumigatus* metabolism: clues to mechanisms of *in vivo* fungal growth and virulence. Med Mycol 47(Suppl 1): S72–79.
75. d'Enfert C (1996) Selection of multiple disruption events in *Aspergillus fumigatus* using the orotidine-5′-decarboxylase gene, pyrG, as a unique transformation marker. Curr Genet 30: 76–82.
76. D'Enfert C, Diaquin M, Delit A, Wuscher N, Debeaupuis JP, et al. (1996) Attenuated virulence of uridine-uracil auxotrophs of *Aspergillus fumigatus*. Infect Immun 64: 4401–4405.
77. Shimizu K, Keller NP (2001) Genetic involvement of a cAMP-dependent protein kinase in a G protein signaling pathway regulating morphological and chemical transitions in *Aspergillus nidulans*. Genetics 157: 591–600.
78. McCluskey K, Wiest A, Plamann M (2010) The Fungal Genetics Stock Center: a repository for 50 years of fungal genetics research. J Biosci 35: 119–126.
79. Silar P (1995) Two new easy to use vectors for transformation. Fungal Genet Newsl 42: 73.
80. Cramer RA, Lawrence CB (2003) Cloning of a gene encoding an Alt a 1 isoallergen differentially expressed by the necrotrophic fungus *Alternaria brassicicola* during *Arabidopsis* infection. Appl Environ Microbiol 69: 2361–2364.
81. Steinbach WJ, Benjamin DK, Jr., Trasi SA, Miller JL, Schell WA, et al. (2004) Value of an inhalational model of invasive aspergillosis. Med Mycol 42: 417–425.
82. Li H, Barker BM, Grahl N, Puttikamonkul S, Bell JD, et al. (2011) The small GTPase RacA mediates intracellular reactive oxygen species production, polarized growth, and virulence in the human fungal pathogen *Aspergillus fumigatus*. Eukaryot Cell 10: 174–186.
83. Hohl TM, Feldmesser M, Perlin DS, Pamer EG (2008) Caspofungin modulates inflammatory responses to *Aspergillus fumigatus* through stage-specific effects on fungal beta-glucan exposure. J Infect Dis 198: 176–185.

Aspergillus fumigatus mitochondrial electron transport chain mediates oxidative stress homeostasis, hypoxia responses, and fungal pathogenesis

Nora Grahl[1], Taisa Magnani Dinamarco[2], Sven D. Willger[1] Gustavo H. Goldman[2] and Robert A. Cramer[1]*

[1]Department of Immunology and Infectious Diseases, Montana State University, Bozeman, MT, USA.

[2]Laboratório Nacional de Ciência e Tecnologia do Bioetanol – CTBE, Caixa Postal 6170, 13083-970 Campinas, São Paulo, Brazil and [†]Faculdade de Ciências Farmacêuticas de Ribeirão Preto, Universidade de São Paulo, Brazil.

*Contact: Robert A. Cramer, Department of Immunology and Infectious Diseases, Montana State University, PO Box 173610 Bozeman, MT 59717. Tel: 406-994-7467, Fax: 406-994-4303, email: rcramer@montana.edu

Running Title: Mitochondrial respiration and fungal pathogenesis

Abstract

We previously observed that hypoxia is an important component of host microenvironments during pulmonary fungal infections. However, mechanisms of fungal growth in these *in vivo* hypoxic conditions are poorly understood. Here, we report that oxidative respiration is active in hypoxia (1% oxygen) and critical for fungal pathogenesis. An *Aspergillus fumigatus* alternative oxidase (*aoxA*) null mutant displays increases in total cellular protein damage by oxidation, susceptibility to reactive oxygen species, and killing by macrophages but no loss in virulence. In contrast, a cytochrome C (*cycA*) mutant was found to be significantly impaired in germination, and growth in normoxia and hypoxia and displayed attenuated virulence. Intriguingly, the loss of *cycA* results in increased levels of AoxA activity, which results in increased resistance to oxidative stress, macrophage killing, and persistence in murine lungs. Our results demonstrate a previously unidentified role for fungal mitochondrial respiration in the pathogenesis of *Aspergillosis*.

Introduction

Aspergillus fumigatus is commonly found in soil and organic debris where it plays an essential role in carbon and nitrogen recycling (Millner *et al.*, 1977, Tekaia & Latge, 2005, Rhodes, 2006). In addition to its role as an environmental composter, *A. fumigatus* is considered an important pathogen of avian species (Beernaert *et al.*, 2010). Over the last three decades this ubiquitous mold has become one of the main causes of invasive fungal infections in humans with immunodeficiency (Singh & Paterson, 2005, Tekaia & Latge, 2005).

To colonize, infect, and invade a host to cause disease *A. fumigatus* has to adapt its metabolism to generate energy in diverse host microenvironments. Most eukaryotic organisms utilize aerobic or oxidative respiration for energy generation, which is the most efficient pathway to produce energy in form of adenosine triphosphate (ATP). In the mitochondrial respiratory chain, electrons are transported over several complexes to the final electron acceptor, molecular oxygen, which is coupled to proton translocation (Figure S1). The resultant proton gradient over the inner mitochondrial membrane is used for ATP synthesis.

The conventional respiratory chain consists of 4 main large protein complexes. Complex I (NADH:ubiquinone oxidoreductase) transfers electrons from NADH to ubiquinone coupled with the translocation of protons across the inner mitochondrial membrane (Figure S1) (Joseph-Horne *et al.*, 2001). Electrons from succinate, which is produced by the TCA cycle, reach ubiquinone via Complex II (Succinate-Ubiquinone oxidoreductase) and this step is not coupled with proton transfer over the membrane (Figure S1). From the ubiquinone pool electrons are transferred through complex III (ubiquinol:cytochrome C oxidoreductase), cytochrome C, and complex IV (cytochrome C oxidase) to oxygen, resulting in the generation of water. Protons are

pumped over the inner mitochondrial membrane by both, complex III and IV, during electron transfer and the resulting proton gradient is used by complex V (ATP synthase) to generate ATP (Figure S1) (Joseph-Horne et al., 2001). In addition to this linear respiratory chain, it has been observed that several plants and fungi possess a branched electron transport chain including alternative NADH:ubiquinone oxidoreductases, that act in parallel with complex I, and an alternative oxidase catalyzing the electron transfer from reduced ubiquinone directly to oxygen, bypassing the main cytochrome respiratory pathway (Figure S1) (Johnson *et al.*, 2003, Kirimura *et al.*, 1999, Moore & Siedow, 1991, Sakajo *et al.*, 1993, Akhter *et al.*, 2003, Martins *et al.*, 2011, Avila-Adame & Koller, 2002, Carneiro *et al.*, 2007, Joseph-Horne et al., 2001).

For *A. fumigatus* the presence of a functional conventional respiratory chain, containing complex I to IV, has been suggested (Tudella *et al.*, 2004). In addition, a gene encoding a functional alternative oxidase was identified in *A. fumigatus* and evidence for an alternative NADH:ubiquinone oxidoreductase has been found (Tudella et al., 2004, Magnani *et al.*, 2007, Magnani *et al.*, 2008). However, the role of the alternative oxidase and mitochondrial respiratory chain in *A. fumigatus* virulence has not been explored.

In a recent study we observed that *A. fumigatus* is exposed to microenvironments with limited oxygen levels (hypoxia) *in vivo* during invasive pulmonary aspergillosis (Grahl *et al.*, 2011). We found that *A. fumigatus* adapts its metabolism to hypoxic environments by activating ethanol (EtOH) fermentation. However, loss of EtOH fermentation had no effect on growth in hypoxic conditions, and furthermore, *A. fumigatus* showed growth on non-fermentable carbon sources suggesting that the mold is able to generate energy by respiration in hypoxia (Grahl

et al., 2011). In support of these observations, a recent *A. fumigatus* proteomics study showed that glycolysis, TCA cycle, and respiratory related proteins were increased in response to hypoxic growth conditions (Vodisch *et al.*, 2011). Furthermore, for *Saccharomyces cerevisiae* it has been suggested that the electron transport chain (ETC) is involved in oxygen sensing, hypoxic signaling, and hypoxic gene induction (Guzy *et al.*, 2007, Poyton *et al.*, 2009a, Poyton *et al.*, 2009b, Kwast *et al.*, 1999). In the human fungal pathogen *Cryptococcus neoformans,* an *Agrobacterium tumefaciens* mediated mutagenesis forward genetics approach identified a key role for fungal mitochondria in hypoxia adaptation (Ingavale *et al.*, 2008). However, it is unclear if loss of the identified genes attenuates virulence of this important pathogen. Altogether, these findings indicate that oxidative respiration might play an important role for adaptation to oxygen limiting conditions and potentially the virulence of *A. fumigatus* and other human fungal pathogens.

In this study we observe that the main mitochondrial respiratory pathway via cytochrome C is important for *A. fumigatus* germination and growth in normoxia and hypoxia. We also observe that the conventional ETC and the alternative oxidase are involved in susceptibility and resistance to oxidative stress and macrophage killing respectively. Importantly, we show for the first time that the respiration chain plays an important role in *A. fumigatus* pathogenesis.

Results

A functional mitochondrial respiration chain with increased alternative oxidase activity is present in *A. fumigatus* under hypoxic conditions

In order to answer the question whether *A. fumigatus* is able to utilize oxidative respiration to generate energy under hypoxic conditions, we performed an oxygen consumption assay with wild-type *A. fumigatus* grown in normoxia and hypoxia. Oxygen uptake confirmed the presence of a functional conventional respiration chain, and suggested active forms of an external alternative NADH:ubiquinone oxidoreductase and an alternative oxidase (AOX) (Figure 1). Expectedly, the overall oxygen consumption is lower in hypoxia. However, the respiration chain is less susceptible to complex IV inhibitor KCN under hypoxic conditions with a decrease of oxygen consumption of only 37.3% compared to 65.7% in normoxia. In addition, 4-times as much SHAM had to be added to *A. fumigatus* in hypoxic conditions to reach the same oxygen consumption rate as in normoxia indicating increased activity of AOX in hypoxia (Figure 1). Altogether, these results show that a functional mitochondrial ETC with increased AOX activity is present under hypoxic growth conditions.

Given that mitochondria and the ETC are associated with oxygen sensing, hypoxic signaling, and hypoxia adaptation in other organisms (Guzy et al., 2007, Poyton et al., 2009a, Poyton et al., 2009b, Ingavale et al., 2008), we hypothesized that respiration and especially the AOX might play an important role for *A. fumigatus* adaptation to hypoxic environments that occur *in vivo* during fungal pathogenesis.

Generation of alternative oxidase and cytochrome C null mutant strains

To test our hypothesis we generated null mutants of the AOX (AoxA) and cytochrome C (CycA) by replacement of the coding sequence in *A. fumigatus* strain CEA17 with the auxotrophic marker *pyrG* from *A. parasiticus* (Figure S2). To be able to attribute all resulting phenotypes specifically to the absence of *aoxA* or *cycA* we ectopically re-introduced the respective wild type (WT) alleles into Δ*aoxA* and Δ*cycA* (resulting in *aoxA* recon and *cycA* recon). Successful gene replacement and reconstitution were verified by PCR analyses (data not shown) and Southern blot (Figure S2).

Next, we examined mRNA abundance changes of *cycA* and *aoxA* in the null mutants compared to the WT over a time course of hypoxia exposure to determine if the loss of either gene impacts the expression of the other. In WT and Δ*aoxA, cycA* mRNA abundance increased as an early response to hypoxia, while *cycA* transcript decreased after 4 and 12h (Figure S3A). Overall the normalized fold expression of *cycA* is the same in WT and Δ*aoxA* indicating that loss of AOX might not have an impact on conventional respiration. However in Δ*cycA*, the normalized fold expression of *aoxA* is significantly increased compared to the WT, suggesting an important role for the AOX in this null mutant (Figure S3B).

In a previous *A. nidulans* study it was found that a CycA mutant produces high levels of EtOH in the presence of a fermentable carbon source (Bradshaw *et al.*, 2001). To test if *A. fumigatus* also switches to EtOH fermentation in response to a blockage in traditional respiration, we examined the mRNA abundance of the pyruvate decarboxylase PdcA and the alcohol dehydrogenase AlcC. Previously, both have been shown to be required for EtOH fermentation in *A. fumigatus* under hypoxic conditions (Grahl et al., 2011). The WT and Δ*aoxA* showed a strong induction of

pdcA and *alcC* transcript especially after 2h of hypoxia exposure. Δ *cycA* showed mostly WT levels of normalized fold expression for both transcripts, however, this mutant lacks the strong spike in mRNA abundance at the 2h time point (Figure S3 A and B). In contrast to the WT and *cycA* recon no increase in PDC activity and no EtOH production could be detected for Δ*cycA* in response to hypoxic conditions (data not shown). Altogether, these results suggest that *A. fumigatus* does not switch to EtOH fermentation like *A. nidulans* after loss of cytochrome C function.

To verify that loss of *aoxA* and *cycA* resulted in functional AOX and CycA mutants, we examined the oxygen consumption of both strains after treatment with different inhibitors (Figure 2). As expected for an AOX mutant, Δ*aoxA* showed loss of cyanide resistant respiration compared to the WT in normoxia and hypoxia (Figure 2 and S4). In contrast, the oxygen consumption of Δ *cycA* is not impaired by the addition of KCN or Antimycin A, but by the AOX inhibitor SHAM (Figure 2 and S5). In addition, inhibition of the oxygen uptake by SHAM is decreased in Δ *cycA* in comparison to the WT and reconstituted strain, which, together with the mRNA abundance data, strongly suggest that more AOX activity is present in the absence of CycA.

Loss of the conventional ETC results in delayed germination and strongly reduced hyphal growth

Next, we examined the role of *cycA* and *aoxA* in germination and hyphal growth of *A. fumigatus*. Δ*cycA* showed a delay in germination as evidenced by a 50% germination rate at 10h of incubation, while the corresponding WT and reconstituted strain reach 50% germination after 5-6h. In addition, for WT and *cycA* recon germination occurs over a time period of 3h compared to 4.5h for the mutant. In

contrast, no change in germination rate was found for Δ*aoxA*. Radial growth was not impaired in the *aoxA* mutant, while loss of *cycA* resulted in reduced growth on the fermentable carbon source glucose (after 96h WT 7.87 ± 0.12 cm; Δ*cycA* 3.70 ± 0.26 cm) and growth was nearly abandoned on the non-fermentable carbon sources glycerol and EtOH (data not shown). Hypoxic growth conditions further reduced growth of Δ*cycA* (after 96h WT 7.53 ± 0.06; Δ*cycA* 2.37 ± 0.15 cm). Overall, our results show that conventional oxidative respiration is important for WT rates of germination and hyphal growth of *A. fumigatus* in both normoxic and hypoxic conditions.

Alternative oxidase is critical for resistance to oxidative stress and macrophage killing

As it has been previously reported that AOX plays a role in resistance to oxidative stress (Akhter et al., 2003, Avila-Adame & Koller, 2002, Magnani et al., 2008, Martins et al., 2011), we determined if loss of AoxA results in higher intracellular levels of reactive oxygen species (ROS). Proteins are one of the major targets of oxygen free radicals and can be used as an indirect measurement of intracellular ROS. Utilizing the OxyBlot protein oxidation detection method we found that exposure to hypoxia increased levels of oxidized proteins in *A. fumigatus* and that loss of AoxA function results in even further increases in protein oxidation (Figure 3). This result suggests that intracellular ROS levels are elevated in hypoxia and by loss of AoxA. In further support of these findings, we found that Δ*aoxA* is significantly more susceptible to external ROS (Figure 4A). We also examined the ability of macrophage-like cells to kill Δ*aoxA* conidia (Figure 4B). As presented in figure 4B, a significant increase in conidia killing was observed between the WT and

Δ*aoxA.* We conclude that AOX is involved in resistance to oxidative stress and macrophage killing of *A. fumigatus*.

Δ*cycA* is less susceptible to ROS and macrophage killing

As oxygen consumption assays and real-time PCR results suggest an increase in AoxA activity in Δ*cycA*, we next examined the resistance of this mutant to ROS and killing by macrophages. Interestingly, Δ*cycA* is significantly more resistant to ROS compared to the WT and reconstituted strain (Figure 4C). For the macrophage-killing assay, we performed a 5 and 9h co-incubation to account for the germination defect of Δ*cycA* (see Figure 4 D and E). After 5h of co-incubation, over 80% of Δ *cycA* conidia survived compared to less than 20% for the WT and reconstituted strain. After a 9h co-incubation the survival of Δ*cycA* conidia was still more than 80% and significantly higher than WT and *cycA* recon (Figure 4E). Taken together, these results suggest that loss of *cycA* results in increased resistance to macrophage killing of *A. fumigatus*.

Mitochondrial ETC via cytochrome C is important for fungal virulence

Next, we sought to determine whether CycA and AoxA were required for *A. fumigatus* virulence. To answer this question we utilized three immunologically distinct murine models of invasive pulmonary aspergillosis (IPA) as previously described (Grahl et al. 2011). Despite the increased susceptibility to oxidative stress and macrophage killing, Δ*aoxA* showed no difference in virulence to the WT and reconstituted strain (data not shown). Given the different, yet severe, forms of immunosuppression in murine models of IPA, this result is not surprising. In contrast, the loss of CycA resulted in a significant attenuation in virulence in a *Galleria*

mellonella insect model (data not shown) and all three murine IPA models (Figure 5). Given the *in vitro* growth attenuation of Δ*cycA* in both normoxia and hypoxia, we anticipated that the virulence attenuation was due to a severe reduction in *in vivo* fungal growth. However, surprisingly, histopathology revealed significant hyphal growth of Δ*cycA* in the murine lung (Figure 6A). Consistent with the germination defect seen *in vitro*, Δ*cycA* exhibits delayed growth *in vivo* on day 2 post inoculation (p.i.). By day 4, however, the mutant grows extended hyphae comparable to the WT (Figure 6A). Histology of WT inoculated corticosteroid treated mice, show expected fungal growth, strong inflammation, and recruitment of immune cells, while lung histopathology of mice inoculated with Δ*cycA* show a reduced influx of immune cells (Figure 6B).

Given the significant amount of fungal growth observed in Δ*cycA* inoculated mice, we elected to follow the survivors for an additional period of time. In the chemotherapy model, 40% of Δ*cycA*-inoculated mice were still alive on day 21 p.i., while in the corticosteroid model 50% of mice survived until day 14 p.i. No mice perished in the X-CGD mouse model up to day 29 p.i. (Figure 5). Survivors showed no obvious symptoms of IPA.

However, surprisingly, histopathology analysis of *cycA* inoculated survivors in the chemotherapy and X-CGD mouse model revealed persistence of fungal hyphae in granuloma-like structures on day 21 and day 29 respectively (Figure 7). The lungs of mice treated only with a corticosteroid also showed persistence of *cycA* hyphae, but no granuloma-like lesions up to day 28 p.i. (data not shown). Granuloma-like lesions occurred in all survivors of the chemotherapy model and 80% of the CGD survivors. Chemotherapy model survivor lesions are characterized by substantial fungal hyphae in the center of the lesions together with macrophages and neutrophils

(Figure 7D to F). In the smaller lesions a ring of macrophages (Figure 7A, arrow) is surrounding the lesion center, while in bigger lesions a ring of neutrophils is present (Figure 7B and C, arrows). On the outside of these rings of immune cells is a layer of epithelial-like cells (Figure 7C, arrowhead). GMS staining revealed a layer of fungal debris, which appears to be located directly outside of the neutrophil-ring (Figure 7 E and F, arrow). Culture of the lungs of these surviving mice revealed that live fungus persists in these lesions.

Granuloma-like lesions in the X-CGD mice appear more organized and are more localized than the lesions in the chemotherapy model. The center of the lesions consists of mainly neutrophils and some fungal hyphae, surrounded by a ring of macrophages (Figure 7 G to K, arrow). Some of these macrophages are multi-nuclei giant cells that started moving into the center of the lesions (Figure 7 I). In addition, eosinophils can be seen at the site of infection (Figure 7 I and L, blue arrows). As also seen in the chemotherapy model, the outside most layer of the lesions seems to consist of epithelial-like cells (Figure 7 I, arrowhead) suggesting that the immune system tries to wall off these lesions to prevent further tissue damage and dissemination of the fungus. Taken together, these results suggest that the mitochondrial ETC of *A. fumigatus* plays a critical role in the pathogenesis of IPA.

Discussion

In a recent study we showed that the oxygen supply is limited in murine models of IPA (Grahl et al., 2011). In addition, data from this study also suggest that *A. fumigatus* is able to utilize alternative energy producing pathways like fermentation in response to *in vivo* hypoxic conditions, which can subsequently alter the host immune response. However, the switch to fermentation based metabolism was found to not be essential for growth under oxygen-limitation, suggesting that *A. fumigatus* is able to generate energy independent of fermentation (Grahl et al., 2011). In this study we continue our research on how *A. fumigatus* adapts to oxygen limiting environments. We observed that fungal mitochondrial respiration is highly active under hypoxic conditions and is involved in mediating resistance to oxidative stress. Importantly, we show for the first time that oxidative respiration plays an important role in IPA pathogenesis.

Oxygen consumption assays indicated an increased role for an alternative oxidase (AOX) when *A. fumigatus* is exposed to hypoxia. Thus, the occurrence of an active mitochondrial respiratory chain and substantial AOX activity under hypoxia led us to hypothesize that these components were critical for *A. fumigatus* to adapt to hypoxia and cause disease. While loss of AoxA had no effect on germination and growth of *A. fumigatus*, a *cycA* null mutant displayed delayed and slower germination and showed a significant growth defect. These results are in agreement with observations in *A. nidulans* and *Neurospora crassa*, where a *cycA* null mutant strain was also characterized by delayed germination and slow growth (Bradshaw et al., 2001, Bottorff *et al.*, 1994). However, in *A. nidulans* the loss of CycA resulted in complete growth inhibition on non-fermentable carbon sources and in increased production of EtOH in normoxia (Bradshaw et al., 2001).

In contrast, the *A. fumigatus* Δ*cycA* showed growth on non-fermentable carbon sources and surprisingly no EtOH production could be detected. Furthermore, Δ*cycA* showed decreased growth in hypoxia and lost the ability to induce EtOH fermentation in response to hypoxic conditions compared to WT and the reconstituted strain, suggesting that the fungal ETC is involved in activation of this process in *A. fumigatus*. In addition, our data suggest that *A. fumigatus* can still use the remaining components of the ETC to produce energy. In the plant pathogenic fungus *Botrytis cinerea* it has been shown that this organism switches the electron flow from the main cytochrome pathway to an alternative pathway utilizing complex I, UBQ, and the AOX after 48h of growth in liquid media. The complex I-AOX pathway can drive ATP synthesis without any observable loss of cell viability (Tamura, 1999). In addition, early studies on *A. nidulans* and *Aspergillus niger* showed that young cultures predominantly utilize the main cytochrome respiration pathway, while respiration via AOX increased at later stages of growth (Tudella et al., 2004, Kirimura, 1987). Together with the fact that we observed increased AoxA levels, no EtOH production, and growth on non-fermentable carbon sources, this indicates that the *cycA* deletion mutant likely utilizes the alternative complex I-AoxA pathway to generate energy.

In previous studies in the model yeast *Saccharomyces cerevisiae*, it has been proposed that the fungal ETC is involved in oxygen sensing, growth in hypoxia, and hypoxic gene regulation via production of reactive oxygen and nitrogen species (ROS, RNS) (Guzy et al., 2007, Ingavale et al., 2008, Poyton et al., 2009a, Poyton et al., 2009b). ROS are generated during normal cellular metabolism by the mitochondrial ETC and the cellular redox system (Richter *et al.*, 1988). In general, it is believed that the two sites of ROS production in the mitochondrial ETC are at complex I and III (Poyton et al., 2009b). Several studies have reported that exposure

to hypoxia results in an increase in oxidative stress suggesting that the generated ROS may act as a putative second messenger that activates redox-sensitive transcription factors to enable hypoxia adaptation (Dirmeier *et al.*, 2002, Chandel & Budinger, 2007, Guzy et al., 2007). In agreement with these findings, we observed an increase in oxidative protein damage in WT *A. fumigatus* after exposure to hypoxia.

Beside ROS, RNS, produced by complex IV of the ETC have been suggested to play an important role in oxygen sensing and hypoxic signaling (Castello *et al.*, 2006, Poyton et al., 2009a, Poyton et al., 2009b). Thus, in the *cycA* deletion mutant ROS can probably still be produced via complex I, while RNS cannot be produced by complex IV, suggesting that loss of this signal might result in loss of EtOH fermentation activation. However, further experiments are needed to support this hypothesis.

ROS and RNS cause damage to cellular components like nucleic acids, lipids, and proteins and, if unregulated, will result in apoptosis. Because of this, cells have developed various antioxidant defenses like superoxide dismutase and catalase (Lambou *et al.*, 2010, Paris *et al.*, 2003). In addition, the AOX has been found to play a role in limiting mitochondrial ROS formation and oxidative stress in general in different organisms (Akhter et al., 2003, Avila-Adame & Koller, 2002, Magnani et al., 2008, Martins et al., 2011, Purvis, 1997, Wagner & Moore, 1997). In agreement with this, we observed increased oxidative damage of proteins, indicating raised intracellular ROS, in Δ*aoxA* and a decreased resistance to exogenous ROS. In contrast, Δ*cycA* displayed a significant increase in resistance against exogenous ROS, which is in accordance with the finding that normalized fold expression of *aoxA* was significantly increased and that this mutant showed increased AOX activity in the

oxygen consumption assays. Increased resistance to the AOX inhibitor SHAM has also been reported for an *A. nidulans* CycA mutant (Bradshaw et al., 2001).

During infection *A. fumigatus* is attacked in part by ROS produced by phagocytic cells, and in agreement with the oxidative stress data, we observed an increase in susceptibility of Δ*aoxA* to macrophage killing, while Δ*cycA* showed increased resistance. Utilizing RNAi, Magnani *et al.* silenced the *A. fumigatus aoxA* gene and also found an increase in macrophage killing of the fungus (Magnani et al., 2008). Altogether, the *in vitro* data suggest an important role for AOX in the defense against ROS and resistance to killing by macrophages.

In *C. neoformans* an AOX mutant was found to be significantly less virulent than the WT (Akhter et al., 2003). However, surprisingly in a mouse model of IPA loss of AoxA did not result in any changes in mortality, which might be based on the fact that *A. fumigatus* possess multiple genes encoding for superoxide dismutases (SODs) and catalases to fight oxidative stress *in vivo* (Lambou et al., 2010, Paris et al., 2003). In contrast, the more oxidative stress resistant cytochrome C null mutant is attenuated in virulence in all mouse models tested. However, it is unclear as to the impact of host derived ROS on the virulence of *A. fumigatus.* Null mutants in the key ROS homeostasis transcriptional regulator Yap1 are also not attenuated in virulence and as are null mutants in catalases and SODs (Lambou et al., 2010, Lessing *et al.*, 2007, Qiao *et al.*, 2008). These results may be influenced by the suppressed activity of macrophages and other innate effector cells in murine models of IPA which all use some form of chemical mediated immunosuppression. However, the clinical observation that individuals with the genetic disease CGD are highly susceptible to *Aspergillus* infections still supports the hypothesis that ROS production is required for full resistance to fungal infection.

It is likely that the attenuation in virulence of Δ*cycA* is due to the delay in germination and reduced growth rate of this mutant, as well as its increased resistance to oxidative stress and innate effector cell killing. Still, the amount of *in vivo* growth of Δ*cycA* was surprising considering the *in vitro* phenotypes. Accordingly, lung histology of the chemotherapy model show extended hyphae of Δ*cycA* compared to significantly shorter hyphae in the corticosteroid model. The difference between the two models lies in the inflammatory response. While the inflammatory response is nearly absent in the chemotherapy model, the corticosteroid model is characterized by a hyper-inflammatory response and increased hypoxia (Grahl et al. 2011). As a result of this, in the corticosteroid model the Δ*cycA* strain is surrounded by immune cells, which contribute to the hypoxic microenvironment, and growth of the Δ*cycA* strain is even further reduced in hypoxic conditions.

One of the most surprising and potentially significant findings of our study was that mice are not able to clear Δ*cycA* as nearly all survivors in the 3 mouse models still show fungal hyphae in the lungs after 14, 21, and 29 days respectively. Fungal growth even increased during the time course of infection and hyphae that were recovered from mice at the end of the experiment were still viable. To contain the area of fungal infection and tissue destruction, the immune system of the host started building granuloma-like lesions observed in the chemotherapy model on day 21 p.i. and in the CGD model on day 29 p.i.. The granuloma-like lesions consist mainly of neutrophils and macrophages, cells that are known to be critical for defense against *A. fumigatus*.

Granuloma-like lesions in X-CGD mice seem to be more highly organized structures. In addition to neutrophils and macrophages, giant cells and eosinophils are present. Giant cells are a union of several distinct cells, which are usually

macrophages. The nuclei of the giant cells observed in the X-CGD mice on day 29 have their nuclei in the cell periphery, which is a characteristic for Langhans giant cells that are usually found in granulomatous conditions (Litvinov & Ariel, 2005). In addition, the occurrence of giant cells has been described for granulomas of CGD patients (Hotchi *et al.*, 1980). Eosinophils are usually present during allergic reactions to *A. fumigatus* like allergic bronchopulmonary aspergillosis or aspergillomas (Patterson & Strek, 2010, Jelihovsky, 1983), indicating that extended exposure to *A. fumigatus* antigens might result in Th2 mediated type disease. As an animal model of chronic *Aspergillus* colonization, which is characteristic of ABPA and aspergillomas is currently lacking, it is intriguing to speculate that Δ*cycA* can be utilized to develop such an important model. This line of inquiry is currently being pursued in our laboratory.

Altogether, we conclude that the combination of slow growth and oxidative stress resistance is the reason why Δ*cycA* virulence is attenuated and the immune system is unable to clear the fungal material. However, because of the slow growth the host immune system is able to form granuloma-like lesions to contain the fungal infection. Taken together, our results suggest a critical role for the mitochondrial respiration chain in *Aspergillus* pathogenesis, and beg intriguing questions about how this system contributes to hypoxia signaling and *in vivo* fungal growth.

Experimental Procedures

Strains and Media

A. fumigatus strain CEA17 (gift from Dr. J.P. Latgé, Institut Pasteur, Paris, France) was used to generate the *aoxA* (AFUB_022090; Δ*aoxA*::*A. parasiticus pyrG pyrG1*), and *cycA* (AFUB_028740; Δ*cycA*::*A. parasiticus pyrG pyrG1*) null mutants. *A. fumigatus* strain CEA17 is a uracil-auxotrophic (*pyrG1*) mutant of *A. fumigatus* strain CBS144.89 (d'Enfert, 1996, D'Enfert *et al.*, 1996). All mutant and reconstituted strains were generated and confirmed following methods as we have previously described (Willger et al. 2008, Grahl et al. 2011). In this study, we used CBS144.89 (gift from Dr. J.P. Latgé, Institut Pasteur, Paris, France) as the wild type strain (WT) in all experiments, Δ*aoxA*, Δ*cycA*, and the ectopic complemented controls, *aoxA* recon (Δ*aoxA*::*A. parasiticus pyrG* + *aoxA*) and *cycA* recon (Δ*cycA*::*A. parasiticus pyrG* + *cycA*). All strains were routinely grown in glucose minimal medium (GMM) with appropriate supplements as previously described (Shimizu & Keller, 2001) at 37ºC. An addition of 1.2M sorbitol to GMM (SMM) had to be used to promote conidiation of the Δ*cycA* strain on solid media. Growth tests were performed on GMM containing 1% glucose or GlyMM with 2% glycerol and EMM containing 2% ethanol as the sole carbon source.

Oxygen consumption assay

Germlings were obtained by growing $1x10^8$ conidia of each respective strain in 50 ml of GMM medium for 24h at 37°C, in normoxic or hypoxic conditions. They were harvested by centrifugation and incubated for 5h (90 rpm) in a standard solution used for *A. fumigatus* protoplasting (Osmani *et al.*, 1987) at 30°C to partially disrupt the cell wall. After incubation, germlings were washed three times with and resuspended in

buffer containing 0.7mM sorbitol, 10mM HEPES-KOH pH7.2, and kept in this buffer on ice during the measurements Oxygen uptake was measured with a Clark-type electrode fitted to a Gilson oxygraph (Gilson Medical Electronics Inc., Middleton, WI, USA) (Tudella et al., 2004) in 1.8 ml of standard incubation medium containing 0.7mM sorbitol, 10mM HEPES-KOH ph 7.2, 5mM $MgCl_2$, 0.5mM EGTA, 0.5% w/v BSA, and 2.5mM KH_2PO_4, 5µM Digitonin, and an appropriate substrate, at 30°C (Tudella et al., 2004). The initial solubility of oxygen in the reaction buffer was considered to be 445 ng atoms of O/ml (Helmerhorst *et al.*, 2002). Further additions are indicated in the figure legends. Respiratory parameters were determined as previously described (Chance & Williams, 1956, Tudella et al., 2004).

Hypoxic cultivation

If not indicated otherwise, strains were routinely grown on or in GMM at 37ºC. Normoxic conditions were considered general atmospheric levels within the lab (~21%). For hypoxic conditions an INVIVO$_2$ 400 Hypoxia Workstation (Ruskinn Technology Limited, Bridgend, UK) was used. For these experiments, the O_2 set point was 1% and the CO_2 set point was 5%. Oxygen levels were maintained with 94% N_2 and a gas regulator. Colony growth was quantified as previously described (Willger *et al.*, 2008).

Isolation of total RNA and transcriptional profiling

Cultures were grown aerobically over night. For normoxic growth, 50 ml of GMM were inoculated with 100 µl of the over night culture and incubated in atmospheric conditions. For hypoxic growth, 15 ml of the overnight culture and 15 ml fresh media were placed in the hypoxic chamber. Cultures were incubated for an additional 24h at

37°C, 120 rpm. RNA extraction and real-time PCR assays were performed as previously described (Grahl et al., 2011). Data was analyzed with the Bio-Rad iQ5 2.0 Standard Edition Optical System Software. The ΔΔCt method of analysis was used to determine fold changes of gene expression in the mutants relative to the WT CBS144.89 strain.

Germination assay

To determine germination rates, 10 ml GMM were inoculated with $1x10^7$ conidia/ml of each respective strain and incubated at 37°C, 300 rpm. Starting after 3h of incubation, 500 µl of each culture are transferred to screw capped tubes containing 0.1 mm glass beads, placed in a bead beater (BioSpec Products, Inc., Bartlesville, OK, USA) and beat for 20 s to break up clumps. The number of conidia and germlings is determined by microscopic analyses. After germination started, culture samples are taken every 30 minutes until a stable germination rate is reached. Experiments were done in three biological replicates.

Detection of protein oxidation

Oxidative modification of proteins by oxygen free radicals was monitored by immunoblot analysis of carbonyl groups using the OxyBlot Protein Oxidation Detection Kit according to the manufacturers instructions (Chemicon International Inc., now Millipore, Billerica, MA, USA). Immunoblotting was used for detection according to the kit instructions. The oxidative status of proteins was analyzed quantitatively by densitometry analysis using the Image J program (available at http://rsbweb.nih.gov/ij/download.html).

ROS sensitivity

200 conidia in 100 µl 0.01% tween 80 were plated on GMM plates and incubated at 30°C until microscopic germlings appeared. Plates were overlayed with 10 ml of a 1.25mM H_2O_2 solution or sterile water as a control. After 10 min incubation at 37°C, the 10 ml were aspirated and the plates were washed 2x with sterile water. Following an overnight incubation at 37°C colonies were counted and the percentage of surviving colonies versus the control was calculated. For the menadione growth inhibition assay $1x10^6$ conidia were plated on GMM plates, a small circular filter paper place in the center, and 5 µl of a 16 mg/ml menadione solution or, as a control, 96% ethanol were dropped directly on the filter paper. Plates were incubated for 72h at 37°C and the growth inhibition zone was determined. Experiments were done in 3 biological repetitions.

Macrophage assay

Macrophage killing of conidia was measured as previously described with minor modification (Willger et al., 2008). The percentage of colony forming units (CFU) from conidia:marcophage co-incubation was determined relative to control conidia harvested at the 1h time point (set to 100%). Experiments were performed in triplicate for each *A. fumigatus* strain.

Murine models

The virulence of the *A. fumigatus* strains was tested in three immunologically distinct murine models of invasive pulmonary aspergillosis as we have previously described (Grahl et al. 2011). CD1 male and female mice, 6-8 weeks old were used in all experiments for the corticosteroid and chemotherapeutic murine models. For

the Chronic Granulomatous Disease (CGD) murine model, 8-10 week old mice with a null allele corresponding to the X-linked gp91^{phox} component of NADPH oxidase (B6.129S6-Cyb^{btm1Din}) were bred in the ARC at Montana State University (Morgenstern *et al.*, 1997).

For survival studies and histopathology, 10 mice per *A. fumigatus* strain (CBS144.89, Δ*aoxA*, *aoxA* recon, Δ*cycA, cycA* recon) were inoculated intranasally with 1x10^6 conidia in 40 μl for the corticosteroid and chemotherapeutic model and 1x10^5 in 40 μl for the CGD mouse model. Mock control mice were inoculated with 40 μl of 0.01% Tween 80. Mice were observed for up to 29 days after *A. fumigatus* challenge. Any animals showing distress were immediately sacrificed and recorded as deaths within 24h. No mock infected animals perished in any murine model in all experiments. Lungs from all mice sacrificed on different time points during the experiment were removed for histopathology. All animal experiments were repeated in duplicate.

Ethics Statement

This study was carried out in strict accordance with the recommendations in the Guide for the Care and Use of Laboratory Animals of the National Institutes of Health. The animal experimental protocol was approved by the Institutional Animal Care and Use Program (IACUC) at Montana State University (Federal-Wide Assurance Number: A3637-01).

Histopathology

For histopathology, mice were inoculated as described above, and sacrificed at set time points after *A. fumigatus* challenge and hematoxylin and eosin (H&E) or

Gomori methenamine silver (GMS) stains were performed as previously described (Willger et al. 2008, Grahl et al. 2011).

Statistical analysis

Data were analyzed using two-tailed Student's t-tests (GraphPad Prism 5.0) to compare two groups of data, and considered significant as indicated in the figure legends. Log-rank tests were utilized to determine significance of survival in animal studies.

Acknowledgements

The author's would like to thank Dr. Allen Harmsen and members of the Harmsen laboratory, especially Katie Rowse, in the department of Immunology and Infectious Diseases at Montana State University for useful insights into lung histopathology interpretation. Work in this study was supported by funding from the National Institutes of Health, COBRE grant RR020185 (M. Quinn PI, RAC project 2 leader), NIH/NIAID grant R01AI81838 (RAC), equipment grant from the M. J. Murdock Charitable Trust, the Montana State University Agricultural Experiment Station, and Fundação de Amparo a Pesquisa do Estado de São Paulo (FAPESP) and Conselho Nacional de Desenvolvimento Científico e Tecnológico (CNPq) from Brazil (GHG).

References

Akhter, S., H. C. McDade, J. M. Gorlach, G. Heinrich, G. M. Cox & J. R. Perfect, (2003) Role of alternative oxidase gene in pathogenesis of *Cryptococcus neoformans*. *Infect Immun* **71**: 5794-5802.

Avila-Adame, C. & W. Koller, (2002) Disruption of the alternative oxidase gene in *Magnaporthe grisea* and its impact on host infection. *Molecular plant-microbe interactions : MPMI* **15**: 493-500.

Beernaert, L. A., F. Pasmans, L. Van Waeyenberghe, F. Haesebrouck & A. Martel, (2010) *Aspergillus* infections in birds: a review. *Avian pathology : journal of the W.V.P.A* **39**: 325-331.

Bottorff, D. A., S. Parmaksizoglu, E. G. Lemire, J. W. Coffin, H. Bertrand & F. E. Nargang, (1994) Mutations in the structural gene for cytochrome c result in deficiency of both cytochromes aa3 and c in *Neurospora crassa*. *Curr Genet* **26**: 329-335.

Bradshaw, R. E., D. M. Bird, S. Brown, R. E. Gardiner & P. Hirst, (2001) Cytochrome c is not essential for viability of the fungus *Aspergillus nidulans*. *Molecular genetics and genomics : MGG* **266**: 48-55.

Carneiro, P., M. Duarte & A. Videira, (2007) The external alternative NAD(P)H dehydrogenase NDE3 is localized both in the mitochondria and in the cytoplasm of *Neurospora crassa*. *J Mol Biol* **368**: 1114-1121.

Castello, P. R., P. S. David, T. McClure, Z. Crook & R. O. Poyton, (2006) Mitochondrial cytochrome oxidase produces nitric oxide under hypoxic conditions: implications for oxygen sensing and hypoxic signaling in eukaryotes. *Cell metabolism* **3**: 277-287.

Chance, B. & G. R. Williams, (1956) The respiratory chain and oxidative phosphorylation. *Advances in enzymology and related subjects of biochemistry* **17**: 65-134.

Chandel, N. S. & G. R. Budinger, (2007) The cellular basis for diverse responses to oxygen. *Free radical biology & medicine* **42**: 165-174.

d'Enfert, C., (1996) Selection of multiple disruption events in *Aspergillus fumigatus* using the orotidine-5'-decarboxylase gene, pyrG, as a unique transformation marker. *Curr Genet* **30**: 76-82.

D'Enfert, C., M. Diaquin, A. Delit, N. Wuscher, J. P. Debeaupuis, M. Huerre & J. P. Latge, (1996) Attenuated virulence of uridine-uracil auxotrophs of *Aspergillus fumigatus*. *Infect Immun* **64**: 4401-4405.

Dirmeier, R., K. M. O'Brien, M. Engle, A. Dodd, E. Spears & R. O. Poyton, (2002) Exposure of yeast cells to anoxia induces transient oxidative stress. Implications for the induction of hypoxic genes. *The Journal of biological chemistry* **277**: 34773-34784.

Grahl, N., S. Puttikamonkul, J. M. Macdonald, M. P. Gamcsik, L. Y. Ngo, T. M. Hohl & R. A. Cramer, (2011) *In vivo* Hypoxia and a Fungal Alcohol Dehydrogenase Influence the Pathogenesis of Invasive Pulmonary Aspergillosis. *PLoS Pathog* **7**: e1002145.

Guzy, R. D., M. M. Mack & P. T. Schumacker, (2007) Mitochondrial complex III is required for hypoxia-induced ROS production and gene transcription in yeast. *Antioxidants & redox signaling* **9**: 1317-1328.

Helmerhorst, E. J., M. P. Murphy, R. F. Troxler & F. G. Oppenheim, (2002) Characterization of the mitochondrial respiratory pathways in *Candida albicans*. *Biochimica et biophysica acta* **1556**: 73-80.

Hotchi, M., M. Fujiwara, S. Hata & T. Nasu, (1980) Chronic granulomatous disease associated with peculiar *Aspergillus* lesions. Patho-anatomical report based on two autopsy cases and a brief review of all autopsy cases reported in Japan. *Virchows Archiv. A, Pathological anatomy and histology* **387**: 1-15.

Ingavale, S. S., Y. C. Chang, H. Lee, C. M. McClelland, M. L. Leong & K. J. Kwon-Chung, (2008) Importance of mitochondria in survival of *Cryptococcus neoformans* under low oxygen conditions and tolerance to cobalt chloride. *PLoS Pathog* **4**: e1000155.

Jelihovsky, T., (1983) The structure of bronchial plugs in mucoid impaction, bronchocentric granulomatosis and asthma. *Histopathology* **7**: 153-167.

Johnson, C. H., J. T. Prigge, A. D. Warren & J. E. McEwen, (2003) Characterization of an alternative oxidase activity of *Histoplasma capsulatum*. *Yeast* **20**: 381-388.

Joseph-Horne, T., D. W. Hollomon & P. M. Wood, (2001) Fungal respiration: a fusion of standard and alternative components. *Biochimica et biophysica acta* **1504**: 179-195.

Kirimura, K., Hirowatari, Y., Usami, S., (1987) Alterations of respiratory systems in *Aspergillus niger* under the conditions of citric acid fermentation. *Agric Biol Chem* **51**: 1299-1303.

Kirimura, K., M. Yoda & S. Usami, (1999) Cloning and expression of the cDNA encoding an alternative oxidase gene from *Aspergillus niger* WU-2223L. *Curr Genet* **34**: 472-477.

Kwast, K. E., P. V. Burke, B. T. Staahl & R. O. Poyton, (1999) Oxygen sensing in yeast: evidence for the involvement of the respiratory chain in regulating the transcription of a subset of hypoxic genes. *Proc Natl Acad Sci U S A* **96**: 5446-5451.

Lambou, K., C. Lamarre, R. Beau, N. Dufour & J. P. Latge, (2010) Functional analysis of the superoxide dismutase family in *Aspergillus fumigatus*. *Mol Microbiol* **75**: 910-923.

Lessing, F., O. Kniemeyer, I. Wozniok, J. Loeffler, O. Kurzai, A. Haertl & A. A. Brakhage, (2007) The *Aspergillus fumigatus* transcriptional regulator AfYap1 represents the major regulator for defense against reactive oxygen intermediates but is dispensable for pathogenicity in an intranasal mouse infection model. *Eukaryot Cell* **6**: 2290-2302.

Litvinov, A. V. & B. M. Ariel, (2005) [Historical reference: giant multinuclear cells in tubercular granuloma]. *Problemy tuberkuleza i boleznei legkikh*: 59-61.

Magnani, T., F. M. Soriani, P. Martins Vde, A. C. Policarpo, C. A. Sorgi, L. H. Faccioli, C. Curti & S. A. Uyemura, (2008) Silencing of mitochondrial alternative oxidase gene of *Aspergillus fumigatus* enhances reactive oxygen species production and killing of the fungus by macrophages. *Journal of bioenergetics and biomembranes* **40**: 631-636.

Magnani, T., F. M. Soriani, V. P. Martins, A. M. Nascimento, V. G. Tudella, C. Curti & S. A. Uyemura, (2007) Cloning and functional expression of the mitochondrial alternative oxidase of *Aspergillus fumigatus* and its induction by oxidative stress. *FEMS Microbiol Lett* **271**: 230-238.

Martins, V. P., T. M. Dinamarco, F. M. Soriani, V. G. Tudella, S. C. Oliveira, G. H. Goldman, C. Curti & S. A. Uyemura, (2011) Involvement of an alternative oxidase in oxidative stress and mycelium-to-yeast differentiation in *Paracoccidioides brasiliensis*. *Eukaryot Cell* **10**: 237-248.

Millner, P. D., P. B. Marsh, R. B. Snowden & J. F. Parr, (1977) Occurrence of *Aspergillus fumigatus* during composting of sewage sludge. *Appl Environ Microbiol* **34**: 765-772.

Moore, A. L. & J. N. Siedow, (1991) The regulation and nature of the cyanide-resistant alternative oxidase of plant mitochondria. *Biochimica et biophysica acta* **1059**: 121-140.

Morgenstern, D. E., M. A. Gifford, L. L. Li, C. M. Doerschuk & M. C. Dinauer, (1997) Absence of respiratory burst in X-linked chronic granulomatous disease mice leads to abnormalities in both host defense and inflammatory response to *Aspergillus fumigatus*. *J Exp Med* **185**: 207-218.

Osmani, S. A., G. S. May & N. R. Morris, (1987) Regulation of the mRNA levels of nimA, a gene required for the G2-M transition in *Aspergillus nidulans*. *The Journal of cell biology* **104**: 1495-1504.

Paris, S., D. Wysong, J. P. Debeaupuis, K. Shibuya, B. Philippe, R. D. Diamond & J. P. Latge, (2003) Catalases of *Aspergillus fumigatus*. *Infect Immun* **71**: 3551-3562.

Patterson, K. & M. E. Strek, (2010) Allergic bronchopulmonary aspergillosis. *Proceedings of the American Thoracic Society* **7**: 237-244.

Poyton, R. O., K. A. Ball & P. R. Castello, (2009a) Mitochondrial generation of free radicals and hypoxic signaling. *Trends in endocrinology and metabolism: TEM* **20**: 332-340.

Poyton, R. O., P. R. Castello, K. A. Ball, D. K. Woo & N. Pan, (2009b) Mitochondria and hypoxic signaling: a new view. *Annals of the New York Academy of Sciences* **1177**: 48-56.

Purvis, A. C., (1997) Role of the alternative oxidase in limiting superoxide production by plant mitochondria. *Physiologia Plantarum* **100**: 165-170.

Qiao, J., D. P. Kontoyiannis, R. Calderone, D. Li, Y. Ma, Z. Wan, R. Li & W. Liu, (2008) *Afyap*1, encoding a bZip transcriptional factor of *Aspergillus fumigatus*, contributes to oxidative stress response but is not essential to the virulence of this pathogen in mice immunosuppressed by cyclophosphamide and triamcinolone. *Med Mycol* **46**: 773-782.

Rhodes, J. C., (2006) *Aspergillus fumigatus*: growth and virulence. *Med Mycol* **44 Suppl 1**: S77-81.

Richter, C., J. W. Park & B. N. Ames, (1988) Normal oxidative damage to mitochondrial and nuclear DNA is extensive. *Proc Natl Acad Sci U S A* **85**: 6465-6467.

Sakajo, S., N. Minagawa & A. Yoshimoto, (1993) Characterization of the alternative oxidase protein in the yeast *Hansenula anomala*. *FEBS Lett* **318**: 310-312.

Shimizu, K. & N. P. Keller, (2001) Genetic involvement of a cAMP-dependent protein kinase in a G protein signaling pathway regulating morphological and chemical transitions in *Aspergillus nidulans*. *Genetics* **157**: 591-600.

Singh, N. & D. L. Paterson, (2005) *Aspergillus* infections in transplant recipients. *Clin Microbiol Rev* **18**: 44-69.

Tamura, H., Mizutani, A., Yukioka, H., Miki, N., Ohba, K. and Masuko, M., (1999) Effect of the methoxyiminoacetamide fungicide, SSF129, on respiration activity in *Botrytis cinerea*. *Pesticide Science* **55**: 681-686.

Tekaia, F. & J. P. Latge, (2005) *Aspergillus fumigatus*: saprophyte or pathogen? *Curr Opin Microbiol* **8**: 385-392.

Tudella, V. G., C. Curti, F. M. Soriani, A. C. Santos & S. A. Uyemura, (2004) *In situ* evidence of an alternative oxidase and an uncoupling protein in the respiratory chain of *Aspergillus fumigatus*. *The international journal of biochemistry & cell biology* **36**: 162-172.

Vodisch, M., K. Scherlach, R. Winkler, C. Hertweck, H. P. Braun, M. Roth, H. Haas, E. R. Werner, A. A. Brakhage & O. Kniemeyer, (2011) Analysis of the *Aspergillus fumigatus* proteome reveals metabolic changes and the activation of the pseurotin A biosynthesis gene cluster in response to hypoxia. *Journal of proteome research* **10**: 2508-2524.

Wagner, A. M. & A. L. Moore, (1997) Structure and function of the plant alternative oxidase: its putative role in the oxygen defence mechanism. *Bioscience reports* **17**: 319-333.

Willger, S. D., S. Puttikamonkul, K. H. Kim, J. B. Burritt, N. Grahl, L. J. Metzler, R. Barbuch, M. Bard, C. B. Lawrence & R. A. Cramer, Jr., (2008) A sterol-regulatory element binding protein is required for cell polarity, hypoxia adaptation, azole drug resistance, and virulence in *Aspergillus fumigatus*. *PLoS Pathog* **4**: e1000200.

Figure legends:

Figure 1: Oxygen Consumption in normoxic and hypoxic conditions. The following components were added to the spheroblasts in 1.8mL respiration medium (10mM Hepes–KOH, 0.7mM Sorbitol pH 7.2, 5mM $MgCl_2$, 2.5mM KH_2PO_4, 0.5mM EGTA, 0.5% (w/v) BSA, 5mmol Digitonin): substrate cocktail (10mM glutamate, 10mM malate, 10mM pyruvate, 10mM α-ketoglutarate) (activates respiration via complex I); 10mM succinate (complex II); 2mM NADH (stimulates external NADH:ubiquinone oxidoreductases); 400nmol ADP (switch to actively respiring state); 2μg Oligomycin (complex V inhibitor); 5μM FCCP (disconnects electron transport and phosphorylation system); 1mM KCN (complex IV inhibitor); 2.5mM SHAM (alternative oxidase inhibitor). The oxygen uptake showed an active mitochondrial ETC and also an increased alternative oxidase activity under hypoxic conditions.

Figure 2: Oxygen consumption in Δ*aoxA* and Δ*cycA*. The following components were added to the spheroblasts: substrate cocktail (10mM glutamate, 10mM malate, 10mM pyruvate, 10mM α-ketoglutarate) (activate respiration via complex I); 0.5mM Flavone (alternative NADH:ubiquinone oxidoreductase inhibitor); 10mM Malonate (complex II inhibitor); 1mM KCN (complex IV inhibitor); 0.5μM Antimycin A (complex III inhibitor); 2.5mM SHAM (alternative oxidase inhibitor). Functional null mutants were verified by the addition of KCN, which resulted in complete inhibition of respiration in Δ*aoxA* and respiration of Δ*cycA* was Antimycin A or KCN resistant. In addition, AOX activity is increased in Δ*cycA* compared to WT.

Figure 3: Loss of *aoxA* results in increased protein damage by ROS. **(A)** Western blot analysis of carbonyl groups and **(B)** quantitative densitometry analysis show an increase in oxidative protein modification in response to hypoxia in the WT and an even further increase in Δ*aoxA*. SDS-PAGE gel is shown as a protein loading control.

Figure 4: ROS and Macrophage susceptibility altered in Δ*aoxA* and Δ*cycA*. **(A)** ROS susceptibility assay. Data is expressed as percentage of surviving colonies. A significant increase in sensitivity could be observed for Δ*aoxA*. **(B)** RAW264.7 cells were inoculated with $1x10^6$ conidia of WT, Δ*aoxA*, and *aoxA* recon. Shown is the percent of recovered conidia after 4h compared to 1h incubation. Conidia survival of Δ*aoxA* is significantly reduced compared to WT. **(C)** $1x10^6$ conidia were spread on GMM plates, a circular filter paper placed in the center with menadione or EtOH (control). After 72h the inhibition zone was measured. **(D)** J774 cells and conidia of WT, Δ*cycA*, and *cycA* recon were co-incubated for 1h, followed by an additional 4 or 8h. Shown is the percent of recovered conidia after 5 or 9h compared to 1h incubation. Each value represents mean and standard error of three biological replicates. (*$p < 0.05$).

Figure 5: Cytochrome C is required for *A. fumigatus* virulence. **(A)** Outbred CD-1 mice (n = 10) and chemotherapy model of IPA. Mice were inoculated intranasally (IN) with $1x10^6$ conidia in 40 μl of WT, Δ*cycA*, and *cycA* recon strain. **(B)** Outbred CD-1 mice (n = 10) and corticosteroid model of IPA. Mice were inoculated IN with $1x10^6$ conidia of WT and Δ*cycA*. **(C)** $gp91^{phox-/-}$ mice (n = 10) were challenged IN with $1x10^5$ conidia of the indicated strains. A log rank test was used for pair wise comparison of

survival levels among the different strain groups. Δ*cycA* is significantly less virulent than the WT and reconstituted strain in all mouse models tested. (*p < 0.05).

Figure 6: Histopathology of chemotherapy and corticosteroid models. Hematoxylin and eosin (H&E) or Gommori's methenamine silver (GMS) stains are shown. **(A)** In the chemotherapy IPA model WT inoculated mice show substantial fungal growth and influx of immune cells as early as day 2 p.i., while Δ*cycA* growth is reduced compared to the WT on day 2 p.i.. On day 4 and 5 p.i. Δ*cycA* inoculated mice show fungal growth comparable to the WT. **(B)** Lung histopathology of corticosteroid model mice showed reduced fungal growth and influx of immune cells in Δ*cycA* inoculated mice compared to the WT. Bar = 100 μm.

Figure 7: Representative histopathology of Δ*cycA* inoculated survivors. Hematoxylin and eosin (H&E) or Gommori's methenamine silver (GMS) stains of lungs showed localized inflammation, necrosis, and fungal growth in granuloma-like lesions. Chemotherapy model survivor histopathology showed substantial fungal growth within the lesions **(D to F)** and rings of macrophages **(A, arrow)** or neutrophils **(B, arrow)** surrounding the fungal tissue, with epithelial-like cells representing the most outside cell layer **(C, arrowhead)**. Fungal growth in granuloma-like lesions of CGD mouse model survivors was greatly reduced **(J and K)**. The structure of lesions was highly conserved with neutrophils in the center surrounded by macrophages **(arrows)** and epithelial-like cells **(arrowhead) (G and H)**. Giant cells **(black arrow)** and eosinophils **(blue arrow)** could be observed in or at the periphery of the lesions **(J)**. **(L)** represents a close up of the eosinophils **(blue arrows)** in **(J)**. **(A)** to **(K)** Bar = 200 μm; **(L)** Bar = 10 μm.

Supplemental information:

Figure S1: Schematic of the fungal mitochondrial ETC. Electrons are transported to the ubiquinone pool (UBQ) from NADH by complex I (I) or internal (int1) and external (ext1, ext2) alternative NADH:ubiquinone oxidoreductase, and from succinate by complex II (II). From the UBQ electrons are channeled through complex III (III), cytochrome C (c), and complex IV (IV) or directly by the alternative oxidase (AOX) to oxygen as the terminal electron acceptor. Simultaneous to the electron transport, protons are pumped over the inner mitochondrial membrane by complex I, III, and IV. This proton gradient is used by the ATP synthase (complex V) to generate ATP.

Figure S2: Generation and confirmation of CycA and AoxA null mutants in *A. fumigatus*. Schematic of WT, CycA **(A)**, and AoxA **(B)** null mutant genomic loci. **(A)** Southern blot analysis of WT, Δ*cycA*, and *cycA* recon strains as well as **(B)** WT, Δ*aoxA*, *aoxA* recon strains. Genomic DNA form the respective strains was isolated and digested overnight with *Hin*dIII. An approximate 1 kb genomic region was utilized as a probe. The expected hybridization patterns and sizes were observed for all strains tested. In addition, confirmation of ectopic reconstitution was confirmed by the presence of the WT locus hybridization signal and persistence of the null mutant locus.

Figure S3: Normalized fold expression of *cycA*, *aoxA*, *pdcA*, and *alcC* in *A. fumigatus* WT, Δ*cycA*, and Δ*aoxA* strains after exposure to normoxia or different periods of hypoxia. Each strain was grown for 12h at 37°C under normoxic conditions. After time point 0h samples were harvested, the remaining cultures were

incubated for an additional 1, 2, 4, or 12h under hypoxic conditions before harvest. Quantification of mRNA was achieved by quantitative real-time PCR. Values are normalized to *tefA* and shown relative to WT 0h. Results are shown for one representative biological repetition.

Figure S4: Oxygen consumption of WT and Δ*aoxA* strains under hypoxic conditions. A functional alternative oxidase mutant was verified by the addition of 1 mM KCN, resulted in complete inhibition of respiration in the Δ*aoxA* strain.

Figure S5: Oxygen consumption of WT and Δ*cycA* strains under hypoxic conditions. A functional cytochrome C mutant was verified since respiration of the Δ*cycA* strains was Antimycin (AA) or KCN resistant. In addition, an increased alternative oxidase activity is detectable in the mutant strain.

Table S1: Oligonucleotides utilized in this study

Figures:

Figure 1:

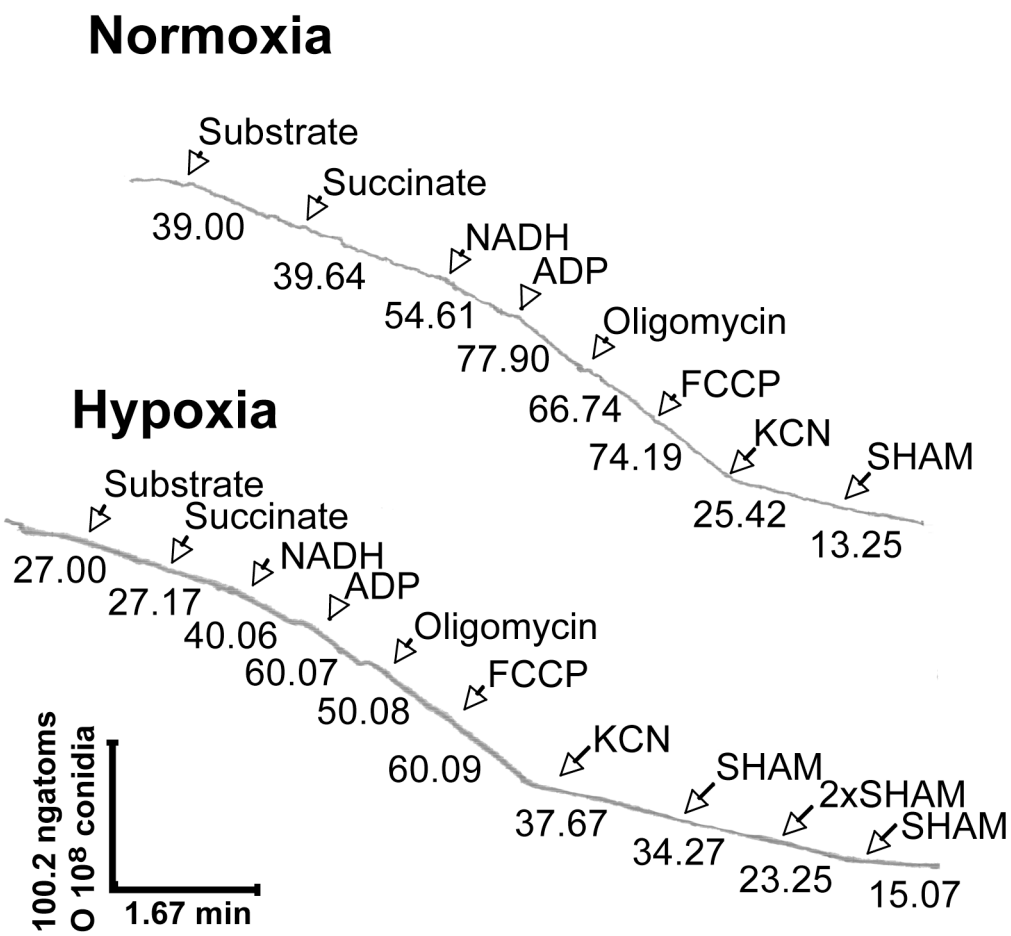

Figure 2:

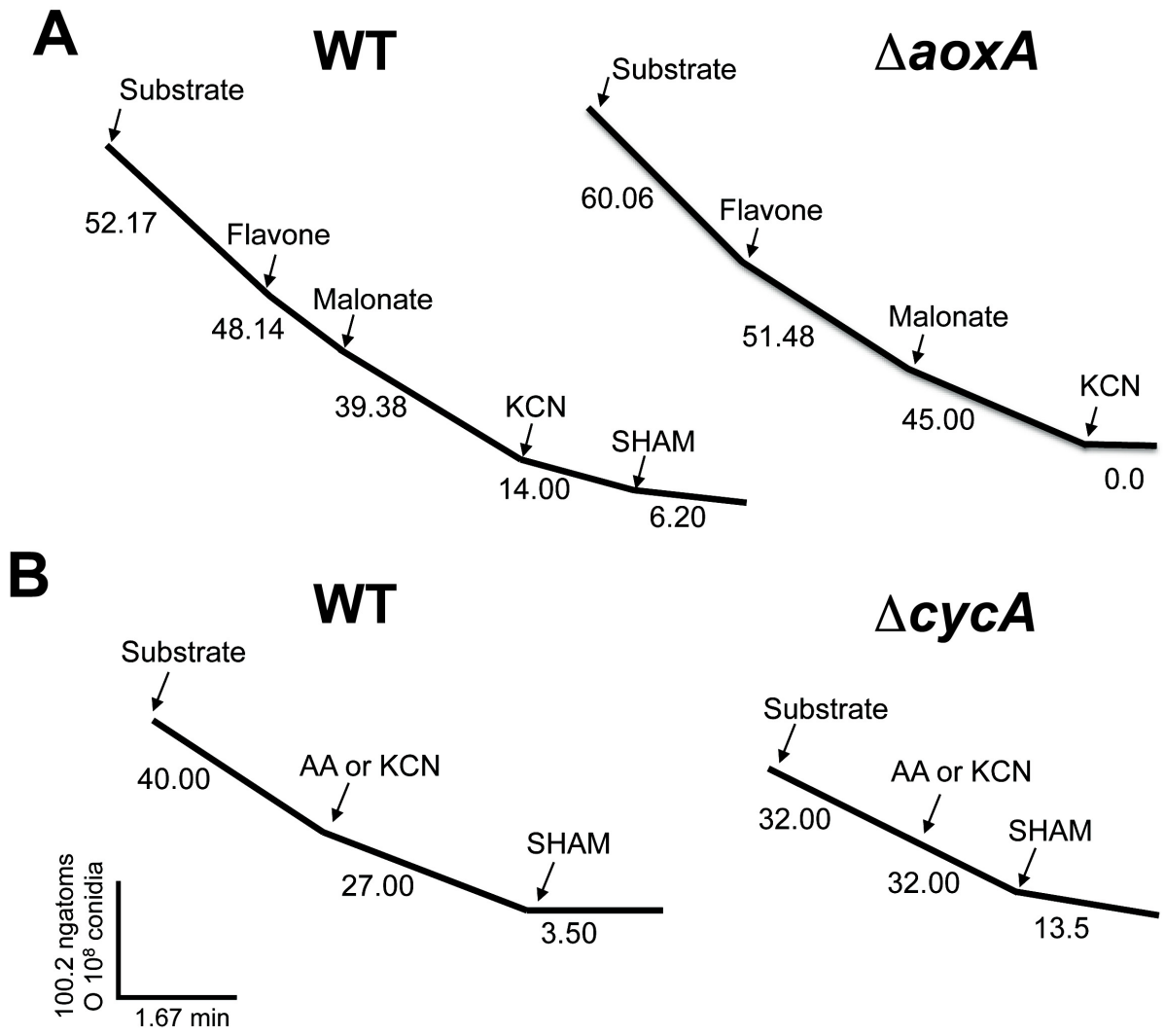
A
WT
Substrate
52.17
Flavone
48.14
Malonate
39.38
KCN
14.00
SHAM
6.20
ΔaoxA
Substrate
60.06
Flavone
51.48
Malonate
45.00
KCN
0.0
B
WT
Substrate
40.00
AA or KCN
27.00
SHAM
3.50
100.2 ngatoms O 10^8 conidia
1.67 min
ΔcycA
Substrate
32.00
AA or KCN
32.00
SHAM
13.5

Figure 3:

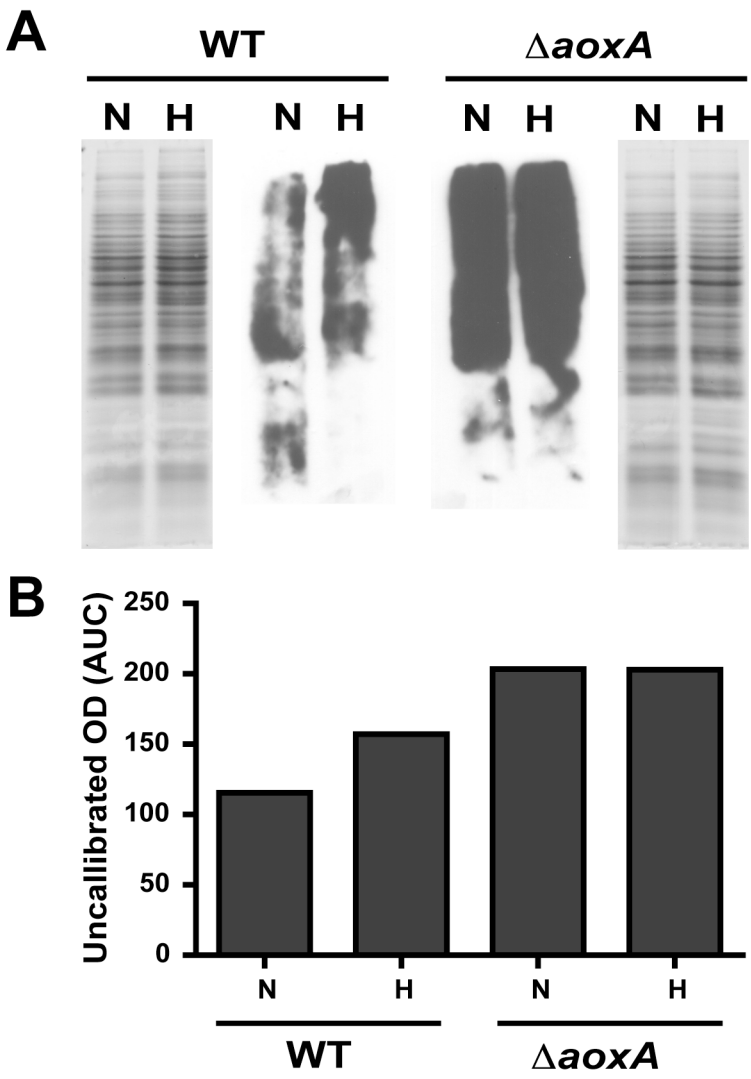
A
WT
ΔaoxA
N H N H N H N H
B
Uncallibrated OD (AUC)
250
200
150
100
50
0
N H N H
WT
ΔaoxA

Figure 4:

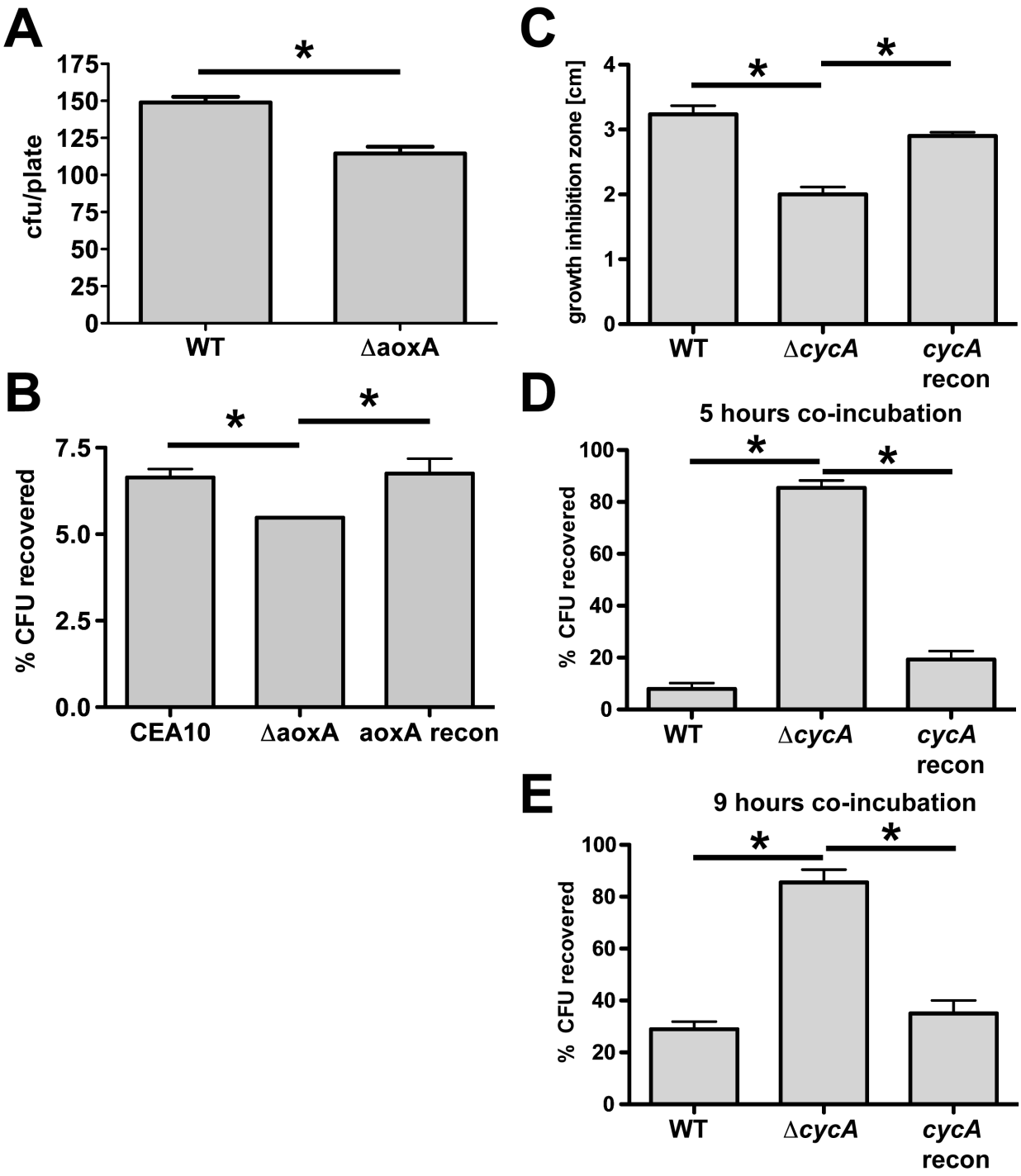
A
cfu/plate
175
150
125
100
75
50
25
0
*
WT
ΔaoxA
B
% CFU recovered
7.5
5.0
2.5
0.0
*
*
CEA10
ΔaoxA
aoxA recon
C
growth inhibition zone [cm]
4
3
2
1
0
*
*
WT
ΔcycA
cycA recon
D
5 hours co-incubation
% CFU recovered
100
80
60
40
20
0
*
*
WT
ΔcycA
cycA recon
E
9 hours co-incubation
% CFU recovered
100
80
60
40
20
0
*
*
WT
ΔcycA
cycA recon

Figure 5:

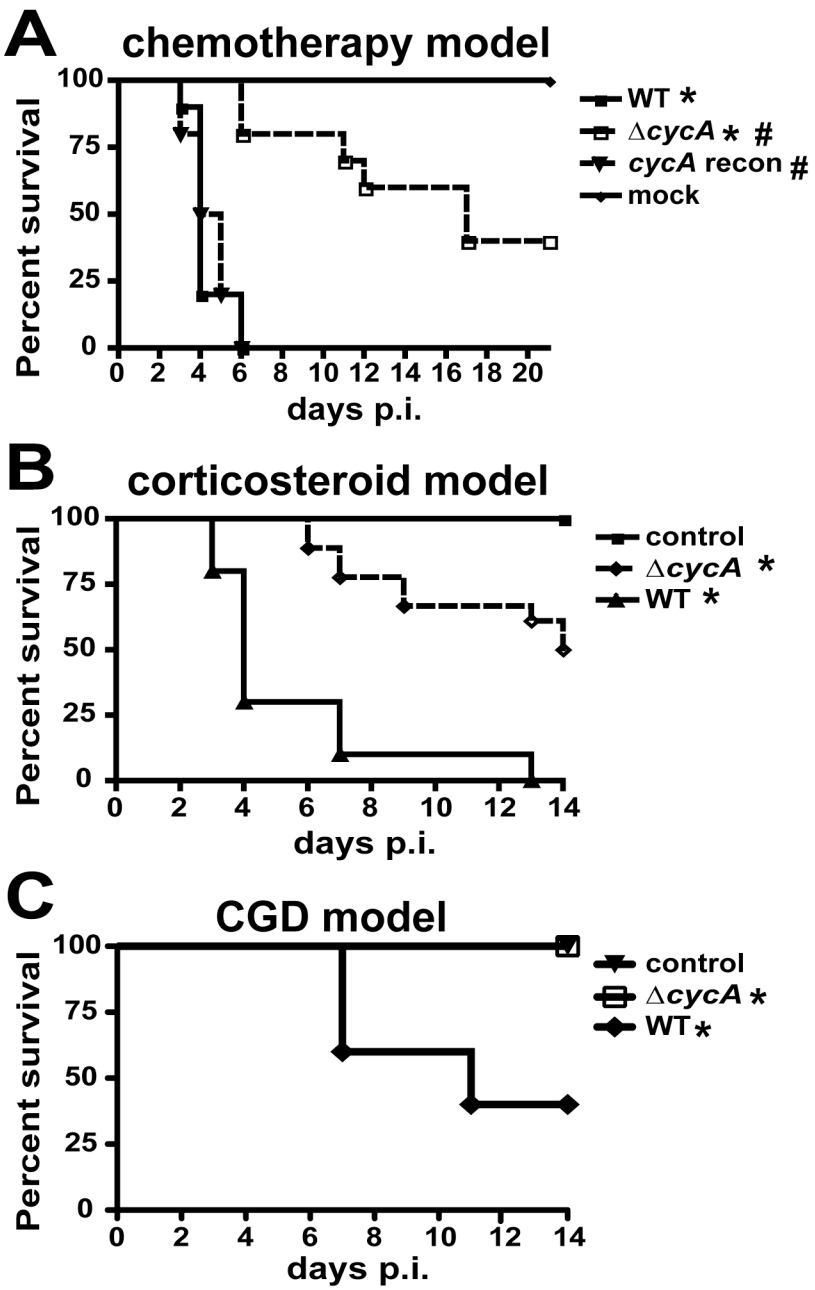
A
chemotherapy model
Percent survival
100
75
50
25
0
0 2 4 6 8 10 12 14 16 18 20
days p.i.
WT *
ΔcycA * #
cycA recon #
mock
B
corticosteroid model
Percent survival
100
75
50
25
0
0 2 4 6 8 10 12 14
days p.i.
control
ΔcycA *
WT *
C
CGD model
Percent survival
100
75
50
25
0
0 2 4 6 8 10 12 14
days p.i.
control
ΔcycA *
WT *

Figure 6:

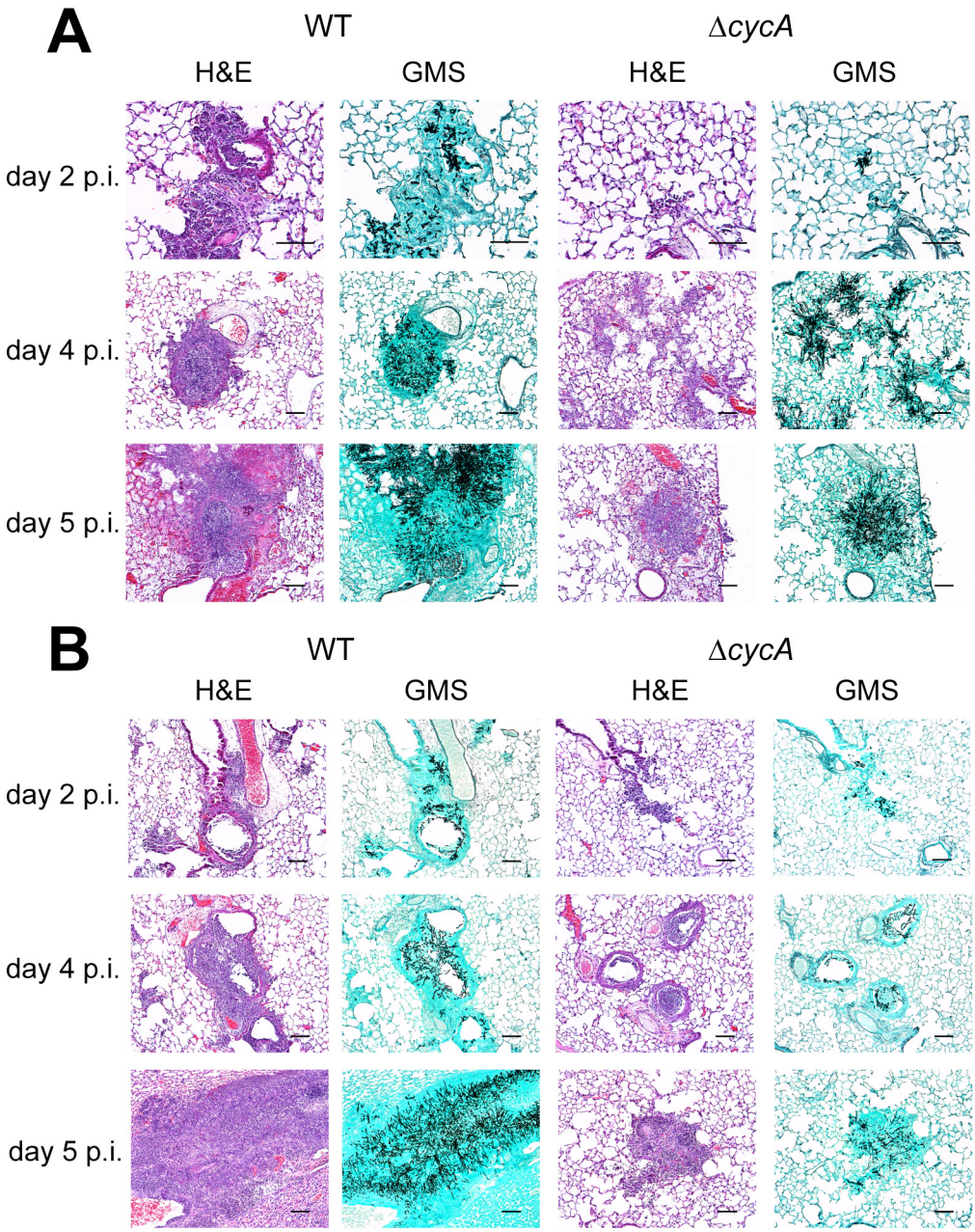
A
WT
ΔcycA
H&E
GMS
H&E
GMS
day 2 p.i.
day 4 p.i.
day 5 p.i.
B
WT
ΔcycA
H&E
GMS
H&E
GMS
day 2 p.i.
day 4 p.i.
day 5 p.i.

Figure 7:

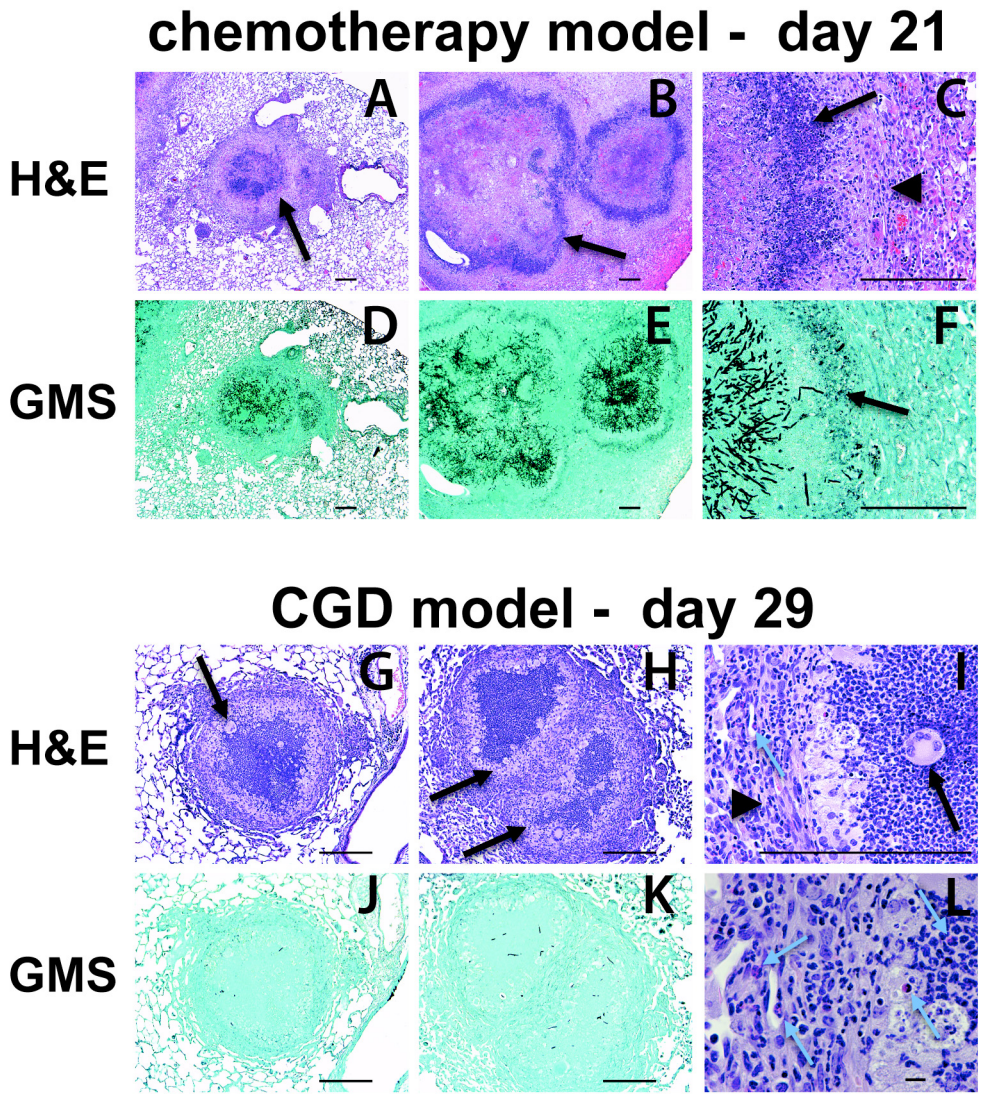
chemotherapy model - day 21
H&E
GMS
A
B
C
D
E
F
CGD model - day 29
H&E
GMS
G
H
I
J
K
L

Figure S1:

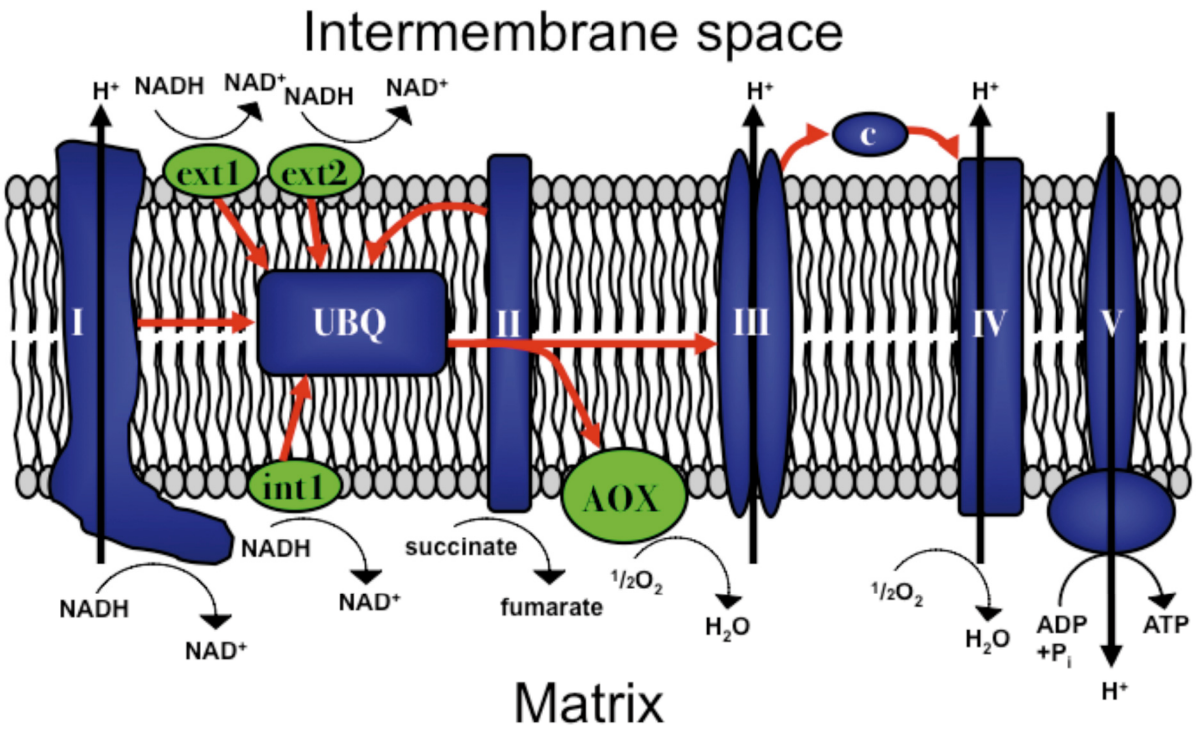
Intermembrane space
H+
NADH
NAD+
NADH
NAD+
ext1
ext2
UBQ
I
II
III
IV
V
c
H+
H+
int1
AOX
NADH
NAD+
succinate
fumarate
1/2O2
H2O
1/2O2
H2O
ADP
+Pi
ATP
H+
NADH
NAD+
Matrix

Figure S2:

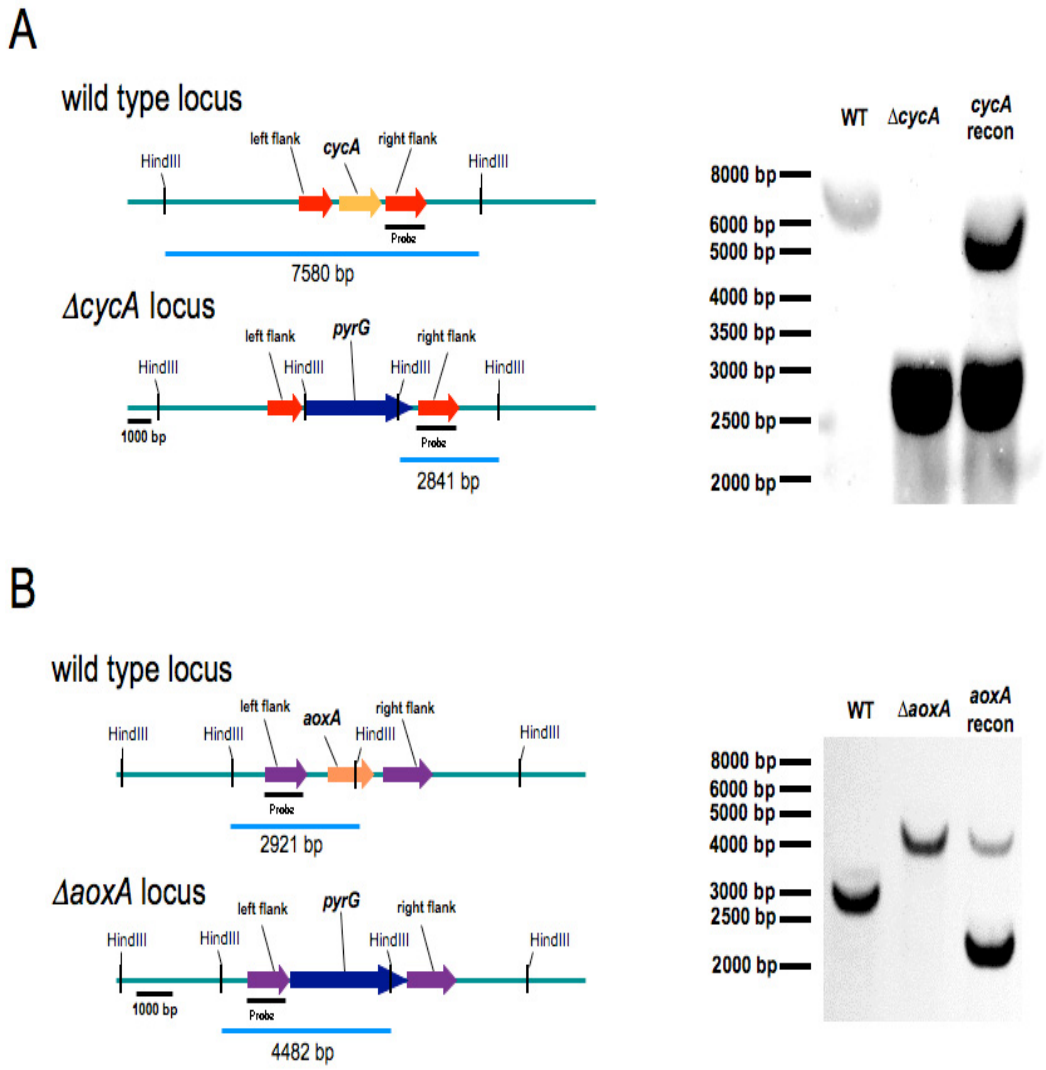
A
wild type locus
HindIII
left flank
cycA
right flank
HindIII
Probe
7580 bp
ΔcycA locus
HindIII
left flank
pyrG
right flank
HindIII
HindIII
HindIII
HindIII
1000 bp
Probe
2841 bp
WT
ΔcycA
cycA recon
8000 bp
6000 bp
5000 bp
4000 bp
3500 bp
3000 bp
2500 bp
2000 bp
B
wild type locus
HindIII
HindIII
left flank
aoxA
right flank
HindIII
HindIII
Probe
2921 bp
ΔaoxA locus
HindIII
HindIII
left flank
pyrG
right flank
HindIII
HindIII
1000 bp
Probe
4482 bp
WT
ΔaoxA
aoxA recon
8000 bp
6000 bp
5000 bp
4000 bp
3000 bp
2500 bp
2000 bp

Figure S3:

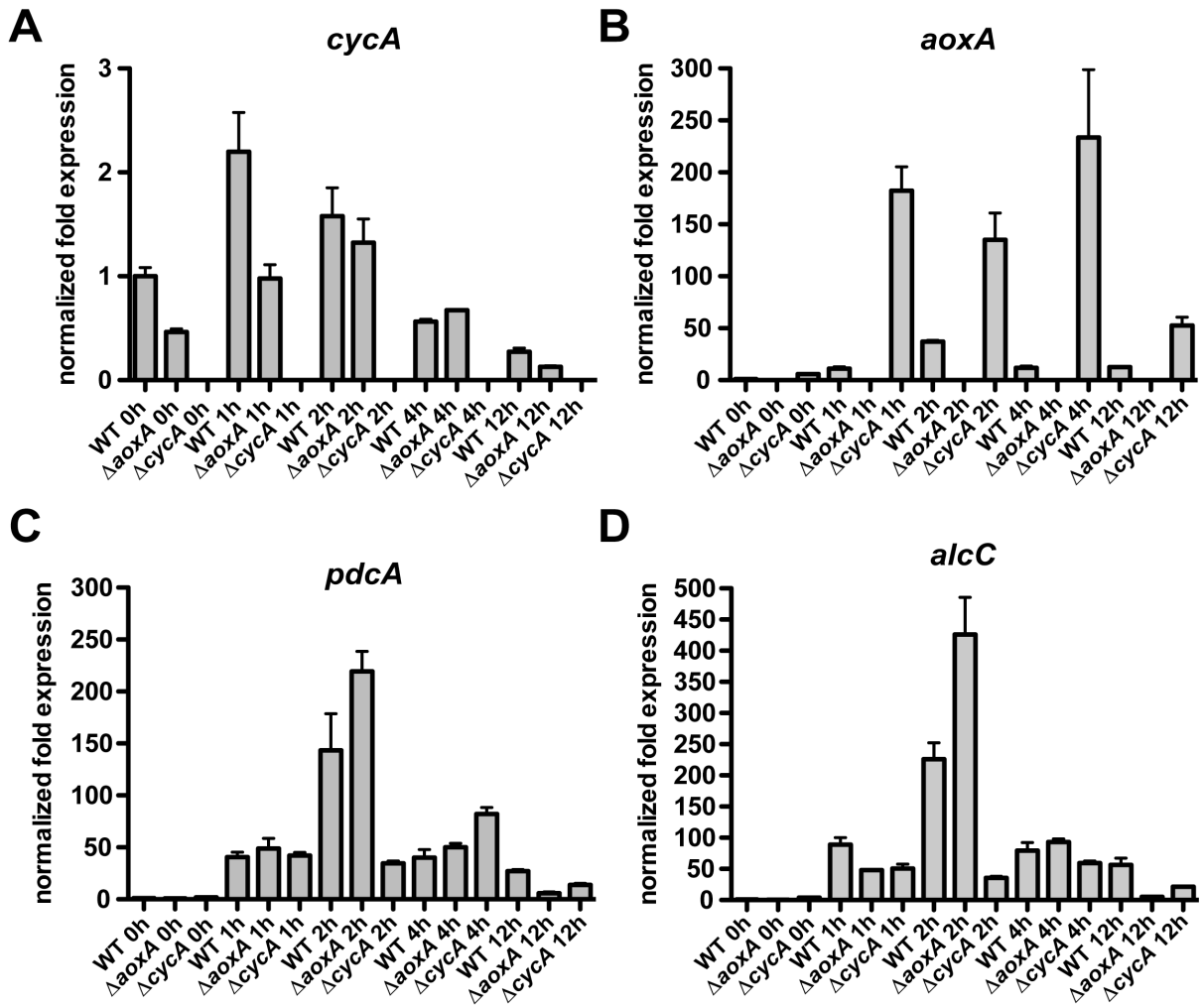
A
cycA
normalized fold expression
3
2
1
0
B
aoxA
normalized fold expression
300
250
200
150
100
50
0
C
pdcA
normalized fold expression
300
250
200
150
100
50
0
D
alcC
normalized fold expression
500
450
400
350
300
250
200
150
100
50
0
WT 0h
ΔaoxA 0h
ΔcycA 0h
WT 1h
ΔaoxA 1h
ΔcycA 1h
WT 2h
ΔaoxA 2h
ΔcycA 2h
WT 4h
ΔaoxA 4h
ΔcycA 4h
WT 12h
ΔaoxA 12h
ΔcycA 12h

Figure S4:

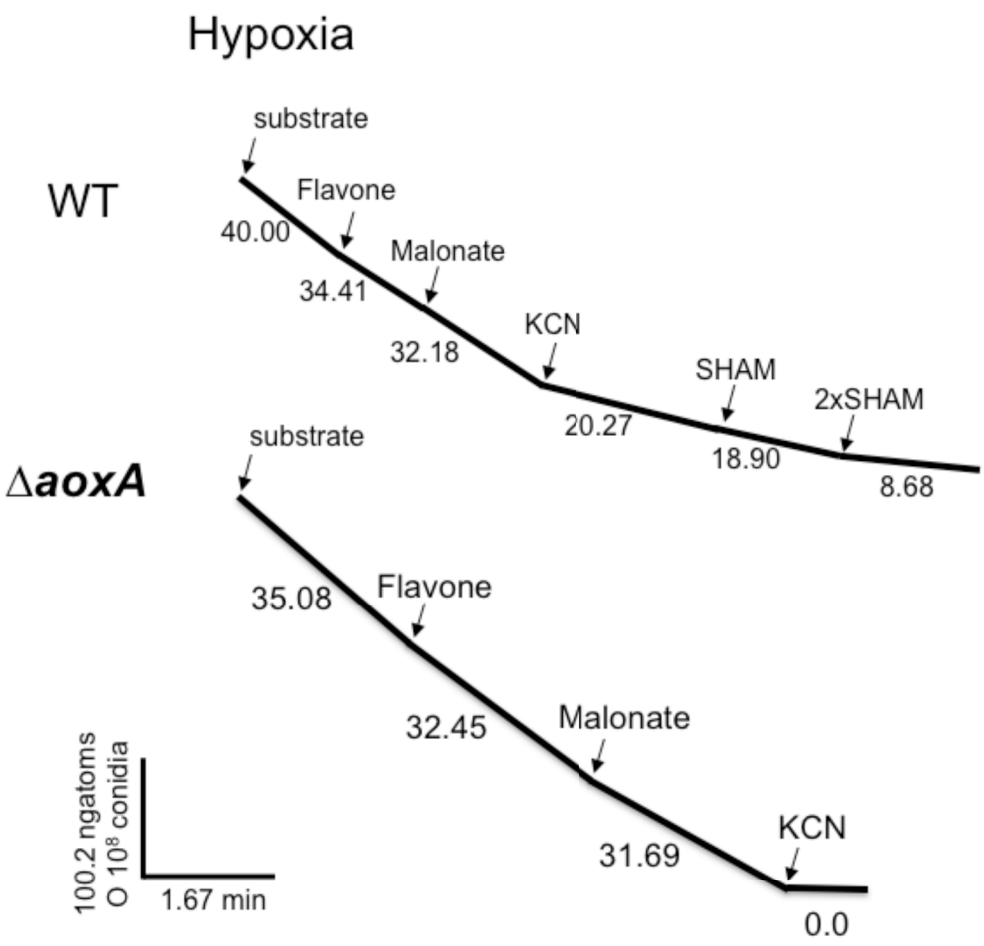
Hypoxia
WT
substrate
Flavone
40.00
Malonate
34.41
KCN
32.18
SHAM
20.27
2xSHAM
18.90
8.68
ΔaoxA
substrate
35.08
Flavone
32.45
Malonate
31.69
KCN
0.0
100.2 ngatoms O 10^8 conidia
1.67 min

Figure S5:

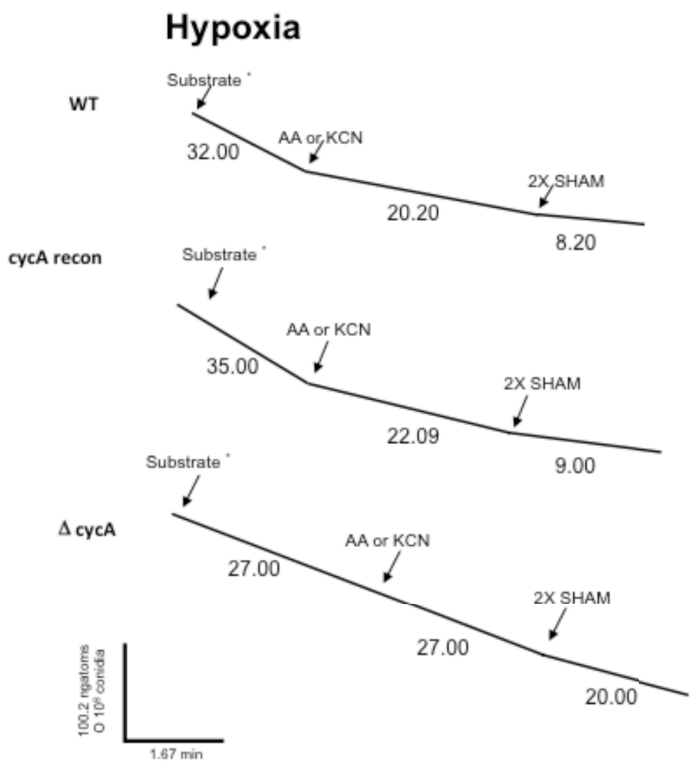
Hypoxia
WT
Substrate
32.00
AA or KCN
20.20
2X SHAM
8.20
cycA recon
Substrate
35.00
AA or KCN
22.09
2X SHAM
9.00
Δ cycA
Substrate
27.00
AA or KCN
27.00
2X SHAM
20.00
100.2 ngatoms O 10⁶ conidia
1.67 min

Tables:

Table S1:

Name	Sequence
cycA_RT_fw	ACTCTACCATGGTTGGCATTGCAG
cycA_RT_rev	GCGACAAAGTTTCCCAGACAAGGT
aoxA_RT_fw	TTCATGCGACTCATGGTTCTCGGA
aoxA_RT_rev	TTTGATGGCCCGAGTGTAGGTGAT
pdcA_RT_fw	TCACTTTGCAGGAGATCAGCACCA
pdcA_RT_rev	TCATTGTAGCTCGCATCCCATCCA
alcC_RT_fw	AGCAAGCTACGGATTATGTCCGCT
alcC_RT_refv	TGGTGATCATCTTGACGACGGTGT
tefA_RT_fw (house keeping gene)	GTGACTCCAAGAACGATCCC
tefA_RT_rev (house keeping gene)	AGAACTTGCAAGCAATGTGG
cycA_KO_left flank_fw	CGTGACTACGTAGAACACAGTAGC
cycA_KO_left flank_rev	**CCAACTTAATCGCCTTGCAGCACA**AGAGCCTGGAGAATCAATTGGG
pyrG_cycA_overlap_fw	CCCAATTGATTCTCCAGGCTCT**TGTGCTGCAAGGCGATTAAGTTGG**
pyrG_cycA_overlap_rev	**AGGACAATGGACAATTCTGCACGC**TCCGGCTCGTATGTTGTGTGGAAT
cycA_KO_right flank_fw	**ATTCCACACAACATACGAGCCGGA**GCGTGCAGAATTGTCCATTGTCCT
cycA_KO_right flank_rev	CTTGCATCAAACGGACCAGCACAT
cycA_nested_fw	GGGGACAAGTTTGTACAAAAAAGCAGGCTAGATGTTCCGCCACTGATAGGT
cycA_nested_rev	GGGGACCACTTTGTACAAGAAAGCTGGGTAGAAGCACCCACGTTAGTTAGCAG
cycA_KO_check_fw	TATATGGCAGGCGTAAGTGAGGGT
cycA_KO_check_rev	ACGGGAAGATGCAAGACATGGGAA
cycA_recon_fw	CT***GCGGCCGC***ATGCCTCATGTCCGCTACATTT CC
cycA_recon_rev	CA***ACTAGT***TGCTGATTGGTCCATCACGAGGAT
cycA_recon_check_fw	TCGCATCTCGTCGTCACAGTTCAA
cycA_recon_check_rev	ACGTGATCAGGTCGTTCCTTTCCT
aoxA_KO_left flank_fw	CA***GTCGAC***CGTGCAGTTGAATACGGGCTGAAA
aoxA_KO_left flank_rev	CT***GAATTC***GAACCAGCGGGCTGAATCCAATTT
aoxA_KO_right flank_fw	TC***CCGCGG***TACATGCCAGCGCTTCTCTTCTCT
aoxA_KO_right flank_rev	GA***GAGCTC***ACCGAGCATTAGGTGTCAACAGGA
aoxA_KO_check_fw	AAAGCTGCGGAGAGAAGAGGACAA
aoxA_KO_check_rev	ATAGTAAACCTTGGCCGCTCGGAT
aoxA_recon_fw	GC***ACTAGT***CGTGCAGTTGAATACGGGCTGAAA
aoxA_recon_rev	AA***GCGGCCGC***TGTCTCACTTCGATCGCTGTTGGT
aoxA_recon_check_fw	AAGGCTCCTCACATCAAGGAGGTT
aoxA_recon_check_rev	ATGCATGCGCTCATTGTATGCCTC
recon_construct_ amplification_fw	ATCCTTGAAGCTGTCCCTGATGGT
recon_construct_ amplification_rev	TCCGGCTCGTATGTTGTGTGGAAT
bold = pyrG sequence	
underlinded = attB sites gateway cloning	
bold italic = added restriction sites	

4. Discussion

To successfully colonize a host and cause disease *A. fumigatus* has to be able to adapt to a variety of *in vivo* environmental challenges. In this dissertation, I provide evidence that hypoxia is an important clinically relevant stress in murine models of IPA. During pathogenesis, growth of the fungus and subsequent influx of recruited immune effector cells cause significant host tissue damage and decreased tissue perfusion that limits infection site oxygen availability (Matherne *et al.*, 1990, Van Belle *et al.*, 1987, Rustad *et al.*, 2009). To determine whether hypoxia actually occurs in the lung during IPA, the hypoxia marker pimonidazole hydrochloride was used in three clinically relevant murine models of IPA. Pimonidazole hydrochloride is an investigational oncology probe used as a hypoxia-imaging agent in clinical studies to detect reduced oxygen concentrations in animal and human tumors (Raleigh *et al.*, 1998, Ljungkvist *et al.*, 2000, Raleigh *et al.*, 2001, Raleigh *et al.*, 2000, Kizaka-Kondoh & Konse-Nagasawa, 2009). Furthermore, it has been used to demonstrate that hypoxic regions occur in tuberculosis granulomas (Via *et al.*, 2008). Staining with pimonidazole hydrochloride identifies hypoxic regions ($O_2 \leq 1.5\%$), but does not determine exact oxygen concentrations.

In three immunologically distinct murine models of invasive pulmonary aspergillosis (chemotherapeutic, corticosteroid, and X-CGD) hypoxic microenvironments could be found, as evidenced by the formation of a stable adduct between reduced pimonidazole and host proteins at sites of *A. fumigatus* infection (Grahl *et al.*, 2011). In addition, the results suggest that the influx and activity of host cells are strong contributors to the development of hypoxia, and that fungal activities or components also contribute to hypoxic lesions (Grahl *et al.*, 2011). From these studies, it is clear that the underlying host immune response is a critical factor in hypoxia development. Altogether, this is the first confirmation that *in vivo* hypoxic microenvironments occur during an invasive fungal infection and adds another *in vivo* stress to the list of environmental challenges human fungal pathogens must adapt to cause lethal disease. In the future it will be intriguing to test whether hypoxia occurs in other models of fungal infection. These studies await to be undertaken. Furthermore, the relative contributions of pathogen and host cells to the generation of hypoxia at the site of infection are likely to be pathogen-host specific, which represents an important line of future inquiry for a diverse array of pathosystems.

As *A. fumigatus* has to face hypoxic environments *in vivo* as well as in its ecological niche, the compost microflora (Grahl *et al.*, 2011, Wang W, 2007), it is more than likely that this mold possesses mechanisms to sense, adapt to, and grow in these oxygen-limiting conditions. Indeed multiple oxygen sensing pathways have been described in fungi. However, it seems that these organisms mainly sense oxygen through intracellular heme and sterol levels, although some other sterol- and heme-independent pathways have been described (reviewed in: (Grahl & Cramer, 2010). Heme and sterol are important cellular components that are essential for the survival of eukaryotic organisms. Environmental oxygen concentrations directly affect cellular heme and sterol levels, as the biosynthesis of both molecules requires oxygen, making it possible for the cell to indirectly sense oxygen through changes in heme and sterol levels (Labbe-Bois, 1990, Hughes *et al.*, 2007).

A heme-sensing pathway involving the heme-Hap1p complex and the hypoxic gene repressors Rox1p and Mot3p has been described in the baker's yeast *S. cerevisiae*. However, so far no heme-sensing pathway has been identified in any of the major human fungal pathogens, while sterol-sensing mechanisms involving SREBP analogs or orthologs have been found and studied (reviewed in: (Grahl & Cramer, 2010, Bien & Espenshade, 2010). In this context, the SREBP ortholog, SrbA, has been recently identified and characterized in *A. fumigatus* and it was found that SrbA is crucial for sterol biosynthesis, growth under hypoxic conditions, and resistance to azole antifungal agents (Figure 2) (Willger *et al.*, 2008). The same characteristics had also been shown for the SREBP null mutants in the yeasts *S. pombe* and *C. neoformans* suggesting that some roles of SREBPs are conserved between yeasts and filamentous fungi (Hughes *et al.*, 2005, Chang *et al.*, 2007, Chun *et al.*, 2007, Willger *et al.*, 2008, Grahl & Cramer, 2010). Interestingly, the finding that SrbA plays an important role in fungal morphology suggests additional functions of SREBPs in filamentous fungi (Willger *et al.*, 2008).

However, to date the mechanisms arresting *A. fumigatus* growth, in response to hypoxia, after loss of SrbA are not fully understood. Analysis of transmission electron micrographs suggested a defect in vesicle translocation and formation, which may be due to altered sterol levels. It is likely that the inability of the mutant to grow in hypoxia is related to the perturbation in sterol biosynthesis, as hypoxia probably potentiates the alterations in sterol levels seen in normoxia (Willger *et al.*, 2008). However, further studies have to be done to verify this hypothesis.

Significantly, it was shown that the SREBP pathway is important for virulence of the human fungal pathogens *A. fumigatus* and *C. neoformans* (Chang *et al.*, 2007, Chun *et al.*, 2007, Willger *et al.*, 2008). While loss of SREBP was found to be unnecessary to initiate an infection, they were required for normal disease progression, which suggests an important role of the fungal SREBP pathway in adaptation to the host environment (Figure 2) (Willger *et al.*, 2008, Bien *et al.*, 2009, Chang *et al.*, 2009). Furthermore, the finding that hypoxia occurs at the site of *A. fumigatus* infection (Grahl *et al.*, 2011) strongly suggests that the inability of the SrbA null mutant to grow in hypoxic microenvironments is primarily responsible for the nearly avirulent phenotype of the mutant (Willger *et al.*, 2008). In addition, also in the mammalian brain, one of the primary sites of *C. neoformans* infection, oxygen levels are low with ~1 to 5% (Sharp & Bernaudin, 2004) and, consequently, a *C. neoformans* Sre1 mutant failed to cause fatal meningoencephalitis (Chang *et al.*, 2009). However, despite this evidence, it is not yet possible to conclude that the virulence defects of the *A. fumigatus* and *C. neoformans* SREBP mutants is solely due to low oxygen concentrations found *in vivo* at the site of infection. Fungal SREBPs transcriptionally regulate a significant number of genes in the respective fungal genomes, suggesting that other SREBP-mediated pathways like maintenance of cell polarity or response to low iron availability may also be important for virulence (Figure 2). In fact, a recent study in *A. fumigatus* showed that SrbA is critical for regulation of iron acquisition, particularly through regulation of siderophore production and iron uptake (Blatzer *et al.*, in press). As *A. fumigatus* iron uptake mutants are also attenuated in virulence, this study suggests a potential role for SrbA mediated iron regulation in fungal virulence (Blatzer *et al.*, in press).

However, which SREBP transcriptional targets are required for growth in hypoxia and in the host remains to be elucidated. In addition, to be able to completely understand the role of the SREBP pathway in *A. fumigatus* hypoxia adaptation and pathogenesis, future studies will need to define the exact mechanism of how SrbA is activated in response to hypoxic conditions. Despite extensive bioinformatics analyses, no functional homologs of other known SREBP pathway components can be found in *A. fumigatus* (Willger *et al.*, 2008, Willger and Cramer personal communication), indicating that while some aspects of SREBP signaling may be conserved, the composition of the pathway seems to be significantly different in *A. fumigatus* and awaits to be elucidated.

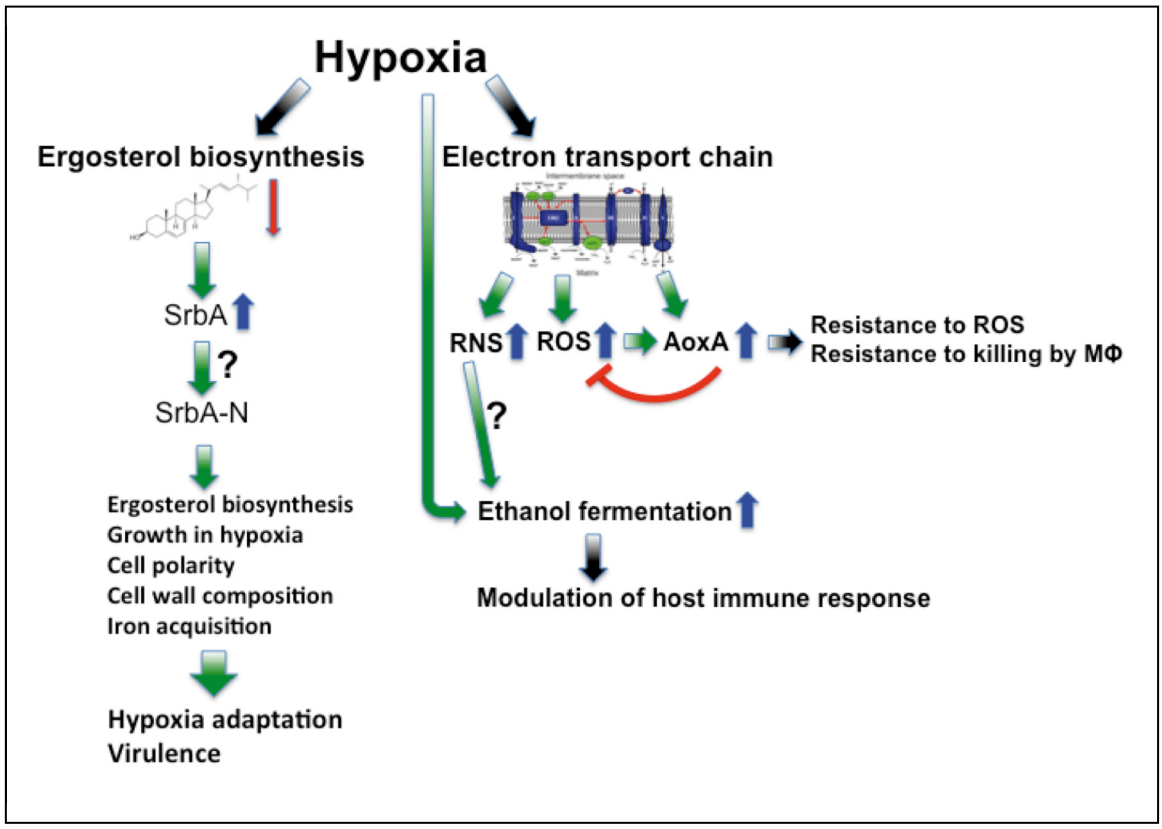

Figure 2: Schematic of known and probable *A. fumigatus* hypoxia adaptation mechanisms. In hypoxic conditions decreasing ergosterol biosynthesis results in increased sterol element binding protein (SrbA) levels and leads to cleavage of SrbA and the release of the N-terminal transcription factor domain, SrbA-N. SrbA-N translocates to the nucleus and activates transcription of genes involved in multiple pathways important for hypoxia adaptation and virulence. In addition, hypoxia causes increased production of reactive oxygen (ROS) and nitrogen (RNS) species, probably produced by the mitochondrial electron transport chain. This results in increased presence of the alternative oxidase (AoxA). AoxA decreases ROS production and mediates resistance to extracellular ROS and killing by macrophages (MΦ). Additionally, hypoxic conditions induce ethanol fermentation. This activation is possibly mediated by RNS produced by the electron transport chain. Ethanol fermentation is also involved in the modulation of the host immune response by decreasing the influx of neutrophils to the site of infection.

In addition to the ability to sense changes in oxygen concentrations, metabolic adaptability and flexibility are important attributes of pathogens to survive and grow in hypoxic microenvironments. Our current knowledge of metabolic pathways used by *A. fumigatus* and other pathogenic fungi under hypoxic conditions and *in vivo* during fungal pathogenesis is limited. Interestingly, a global *in vivo* metabolite screen utilizing ^{1}H-NMR of broncheoalveolar lavage fluid identified ethanol in the lungs of mice inoculated with *A. fumigatus* indicating that fermentation may be a mechanism by which this mold adapts to the host environment (Grahl *et al.*, 2011). Further supporting a role of fermentation during fungal pathogenesis is the finding of ethanol in cerebral tissue of rats infected with *C. neoformans* (Himmelreich *et al.*, 2001).

Most eukaryotic cells, like *A. fumigatus*, obligatorily use oxygen to carry out many of their biochemical reactions. Molecular oxygen is critical for several

biosynthetic pathways like biosynthesis of sterols, heme, mono- and poly-unsaturated fatty acids, or nicotinamide adenine dinucleotide (NAD^+) (Raymond & Segre, 2006, Goldfine, 1965, Summons *et al.*, 2006, Labbe-Bois, 1990, Hughes *et al.*, 2007). In addition, oxygen is a key component of energy production where it functions as a terminal electron acceptor in the formation of ATP from glucose during aerobic respiration. When exposed to microenvironments with limited levels of oxygen, many microorganisms utilize fermentation as a potential metabolic mechanism for dealing with the lack of oxygen (Zhou *et al.*, 2010, Panagiotou *et al.*, 2005, Kiers *et al.*, 1998, Merico *et al.*, 2009, van Dijken *et al.*, 1986, Lara *et al.*, 2009, Ismond *et al.*, 2003). Fermentation allows the cell to replenish sources of NAD^+ and thus generate ATP through continued use of glycolysis.

In the human fungal pathogens *A. fumigatus*, *C. neoformans*, and *C. albicans,* it has been observed that hypoxia induces expression of genes involved in ethanol fermentation (Grahl *et al.*, 2011, Chun *et al.*, 2007, Setiadi *et al.*, 2006). In addition, *A. nidulans*, *A. parasiticus*, and *A. fumigatus* produce ethanol in response to *in vitro* hypoxic conditions (Grahl *et al.*, 2011, Kelly *et al.*, 1990, Lockington *et al.*, 1997, Sanchis *et al.*, 1994). Altogether, this data suggests an important role for ethanol fermentation in fungal adaptation and growth under oxygen limited conditions (Figure 2). However, while *A. fumigatus* appears to utilize ethanol fermentation *in vivo*, this mechanism of energy generation is not essential for *in vitro* hypoxic growth, suggesting that other fermentation pathways exist and/or that sufficient mitochondrial respiration still occurs under the examined conditions.

Loss of ethanol fermentation via genetic mutation of either pyruvate decarboxylase or alcohol dehydrogenase did not affect the ability of *A. fumigatus* to cause lethal disease in any of our murine models. However, the loss of the alcohol dehydrogenase (AlcC), involved in ethanol fermentation in response to hypoxia, significantly altered the host immune response to the fungus as evidenced by increased neutrophil recruitment and alteration in cytokine production in mice inoculated with an *alcC* null mutant (Grahl *et al.*, 2011). This suggests that *A. fumigatus* is able to partially suppress localized immune responses by utilizing ethanol fermentation in response to hypoxic microenvironments during IPA (Figure 2). However, to confirm this hypothesis more sensitive and reliable ethanol detection methods need to be developed. Overall, these results suggest that fungal responses to hypoxia *in vivo* may not only affect fungal growth directly, but also affect the production of fungal metabolites that can subsequently alter host immune responses.

Thus, the effects of hypoxia on fungal pathogenesis are likely to be more complex than simply altering rates of fungal growth. Consequently, in future studies it will be intriguing to elucidate how different fungal metabolites produced in response to oxygen-limited conditions influence host-pathogen interactions.

As mentioned above, the fact that loss of ethanol fermentation had no effect on growth in hypoxic conditions, together with the finding that *A. fumigatus* showed growth on non-fermentable carbon sources suggests that the mold is able to generate energy by respiration in hypoxia (Grahl *et al.*, 2011). Indeed further studies on respiration in hypoxia found that the fungal respiration chain is active under hypoxic conditions and is most likely used to support *A. fumigatus* growth (Grahl *et al.*, 2011, Grahl *et al*. submitted).

The eukaryotic respiration chain consists of a conventional linear electron transport chain involving core respiration complexes I, II, III, and IV, as well as the ubiquinone pool and the ATP synthase also referred to as complex V. In addition, fungi possess alternative NADH:ubiquinone oxidoreductases and an alternative oxidase (Joseph-Horne *et al.*, 2001). Utilizing oxygen consumption assays, all components of the mitochondrial electron transport chain can be found in *A. fumigatus* in normoxic and hypoxic conditions. Importantly, alternative oxidase activity is significantly elevated after growth in hypoxia indicating an increased role of this enzyme under these conditions (Figure 2) (Grahl *et al*. submitted).

The alternative oxidase has been shown to play a role in limiting mitochondrial reactive oxygen species (ROS) formation and oxidative stress in *A. fumigatus* (Figure 2) and other organisms (Purvis, 1997, Wagner & Moore, 1997, Avila-Adame & Koller, 2002, Akhter *et al.*, 2003, Magnani *et al.*, 2007, Magnani *et al.*, 2008, Martins *et al.*, 2011, Grahl *et al*. submitted). In addition, several studies have reported that exposure to hypoxia results in an increase of oxidative stress, which is also observed in *A. fumigatus* (Figure 2) (Dirmeier *et al.*, 2002, Chandel & Budinger, 2007, Guzy *et al.*, 2007, Grahl *et al*. submitted). Taken together, these data indicate that the increased alternative oxidase activity in hypoxia might be a result of elevated intracellular ROS production from mitochondrial respiration (Figure 2). Furthermore, during infection, pathogens like *A. fumigatus* and *C. neoformans* are attacked by ROS produced by phagocytic cells and the alternative oxidase is also involved in resistance to this extracellular oxidative stress (Figure 2) (Magnani *et al.*, 2008, Akhter *et al.*, 2003, Grahl *et al*. submitted). In agreement, a cytochrome C null mutant of *A. fumigatus* displaying increased levels of alternative oxidase activity was found

to be hyper-resistant to oxidative stress and killing by macrophages (Grahl *et al*. submitted). The same cytochrome C mutant showed delayed germination and a significant growth defect, which had also been observed in *Neurospora crassa* and *A. nidulans* (Bradshaw *et al.*, 2001, Bottorff *et al.*, 1994, Grahl *et al*. submitted).

In contrast to *A. nidulans* loss of cytochrome C did not result in complete growth inhibition on non-fermentable carbon sources and no ethanol production on the fermentable carbon source glucose could be observed in *A. fumigatus*. Furthermore, the *cycA* mutant showed decreased growth in hypoxia and lost the ability to induce ethanol fermentation in response to hypoxic conditions, suggesting an involvement of the fungal electron transport chain in this process in *A. fumigatus* (Figure 2) (Grahl *et al*. submitted). In previous studies in yeast, it has been proposed that the fungal respiratory chain is involved in oxygen sensing, growth in hypoxia, and hypoxic gene regulation, and that ROS and reactive nitrogen species (RNS) produced by the respiration chain are involved in this process (Kwast *et al.*, 1999, David & Poyton, 2005, Castello *et al.*, 2006, Guzy *et al.*, 2007, Ingavale *et al.*, 2008, Poyton *et al.*, 2009a, Poyton *et al.*, 2009b).

In general, it is believed that the two sites of ROS production in the mitochondrial respiratory chain are at complex I and III (Poyton *et al.*, 2009b), and in addition, several studies have suggested that increased oxidative stress observed in hypoxia may act as a putative second messenger that activates redox-sensitive transcription factors to enable hypoxia adaptation (Dirmeier *et al.*, 2002, Chandel & Budinger, 2007, Guzy *et al.*, 2007). Beside ROS, RNS produced by complex IV of the electron transport chain have been suggested to play an important role in oxygen sensing and hypoxic signaling (Castello *et al.*, 2006, Poyton *et al.*, 2009a, Poyton *et al.*, 2009b). Thus, as a cytochrome C mutant of *A. fumigatus* seems to be able to utilize the alternative complex I - alternative oxidase pathway to generate energy, this mutant probably still produces ROS via complex I (Grahl *et al*. submitted) However, loss of cytochrome C blocks the conventional electron transport chain after complex III and with that loses the ability to produce RNS by complex IV. Altogether, this suggests that loss of the RNS signal via complex IV might be the reason for loss of ethanol fermentation activation in the cytochrome C mutant in response to hypoxic conditions (Figure 2).

Surprisingly, the more oxidative stress resistant cytochrome C mutant is attenuated in virulence, while the loss of alternative oxidase did not result in any mortality changes, which is in contrast to findings in *C. neoformans* (Akhter *et al.*,

2003, Grahl *et al*. submitted). The missing virulence defect of the alternative oxidase mutant might be based on the fact that *A. fumigatus* possesses multiple genes encoding for superoxide dismutase and catalase to fight oxidative stress *in vivo* (Lambou *et al.*, 2010, Paris *et al.*, 2003) or that, *C. neoformans* cannot generate energy in the absence of a functional alternative oxidase. As *C. neoformans* also has multiple SODs and catalases, this latter hypothesis is most likely (Cox *et al.*, 2003, Giles *et al.*, 2005, Giles *et al.*, 2006). Overall, the data indicate that mitochondria are involved in hypoxia adaptation of *A. fumigatus* and future studies will determine whether the respiration chain and ROS/RNS are involved in oxygen sensing, hypoxic signaling, and hypoxic gene regulation as it has been suggested for *S. cerevisiae*.

Interestingly, histopathology analysis of mice inoculated with the *A. fumigatus* cytochrome C mutant led to the hypothesis that the combination of slow growth and oxidative stress resistance is the reason why the virulence is attenuated and the immune system is unable to clear the fungus. However, because of the slow growth the host immune system is able to form granuloma-like lesions to contain the fungal infection. These lesions are most likely regions of limited oxygen supply, which would even further decrease hyphal growth of the cytochrome C mutant. In agreement with this hypothesis the mutant seems to be unable to grow out of these lesions (Grahl *et al*. submitted). Significantly, an influx of eosinophils, which is connected with two other *A. fumigatus* diseases, ABPA and aspergilloma, could be observed. Future experiments will show whether infections with this deletion mutant can be used as a potential mouse model to study these Th2 type diseases and/or chronic aspergillosis (Grahl *et al*. submitted).

Taken together, the aforementioned studies suggest an important link between hypoxia adaptation and fungal pathogenesis for *A. fumigatus* and other human fungal pathogens. However, our understanding of fungal hypoxia adaptation mechanisms and their link to pathogenesis is still limited. Importantly, while adaptation to oxygen-limited conditions is likely to be critical for *in vivo* growth of the fungal pathogen, other subtle effects of hypoxia on fungal metabolism are likely to influence the host-fungal interaction. Furthermore, occurrence of hypoxia at the site of infection most likely affects the immune response of the host and with that probably influences the course of fungal infection. In fact, a link between host hypoxic responses and bactericidal activities of phagocytic cells has been shown and suggests that such responses are also critical for fungal infections (Nizet & Johnson,

2009, Cramer *et al.*, 2003, Peyssonnaux *et al.*, 2005, Peyssonnaux *et al.*, 2007, Rius *et al.*, 2008).

In summary, data from this dissertation and other seminal studies to date largely support the hypothesis that the ability to sense, adapt to, and grow in hypoxic conditions is a virulence attribute of *A. fumigatus* and other human fungal pathogens. A significant take home message from this work is that it might be of great interest to conduct future *in vitro* experiments on fungal mutants and/or host cell responses to fungal pathogens in hypoxic environments to attempt to simulate *in vivo* microenvironments. Traditionally, most fungal-host interaction studies are conducted in normoxic conditions, which may miss some important nuances of these interactions that occur *in vivo*. In addition, hypoxia adaptation mechanisms and their potential influence on host-pathogen interaction should be considered, not only for fungal infections, but for all microbial pathogens.

For example, many important bacterial human pathogens are obligate (i.e. *Clostridium* spp.) or facultative (i.e. *Staphylococcus* spp.) anaerobes and exhibit remarkable adaptability to diverse oxygen concentrations. Furthermore, all major pathogens of the human lower gastrointestinal tract are facultative anaerobes (Marteyn *et al.*, 2011). In addition, different oxygen sensing mechanisms in bacteria have been described, as well as changes in pathogen-host cell interactions (Marteyn *et al.*, 2011). Other human prokaryotic pathogens such as *Pseudomonas aeruginosa* and *Mycobacterium tuberculosis* are obligate aerobes and generally are thought to require hypoxia adaptation mechanisms as part of their ability to persist in the lung and cause disease (Rustad *et al.*, 2009, Hassett *et al.*, 2009). Altogether, one could hypothesize that the ability to adapt to and prevail in oxygen-limited conditions is a global virulence attribute/factor of microbial pathogens like for example the ability to grow at 37°C. However, more research needs to be done to test this hypothesis.

Finally, from a translational perspective, it is highly probable that an increased understanding of hypoxia and its impact on fungal pathogenesis could lead to improved therapeutic options for these often lethal infections. The SREBP pathway in fungal pathogens represents a promising target for antifungal therapy development. SREBP orthologs, analogs, and SREBP-like proteins have been identified in several pathogenic fungi, indicating an important and most likely conserved role of SREBPs (Grahl & Cramer, 2010, Bien & Espenshade, 2010). Importantly, studies of the human fungal pathogens *C. neoformans* and *A. fumigatus* showed that mutants of the respective SREBP are hypersensitive to the triazole class of antifungals which

are commonly prescribed to treat fungal infections (Chang *et al.*, 2007, Chun *et al.*, 2007, Willger *et al.*, 2008). In addition, a homozygous deletion of the SREBP analog Upc2p in *C. albicans* also resulted in hypersensitivity to triazoles (Silver *et al.*, 2004). Furthermore, it is interesting to note that disruption of the SREBP pathway in *C. neoformans* converts the fungistatic activity of the triazole class of antifungals to fungicidal, meaning that instead of only blocking fungal cell growth these cells can be directly killed (Bien *et al.*, 2009). As immunocompromised patients are more or less unable to clear fungal cells and have to under go long-term antifungal treatment when an infection is diagnosed, the fact that inhibitors of fungal SREBPs may act synergistically with current antifungal drugs to more effectively and rapidly clear fungal infections is of great interest and should be explored in future studies.

5. Summary

Aspergillus fumigatus is a ubiquitous mold found in soil and organic debris that is currently the most frequent cause of airborne invasive fungal infections in immunocompromised individuals. The high mortality rate of invasive pulmonary aspergillosis indicates that increased efforts to disclose the principles of *A. fumigatus* pathogenicity are necessary. However, to date no sophisticated virulence factor has been identified for *A. fumigatus*. In contrast, it has been proposed that this human fungal pathogen is able to establish infection due to its robustness and ability to adapt to a wide range of environmental conditions. Those mechanisms involved in adaptation to host environments and allowing onset of an infection, we call virulence attributes. Importantly, over the last years increasing evidence has been found that oxygen-limited conditions occur during fungal pathogenesis in which both the pathogen and host cells must survive. In this study the hypothesis that hypoxia is a stress faced *in vivo* by *A. fumigatus* and that the ability to sense, adapt to, and grow in hypoxic conditions is a virulence attribute of this human fungal pathogen was tested and largely supported by our data.

Utilizing pimonidazole hydrochloride staining in three immunologically distinct and clinically relevant IPA murine models, it was shown for the first time that hypoxic microenvironments occur at sites of *A. fumigatus* infection. In addition, the results suggest that both the influx and activity of host cells and the pathogen contribute to these hypoxic lesions. Thus, *A. fumigatus* has to be able to adapt to these oxygen-limited conditions in order to cause disease. In this context, a SREBP ortholog was identified and characterized in *A. fumigatus*. Importantly, a null mutant of this SREBP was shown to be unable to grow in hypoxia and virtually avirulent. However, further studies need to be done to be absolutely certain that the inability of this mutant to cause disease is solely based on the hypoxic growth defect and not on other pleiotropic factors. Importantly, oxygen sensing and hypoxia adaptation mechanisms like the SREBP pathway can be identified in the model yeasts *Saccharomyces cerevisiae* and *Schizosaccharomyces pombe* as well as in human fungal pathogens *Cryptococcus neoformans*, *Candida albicans*, and *A. fumigatus* suggesting an important role for these mechanisms for fungal biology and virulence.

In addition, it was found that *A. fumigatus* utilizes ethanol fermentation *in vivo* and that ethanol fermentation is induced under hypoxic conditions *in vitro*. While

fermentation was shown to not be essential for growth of *A. fumigatus* in hypoxia and fungal virulence, it was found that loss of the alcohol dehydrogenase involved in ethanol fermentation under hypoxic conditions resulted in significant changes in the host immune response as evidenced by increased neutrophil recruitment and alteration in cytokine production. Thus, the effects of hypoxia on fungal pathogenesis are likely to be more complex than simply altering rates of fungal growth.

Lastly, it was found that the conventional mitochondrial electron transport chain of *A. fumigatus* seems to be involved in hypoxic signaling as a deletion of cytochrome C resulted in a loss of ethanol fermentation activation in response to hypoxia. Furthermore, the electron transport chain plays a role in growth under hypoxic conditions, as well as the oxidative stress response, and is important for *A. fumigatus* pathogenesis.

Overall, the presented data shows that hypoxia occurs at the site of *A. fumigatus* infection and it suggests an important previously unidentified link between hypoxia adaptation and fungal pathogenesis of *A. fumigatus*.

6. Zusammenfassung

Aspergillus fumigatus ist ein Schimmelpilz, der normalerweise im Erdreich zu finden ist und an der Mineralisierung biologischem Materials beteiligt ist. Daneben ist *A. fumigatus* allerdings in der Lage, den Menschen zu besiedeln und zurzeit verantwortlich für die meisten invasiven Pilzinfektionen in Patienten mit geschwächtem Immunsystem. Diese Infektionen sind schwer zu behandeln und verlaufen häufig tödlich. Die Grundlagen der Pathogenität von *A. fumigatus* sind nicht geklärt und es ist bisher nicht gelungen traditionelle Virulenzfaktoren für *A. fumigatus* zu identifizieren. Vielmehr wird vermutet, dass Fitness und Anpassungsfähigkeit an verschiedenste Umweltbedingungen dem Pilz eine Infektion des Wirts ermöglichen. In diesem Zusammenhang wurden in den letzten Jahren vermehrt Beweise dafür gefunden, dass sauerstoffarme Bedingungen während der Infektion auftreten, an die sich Pathogen und Immunzellen anpassen müssen. In der vorliegenden Arbeit wurde die Hypothese getestet, ob *A. fumigatus* während der Infektion hypoxischen Bedingungen ausgesetzt ist und ob die Fähigkeiten zu Wahrnehmung, Adaptation, und des Wachstums in sauerstoffarmer Umgebung ein Virulenzmerkmal von *A. fumigatus* darstellen könnte.

Mit Hilfe des Hypoxiamarkers Pimonidazol-Hydrochlorid wurde gezeigt, dass sauerstoffarme Bedingungen während einer Infektionen mit *A. fumigatus* in drei immunologisch verschiedenen Mausmodellen auftreten. Diese hypoxischen Bedingungen scheinen vor allem aus dem Zustrom und der Aktivität der Immunzellen zu resultieren, aber auch Wachstum und Ausschüttung von Metaboliten des Pilzes tragen dazu bei. Demzufolge muss *A. fumigatus* über Mechanismen verfügen sich an sauerstoffarme Bedingungen anzupassen, um eine Erkrankung auslösen zu können.
In diesem Zusammenhang wurde in *A. fumigatus* ein Protein, SrbA, identifiziert und charakterisiert. SrbA ist ein Ortholog von SREBP, das als Transkriptionsfaktor in höheren Eukaryonten die genetische Antwort auf Sterolmangel reguliert. Es wurde gezeigt, dass eine *srbA*-Deletionsmutante unfähig ist unter sauerstoffarmen Bedingungen zu wachsen und damit fast vollständig avirulent ist.

Mechanismen der Sauerstoffdetektion und Hypoxiaanpassung sowie der SREBP Signalweg konnten in den Modellorganismen *Saccharomyces cerevisiae* und *Schizosaccharomyces pombe*, ebenso wie in den pathogenen Pilzen *C. neoformans*,

C. albicans und *A. fumigatus* identifiziert werden. Dies suggeriert, dass diese Mechanismen eine wichtige Rolle für die Biologie und Virulenz der Pilze spielen.

Des Weiteren wurde gezeigt, dass *A. fumigatus* Ethanolfermentation *in vivo* nutzt und dass *in vitro* unter sauerstoffarmen Bedingungen die ethanolische Gärung induziert wird. Während dieser Stoffwechsel für das Wachstum unter hypoxischen Bedingungen und für die Virulenz von *A. fumigatus* nicht essentiell ist, konnte gezeigt werden, dass der Verlust der Alkoholdehydrogenase C, die in der Ethanolfermentation unter hypoxischen Bedingungen eine Rolle spielt, signifikante Veränderungen der Immunantwort hervorruft. Demzufolge sind Auswirkungen der Sauerstoffarmut auf die Krankheitsentstehung wahrscheinlich viel komplexer, als bloße Modifizierungen des Wachstumverhaltens.

Abschließend konnte gezeigt werden, dass die konventionelle mitochondriale Elektronentransportkette von *A. fumigatus* eine wichtige Rolle für das Wachstum in Hypoxia und für die Pathogenität spielt. Außerdem scheint die Elektrontransportkette in hypoxische Signalwege involviert zu sein, da die Deletion von Cytochrom C zum Verlust der Aktivierung der Ethanolfermentation unter hypoxischen Bedingungen führte.

Zusammenfassend zeigen die hier präsentierten Daten, dass Hypoxia während einer Infektion mit *A. fumigatus* auftritt und dass eine Verbindung zwischen Anpassung an hypoxische Bedingungen und der Pathogenität des humanpathogenen Pilzes besteht.

7. References

Akhter, S., H. C. McDade, J. M. Gorlach, G. Heinrich, G. M. Cox & J. R. Perfect, (2003) Role of alternative oxidase gene in pathogenesis of *Cryptococcus neoformans*. *Infect Immun* **71**: 5794-5802.

Antunes, J., A. Fernandes, L. M. Borrego, P. Leiria-Pinto & J. Cavaco, (2010) Cystic fibrosis, atopy, asthma and ABPA. *Allergologia et immunopathologia* **38**: 278-284.

Arnold, F., D. West & S. Kumar, (1987) Wound healing: the effect of macrophage and tumour derived angiogenesis factors on skin graft vascularization. *British journal of experimental pathology* **68**: 569-574.

Avila-Adame, C. & W. Koller, (2002) Disruption of the alternative oxidase gene in *Magnaporthe grisea* and its impact on host infection. *Molecular plant-microbe interactions : MPMI* **15**: 493-500.

Baddley, J. W., D. R. Andes, K. A. Marr, D. P. Kontoyiannis, B. D. Alexander, C. A. Kauffman, R. A. Oster, E. J. Anaissie, T. J. Walsh, M. G. Schuster, J. R. Wingard, T. F. Patterson, J. I. Ito, O. D. Williams, T. Chiller & P. G. Pappas, (2010) Factors associated with mortality in transplant patients with invasive aspergillosis. *Clin Infect Dis* **50**: 1559-1567.

Beffa, T., F. Staib, J. Lott Fischer, P. F. Lyon, P. Gumowski, O. E. Marfenina, S. Dunoyer-Geindre, F. Georgen, R. Roch-Susuki, L. Gallaz & J. P. Latge, (1998) Mycological control and surveillance of biological waste and compost. *Med Mycol* **36 Suppl 1**: 137-145.

Bien, C. M., Y. C. Chang, W. D. Nes, K. J. Kwon-Chung & P. J. Espenshade, (2009) *Cryptococcus neoformans* Site-2 protease is required for virulence and survival in the presence of azole drugs. *Mol Microbiol* **74**: 672-690.

Bien, C. M. & P. J. Espenshade, (2010) Sterol regulatory element binding proteins in fungi: hypoxic transcription factors linked to pathogenesis. *Eukaryot Cell* **9**: 352-359.

Blatzer, M., B. Barker, S. Willger, N. Beckmann, S. Blosser, E. Cornish, A. Mazurie, N. Grahl, H. Haas & R. Cramer, (in press) SREBP cooridnates iron and ergosterol homeostasis to mediate triazole drug and hypoxia responses in the human fungal pathogen *Aspergillus fumigatus*. *PLoS Genet*.

Bodey, G., B. Bueltmann, W. Duguid, D. Gibbs, H. Hanak, M. Hotchi, G. Mall, P. Martino, F. Meunier, S. Milliken, S. Naoe, M. Okudaira, D. Scevola & J. van't Wout, (1992) Fungal infections in cancer patients: an international autopsy survey. *European journal of clinical microbiology & infectious diseases : official publication of the European Society of Clinical Microbiology* **11**: 99-109.

Bottorff, D. A., S. Parmaksizoglu, E. G. Lemire, J. W. Coffin, H. Bertrand & F. E. Nargang, (1994) Mutations in the structural gene for cytochrome c result in deficiency of both cytochromes aa3 and c in *Neurospora crassa*. *Curr Genet* **26**: 329-335.

Bradshaw, R. E., D. M. Bird, S. Brown, R. E. Gardiner & P. Hirst, (2001) Cytochrome c is not essential for viability of the fungus *Aspergillus nidulans*. *Molecular genetics and genomics : MGG* **266**: 48-55.

Brakhage, A. A., S. Bruns, A. Thywissen, P. F. Zipfel & J. Behnsen, (2010) Interaction of phagocytes with filamentous fungi. *Curr Opin Microbiol* **13**: 409-415.

Brock, M., G. Jouvion, S. Droin-Bergere, O. Dussurget, M. A. Nicola & O. Ibrahim-Granet, (2008) Bioluminescent *Aspergillus fumigatus*, a new tool for drug efficiency testing and *in vivo* monitoring of invasive aspergillosis. *Appl Environ Microbiol* **74**: 7023-7035.

Carlsson, P. O., F. Palm, A. Andersson & P. Liss, (2001) Markedly decreased oxygen tension in transplanted rat pancreatic islets irrespective of the implantation site. *Diabetes* **50**: 489-495.

Castello, P. R., P. S. David, T. McClure, Z. Crook & R. O. Poyton, (2006) Mitochondrial cytochrome oxidase produces nitric oxide under hypoxic conditions: implications for oxygen sensing and hypoxic signaling in eukaryotes. *Cell metabolism* **3**: 277-287.

Chandel, N. S. & G. R. Budinger, (2007) The cellular basis for diverse responses to oxygen. *Free radical biology & medicine* **42**: 165-174.

Chandrasekar, P., (2011) Management of invasive fungal infections: a role for polyenes. *J Antimicrob Chemother* **66**: 457-465.

Chang, Y. C., C. M. Bien, H. Lee, P. J. Espenshade & K. J. Kwon-Chung, (2007) Sre1p, a regulator of oxygen sensing and sterol homeostasis, is required for virulence in *Cryptococcus neoformans*. *Mol Microbiol* **64**: 614-629.

Chang, Y. C., S. S. Ingavale, C. Bien, P. Espenshade & K. J. Kwon-Chung, (2009) Conservation of the sterol regulatory element-binding protein pathway and its pathobiological importance in *Cryptococcus neoformans*. *Eukaryot Cell* **8**: 1770-1779.

Chazalet, V., J. P. Debeaupuis, J. Sarfati, J. Lortholary, P. Ribaud, P. Shah, M. Cornet, H. Vu Thien, E. Gluckman, G. Brucker & J. P. Latge, (1998) Molecular typing of environmental and patient isolates of *Aspergillus fumigatus* from various hospital settings. *J Clin Microbiol* **36**: 1494-1500.

Chen, S. C., M. A. Slavin & T. C. Sorrell, (2011) Echinocandin antifungal drugs in fungal infections: a comparison. *Drugs* **71**: 11-41.

Chun, C. D., O. W. Liu & H. D. Madhani, (2007) A link between virulence and homeostatic responses to hypoxia during infection by the human fungal pathogen *Cryptococcus neoformans*. *PLoS Pathog* **3**: e22.

Cooney, N. M. & B. S. Klein, (2008) Fungal adaptation to the mammalian host: it is a new world, after all. *Curr Opin Microbiol* **11**: 511-516.

Cox, G. M., T. S. Harrison, H. C. McDade, C. P. Taborda, G. Heinrich, A. Casadevall & J. R. Perfect, (2003) Superoxide dismutase influences the virulence of *Cryptococcus neoformans* by affecting growth within macrophages. *Infect Immun* **71**: 173-180.

Cramer, T., Y. Yamanishi, B. E. Clausen, I. Forster, R. Pawlinski, N. Mackman, V. H. Haase, R. Jaenisch, M. Corr, V. Nizet, G. S. Firestein, H. P. Gerber, N. Ferrara & R. S. Johnson, (2003) HIF-1alpha is essential for myeloid cell-mediated inflammation. *Cell* **112**: 645-657.

Dagenais, T. R. & N. P. Keller, (2009) Pathogenesis of *Aspergillus fumigatus* in Invasive Aspergillosis. *Clin Microbiol Rev* **22**: 447-465.

David, P. S. & R. O. Poyton, (2005) Effects of a transition from normoxia to anoxia on yeast cytochrome c oxidase and the mitochondrial respiratory chain: implications for hypoxic gene induction. *Biochimica et biophysica acta* **1709**: 169-180.

Davies, B. S. & J. Rine, (2006) A role for sterol levels in oxygen sensing in *Saccharomyces cerevisiae*. *Genetics* **174**: 191-201.

Denning, D. W., A. Marinus, J. Cohen, D. Spence, R. Herbrecht, L. Pagano, C. Kibbler, V. Kcrmery, F. Offner, C. Cordonnier, U. Jehn, M. Ellis, L. Collette & R. Sylvester, (1998) An EORTC multicentre prospective survey of invasive aspergillosis in haematological patients: diagnosis and therapeutic outcome. EORTC Invasive Fungal Infections Cooperative Group. *The Journal of infection* **37**: 173-180.

Dewhirst, M. W., (1998) Concepts of oxygen transport at the microcirculatory level. *Semin Radiat Oncol* **8**: 143-150.

Dirmeier, R., K. M. O'Brien, M. Engle, A. Dodd, E. Spears & R. O. Poyton, (2002) Exposure of yeast cells to anoxia induces transient oxidative stress. Implications for the induction of hypoxic genes. *The Journal of biological chemistry* **277**: 34773-34784.

Erecinska, M. & I. A. Silver, (2001) Tissue oxygen tension and brain sensitivity to hypoxia. *Respir Physiol* **128**: 263-276.

Erjavec, Z., H. Kluin-Nelemans & P. E. Verweij, (2009) Trends in invasive fungal infections, with emphasis on invasive aspergillosis. *Clin Microbiol Infect* **15**: 625-633.

Giles, S. S., I. Batinic-Haberle, J. R. Perfect & G. M. Cox, (2005) *Cryptococcus neoformans* mitochondrial superoxide dismutase: an essential link between antioxidant function and high-temperature growth. *Eukaryot Cell* **4**: 46-54.

Giles, S. S., J. E. Stajich, C. Nichols, Q. D. Gerrald, J. A. Alspaugh, F. Dietrich & J. R. Perfect, (2006) The *Cryptococcus neoformans* catalase gene family and its role in antioxidant defense. *Eukaryot Cell* **5**: 1447-1459.

Goldfine, H., (1965) The evolution of oxygen as a biosynthetic reagent. *The Journal of general physiology* **49**: Suppl:253-274.

Goodley, J. M., Y. M. Clayton & R. J. Hay, (1994) Environmental sampling for aspergilli during building construction on a hospital site. *The Journal of hospital infection* **26**: 27-35.

Grahl, N. & R. A. Cramer, Jr., (2010) Regulation of hypoxia adaptation: an overlooked virulence attribute of pathogenic fungi? *Med Mycol* **48**: 1-15.

Grahl, N., S. Puttikamonkul, J. M. Macdonald, M. P. Gamcsik, L. Y. Ngo, T. M. Hohl & R. A. Cramer, (2011) *In vivo* Hypoxia and a Fungal Alcohol Dehydrogenase Influence the Pathogenesis of Invasive Pulmonary Aspergillosis. *PLoS Pathog* **7**: e1002145.

Guzy, R. D., M. M. Mack & P. T. Schumacker, (2007) Mitochondrial complex III is required for hypoxia-induced ROS production and gene transcription in yeast. *Antioxidants & redox signaling* **9**: 1317-1328.

Hall, L. A. & D. W. Denning, (1994) Oxygen requirements of *Aspergillus* species. *J Med Microbiol* **41**: 311-315.

Hassett, D. J., M. D. Sutton, M. J. Schurr, A. B. Herr, C. C. Caldwell & J. O. Matu, (2009) *Pseudomonas aeruginosa* hypoxic or anaerobic biofilm infections within cystic fibrosis airways. *Trends Microbiol* **17**: 130-138.

Herbrecht, R., D. W. Denning, T. F. Patterson, J. E. Bennett, R. E. Greene, J. W. Oestmann, W. V. Kern, K. A. Marr, P. Ribaud, O. Lortholary, R. Sylvester, R. H. Rubin, J. R. Wingard, P. Stark, C. Durand, D. Caillot, E. Thiel, P. H. Chandrasekar, M. R. Hodges, H. T. Schlamm, P. F. Troke & B. de Pauw, (2002) Voriconazole versus amphotericin B for primary therapy of invasive aspergillosis. *The New England journal of medicine* **347**: 408-415.

Himmelreich, U., T. E. Dzendrowskyj, C. Allen, S. Dowd, R. Malik, B. P. Shehan, P. Russell, C. E. Mountford & T. C. Sorrell, (2001) Cryptococcomas distinguished from gliomas with MR spectroscopy: an experimental rat and cell culture study. *Radiology* **220**: 122-128.

Hon, T., A. Dodd, R. Dirmeier, N. Gorman, P. R. Sinclair, L. Zhang & R. O. Poyton, (2003) A mechanism of oxygen sensing in yeast. Multiple oxygen-responsive steps in the heme biosynthetic pathway affect Hap1 activity. *The Journal of biological chemistry* **278**: 50771-50780.

Hoot, S. J., B. G. Oliver & T. C. White, (2008) *Candida albicans* UPC2 is transcriptionally induced in response to antifungal drugs and anaerobicity through Upc2p-dependent and -independent mechanisms. *Microbiology* **154**: 2748-2756.

Hospenthal, D. R., K. J. Kwon-Chung & J. E. Bennett, (1998) Concentrations of airborne *Aspergillus* compared to the incidence of invasive aspergillosis: lack of correlation. *Med Mycol* **36**: 165-168.

Hughes, A. L., C. Y. Lee, C. M. Bien & P. J. Espenshade, (2007) 4-Methyl sterols regulate fission yeast SREBP-Scap under low oxygen and cell stress. *The Journal of biological chemistry* **282**: 24388-24396.

Hughes, A. L., B. L. Todd & P. J. Espenshade, (2005) SREBP pathway responds to sterols and functions as an oxygen sensor in fission yeast. *Cell* **120**: 831-842.

Ibrahim-Granet, O., G. Jouvion, T. M. Hohl, S. Droin-Bergere, F. Philippart, O. Y. Kim, M. Adib-Conquy, R. Schwendener, J. M. Cavaillon & M. Brock, (2010) *In vivo* bioluminescence imaging and histopathopathologic analysis reveal distinct roles for resident and recruited immune effector cells in defense against invasive aspergillosis. *BMC Microbiol* **10**: 105.

Ingavale, S. S., Y. C. Chang, H. Lee, C. M. McClelland, M. L. Leong & K. J. Kwon-Chung, (2008) Importance of mitochondria in survival of *Cryptococcus neoformans* under low oxygen conditions and tolerance to cobalt chloride. *PLoS Pathog* **4**: e1000155.

Ismond, K. P., R. Dolferus, M. de Pauw, E. S. Dennis & A. G. Good, (2003) Enhanced low oxygen survival in *Arabidopsis* through increased metabolic flux in the fermentative pathway. *Plant Physiol* **132**: 1292-1302.

Joseph-Horne, T., D. W. Hollomon & P. M. Wood, (2001) Fungal respiration: a fusion of standard and alternative components. *Biochimica et biophysica acta* **1504**: 179-195.

Kelly, J. M., M. R. Drysdale, H. M. Sealy-Lewis, I. G. Jones & R. A. Lockington, (1990) Alcohol dehydrogenase III in *Aspergillus nidulans* is anaerobically induced and post-transcriptionally regulated. *Mol Gen Genet* **222**: 323-328.

Kiers, J., A. M. Zeeman, M. Luttik, C. Thiele, J. I. Castrillo, H. Y. Steensma, J. P. van Dijken & J. T. Pronk, (1998) Regulation of alcoholic fermentation in batch and chemostat cultures of *Kluyveromyces lactis* CBS 2359. *Yeast* **14**: 459-469.

Kizaka-Kondoh, S. & H. Konse-Nagasawa, (2009) Significance of nitroimidazole compounds and hypoxia-inducible factor-1 for imaging tumor hypoxia. *Cancer Sci* **100**: 1366-1373.

Kwast, K. E., P. V. Burke, B. T. Staahl & R. O. Poyton, (1999) Oxygen sensing in yeast: evidence for the involvement of the respiratory chain in regulating the transcription of a subset of hypoxic genes. *Proc Natl Acad Sci U S A* **96**: 5446-5451.

Labbe-Bois, R., Labbe P., (1990) Tetrapyrrole and heme biosynthesis in the yeast *Saccharomyces cerevisiae*. In: Biosynthesis of Heme and Chlorophylls. H. A. Dailey (ed). New York: McGraw-Hill Publishing Co., pp. 235-285.

Lambou, K., C. Lamarre, R. Beau, N. Dufour & J. P. Latge, (2010) Functional analysis of the superoxide dismutase family in *Aspergillus fumigatus*. *Mol Microbiol* **75**: 910-923.

Lara, A. R., H. Taymaz-Nikerel, M. R. Mashego, W. M. van Gulik, J. J. Heijnen, O. T. Ramirez & W. A. van Winden, (2009) Fast dynamic response of the fermentative metabolism of *Escherichia coli* to aerobic and anaerobic glucose pulses. *Biotechnol Bioeng* **104**: 1153-1161.

Latge, J. P., (1999) *Aspergillus fumigatus* and aspergillosis. *Clin Microbiol Rev* **12**: 310-350.

Latge, J. P., (2001) The pathobiology of *Aspergillus fumigatus*. *Trends Microbiol* **9**: 382-389.

Ljungkvist, A. S., J. Bussink, P. F. Rijken, J. A. Raleigh, J. Denekamp & A. J. Van Der Kogel, (2000) Changes in tumor hypoxia measured with a double hypoxic marker technique. *Int J Radiat Oncol Biol Phys* **48**: 1529-1538.

Lockington, R. A., G. N. Borlace & J. M. Kelly, (1997) Pyruvate decarboxylase and anaerobic survival in *Aspergillus nidulans*. *Gene* **191**: 61-67.

Magnani, T., F. M. Soriani, P. Martins Vde, A. C. Policarpo, C. A. Sorgi, L. H. Faccioli, C. Curti & S. A. Uyemura, (2008) Silencing of mitochondrial alternative oxidase gene of *Aspergillus fumigatus* enhances reactive oxygen species production and killing of the fungus by macrophages. *Journal of bioenergetics and biomembranes* **40**: 631-636.

Magnani, T., F. M. Soriani, V. P. Martins, A. M. Nascimento, V. G. Tudella, C. Curti & S. A. Uyemura, (2007) Cloning and functional expression of the mitochondrial alternative oxidase of *Aspergillus fumigatus* and its induction by oxidative stress. *FEMS Microbiol Lett* **271**: 230-238.

Marr, K. A., R. A. Carter, M. Boeckh, P. Martin & L. Corey, (2002) Invasive aspergillosis in allogeneic stem cell transplant recipients: changes in epidemiology and risk factors. *Blood* **100**: 4358-4366.

Marteyn, B., F. B. Scorza, P. J. Sansonetti & C. Tang, (2011) Breathing life into pathogens: the influence of oxygen on bacterial virulence and host responses in the gastrointestinal tract. *Cell Microbiol* **13**: 171-176.

Martins, V. P., T. M. Dinamarco, F. M. Soriani, V. G. Tudella, S. C. Oliveira, G. H. Goldman, C. Curti & S. A. Uyemura, (2011) Involvement of an alternative oxidase in oxidative stress and mycelium-to-yeast differentiation in *Paracoccidioides brasiliensis*. *Eukaryot Cell* **10**: 237-248.

Matherne, G. P., J. P. Headrick, S. D. Coleman & R. M. Berne, (1990) Interstitial transudate purines in normoxic and hypoxic immature and mature rabbit hearts. *Pediatr Res* **28**: 348-353.

Mayr, A. & C. Lass-Florl, (2011) Epidemiology and antifungal resistance in invasive Aspergillosis according to primary disease: review of the literature. *European journal of medical research* **16**: 153-157.

McCormick, A., J. Loeffler & F. Ebel, (2010) *Aspergillus fumigatus*: contours of an opportunistic human pathogen. *Cell Microbiol* **12**: 1535-1543.

McNeil, M. M., S. L. Nash, R. A. Hajjeh, M. A. Phelan, L. A. Conn, B. D. Plikaytis & D. W. Warnock, (2001) Trends in mortality due to invasive mycotic diseases in the United States, 1980-1997. *Clin Infect Dis* **33**: 641-647.

Merico, A., S. Galafassi, J. Piskur & C. Compagno, (2009) The oxygen level determines the fermentation pattern in *Kluyveromyces lactis*. *FEMS Yeast Res* **9**: 749-756.

Mikulska, M., A. M. Raiola, B. Bruno, E. Furfaro, M. T. Van Lint, S. Bregante, A. Ibatici, V. Del Bono, A. Bacigalupo & C. Viscoli, (2009) Risk factors for invasive aspergillosis and related mortality in recipients of allogeneic SCT from alternative donors: an analysis of 306 patients. *Bone marrow transplantation* **44**: 361-370.

Millner, P. D., P. B. Marsh, R. B. Snowden & J. F. Parr, (1977) Occurrence of *Aspergillus fumigatus* during composting of sewage sludge. *Appl Environ Microbiol* **34**: 765-772.

Morgan, J., K. A. Wannemuehler, K. A. Marr, S. Hadley, D. P. Kontoyiannis, T. J. Walsh, S. K. Fridkin, P. G. Pappas & D. W. Warnock, (2005) Incidence of invasive aspergillosis following hematopoietic stem cell and solid organ transplantation: interim results of a prospective multicenter surveillance program. *Med Mycol* **43 Suppl 1**: S49-58.

Moss, R. B., (2010) Allergic bronchopulmonary aspergillosis and *Aspergillus* infection in cystic fibrosis. *Current opinion in pulmonary medicine* **16**: 598-603.

Mylonakis, E., T. F. Barlam, T. Flanigan & J. D. Rich, (1998) Pulmonary aspergillosis and invasive disease in AIDS: review of 342 cases. *Chest* **114**: 251-262.

Nash, G., R. Irvine, R. L. Kerschmann & B. Herndier, (1997) Pulmonary aspergillosis in acquired immune deficiency syndrome: autopsy study of an emerging pulmonary complication of human immunodeficiency virus infection. *Human pathology* **28**: 1268-1275.

Nizet, V. & R. S. Johnson, (2009) Interdependence of hypoxic and innate immune responses. *Nat Rev Immunol* **9**: 609-617.

Panagiotou, G., S. G. Villas-Boas, P. Christakopoulos, J. Nielsen & L. Olsson, (2005) Intracellular metabolite profiling of *Fusarium oxysporum* converting glucose to ethanol. *J Biotechnol* **115**: 425-434.

Paris, S., D. Wysong, J. P. Debeaupuis, K. Shibuya, B. Philippe, R. D. Diamond & J. P. Latge, (2003) Catalases of *Aspergillus fumigatus*. *Infect Immun* **71**: 3551-3562.

Park, M. K., R. A. Myers & L. Marzella, (1992) Oxygen tensions and infections: modulation of microbial growth, activity of antimicrobial agents, and immunologic responses. *Clin Infect Dis* **14**: 720-740.

Patel, R. & C. V. Paya, (1997) Infections in solid-organ transplant recipients. *Clin Microbiol Rev* **10**: 86-124.

Patterson, K. & M. E. Strek, (2010) Allergic bronchopulmonary aspergillosis. *Proceedings of the American Thoracic Society* **7**: 237-244.

Perfect, J. R., G. M. Cox, J. Y. Lee, C. A. Kauffman, L. de Repentigny, S. W. Chapman, V. A. Morrison, P. Pappas, J. W. Hiemenz & D. A. Stevens, (2001) The impact of culture isolation of *Aspergillus* species: a hospital-based survey of aspergillosis. *Clin Infect Dis* **33**: 1824-1833.

Peyssonnaux, C., P. Cejudo-Martin, A. Doedens, A. S. Zinkernagel, R. S. Johnson & V. Nizet, (2007) Cutting edge: Essential role of hypoxia inducible factor-1alpha in development of lipopolysaccharide-induced sepsis. *J Immunol* **178**: 7516-7519.

Peyssonnaux, C., V. Datta, T. Cramer, A. Doedens, E. A. Theodorakis, R. L. Gallo, N. Hurtado-Ziola, V. Nizet & R. S. Johnson, (2005) HIF-1alpha expression regulates the bactericidal capacity of phagocytes. *J Clin Invest* **115**: 1806-1815.

Post, M. J., C. Lass-Floerl, G. Gastl & D. Nachbaur, (2007) Invasive fungal infections in allogeneic and autologous stem cell transplant recipients: a single-center study of 166 transplanted patients. *Transplant infectious disease : an official journal of the Transplantation Society* **9**: 189-195.

Poyton, R. O., K. A. Ball & P. R. Castello, (2009a) Mitochondrial generation of free radicals and hypoxic signaling. *Trends in endocrinology and metabolism: TEM* **20**: 332-340.

Poyton, R. O., P. R. Castello, K. A. Ball, D. K. Woo & N. Pan, (2009b) Mitochondria and hypoxic signaling: a new view. *Annals of the New York Academy of Sciences* **1177**: 48-56.

Purvis, A. C., (1997) Role of the alternative oxidase in limiting superoxide production by plant mitochondria. *Physiologia Plantarum* **100**: 165-170.

Raleigh, J. A., D. P. Calkins-Adams, L. H. Rinker, C. A. Ballenger, M. C. Weissler, W. C. Fowler, Jr., D. B. Novotny & M. A. Varia, (1998) Hypoxia and vascular endothelial growth factor expression in human squamous cell carcinomas using pimonidazole as a hypoxia marker. *Cancer Res* **58**: 3765-3768.

Raleigh, J. A., S. C. Chou, E. L. Bono, D. E. Thrall & M. A. Varia, (2001) Semiquantitative immunohistochemical analysis for hypoxia in human tumors. *Int J Radiat Oncol Biol Phys* **49**: 569-574.

Raleigh, J. A., S. C. Chou, D. P. Calkins-Adams, C. A. Ballenger, D. B. Novotny & M. A. Varia, (2000) A clinical study of hypoxia and metallothionein protein expression in squamous cell carcinomas. *Clin Cancer Res* **6**: 855-862.

Raymond, J. & D. Segre, (2006) The effect of oxygen on biochemical networks and the evolution of complex life. *Science* **311**: 1764-1767.

Rex, J. H., J. E. Bennett, J. I. Gallin, H. L. Malech, E. S. DeCarlo & D. A. Melnick, (1991) *In vivo* interferon-gamma therapy augments the in vitro ability of chronic granulomatous disease neutrophils to damage *Aspergillus* hyphae. *J Infect Dis* **163**: 849-852.

Rhodes, J. C., (2006) *Aspergillus fumigatus*: growth and virulence. *Med Mycol* **44 Suppl 1**: S77-81.

Ribaud, P., C. Chastang, J. P. Latge, L. Baffroy-Lafitte, N. Parquet, A. Devergie, H. Esperou, F. Selimi, V. Rocha, F. Derouin, G. Socie & E. Gluckman, (1999) Survival and prognostic factors of invasive aspergillosis after allogeneic bone marrow transplantation. *Clin Infect Dis* **28**: 322-330.

Ribrag, V., F. Dreyfus, A. Venot, V. Leblong, J. J. Lanore & B. Varet, (1993) Prognostic factors of invasive pulmonary aspergillosis in leukemic patients. *Leukemia & lymphoma* **10**: 317-321.

Richardson, D. J., (2000) Bacterial respiration: a flexible process for a changing environment. *Microbiology* **146 (Pt 3)**: 551-571.

Riscili, B. P. & K. L. Wood, (2009) Noninvasive pulmonary *Aspergillus* infections. *Clinics in chest medicine* **30**: 315-335, vii.

Rius, J., M. Guma, C. Schachtrup, K. Akassoglou, A. S. Zinkernagel, V. Nizet, R. S. Johnson, G. G. Haddad & M. Karin, (2008) NF-kappaB links innate immunity to the hypoxic response through transcriptional regulation of HIF-1alpha. *Nature* **453**: 807-811.

Rustad, T. R., A. M. Sherrid, K. J. Minch & D. R. Sherman, (2009) Hypoxia: a window into *Mycobacterium tuberculosis* latency. *Cell Microbiol* **11**: 1151-1159.

Sanchis, V., I. Vinas, I. N. Roberts, D. J. Jeenes, A. J. Watson & D. B. Archer, (1994) A pyruvate decarboxylase gene from *Aspergillus parasiticus*. *FEMS Microbiol Lett* **117**: 207-210.

Segal, B. H., W. Han, J. J. Bushey, M. Joo, Z. Bhatti, J. Feminella, C. G. Dennis, R. R. Vethanayagam, F. E. Yull, M. Capitano, P. K. Wallace, H. Minderman, J. W. Christman, M. B. Sporn, J. Chan, D. C. Vinh, S. M. Holland, L. R. Romani, S. L. Gaffen, M. L. Freeman & T. S. Blackwell, (2010) NADPH oxidase limits innate immune responses in the lungs in mice. *PloS one* **5**: e9631.

Setiadi, E. R., T. Doedt, F. Cottier, C. Noffz & J. F. Ernst, (2006) Transcriptional response of *Candida albicans* to hypoxia: linkage of oxygen sensing and Efg1p-regulatory networks. *J Mol Biol* **361**: 399-411.

Sharp, F. R. & M. Bernaudin, (2004) HIF1 and oxygen sensing in the brain. *Nature reviews. Neuroscience* **5**: 437-448.

Shi, L., C. D. Sohaskey, B. D. Kana, S. Dawes, R. J. North, V. Mizrahi & M. L. Gennaro, (2005) Changes in energy metabolism of *Mycobacterium tuberculosis* in mouse lung and under *in vitro* conditions affecting aerobic respiration. *Proc Natl Acad Sci U S A* **102**: 15629-15634.

Silver, P. M., B. G. Oliver & T. C. White, (2004) Role of *Candida albicans* transcription factor Upc2p in drug resistance and sterol metabolism. *Eukaryot Cell* **3**: 1391-1397.

Simmen, H. P., H. Battaglia, P. Giovanoli & J. Blaser, (1994) Analysis of pH, pO2 and pCO2 in drainage fluid allows for rapid detection of infectious complications during the follow-up period after abdominal surgery. *Infection* **22**: 386-389.

Smith, I., (2003) *Mycobacterium tuberculosis* pathogenesis and molecular determinants of virulence. *Clin Microbiol Rev* **16**: 463-496.

Snelders, E., W. J. Melchers & P. E. Verweij, (2011) Azole resistance in *Aspergillus fumigatus*: a new challenge in the management of invasive aspergillosis? *Future microbiology* **6**: 335-347.

Studer, L., M. Csete, S. H. Lee, N. Kabbani, J. Walikonis, B. Wold & R. McKay, (2000) Enhanced proliferation, survival, and dopaminergic differentiation of CNS precursors in lowered oxygen. *J Neurosci* **20**: 7377-7383.

Summons, R. E., A. S. Bradley, L. L. Jahnke & J. R. Waldbauer, (2006) Steroids, triterpenoids and molecular oxygen. *Philosophical transactions of the Royal Society of London. Series B, Biological sciences* **361**: 951-968.

Synnott, J. M., A. Guida, S. Mulhern-Haughey, D. G. Higgins & G. Butler, (2010) Regulation of the hypoxic response in *Candida albicans*. *Eukaryot Cell* **9**: 1734-1746.

Tabak, H. H. & W. B. Cooke, (1968) Growth and metabolism of fungi in an atmosphere of nitrogen. *Mycologia* **60**: 115-140.

Tekaia, F. & J. P. Latge, (2005) *Aspergillus fumigatus*: saprophyte or pathogen? *Curr Opin Microbiol* **8**: 385-392.

Thiel, M., A. Chouker, A. Ohta, E. Jackson, C. Caldwell, P. Smith, D. Lukashev, I. Bittmann & M. V. Sitkovsky, (2005) Oxygenation inhibits the physiological tissue-protecting mechanism and thereby exacerbates acute inflammatory lung injury. *PLoS Biol* **3**: e174.

Todd, B. L., E. V. Stewart, J. S. Burg, A. L. Hughes & P. J. Espenshade, (2006) Sterol regulatory element binding protein is a principal regulator of anaerobic gene expression in fission yeast. *Molecular and cellular biology* **26**: 2817-2831.

Trautmann NM, R. T., Krasny ME, (2003) Monitoring Compost pH. In. Ithaca, NY: Cornell University Composting Resources, pp.

Upton, A., K. A. Kirby, P. Carpenter, M. Boeckh & K. A. Marr, (2007) Invasive aspergillosis following hematopoietic cell transplantation: outcomes and prognostic factors associated with mortality. *Clin Infect Dis* **44**: 531-540.

Van Belle, H., F. Goossens & J. Wynants, (1987) Formation and release of purine catabolites during hypoperfusion, anoxia, and ischemia. *Am J Physiol* **252**: H886-893.

van Dijken, J. P., E. van den Bosch, J. J. Hermans, L. R. de Miranda & W. A. Scheffers, (1986) Alcoholic fermentation by 'non-fermentative' yeasts. *Yeast* **2**: 123-127.

van Heerden, I., C. Cronje, S. H. Swart & J. M. Kotze, (2002) Microbial, chemical and physical aspects of citrus waste composting. *Bioresour Technol* **81**: 71-76.

Varkey, J. B. & J. R. Perfect, (2008) Rare and emerging fungal pulmonary infections. *Semin Respir Crit Care Med* **29**: 121-131.

Via, L. E., P. L. Lin, S. M. Ray, J. Carrillo, S. S. Allen, S. Y. Eum, K. Taylor, E. Klein, U. Manjunatha, J. Gonzales, E. G. Lee, S. K. Park, J. A. Raleigh, S. N. Cho, D. N. McMurray, J. L. Flynn & C. E. Barry, 3rd, (2008) Tuberculous granulomas are hypoxic in guinea pigs, rabbits, and nonhuman primates. *Infect Immun* **76**: 2333-2340.

von Eiff, M., N. Roos, W. Fegeler, C. von Eiff, M. Zuhlsdorf, J. Glaser & J. van de Loo, (1994) Pulmonary fungal infections in immunocompromised patients: incidence and risk factors. *Mycoses* **37**: 329-335.

Wagner, A. M. & A. L. Moore, (1997) Structure and function of the plant alternative oxidase: its putative role in the oxygen defence mechanism. *Bioscience reports* **17**: 319-333.

Wang W, W. X., Liu J, Masaharu, I, Yasuo I, Cui Z, (2007) Effect of oxygen concentration on the composting process and maturity. *Compost science & utilization* **vol. 15**: pp. 184-190.

Warn, P. A., A. Sharp, J. Guinea & D. W. Denning, (2004) Effect of hypoxic conditions on *in vitro* susceptibility testing of amphotericin B, itraconazole and micafungin against *Aspergillus* and *Candida*. *J Antimicrob Chemother* **53**: 743-749.

West, J. B., (1984) 1984 Armstrong lecture. Hypoxic man: lessons from extreme altitude. *Aviat Space Environ Med* **55**: 1058-1062.

Westney, G. E., S. Kesten, A. De Hoyos, C. Chapparro, T. Winton & J. R. Maurer, (1996) *Aspergillus* infection in single and double lung transplant recipients. *Transplantation* **61**: 915-919.

White, T. C. & P. M. Silver, (2005) Regulation of sterol metabolism in *Candida albicans* by the *UPC2* gene. *Biochemical Society transactions* **33**: 1215-1218.

Willger, S. D., S. Puttikamonkul, K. H. Kim, J. B. Burritt, N. Grahl, L. J. Metzler, R. Barbuch, M. Bard, C. B. Lawrence & R. A. Cramer, Jr., (2008) A sterol-regulatory element binding protein is required for cell polarity, hypoxia adaptation, azole drug resistance, and virulence in *Aspergillus fumigatus*. *PLoS Pathog* **4**: e1000200.

Wilson, D. M., W. Mubatanhema & Z. Jurjevic, (2002) Biology and ecology of mycotoxigenic *Aspergillus* species as related to economic and health concerns. *Adv Exp Med Biol* **504**: 3-17.

Zhang, L. & A. Hach, (1999) Molecular mechanism of heme signaling in yeast: the transcriptional activator Hap1 serves as the key mediator. *Cellular and molecular life sciences : CMLS* **56**: 415-426.

Zhou, Z., N. Takaya & H. Shoun, (2010) Multi-energy metabolic mechanisms of the fungus *Fusarium oxysporum* in low oxygen environments. *Biosci Biotechnol Biochem* **74**: 2431-2437.

Acknowledgements

My utmost gratitude goes to my two advisors, Dr. Erika Kothe and Dr. Robert A. Cramer for allowing me to conduct the work for my Ph.D. in this format.

Erika, I am very thankful that you were willing to support me with this unusual Ph.D. thesis set-up. Thank you for being so open-minded.

Dr. Robb – thank you, thank you, thank you for the last 4 fantastic years! This thesis would not have been possible without all your help and support. I am deeply grateful for all the helpful discussions and conversations we had over the years. Thank you for believing in me when I did not believe in myself. You have been a fantastic teacher and supervisor, and you will be a good friend forever. ☺ Thank you!

I also want to thank my fellow lab members, co-workers, and friends for all their support and for tolerating my craziness and sometimes overwhelming energy (even early in the morning, I know). I especially want to thank Bridget Barker, my lab-dance partner in crime (may the Gaga be with you!), Katie Rowse, Kelly Shepardson, and Peggy Lehmann for being such good friends and for the countless group therapies on Friday afternoons at Spectators that kept me safe and sound. Cheers ladies!

In addition, I want to thank my friends in Germany that supported me even though I was “on the other side of the world”. My special thanks go to my best friend Dagmar Lyska whose support and insights were invaluable. Schätzelein, du bist unbezahlbar!

And last but not least, I want to thank my family (Grahl’s and Willger’s) for their love and support every step of the way. I especially thank Sven Willger, love of my life, for his patients, love, support, and unshakable faith in me and my skills. Thank you for being there for me. I could not have done this without you. LU

Eigenständigkeitserklärung

Hiermit erkläre ich, dass ich die hier vorgelegte Dissertation mit dem Titel "*In vivo* hypoxia and *Aspergillus fumigatus* pathogenesis" eigenständig und ohne unerlaubte Hilfe angefertigt habe. Die Dissertation wurde in der vorgelegten oder ähnlicher Form noch bei keiner anderen Institution eingereicht. Ich habe bisher keine erfolgreichen oder erfolglosen Promotionsversuche unternommen, um den akademischen Grad doctor rerum naturalium zu erlangen.

Declaration

I hereby declare that I independently wrote the dissertation "*In vivo* hypoxia and *Aspergillus fumigatus* pathogenesis" utilizing only the stated resources. I vouch that the content of this dissertation has not, in part or whole, been submitted or accepted for the award of any Degree at any university or other institutions. To date I have not undertaken any successful or unsuccessful attempts to acquire the degree doctor rerum naturalium.

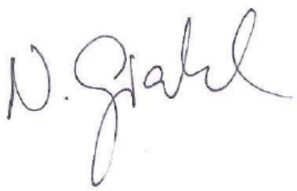

Bozeman, 12.10.2011

Curriculum Vitae

CONTACT INFORMATION

Name Nora Grahl

Address Department of Immunology and Infectious Diseases
Montana State University
960 Technology Blvd
Bozeman, MT 59718

email: nora.grahl@montana.edu

EDUCATION

2007 – current **Ph.D. student**, Biology, Friedrich Schiller University Jena, Germany. (Ph.D. work will be conducted at Montana State University in Bozeman, Montana, USA, in the laboratory and under the supervision of Robert A. Cramer, Ph.D.)
Title: *In vivo* Hypoxia and *Aspergillus fumigatus* pathogenesis

2001 - 2006 **University Student**
Heinrich-Heine University Düsseldorf, Germany
Degree: Diplom Biologin
Diplomawork in the department of Microbiology
Title: Analysis of protein-protein interactions between protein-*O*-mannosyltransferases (PMTs) in *Cryptococcus neoformans*

PROFESIONAL EXPERIENCE

Summer 2010 Student of the 2010 MBL course Medical Mycology: Current Approaches to Fungal Pathogenesis

Spring 2007 Industrial Internship at Henkel KGaA in the department of Enzyme Technology, Düsseldorf Germany

January 2007 Practical lab work at Duke University in Durham, NC USA, in the group of Dr. J. A. Alspaugh, M.D.

Fall 2006 Participation in an exchange program of the DAAD between Germany (group of Prof. J. Ernst; Heinrich-Heine University Düsseldorf) and Spain (group of Prof. J. Pla; Universidad Complutense de Madrid)

PUBLICATIONS

Grahl N, and Cramer, RA (2011) Hypoxia and Fungal Pathogenesis: Is there a link? Eukaryotic Cell (in preparation).

Grahl N, Magnani Dinamarco T, Willger SD, Goldman GH, and Cramer, RA (2011) *Aspergillus fumigatus* mitochondrial electron transport chain mediates oxidative stress homeostasis, hypoxia responses, and fungal pathogenesis. Molecular Microbiology (submitted).

Blatzer M, Barker BM, Willger SD, Beckmann N, Blosser SJ, Cornish EJ, Mazurie A, Grahl N, Haas H, and Cramer RA (2011) SREBP Coordinates Siderophore and Ergosterol Biosynthesis to Mediate Triazole Drug and Hypoxia Responses in a Human Fungal Pathogen. PLoS Genetics (in press).

Feng X, Krishnan K, Richie DL, Aimanianda V, Hartl L, Grahl N, Powers-Fletcher MV, Zhang M, Fuller KK, Nierman WC, Lu LJ, Latge JP, Woollett L, Newman SL, Cramer Jr RA, Rhodes JC, and Askew DS (2011) HacA-independent functions of the ER stress sensor IreA synergize with the canonical UPR to influence virulence traits in the fungal pathogen *Aspergillus fumigatus*. PLoS Pathog (in press).

Grahl N, Puttikamonkul S, Macdonald JM, Gamcsik MP, Ngo LY, Hohl TM, and Cramer, RA (2011) *In vivo* Hypoxia and a Fungal Alcohol Dehydrogenase Influence the Pathogenesis of Invasive Pulmonary Aspergillosis. PLoS Pathog 7(7): e1002145.

Li H, Barker B, Grahl N, Puttikamonkul S, Bell JD, Craven KD, Cramer RA Jr. (2011) The small GTPase RacA mediates intracellular reactive oxygen species production, polarized growth, and virulence in the human fungal pathogen *Aspergillus fumigatus*. Eukaryotic Cell, 10(2):174-86.

Puttikamonkul S, Willger SD, Grahl N, Perfect JR Movahed N, Bothner B, Park S, Paderu P, Perlin DS, Cramer RA Jr. (2010) Trehalose-6-Phosphate Phosphatase is required for cell wall integrity and fungal virulence but not trehalose biosynthesis in the human fungal pathogen *Aspergillus fumigatus*. Molecular Microbiology, 77:891-911.

Grahl, N, and Cramer, RA (2010) Regulation of Hypoxia Adaptation: An Overlooked Virulence Attribute of Pathogenic Fungi? Medical Mycology, 22:1-16.

Kim KH, Willger SD, Park SW, Puttikamonkul S, Grahl N, Cho Y, Mukhopahyay B, Cramer RA Jr., Lawrence CB (2009) TmpL, a transmembrane protein required for intracellular redox homeostasis and virulence in a plant and an animal fungal pathogen. PLoS Pathog 5(11): e1000653.

Willger, Sven D., Grahl, Nora and Cramer Jr, Robert A. (2009)'*Aspergillus fumigatus* metabolism: Clues to mechanisms of in vivo fungal growth and virulence', Medical Mycology, 47:1,S72 — S79.

Willger SD, Puttikamonkul S, Kim KH, Burritt JB, Grahl N, Metzler LJ, Barbuch R, Bard M, Lawrence CB, Cramer RA Jr. (2008) A sterol-regulatory element binding protein is required for cell polarity, hypoxia adaptation, azole drug resistance, and virulence in *Aspergillus fumigatus*. *PLoS Pathog*; 4(11): e1000200.

POSTER PRESENTATIONS

Grahl, N, Puttikamonkul S, Magnani T, MacDonald JM, Gamcsik MP, Goldman GH, and Cramer Jr RA (2011) *In vivo* hypoxia affects the pathogenesis of invasive pulmonary aspergillosis. 4th FEBS Advanced Lecture Course Human Fungal Pathogens: Molecular Mechanisms of Host-Pathogen Interactions and Virulence (May 7-13, 2011, La Colle sur Loup, France).

Grahl, N, Puttikamonkul S, Bushmaker TJ, Magnani T, Macdonald J, Gamcsik M, Goldman G, and Cramer Jr RA (2010) *In vivo* energy metabolism of *A. fumigatus*: implications of *in vivo* hypoxia during fungal pathogenesis. 4th Advances against Aspergillosis Conference (February 4-6 2010, Sheraton Roma, Rome, Italy)

Grahl, N, Macdonald JM, Gamcsik MP, and Cramer Jr RA (2009) Alcohol fermentation and hypoxia adaptation in the pathogenic mold *Aspergillus fumigatus*. Western Region COBRE-INBRE Scientific Conference (September 17-18 2009, Big Sky Resort, Big Sky, Montana)

Grahl, N, Macdonald JM, Gamcsik MP, and Cramer Jr RA (2009) Alcohol fermentation and hypoxia adaptation in the pathogenic mold *Aspergillus fumigatus*. 25th Fungal Genetics Conference (March 17-22 2009, Asilomar Conference Center, Pacific Grove, California)

Grahl, N, Macdonald JM, Gamcsik MP, and Cramer Jr RA (2009) Alcohol fermentation and hypoxia adaptation in the pathogenic mold *Aspergillus fumigatus*. 6th international Aspergillus Meeting (March 15-17 2009, Asilomar Conference Center, Pacific Grove, California)

ORAL PRESENTATIONS

In vivo hypoxia and alcohol dehydrogenase influence the pathogenesis of invasive pulmonary aspergillosis. 2011 Big Sky Mycology Meeting (May 19-20, 2011, Bozeman, Montana, USA).

In vivo hypoxia affects the pathogenesis of invasive pulmonary aspergillosis. 4th FEBS Advanced Lecture Course Human Fungal Pathogens: Molecular Mechanisms of Host-Pathogen Interactions and Virulence (May 7-13, 2011, La Colle sur Loup, France).

In vivo energy metabolism of *Aspergillus fumigatus*. 2010 Big Sky Mycology Meeting (May 13-14, 2010, Bozeman, Montana, USA).

The Trehalose Pathway is Critical for *Aspergillus Fumigatus* Virulence. 4th Advances against Aspergillosis Conference (February 4-6 2010, Rome, Italy) – proxy for Srisombat Puttikamonkul

In vivo energy metabolism of *A. fumigatus*: Implications of *in vivo* hypoxia during fungal pathogenesis. Department of Immunology and Infectious Diseases Seminar Series, Montana State University (September 27th 2009, Bozeman, Montana, USA).

AWARDS

Oral presentation Young Investor Award at the 4th FEBS Advanced Lecture Course Human Fungal Pathogens: Molecular Mechanisms of Host-Pathogen Interactions and Virulence (May 7-13, 2011, La Colle sur Loup, France).

FEBS Youth Trans Travel Award (2011) to attend 4th FEBS Advanced Lecture Course Human Fungal Pathogens: Molecular Mechanisms of Host-Pathogen Interactions and Virulence (May 7-13, 2011, La Colle sur Loup, France).

Oral presentation at the 4th Advances against Aspergillosis Conference (February 4-6 2010, Sheraton Roma, Rome, Italy) was awarded an oral presentation award.

Student Poster Award - 6th international *Aspergillus* Meeting (March 15-17 2009, Asilomar Conference Center, Pacific Grove, California).

Travel award – Fungal genetics society (2009) to attend 25th Fungal Genetics Conference (March 17-22 2009, Asilomar Conference Center, Pacific Grove, California).

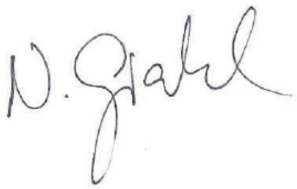

Bozeman, 12.10.2011